THESE POUR OBTENIR LE GRADE DE DOCTEUR DE
L'ECOLE NATIONALE SUPERIEURE DE CHIMIE DE MONTPELLIER

En Chimie et Physico-Chimie des Matériaux

École doctorale Sciences Chimiques Balard (ED459)

Unité de recherche Institut Charles Gerhardt Montpellier UMR 5253

Synthèse et caractérisation de vitrimères de transestérification sans catalyseur

Présentée par **Florian CUMINET**
le 11 octobre 2022

Sous la direction de Sylvain CAILLOL et Éric DANTRAS
Et co-encadrée par Vincent LADMIRAL et Éric LECLERC

Devant le jury composé de

Tatiana BESSET, Directrice de recherche CNRS, INSA Rouen Normandie	Rapporteure
François TOURNILHAC, Directeur de recherche CNRS, ESPCI-Paris	Rapporteur
Frédéric PERUCH, Directeur de recherche CNRS, LCPO (CNRS/Bx INP-ENSCBP/ Univ. Bx)	Président
Rinaldo POLI, Professeur des Universités, Institut National Polytechnique de Toulouse	Invité
Sylvain CAILLOL, Directeur de recherche CNRS, ICGM	Co-directeur de thèse
Éric DANTRAS, Maître de conférences, Université Toulouse 3 Paul Sabatier	Co-directeur de thèse
Vincent LADMIRAL, Directeur de recherche CNRS, ICGM	Co-encadrant
Éric LECLERC, Chargé de recherche CNRS, ICGM	Co-encadrant

ENS C M Chimie Montpellier

UNIVERSITÉ DE MONTPELLIER

REMERCIEMENTS

Je tiens d'abord à remercier Patrick Lacroix-Desmazes, directeur du département Chimie et Matériaux MacroMoléculaires de l'Institut Charles Gerhardt de Montpellier, de m'avoir accueilli au sein de l'équipe pour la majeure partie de ma thèse. Merci à Marc Taillefer, directeur de l'ex-équipe Architectures Moléculaires et Matériaux Nanostructurés au sein de laquelle j'ai travaillé pendant les trois premiers mois de ma thèse, et tout particulièrement à Jean-Marc Campagne, pour m'avoir accueilli dans son groupe. Merci également à Christophe Laurent, directeur du Centre Inter-universitaire de Recherche et d'Ingéniérie des Matériaux de Toulouse, et à Éric Dantras, responsable de l'équipe Physique des Polymères, de m'avoir également accueilli dans leurs locaux.

Merci à l'Institut Carnot Chimie Balard – CIRIMAT d'avoir financé mon projet de thèse.

Je remercie Mme Tatiana Besset et M. François Tournilhac, en leurs qualités de rapporteure et rapporteur, ainsi que M. Frédéric Peruch, en qualité d'examinateur, d'avoir accepté d'évaluer ces travaux de thèse.

Je tiens à exprimer toute ma reconnaissance et ma gratitude envers mes directeurs et encadrants de thèse : Sylvain Caillol, Éric Dantras, Vincent Ladmiral et Éric Leclerc. Merci à tous pour votre aide, votre attention, vos nombreux conseils, votre soutien et votre bienveillance. Merci Sylvain pour les nombreux conseils stratégiques affutés, pour ta présence dans les moments de tension, et pour m'avoir transmis ta vision très appliquée de la science des polymères. Merci Vincent pour m'avoir appris la rigueur, le souci du détail et du mot juste, et la gestion de son temps (« on dormira quand on sera morts », Vincent Ladmiral, 2019), mais également pour l'indulgence dont tu sais faire preuve. Et merci à tous les deux d'avoir souvent illustré cette phrase qui vous va si bien « Ici on fait des choses sérieuses, sans se prendre au sérieux » (Sylvain Caillol, 2021). Merci Éric (Dantras) pour m'avoir appris les rudiments de la physique des polymères, la rigueur en analyse mécanique et la prudence dans les interprétations de résultats. Expliquer la physique à un chimiste n'a pas dû être facile, merci pour ta patience. Tu as trouvé la formule parfaite pour résumer ces trois ans : « Les vitrimères, c'est l'école de la patience » (Éric Dantras, 2021). Merci Éric (Leclerc) pour les 3 mois passés à travailler avec toi, j'ai découvert et appris beaucoup en très peu de temps. Merci pour ta bienveillance, et d'avoir veillé tout au long du projet à corriger mes hypothèses de chimie organique, parfois farfelues. J'ai beaucoup appris au contact de chacun d'entre vous, bien plus que ces quelques lignes ne sauraient le résumer. Vos compétences dans des domaines très variés et vos visions complémentaires de la recherche ont fait la force de cette équipe et ont permis de mener ce projet à son terme. Sans chacun d'entre vous, tout cela n'aurait pas été possible.

Je tiens également à remercier toutes les personnes avec qui j'ai pu collaborer, sur mes travaux de thèse ou sur des sujets transversaux : Jennifer « Jenn », Romain, Anne-Sophie, David, Rinaldo Poli, Sébastien Lemouzy, Cédric Totée, Gilles Silly, Sabine Devautour-Vinot, Paul Iacomi, Maxinne, Baptiste, Julien et

Dimitri. Merci à Marc Guerre et François Tournilhac pour les discussions sur les vitrimères qui ont permis de me faire avancer dans mes questionnements. Merci à Lise Reymond pour son aide sur la synthèse de monomères.

Merci à tous les membres du département C3M « D2 », que j'ai croisé au quotidien, permanents et non-permanents. Merci en particulier à Abdou, Caroline, Christine (J-D), Claire, qui est restée bienveillante à mon égard malgré que j'ai refusé son sujet de thèse, Ghis, que je n'ai pas épargné non plus, Julien, Maxime, Patrick, Rémi et Sylvain Catrouillet, qui s'entête à venir me parler, malgré le peu d'informations utiles que je lui apporte. Merci à Aliénor, Fabien, Gaëlle et Zoé pour la bonne ambiance au bureau et au labo.

Merci aux membres du groupe Jean-Marc Campagne de l'ex-équipe AM_2N : Chayma, Eleonora, pour ton intarissable bonne humeur et ton énergie, Emmanuel, Éric, Georg, Jean-Marc, Liyan, Pierre et Renata, merci pour ta gentillesse. Merci à Pascale pour nos échanges non dénués d'un grain de folie, souvent brefs au détour d'un couloir, mais toujours très agréables.

Merci aux membre de l'équipe Phypol de m'avoir accueilli pendant un mois, et en particulier à Éric et Antoine, pour votre aide et vos conseils sur l'analyse mécanique.

« Une thèse, c'est un marathon de 3 ans » m'a dit un jour un certain Vincent Bouad. Et comme pour un marathon, il est plus facile de tenir sur la durée lorsqu'on est bien entourés. J'ai eu la chance de partager un magnifique appartement pendant 2 ans avec « mes loulous » Maxinne et Guilhem. Je vois dois énormément à tous les deux, pour avoir mis tant de gaîté dans mon quotidien et pour avoir été présents dans les meilleurs moments comme dans les pires. Merci aussi pour tous les supers moments que je ne compte plus, les apéros sur la terrasse à refaire le monde (et surtout le labo !), les vacances incroyables organisées par notre tour-op' de compétition Maxinne, bref, pour ces années incroyables à vos côtés. Merci à Dimitri et à Sébastien pour l'aide précieuse qu'ils m'ont apporté au moment où j'en avait le plus besoin, et dans un autre registre, pour les sessions de course à pied avec Dimitri qui nous ont mené jusqu'au semi-marathon de Montpellier. Merci à Camille et Baptiste d'avoir été nos coachs pendant nos WOD clandestins sur le parking, et à Baptiste pour les « vrais » WOD partagés, après que tu aies passé presque 2 ans à essayer de me convaincre que le CrossFit me plairait. On dirait que tu avais raison ! Merci Elena pour ton énergie (encore une italienne survitaminée, ça fait plaisir !). Merci à Léo, Lorelei, Joshua, Philibert et Camille pour avoir énormément contribué à la bonne ambiance qui règne au labo. Et bien-sûr à Maxime et Morgane, on se voit trop peu, mais c'est toujours avec grand plaisir.

Bien-sûr je n'oublie pas les « anciens », de la génération IAM, ceux qui n'ont connus que les vieux locaux rue de l'Ecole Normale. Heureusement que vous étiez là, pour supporter ces vieux labos vétustes et pas

très rassurants. Merci à tous les membres du « bureau des garçons ~~+ Mélanie~~ + Camille » : Fabien, notre Caliméro à nous, que j'ai grand plaisir à retrouver dans mon labo aujourd'hui, Camille, Benjamin, Vincent et bien sûr Romain. Tu as été mon premier chef, et j'ai beaucoup apprécié de travailler à tes côtés. Tu m'as beaucoup appris et c'est toujours un plaisir de se revoir, même en terre hostile, à des centaines de kilomètres de Montpellier ! Je n'oublie pas Anne-Sophie, qui m'a légué la responsabilité des DSC, sur lesquelles j'ai veillé pendant 2 ans et demi… J'espère avoir été à la hauteur de la tâche. J'ai toujours ton « héritage » dans sa boite, tout neuf, il faudra que je le transmette à Philibert pour poursuivre la lignée. Je pense également à David, avec qui on a échangé pendant des heures sur les vitrimères (ou pas), avec généralement plus de questions sans réponse à la fin qu'au début. A Yvan et Eline, pour les très bonnes soirées avec des chorégraphies parfois… approximatives, un peu comme les souvenirs que j'en ai d'ailleurs ! A Céline pour ta gentillesse et pour ton énergie positive. Enfin, à Mélanie, bien qu'on se soit peu croisés. J'ai gardé en tête cette phrase que tu as dit la première fois qu'on s'est rencontrés : « c'est mon poulain ! ». L'air de rien, elle a fait son chemin dans ma tête et m'a aidé à rentrer plus sereinement dans le projet au début de ma thèse.

Je tiens également à remercier mes deux stagiaires Chloé et Nathan, pour tout le travail accompli. Je finirai par le valoriser, bientôt, c'est promis ! Vous m'avez apporté et appris beaucoup, sans doute plus que vous ne l'imaginez, et je vous en remercie.

Je remercie également tous ceux que j'ai connu avant la thèse et qui ont continué à me suivre de plus ou moins loin pendant ces trois années. Je pense bien sûr à Péroline, Clothilde, Anna, Antoine, Lucas, Sophie et les autres membres des « Kékos » et de la « basse-cour de l'ENSCM », qui se reconnaitront. Un grand merci également à Giovanna, après 12 ans c'est toujours un grand plaisir de se revoir (on devrait faire ça plus souvent !).

Enfin, un énorme merci à ma famille, en particulier à mes parents et à Océane, pour m'avoir soutenu depuis toutes ces années. Je n'en serais pas là si vous n'aviez pas été là, derrière moi. Merci pour votre soutien dans les moments de doutes, de stress, dans les petites galères du quotidien et les galères tout court. Et puis merci de m'avoir supporté aussi… un thésard sous pression ça n'est pas tous les jours facile à vivre. Merci pour les supers moments partagés en vacances, en Normandie, en week-end. Bref, merci pour tout. Je vous aime. D'ailleurs en parlant de vacances… Chat-Wane, on part où pour les prochaines ? J'ai aussi une pensée pour Zen, elle aussi m'a soutenu à sa façon.

Je pense avoir fait le tour. Ces trois années auront été riches en rencontres, malgré les confinements et autres restrictions, et j'espère sincèrement n'avoir oublié personne !

SOMMAIRE

LISTE DES ABREVIATIONS

ATR	*attenuated total reflectance* - réflectance totale atténuée
BADGE	*bisphenol A diglycidyl ether*- diglycidyl éther de bisphénol A
DGEBA	diglycidyl éther de bisphénol A
3D	*three-dimensional* - tridimensionnel
BDE	*bond dissociation energy* - énergie de dissociation d'une liaison
BDGE	*butanediol diglycidyl ether*- diglycidyl éther de butanediol
BMSC	*bis-(methylsalicyl)carbonate*
BPA	*bisphenol A* - bisphénol A
CAN	*covalent adaptable network* - réseau covalent adaptable
CIRIMAT	Centre Inter-universitaire de Recherche et d'Ingénierie des MATériaux
CNRS	Centre National de la Recherche Scientifique
COSY (NMR)	*correlated spectroscopy* - RMN bidimensionnelle par corrélation homonucléaire
CX1	*complex 1* - complexe 1
CX2	c*omplex 2* - complexe 2
DBTL / DBTDL	*dibutyltin dilaurate* - dilaurate de dibutylétain
DBU	*1,8-Diazabicyclo[5.4.0]undec-7-ene* - 1,8-Diazabicyclo[5.4.0]undéc-7-ène
DCM	*dichloromethane*- dichlorométhane
DMA	*dynamic mechanical analysis* - analyse mécanique dynamique
DMF	*dimethylformamide*- diméthylformamide
DMSO	*dimethylsulfoxide* - diméthylsulfoxyde
DMTDA	*dimethylthiotoluenediamine*- diméthylthiotoluènediamine
DPC	*diphenyl carbonate* - diphényl carbonate
DSC	*differential scanning calorimetry* - calorimétrie différentielle à balayage
EDG	*electron donating group* - groupe électrodonneur
EEW	*epoxy equivalent weight* - masse équivalente pour une mole de fonction époxy
EG-AA	*ethylene glycol–bisacetoacetate* - bis(acétoacétate) d'éthylène glycol
EN	en anglais
ESI-	*negative electrospray ionization* - ionisation négative par électronébuliseur
ESI+	*positive electrospray ionization* - ionisation positive par électronébuliseur
Et_2O	*diethyl ether* - éther diéthylique
EWG	*electron withdrawing group* - groupe électroattracteur
FR	en français
FTIR	*Fourier transform infrared spectroscopy* - spectroscopie infrarouge à transformée de Fourier
HRMS	*high resolution mass spectroscopy* - spectroscopie de masse à haute résolution
HSQC (NMR)	*heteronuclear single quantum coherence*
ICGM	Institut Charles Gerhardt de Montpellier
INP-ENSCBP	Institut National Polytechnique - École Nationale Supérieure de Chimie, de Biologie et de Physique
INSA	Institut National des Sciences Appliquées
KWW	Kohlrausch-Williams-Watts (fonction de) **ou** fonction exponentielle étirée
LCPO	Laboratoire de Chimie des Polymères Organiques
MDI	*methylene diphenyl diisocyanate* - 4,4'-diisocyanate de diphénylméthylène
MeCN	*acetonitrile* - acétonitrile
MOCA	*4,4'-methylenebis(2-chlorobenzenamine)*- 4,4'-méthylènebis(2-chloroaniline)
NaOH	*sodium hydroxide* - hydroxyde de sodium
NGP	*neighboring group participation* - participation des groupes voisins **ou** assistance anchimérique

NMR	*nuclear magnetic resonnance* - résonnance magnétique nucléaire (RMN)
P-DAF	*2,2'-(1,4-phenylene)bis(2,2-difluoroacetic acid)* - acide 2,2'-(1,4-phénylène)bis(2,2-difluoroacétique)
P-DAF/BDGE	vitrimère fluoré issu du P-DAF et du BDGE
P-DE	*diethyl 2,2'-(1,4-phenylene)bis(2,2-difluoroacetate)* - 2,2'-(1,4-phénylène)bis(2,2-difluoroacétate) de diéthyle
PDMS	*polydimethylsiloxane* - polydiméthylsiloxane
PEEK	*polyetherketoneketone* - polyéthercétonecétone
PEEKK	*polyetheretherketoneketone* - polyétheréthercétonecétone
PEG	*polyethylene glycol* - polyéthylène glycol
PEK	*polyetherketone* - polyéthercétone
PET	*poly(ethylene terephthalate)* - poly(téréphtalate d'éthylène)
PHU	*polyhydroxyurethane* - polyhydroxyuréthane
PTFE	*polytetrafluoroethylene* - polytétrafluoroéthylène
PTMG	*poly(tetramethylene ether)glycol* ***or*** *polytetrahydrofuran*
PTU	*polythiourethane* - polythiouréthane
PU	*polyurethane* - polyuréthane
ROP	*ring opening polymerization* - polymérisation par ouverture de cycle
RT	*room temperature* - température ambiante
RvOEt	triester α,α-difluoré issu du resvératrol
RvOGly	resvératrol époxydé
RvOH-TAF	triacide α,α-difluoré issu du resvératrol
TBD	*triazabicyclodecene* - triazabicyclodécène
TEA	*triethanolamine* - triéthanolamine
TBAB	*tetrabutylammonium bromide* - bromure de tétrabutylammonium
TGA	*thermogravimetric analysis* - analyse thermogravimétrique
TGDDM	*tetraglycidyl methylenedianiline*- tétraglycidyléther de 4,4'-diaminodiphénylméthane
THF	*tetrahydrofuran* - tétrahydrofurane
TMS	*tetramethylsilane* - tétraméthylsilane
TPE	*1,1,1-Tris(4-hydroxyphenyl)ethane* - 1,1,1-Tris(4-hydroxyphényl)éthane
TPE-TAF	triacide α,α-difluoré issu du 1,1,1-Tris(4-hydroxyphényl)éthane
TPE-TAF/BDGE	vitrimère fluoré issu du TPE-TAF et du BDGE
TPE-TE	triester α,α-difluoré issu du 1,1,1-Tris(4-hydroxyphényl)éthane
TPP	*triphenylphosphine* - triphénylphosphine
TREN	*tris(2-aminoethyl)amine*- tris(2-aminoéthyl)amine
TTS	*transition state* - état de transition
Vm-RvOH	vitrimère fluoré issu du resvératrol (RvOH-TAF et RvOGly)
VU	*vinylogous urethane* ***or*** *enaminone*

INTRODUCTION GENERALE

Depuis l'essor des polymères de synthèse dans les années 1930 jusqu'au début des années 2000, la communauté des polymèristes classifiait les architectures polymères en deux groupes : soit le matériau polymère était formé par un réseau macromoléculaire trimensionnel, soit constitué de chaînes linéaires enchevêtrées. Dans l'industrie, ces deux types d'architecture ont été qualifiées respectivement de thermodurcissable ou de thermoplastique, en fonction de leurs propriétés, notamment de mise en oeuvre. En effet, les thermodurcissables ont une morphologie fixée une fois leur polymérisation achevée. Leur mise en forme se fait à partir du prépolymère, et la morphologie obtenue est fixée après réticulation. Les thermoplastiques, en revanche, sont généralement fusibles après polymérisation, à quelques exceptions près (aramides, PTFE). Cette propriété permet des procédés de mise en œuvre à l'état fondu, par exemple par extrusion, par injection ou encore par calandrage. Les propriétés différentes des thermodurcissables et des thermoplastiques dépendent directement de leur structure macromoléculaire. Un thermodurcissable forme en théorie une seule macromolécule qui occupe tout le volume du matériau, la cohésion du réseau étant liée principalement aux liaisons covalentes qui le composent. Dans le cas d'un thermoplastique, il n'y a pas de liaison covalente entre les chaînes, la cohésion est assurée par les enchevêtrements et les liaisons faibles pouvant intervenir entre ces chaînes (liaisons hydrogènes, liaisons de Van der Waals). Les propriétés de ces deux types de matériaux, qui découlent de leur architecture, sont de ce fait très différentes. Les thermodurcissables permettent d'obtenir de hautes performances mécaniques, et sont généralement plus résistants en température et aux agents chimiques que les thermoplastiques. En revanche ils ne sont pas recyclables par des méthodes mécaniques (extrusion, moulage par compression, etc.) et restent des défis pour le recyclage chimique (dépolymérisation, solvolyse). Les thermoplastiques, à l'inverse, sont la plupart du temps recyclables par procédés mécaniques lorsque la température dépasse leur température de transition vitreuse (T_g), et dans le cas des semi-cristallins leurs températures de fusion. En revanche, leur résistance aux solvants ainsi que leurs propriétés mécaniques et de tenue en température sont généralement plus limitées, à l'exception toutefois de quelques cas particuliers (aramides, PEK, PEEK, PEEKK…).

La vision binaire historique scindant thermodurcissables et thermoplastiques a commencé à être mise à mal avec l'apparition[1] des réseaux covalents adaptables (CAN). Ce type de matériaux est basé sur un réseau tridimensionnel de liaisons covalentes, à l'instar des thermodurcissables. La différence réside dans la capacité de certaines de ces liaisons à s'échanger d'une séquence du réseau polymère à une autre, lorsque le matériau est chauffé à une température suffisante pour activer cet échange. Cette propriété rend le réseau dynamique par chauffage, et permet de remettre en forme ces matériaux. En

[1] Kloxin, C. J.; Bowman, C. N. Chem. Soc. Rev. 2013, 42 (17), 7161–7173.

particulier, l'équipe de Leibler a théorisé en 2011 le concept de vitrimère,[2] un cas particulier de CAN dans lequel l'échange se fait par un mécanisme associatif. Ce mécanisme confère au matériau des propriétés particulières, en particulier rhéologiques et de résistance aux solvants. Cette découverte, basée sur l'échange de liaisons par transestérification, a suscité l'engouement de la communauté des polymèristes. En effet, ce nouveau type de matériaux polymères permet d'envisager l'utilisation de procédés de mise en œuvre traditionnellement réservés aux thermoplastiques, pour des applications pour lesquelles les thermodurcissables sont préférentiellement utilisés. De plus, les réactions d'échange rendent possible la remise en oeuvre de ces matériaux, et propose une solution au problème du recyclage des thermodurcissables, qui reste limité à l'heure actuelle. Suite à la découverte des vitrimères, d'autres réactions d'échange ont été étudiées pour élargir la gamme des propriétés des vitrimères. Un des objectifs principaux a été de trouver des systèmes qui soient dynamiques sans avoir à recourir à des catalyseurs « externes » (non liés au réseau) au sein du matériau. En effet, les vitrimères de transestérification nécessitent l'emploi de catalyseurs en grande quantité (jusqu'à 10 % molaire) afin d'activer la réaction d'échange et rendre les nœuds de réticulation dynamiques. L'utilisation de catalyseurs externes induit un risque de lixiviation de ces espèces chimiques lorsque le matériau est en usage, et un risque de vieillissement prématuré du matériau au moment de son recyclage mécanique. Outre l'utilisation de réactions d'échange qui ne nécessitent pas de catalyseur, une autre stratégie est d'activer des réactions telles que la transestérification, par des groupements disposés sur la macromolécule. Cette stratégie d'activation est l'objet de la présente étude.

[2] Montarnal, D.; Capelot, M.; Tournilhac, F.; Leibler, L. Science 2011, 334 (6058), 965–968.

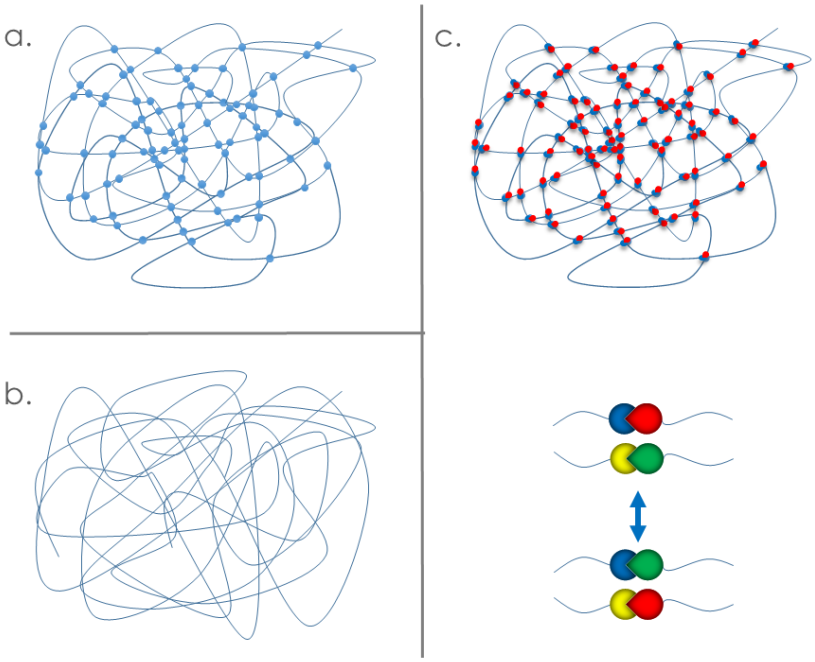

Figure A. Représentation schématique de la structure de (a) réseaux 3D (thermodurcissables), (b) linéaires (thermoplastiques) et (c) CANs avec des nœuds de réticulation échangeables

La transestérification est une réaction de substitution. Elle a lieu par l'attaque d'un groupement hydroxyle nucléophile sur le carbone électrophile du carbonyle de l'ester. Pour activer cette réaction, il est donc possible d'augmenter le caractère nucléophile du groupe hydroxyle, ou d'augmenter le caractère électrophile du carbonyle. C'est cette dernière stratégie qui a été retenue pour ce projet. En particulier, l'objectif est de démontrer la possibilité d'utiliser le fluor comme activateur de transestérification dans des vitrimères polyester. En effet, le fluor, de par sa forte électronégativité, confère aux groupements fluorés des effets inductifs électroattracteur intenses. Ce projet est basé sur le postulat que des atomes de fluor placés à proximité du carbonyle d'un ester vont exercer un effet inductif électroattracteur de manière à diminuer la densité électronique sur le carbone de ce carbonyle, et le rendre plus électrophile (Figure B).

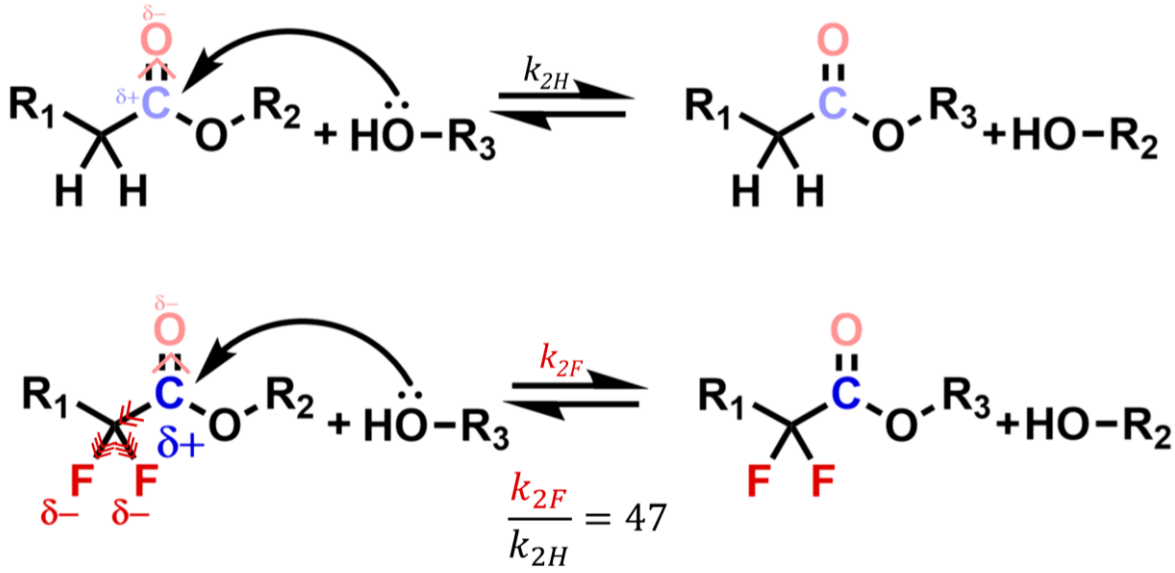

Figure B. Activation de la réaction de transestérification par effet inductif d'atomes de fluor en position α- par rapport au carbonyle de l'ester. L'effet inductif électroattracteur des atomes de fluor augmente le caractère électrophile du carbonyle.

Dans un premier temps, les travaux décrits dans ce manuscrit avaient pour but l'obtention de la preuve de concept à partir d'un premier monomère. Par la suite, des solutions ont été envisagées pour simplifier les synthèses de monomères activés par rapport à la première génération. Enfin, l'utilisation de synthons biosourcés et l'élargissement de la gamme de propriétés des matériaux obtenus ont été étudiés.

Ces travaux ont été menés au sein des départements Chimie et Matériaux Moléculaires (C2M, ex-AM_2N) et Chimie et Matériaux MacroMoléculaires (C3M, ex-IAM) de l'Institut Charles Gerhardt de Montpellier (ICGM) et de l'équipe Physique des Polymères du Centre Interuniversitaire de Recherche et Ingénierie des Matériaux de Toulouse (CIRIMAT). Ils s'inscrivent dans le cadre du projet 16CARN000801 financé par l'institut Carnot Chimie Balard Cirimat.

Dans un premier temps, nous passerons en revue les stratégies d'activation décrites dans la littérature pour les réactions d'échanges employées dans les vitrimères jusqu'à présent. Nous verrons ensuite qu'il est possible d'activer la réaction de transestérification grâce à l'introduction de groupements α,α-difluoroesters afin de synthétiser des vitrimères sans catalyseur. Nous nous attarderons ensuite sur l'étude de la formation de réseaux tridimensionnels à partir de monomères difonctionnels dans ce type de vitrimères. Enfin, nous discuterons de la possibilité d'utiliser des synthons d'origine naturelle pour la synthèse de monomères α,α-difluoro acides carboxylique, et des vitrimères associés.

Ce manuscrit de thèse est essentiellement rédigé sous forme d'une compilation d'articles scientifiques acceptés ou soumis dans des revues internationales à comité de lecture.

CHAPITRE I : ETAT DE L'ART SUR LES REACTIONS D'ECHANGE EMPLOYEES DANS LES VITRIMERES ET LES STRATEGIES POUR LES ACTIVER

Introduction du chapitre I

Les travaux de thèse décrits dans ce manuscrit portent sur des systèmes vitrimère dont le caractère dynamique nécessite habituellement l'emploi de catalyseurs externes. Ces catalyseurs externes sont emprisonnés dans le réseau, mais n'y sont pas liés directement. Ces espèces chimiques peuvent donc migrer vers l'extérieur du polymère. Pour palier ce problème, il est possible d'utiliser des « catalyseurs internes », c'est-à-dire des groupements liés au réseau polymère capables d'activer les fonctions échangeables à proximité. Afin de circonscrire les objectifs du projet, une étude bibliographique a été menée. Elle s'articule autour de deux axes. Le premier consiste en un inventaire des réactions d'échange décrites dans la littérature afin de synthétiser des matériaux vitrimères. Un intérêt particulier a été apporté aux mécanismes d'échanges mis en jeu, connus ou postulés, pour mieux comprendre les leviers existants afin d'activer les échanges dans chaque cas. La nature du mécanisme d'échange, associatif ou dissociatif, a également une influence primordiale sur les propriétés rhéologiques des matériaux obtenus, ce qui a également été développé dans ce chapitre. Le second axe est consacré aux outils déjà décrits pour activer les différentes réactions détaillées auparavant. En particulier, un inventaire des groupements activant les échanges lorsqu'ils sont à proximité a été réalisé. Certains de ces groupements ont été décrits dans des vitrimères et leur influence sur les propriétés dynamiques des matériaux a été étudiée. Cependant, beaucoup de ces groupements ont été utilisés dans d'autres domaines de la chimie, organique notamment, et souvent en solution. L'inventaire de ces groupements a donc pour but de mettre en lumière des possibilités encore inexploitées pour activer les échanges, et potentiellement les mettre à profit dans de futures études dans le domaine des vitrimères.

Au-delà du simple inventaire des groupements activateurs, cette étude a permis de comprendre par quels mécanismes ces groupes activent les échanges (effets inductifs, assistance anchimérique, effets stériques, cyclisation pour stabiliser l'intermédiaire réactionnel, etc.).

Cette étude a permis la publication d'un article de perspective[3] dans le journal *Macromolecules* en mars 2021, qui constitue ce chapitre (Figure C).

[3] Cuminet, F.; Caillol, S.; Dantras, É.; Leclerc, É.; Ladmiral, V. Macromolecules 2021, 54 (9), 3927–3961.

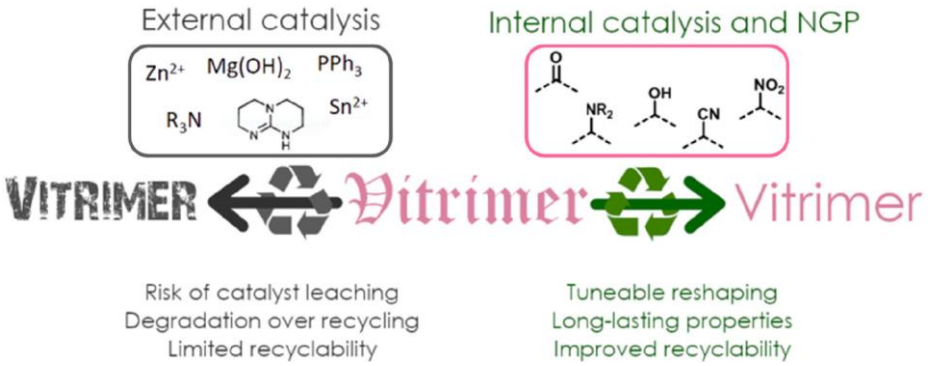

Figure C. Activation of bond exchanges in vitrimers by external catalysis or internal catalysis and neighboring group participation

Neighboring Group Participation and Internal Catalysis Effects on Exchangeable Covalent Bonds: Application to the Thriving Field of Vitrimer Chemistry

Florian Cuminet,[a,b] Sylvain Caillol,[a] Éric Dantras,[b] Éric Leclerc[a] and Vincent Ladmiral[a]

[a]ICGM, Univ Montpellier, CNRS, ENSCM, Montpellier, France
[b]CIRIMAT Physique des Polymères, Université de Toulouse, CNRS, Université Toulouse 3 - Paul Sabatier, 31062 Toulouse, France

1. Abstract

Vitrimers constitute a fascinating class of polymer materials that make the link between the historically opposed 3D networks (thermosets) and linear polymers (thermoplastics). Their chemical resistance, reshaping ability, and unique rheological behavior upon heating make them promising for future applications in industry. However, many vitrimers require the use of high catalyst loadings, which raises concerns for their durability and limits their potential applications. To cope with this issue, internal catalysis and neighboring group participation (NGP) can be used to enhance the reshaping ability of such materials. A few studies report the effect of activating groups on the exchange reactions in vitrimers. Nevertheless, knowledge on this topic remains scarce, although research on vitrimers would greatly benefit from NGP already known in organic chemistry. The present Perspective presents the different types of exchangeable bonds implemented in vitrimers and discusses chemical groups known to have or potentially capable of an enhancing effect on exchange reactions. This analysis is underpinned by a thorough mechanistic discussion of the various exchangeable bonds presented.

1. Introduction

Since the team of L. Leibler discovered and described the first vitrimer in 2011,[1] these materials have attracted tremendous attention in the polymer and materials communities. This enthusiasm is not surprising given the amazing properties of these materials. Nevertheless, though the definition of this concept seems easy to handle at first glance, caution should be taken when classifying new materials as vitrimers. To understand well what a vitrimer is, the usual classification of polymer materials must be clearly recalled. Historically, polymers have been categorized in two main classes: thermoplastics and thermosets. Thermoplastics consist of entangled linear polymer chains that are free one from another. In contrast, in thermosets, polymer chains are linked by covalent bonds that cannot be cleaved without destroying the network.[2] This difference at the molecular scale has consequences on

the macroscopical behavior of these materials. Most thermoplastics are soluble provided that a convenient solvent is used (or exists). In thermosets the solvent is not able to set the chains apart, and the material does not dissolve. Besides this different behavior toward solvents, the other main difference lies in the thermal behavior of these materials. In most cases when thermoplastics are heated, the relative movement of the chains becomes easier. Macroscopically this phenomenon is visible when the material flows.[2] Thermosets cannot flow when heated.[2,3] Reversible reactions involving covalent bonds have been known for many decades, and their possible use in polymers had already been inferred in the 1960s.[4,5] The concept of reversible covalent bonds implemented in polymers led to a new class of materials called CANs, short for covalent adaptable networks. In CANs, polymer chains are covalently cross-linked as in thermosets, but these cross-linking bonds are reversibly cleavable, which leads to properties such as malleability in response to an external stimulus such as temperature or light irradiation.[6] The most iconic reversible reaction used in such materials is probably the Diels−Alder reaction.[7−13] This reaction is reversible upon heating. When this reaction is used to make cross-linked materials, the crosslinking bonds can break upon heating and re-form at lower temperature, thus leading to reshapability (Figure 1C).[6]

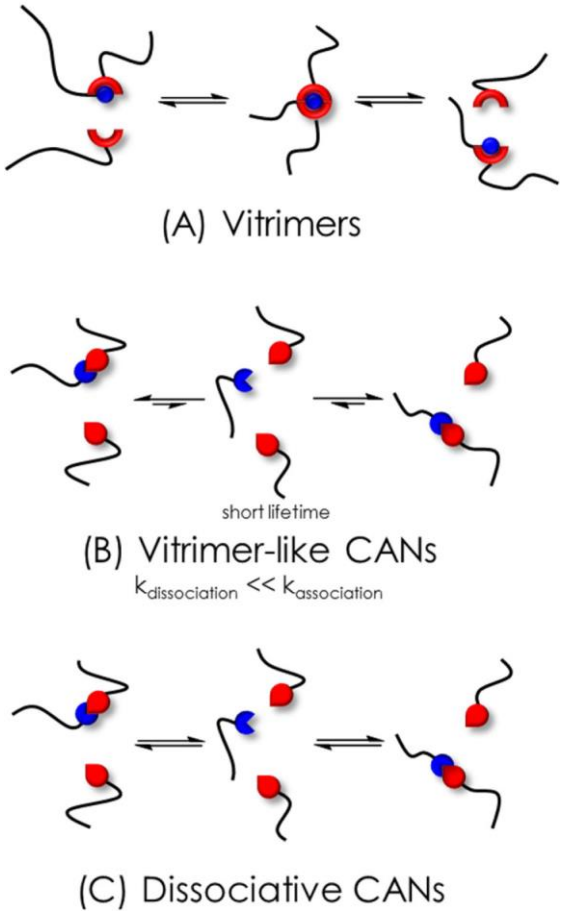

Figure 1. Schematic representations of the mechanisms at work in (A) associative CANs (vitrimers), (B) vitrimer-like dissociative CANs, and (C) dissociative CANs. Vitrimer-like dissociative CANs (B) exhibit a constant Keq over the vitrimer-like temperature regime and a short lifetime of the dissociated state.

Most CANs designed before the year 2010 were based on the dissociative mechanism whereby a bond has to be cleaved before another bond is formed between the dissociated moieties. In 2005, Bowman et al. reported the first CAN based on an associative exchange reaction.[14] Allyl sulfides were used as addition−fragmentation chain transfer agents. The exchange proceeded via a photoinduced radical mechanism allowing constant cross-linking density and network connectivity even though the topology changed.[14] Later, in 2011, Leibler et al.[1] described the first thermally triggered associative CAN, based on transesterification as the exchange reaction. This material exhibited a novel rheological behavior with its viscosity decreasing linearly with increasing temperature. Because this behavior is common in inorganic materials and especially strong glass, this new kind of polymer was coined "vitrimer". On the one hand, vitrimers are often insoluble like thermosets, except for specific cases such as very fast vitrimers for instance.[15,16] On the other hand, they can be reshaped and recycled by heating without precise control over temperature, like glass. Their singular rheological behavior was attributed to the associative mechanism of the bond exchange. In contrast to the majority of dissociative CANs, because vitrimers keep a constant connectivity regardless of the temperature (even the reshaping temperatures), their viscosity only depends on the rate of the exchange reaction. Therefore, the

viscosity and stress−relaxation profiles as a function of temperature follow the Arrhenius law. These behaviors are often considered specific to vitrimers,[1,17−19] although this point has recently been questioned and is debatable. Two visions of what a vitrimer is coexist, depending on whether the chemist's or the physicist's point of view is adopted. The chemist's definition focuses on the exchange mechanism. In consequence, only a CAN based on an associative mechanism is a vitrimer (Figure 1A). In contrast, the physicist defines a vitrimer according to the physical properties. For example, Drockenmuller et al.[20] described a material based on a dissociative mechanism that exhibits an Arrhenius viscosity dependence with temperature. Such materials were designated as "vitrimer-like".[21] The hypothesis to explain such vitrimer-like behavior in dissociative CANs lies in the thermodynamic and kinetic of the exchanges. When the equilibrium constant of dissociative bonds is displaced toward the associated state, though the dissociation−association happens, the overall number of bonds and cross-link density is barely reduced. Kinetically, this happens when the association reaction is much faster than the dissociation reaction. The dissociated state is thus transitory, globally the number of bonds hardly changes, and the network integrity remains virtually unchanged (Figure 1B).[22,23] The Arrhenian rheological behavior can also be observed in a range of temperatures over which the equilibrium constant does not vary much. For instance, Konkolewicz et al. made vitrimer-like dissociative CANs out of anilinium salts. They reported for the adduct formation a ΔH value of −2.8 ± 0.2 kJ mol^{-1} and compared it with the case of Diels−Alder adduct formation with a ΔH value of −157 ± 14 kJ mol^{-1}.[21] Because ΔH is very low for their system, the dependence of Keq with temperature is considered negligible. In this case, the ratio of dissociated and associated bonds over this temperature range is constant (Figure 1B), and the network connectivity does not change.[21,24] With the increasing number of chemical platforms able to undergo exchange discovered, some particular cases of dissociative CANs somewhat blur the boundary with vitrimers.[20,21,25,26] In addition, networks featuring both permanent and exchangeable cross-links are reported to exhibit vitrimer-like stress−relaxation, but within a certain limit as the permanent cross-links induced a residual stress plateau.[27] Such borderline materials indicate that the definition of a vitrimer still remains debatable, depending on the viewpoint adopted. Vitrimers address the problem of thermoset recyclability and thermoplastic vulnerability toward solvents. Therefore, the interest for these materials is growing in industry, as highlighted in recent reviews.[22,28,29] Nonetheless, some characteristics may limit their industrialization. They often display high relaxation times and high viscosity during reprocessing, making them unsuitable for the recycling processes usually found for thermoplastics in industry. Furthermore, most vitrimers rely on catalysts and in some cases on high catalyst loadings.[1] The use of catalysts may generate problems such as limited number of recycling/reshaping cycles due to premature degradation or migration and loss of the catalyst.[30−32] A solution to this issue is the design of vitrimers that do not rely on catalysis. This can be done by using a large excess of exchanging functional

groups[32–34] or by using exchange reactions that do not require any catalyst.[18,35–42] Another strategy, inspired by organic chemistry in solutions, relies on chemical functions near the exchangeable bond to enhance the reaction rate. This effect is called either neighboring group participation (NGP) when the accelerating substituents are at some point covalently bonded to the reaction center during the exchange or internal catalysis for effects at longer distance such as electrostatic interactions, steric effects, or weak bonds.[43] Guan et al.[44] implemented this strategy in boronic ester CANs and enhanced the transesterification rate thanks to neighboring tertiary amines. This effect was later implemented in other kinds of vitrimers featuring ester or silyl ether exchangeable bonds, for instance.[38,45] In their review, Guerre et al.[43] highlighted the few examples of internal catalysis in vitrimers reported so far and the strong potential of this strategy to tune the properties of vitrimers. More recently, Van Lijsebetten et al.[46] also emphasized the power of NGP in dynamic covalent chemistry, especially in polymeric materials, in a very clear and useful tutorial review. To proceed further with this concept, a general outline of the activating groups potentially beneficial to vitrimers would give useful insight for further research on this fast rising topic. Nevertheless, caution should be taken when using NGP as this strategy can sometimes drastically modify the exchange mechanism.[24,43] For instance, transesterification, which usually proceeds via an associative exchange, was reported to follow a dissociative pathway in the presence of specific activating groups.[47,48] Activating groups are a very powerful yet complex tool. Because the case of vitrimer-like dissociative CANs is still debated in the vitrimer community, this Perspective focuses on internal catalysis and NGP in associative exchange reactions, to follow the strict definition of vitrimers. The first part is dedicated to the description of the associative exchange reactions implemented in vitrimers, their mechanisms, and some of the pitfalls a vitrimer scientist should be aware of (Figure 2). Then, in light of this mechanistic discussion, the activating groups potentially useful to tune the properties of vitrimers are briefly presented and discussed. Insights into the activating groups proven to be beneficial on small molecules but not yet implemented in vitrimers are also given. For each kind of exchangeable bond the influence on the kinetics of exchange reactions is discussed as well.

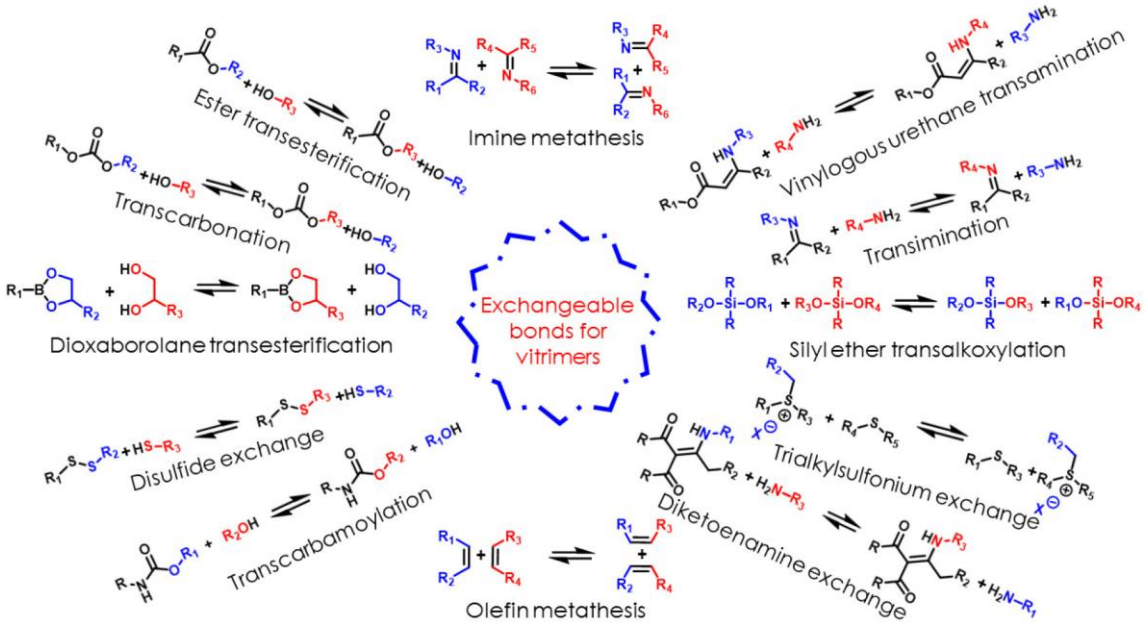

Figure 2. Associative exchangeable bonds for vitrimers' design.

2. Exchangeable Bonds with an Associative Mechanism

Esters.

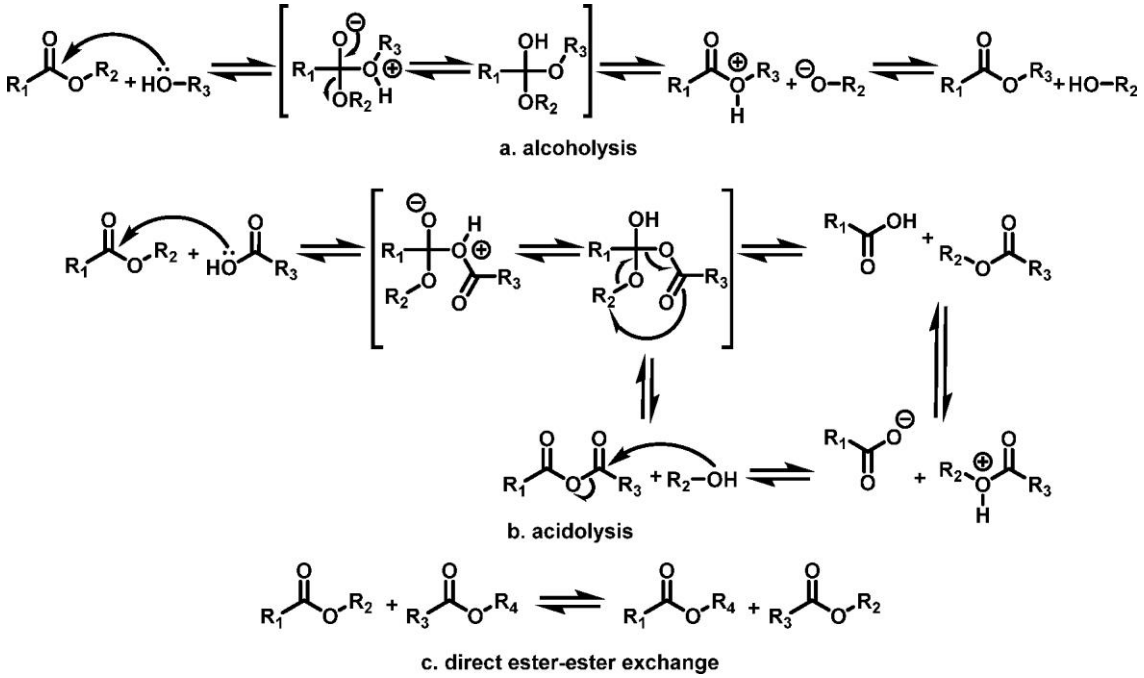

Scheme 1. Ester Exchange Mechanisms: (a) Alcoholysis, (b) Acidolysis, and (c) Direct Ester–Ester Exchange

Esters are probably one of the oldest known exchangeable bonds, as Friedel and Craft, famous for the eponymous reaction, also discovered in 1865 the exchange reaction occurring between two ester groups.[49] Several terms such as ester exchange, ester–ester interchange, interesterification or the

nowadays most commonly used transesterification are considered as synonymous, though they actually encompass several reactions.[50] Actually, three reactions are reported to happen in what is commonly considered as the transesterification equilibrium,[51] namely, alcoholysis, acidolysis, and the genuine transesterification.[49,52–54] Alcoholysis is the main reaction[55] although the direct ester–ester exchange prevails for esters synthesized from aromatic acids over 300 °C.[56] The alcoholysis mechanism proceeds by the attack of the alcohol onto the carbon of the carboxylate. A tetrahedral intermediate is thus formed prior to the elimination of an alkoxy group, leading either to the starting ester or to the exchanged one (Scheme 1a). The mechanism of acidolysis is similar: the nucleophilic oxygen of the acid attacks the electrophilic carbon of the carbonyl moiety of the ester and forms a tetrahedral intermediate, prior to the elimination of the attacking acid, or the exchanged one. Elimination of the alkoxy group on the intermediate can also occur. This produces an anhydride intermediate which reacts immediately with the released alcohol (Scheme 1b).[53,57] The third mechanism is less usual and is described as a concerted interchange (Scheme 1c). This reaction was reported experimentally thanks to kinetics experiment at temperatures over 300 °C.[56] Kotliar et al. pointed out that the enthalpy change during this reaction is near zero, suggesting an associative pathway.[53] Anyway, these three mechanisms are associative. Catalysis does not seem to change this feature as acid-catalyzed transesterification is reported to proceed through an addition/elimination mechanism.[58] Additionally, base catalysis only changes the nucleophile from an alcohol to its more reactive alkoxide counterpart.[59] Transesterification was studied in polymers in the second half of the 20th century, as the exchange reaction is more significant in bulk materials;[49,52,55,60] then this reaction regained popularity among scientists with the development of biodiesel and biofuels. Recently, the interest in biomass valorization and greener fuels has grown, and catalysts such as N-heterocyclic carbenes,[61] calcium oxide,[62] ZrO_2/SO_4,[59] silicates and clays,[63,64] or aluminum chloride[65] were (re)- discovered. Metal-based catalysis (such as Sn, Ti, or Mg[51,54] for instance) draws particular attention as zinc-based catalysts were recently used in the first reported vitrimer.[1] The mechanism involves a Zn^{2+} species, which coordinates to the ester carbonyl group and activates it with respect to the nucleophilic attack of the alcohol or alkoxide and then proceeds via the pathway previously described.[66] In summary, all the catalytic mechanisms encountered so far were associative.

Carbonates.

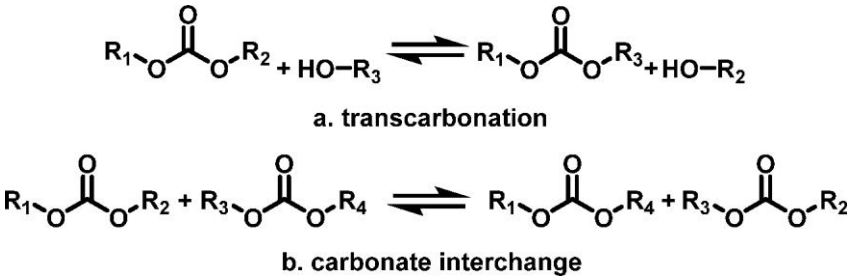

Scheme 2. Exchange Reactions on Carbonates (a) Transcarbonation and (b) Carbonate Interchange

Owing to their structural similarity, carbonates and esters are often compared, and their chemistries are considered very close. As in the case of esters, several names are used for the exchange reactions of carbonate. The exchange between an alcohol and a carbonate is called transcarbonation, carbonate transesterification, or carbonate alcoholysis when the exchange occurs on polycarbonate chains and small alcohols (Scheme 2a). Carbonate interchange refers to the exchange between two carbonates (Scheme 2b). The interest for transcarbonation rose when scientists aimed at synthesizing polycarbonate materials without the use of highly toxic phosgene.[67] The exchange between diphenyl carbonate and bisphenol A was used as a safer pathway to produce polycarbonates. The mechanism involved was similar to ester transesterification[68] and was proven quite recently. In the absence of catalyst, there is a prototropy between the phenol and the carbonate. The deprotonated counterpart (phenolate) is the reactive species toward the electrophilic carbon of the carbonate carbonyl moiety. The reaction proceeds through a tetrahedral intermediate before the elimination of a phenolate (from the starting carbonate or from the reactant).[69,70] However, this exchange is very slow.[67] Transcarbonation is known to be catalyzed by metal-derived catalysts such as tin salts,[71–73] zinc acetate,[74] copper salts,[72] and even a dimetallic iron−manganese cyanide catalyst.[75] Bases are also common catalysts, for instance, magnesium hydroxide,[76] calcium salts,[77,78] or sodium alkoxides.[74,79] All the catalyzed mechanisms described are associative,[69,71,74,76–80] though they are slightly different depending on the type of catalysis employed (Scheme 3). When a base catalyst is used, the carbonate and the alcohol moiety form a prereaction complex (CX1). Then the reaction proceeds via a tetrahedral transition state (TTS) yielding a postreaction complex (CX2) and ultimately the free exchanged species (Scheme 3b).[74] The overall reaction follows an "addition−elimination" mechanism. When a Lewis acid catalyst is employed, such as zinc acetate, a cyclic transition state involving a ternary complex between the carbonate, the alcohol, and the catalyst is formed. Then, the reaction proceeds through a concerted mechanism to generate a postreaction complex, following an addition−elimination mechanism.[74] Direct ester−carbonate interchange has also been reported[81] and described as following an associative pathway as well.

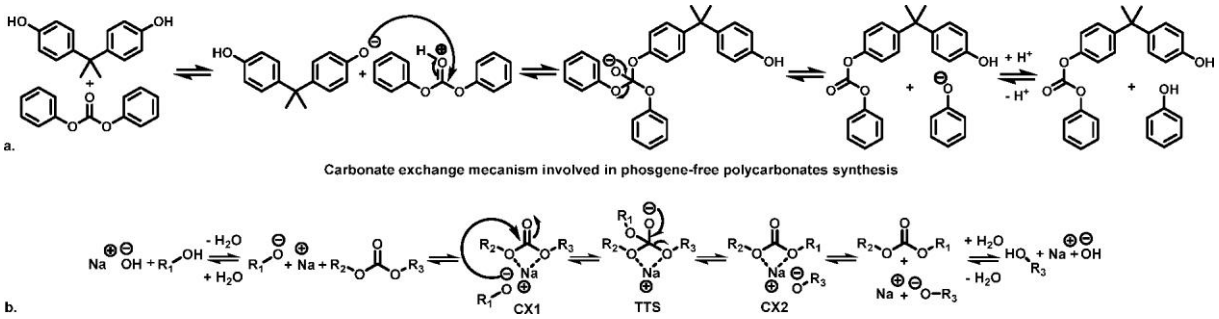

Scheme 3. (a) Transcarbonation Pathway and (b) Catalytic Effect by Bases and Metal Ions

Boronic Esters.

Cyclic boronic esters, also known as dioxaborolanes, are synthesized by condensation of boronic acids with 1,2- and 1,3-diols leading to 5- and 6-membered rings, respectively.[82–84] Boronic acids are used in a wide range of reactions in organic chemistry, as catalysts, pronucleophiles (cross-coupling reactions), or reaction intermediates.[82,85] In carbohydrate chemistry, they are also useful as protective groups for diols and diamines.[82,85,86] Besides, their ability to bond with diols makes boronic esters particularly useful in biology, biochemistry, or chromatography for sugars and diol bearing compounds purification or carbohydrate sensors, for example.[85,87–89] In medicine they are also proposed for drug delivery[90–92] and glucose sensing for diagnostic purposes.[93,94] The key feature of boronic esters is their reversible formation from diols and boronic acids, resulting in dynamic systems with tunable properties. In biological media, this reactivity results in a dissociative mechanism, as boronic esters in aqueous conditions are prone to hydrolysis yielding boronic acids.[95,96] The equilibrium between dissociated boronic acid−diol and associated boronic ester (Scheme 4) was exploited to prepare covalently cross-linked self-healing hydrogels, for example.[97–99]

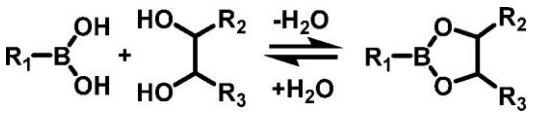

Scheme 4. Equilibrium between Boronic Acid and 1,2-Diol

Over the past few years, growing interest for this functionality has spread in the polymer science community, in particular for the preparation of self-healing polymers.[100,101] Interestingly, Sumerlin et al.[101] showed that two different mechanisms are involved in the exchange reactions occurring in boronic ester-based cross-linked materials. The exchange occurs either via classical boronic ester dissociation and reesterification or via an associative mechanism similar to transesterification, provided that free diol functions are available in the material. As the dissociative mechanism requires water to cleave the boronic ester, it is assumed that in a completely dry environment only the associative transesterification mechanism occurs.[85,102] Guan et al. implemented this associative mechanism in the first boronic ester cross-linked vitrimers.[44] Eventually, Nicolaÿ and Leibler et al.[103]

reported a vitrimer based on a third kind of exchange reaction, namely, the direct metathesis between two boronic ester moieties. Although the exact mechanism of this reaction remains uncertain, the hypothesized transition states and intermediates are expected to have a higher connectivity,[104] as expected for an associative mechanism. Raynaud et al. investigated the mechanism at work in dynamic polymer networks based on pinacol boronates. The experimental and theoretical results corroborate the hypothesis of an associative mechanism as suggested and that the reaction is triggered by adventitious traces of nucleophiles trapped in the medium.[105] Nevertheless, mechanistic studies would be very useful to confirm the associative pathways of boronic ester exchange reactions in anhydrous conditions and to acquire the knowledge required to harness this type of exchange reaction more efficiently.

Sulfur-Containing Bonds.

Disulfides.

For a long time, disulfide bonds have been known to feature an interesting reversible behavior. Historically, this behavior has been used in personal care products. Disulfide bonds naturally occurring in keratin were cleaved by a reducing agent before new bonds were generated by using an oxidant to perform so-called "permanent wave" on hair.[106] This process can be considered as an early chemically reshapable material and was implemented after several decades in reversibly cross-linked polymers.[107,108] Disulfide bonds are also involved in the rubber vulcanization process. Hence, in 1946, Stern and Tobolsky already discussed possible mechanisms for the reshuffling of these bonds to explain stress−relaxation in these materials.[109] The mechanism remained uncertain but usually admitted to be associative.[104] Two possible mechanisms have been discussed: (1) a [2 + 2] metathesis mechanism and (2) a radical mediated [2 + 1] mechanism, where a S−S bond would be homolytically cleaved prior to a radical attack of another S−S bond to yield a three-membered intermediate (Scheme 5).

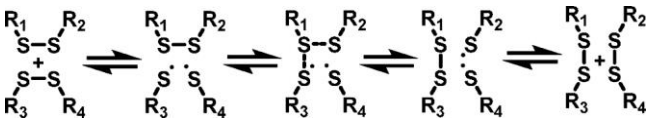

Scheme 5. Disulfide Exchange [2 + 1] Radical Mechanism

To elucidate which mechanism was involved, in silico studies were carried out and concluded that the radical mechanism was more likely to occur.[110−112] This conclusion was verified experimentally by model exchange reactions in the presence of radical traps or radical sources.[113] However, when a nucleophilic catalyst is used, two mechanisms occur simultaneously: the radical mechanism described previously and a thiol-mediated exchange due to the formation of thiolate anions. Moreover, UV light can advantageously activate disulfide metathesis. Thus, materials exhibiting self-healing behavior

upon 5 min exposure to 320−390 nm UV light were synthesized.[114] Although this reaction is convenient to yield self-healing materials,[114−116] its dissociative mechanism may not be suitable to obtain vitrimer properties. Additionally, disulfide metathesis is not always the only mechanism involved. Hence, depending on the synthetic pathways for disulfide-containing polymers and on the stoichiometry chosen, dangling thiol moieties enable thiol/disulfide exchanges. For this reaction the exchange proceeds through an associative mechanism, whereby a disulfide bond is attacked by a thiolate, yielding a new disulfide bond through a three membered transition state (Scheme 6).[111,117] Thus, attention should be paid to stoichiometry when designing a disulfide containing vitrimer or self-healing material.

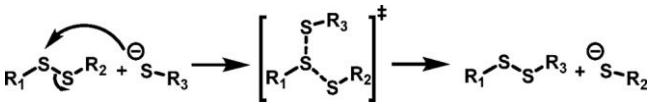

Scheme 6. Thiol−Disulfide Exchange Mechanism

Thioesters.

Recently, Bowman et al. reported thioester dynamic networks.[118] Without neighboring groups the exchange takes place via a purely associative pathway. Nevertheless, when NGP were present, two competitive mechanisms were discussed: a mechanism involving an equilibrium between the associated thioester form and the dissociated thiol/anhydride form and the associative transthioesterification mechanism requiring free thiol moieties.

Meldrum's Acids.

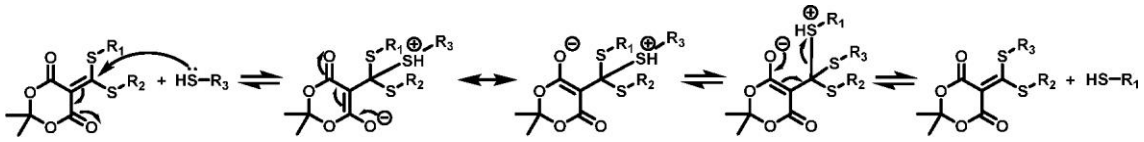

Scheme 7. Mechanism of Meldrum's Acid Exchange with a Thiol as an Example

Sulfur-bearing Meldrum's acids were also described as exchangeable cross-linkers in PDMS vitrimers through an associative mechanism involving thiol moieties (Scheme 7).[119]

Trialkylsulfonium Salts.

In the 1970s, a group at Ghent got interested in poly(propylene sulfide) and the mechanism of its degradation upon incorporation of oxonium salts to introduce sulfonium groups in the material. They reported an exchange reaction between thioethers and trialkylsulfonium likely proceeding through an associative mechanism whereby the sulfur atom of the thioether attacks the α-carbon atom of a sulfonium salt prior to the elimination of the exchanged thioether following an associative pathway (Scheme 8).[120−123]

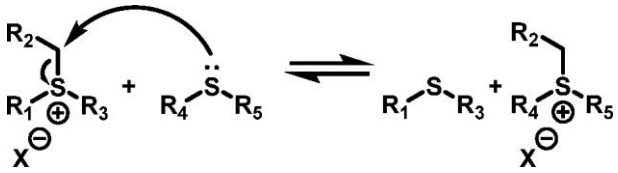

Scheme 8. Proposed Mechanism for Thioether–Sulfonium

The fact that sulfides react with electrophiles (brosylates for instance) and the positively charged sulfonium is a good leaving group comfort the hypothesis of a S_N2 mechanism, while a S_N1 is unlikely considering this pathway would involve a highly unstable primary carbocation. Four decades later, the group of Du Prez studied and updated this forgotten chemistry and implemented it in polythioether networks to prepare catalyst-free vitrimers.[40] Knowledge on this bond exchange chemistry remains scarce, but the promising opportunities offered in rubber recycling[124] might favor more in-depth studies.

Silyl Ether Transalkoxylation and Metathesis.

Silicones represent an $11 billion industry, and production of formulated silicones exceeded 2 Mt in 2013.[125] Silicones are made from silicon, which is also the main component of glass. In the 1950s, polydimethylsiloxanes (PDMS) were reported to exhibit stress−relaxation behavior thanks to a chemical phenomenon of chain exchange, catalyzed by either an acid or a base.[126,127] The acid-catalyzed mechanism was supposed to involve a protonated oxygen atom on the Si−O−Si bond as an intermediate,[127] but this mechanism still seems unclear. The base-catalyzed mechanism was supposed to involve the attack of the basic species onto a silicon atom, consequently cleaving a Si−O−Si bond and yielding an anionic −O−Si group.[127] However, the mechanism leading to the exchange between two polymer chains was not fully elucidated. Surprisingly, the self-healing properties of these materials were somehow forgotten, except for a patent reporting thermally reversible silicone rubbers catalyzed by strong acids, becoming malleable at 150 °C but remaining insoluble and dimensionally stable at room temperature.[128] The self-healing behavior of polysiloxanes was rediscovered in 2012 by McCarthy et al.[129] after the concept of vitrimer was first defined. They studied tetramethylammonium dimethylsilanolate-terminated polysiloxane chains and emphasized that any cross-linked PDMS elastomer could be converted into a self-healable polymer by addition of basic catalysts. The mechanism involved is an associative transsiloxanation. The first step of this mechanism would be the dissociation of the chain-end silanolate−counterion ion pair followed by the attack of the silanolate anion onto a silicon atom and simultaneous cleavage of a Si−O bond (Scheme 9).[130,131] Thus, the ion pair would behave as a dormant species and the silanolate anion as the active one, enabling chain exchange.

Scheme 9. Trans-Siloxanation Mechanism[130]

Other strong bases can be used to generate living chain ends such as the most effective potassium hydroxide and cesium hydroxide, but a major flaw at high temperature is the formation of volatile cyclic oligomers leading to decreases of connectivity and average molar mass.[131] In 2017, Guan et al. used a silyl ether as the exchangeable moiety in cross-linkers to make polystyrene networks, where the exchange reaction involved free hydroxyl groups without ion pairs.[45] Finally, the same group reported an exchange reaction in the absence of free hydroxyl moieties and hypothesized a direct silyl ether metathesis mechanism catalyzed by acids, but the mechanism still remains unclear and further investigations are needed to fully understand the behavior of this material.[132]

Urethanes, Ureas, Thiourethanes, and Hydroxyurethanes.

Polyurethanes (PU) are the fifth largest production of industrial polymers with a global production reaching 20 Mt/y.[133] The urethane bond, alternatively called carbamate, is usually obtained by reaction between an isocyanate and an alcohol and has been known to be reversible at high temperatures for a long time. Ureas are obtained by reaction between isocyanate and amine, and the direct condensation of ureas leads to biuret functions. In the 1950s, PU materials were shown to exhibit stress−relaxation thanks to urethane cleavage.[134] Furthermore, relaxation times were shorter when the material included ureas and biuret bonds,[135] highlighting the increased reactivity of nitrogen in exchange reactions. Catalyst-free vitrimers based on exchangeable urea bonds were also made thanks to bulky groups, which enhances their reactivity toward urea−urea exchange without the need of any catalyst.[136] Nevertheless, the mechanism involved in this process is uncertain. In the early studies on urethane cleavage, the mechanism was suggested to be dissociative, involving the dissociation of the urethane to its initial isocyanate and alcohol moieties,[137] as no free hydroxyl groups was available for transurethanization reaction.[138,139] Even when a free alcohol is available next to a urethane bond, the dissociative pathway occurs most of the time, in some cases along with an associative pathway similar to transesterification (Scheme 1), depending on the system composition and temperature. A low temperature favors the associative mechanism, and reversely, high temperatures favor the dissociative one.[137] In solution, external catalysts such as phosphoryl chloride were shown to favor the associative mechanism between a urethane and a phenol over the dissociative one (Scheme 10).[140] The direct exchange between two urethane moieties via an associative mechanism has been ruled out.[139]

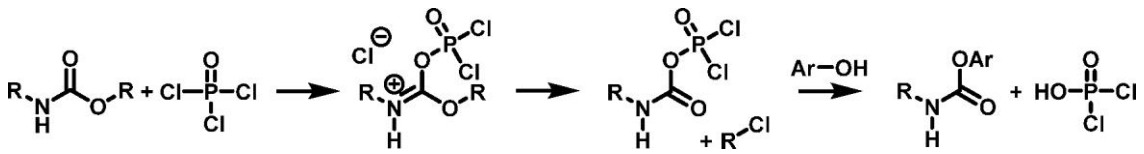

Scheme 10. Phosphoryl Chloride as a Catalyst Favors the Associative Mechanism of Transcarbamoylation with Phenols[140]

Ureas seem to be promising bonds to implement in selfhealing materials as the exchange reaction is much faster.[135] However, the exchange mechanism is similar, with first a dissociation (which rate depends on the steric hindrance of the amine) yielding the starting isocyanate and amine.[141–143] Thus, based on their apparent dissociative mechanism, polyurethanes and polyureas do not seem to be suitable to obtain vitrimer properties. Recently, polythiourethanes (PTU) started to be investigated to make self-healing materials. PTU vitrimers catalyzed by dibutyltin dilaurate were synthesized by reaction of a trithiol with different diisocyanates: isophorone diisocyanate, 1,6- diisocyanatohexane, or tolylene-2,6-diisocyanate. In these materials, the structure of the isocyanate precursor influenced the relaxation time. Aliphatic isocyanate-derived networks displayed much higher relaxation times at 180 °C than their aromatic analogues. The relaxation times of the isophorone diisocyanate- or 1,6-diisocyanatohexane-derived network were 11.1 and 10.7 min, respectively, whereas it was only 2.9 min for the aromatic tolylene-2,6-diisocyanate-based material. Both associative and dissociative exchange mechanisms were reported to be involved in their reprocessability (Scheme 11).[144,145]

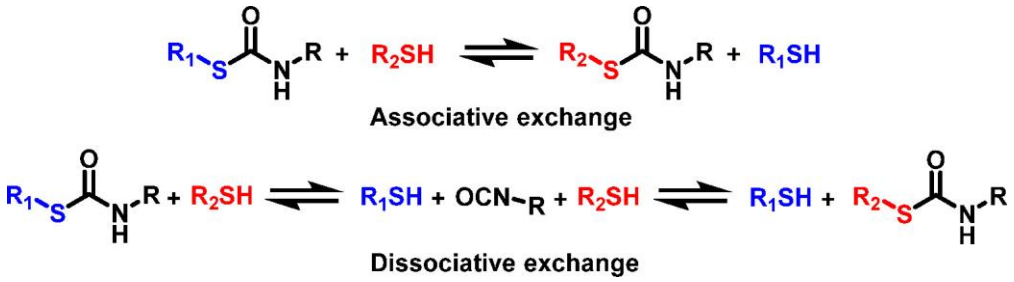

Scheme 11. Associative and Dissociative Exchange Pathways for Polythiourethanes[144,145]

Compared to traditional PU, the case of polyhydroxyurethanes (PHU) prepared from cyclic carbonates and amines may be different. PHU contain hydroxyurethane bonds, which are carbamate bonds with a hydroxyl group at the β-position (Scheme 12) or γ-position. The synthesis of these materials is advantageously greener compared to PU, as it does not involve the use of isocyanates which are toxic substances.

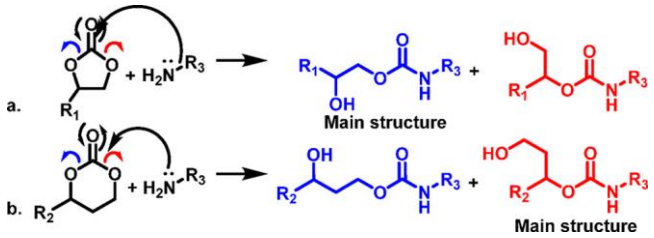

Scheme 12. Synthesis of Polyhydroxyurethanes (PHU) from (a) Five- and (b) Six-Membered Cyclocarbonates Featuring a Substituent at the β-Position

Fortman et al. studied PHU vitrimers and suggested that transcarbamoylation occurred, albeit slowly, and that decomposition and side reactions occurred more easily at high temperatures.[146] In particular, side reactions were observed at 160 °C and over, whereas the decomposition of the urethane linkage to an isocyanate and an alcohol usually occurs over 250 °C. These observations were highly dependent on the type of PHU: five-membered cyclocarbonate-derived PHU (5-CC PHU, Scheme 12a) were more prone to decomposition via dissociative reactions at 180 °C. 5-CC PHU were shown to decompose back to their 5CC amine precursors (Scheme 13a). Several decomposition reactions were hypothesized: reaction of amine with cyclic carbonates by the irreversible decarboxylative mechanism (Scheme 13b), addition of amines to carbamates to form ureas (Scheme 13c), decarboxylative reaction of free hydroxyl groups with cyclic carbonate to form ethers (Scheme 13d) or carbonates (Scheme 13e), and oxazolidone formation, to name a few. These irreversible reactions are responsible for the loss of mechanical properties of the reprocessed materials. On the contrary, the dissociative reversion reaction leading to the starting amine and cyclocarbonate was not observed for 6-CC PHU (Scheme 12b), thus limiting the decomposition reactions. This suggests that the associative transcarbamoylation may be responsible for the stress−relaxation behavior observed for these 6-CC PHU materials.[139,147]

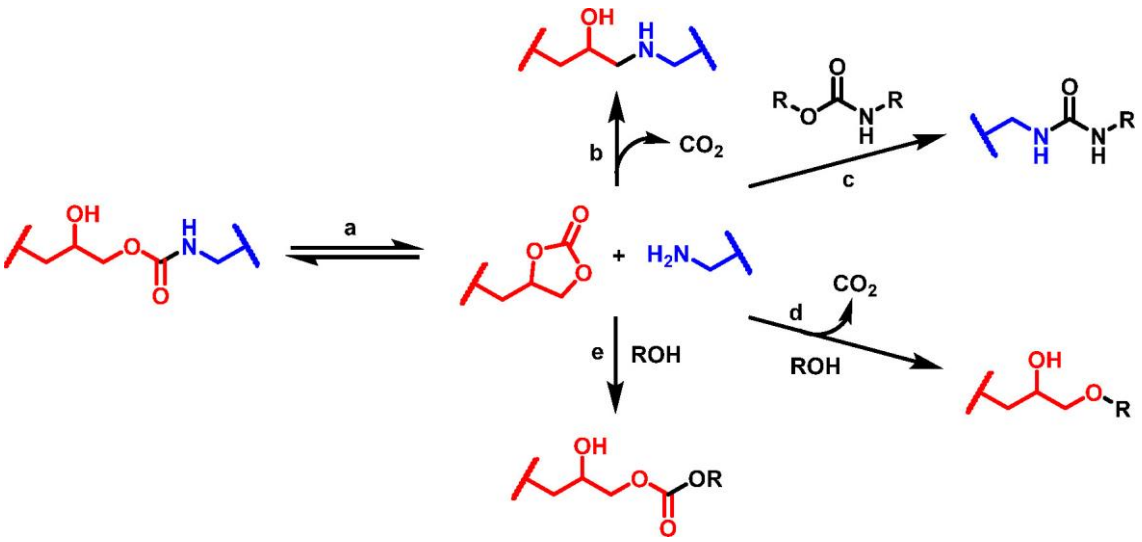

Scheme 13. (a) Reversion of 5-CC PHU to the Original 5-CC and Amine and Hypothesized Decomposition Reactions (b) by Decarboxylation, (c) by Formation of Urea, (d) by Formation of Ether, and (e) by Formation of Carbonate[147]

Chen et al. also pointed out that two simultaneous mechanisms were responsible for the network rearrangement of their 5-CC PHU, the associative transcarbamoylation and the dissociative reversible cyclocarbonate aminolysis, yielding back the initial cyclocarbonate and amine.[148] Because two main reactions seem to be accountable for the stress−relaxation behavior of PHU and PTU and because one is associative whereas the other is dissociative, one can rule out this chemistry for associative CANs. However, more research could be done to favor the associative mechanism over the dissociative one, investigating the effects of catalysts, the network morphology, or the monomer structure, for example.

Olefin Metathesis.

In the early days of petrochemistry, investigations led on propane cracking revealed that cracking of propylene at 752 °C under 0.2 atm yielded 23−24 mol % of butylene and ethylene.[149] The overall reaction equation is similar to a metathesis. However, this reaction is inexploitable under such conditions that do not allow any control. Olefin metathesis was then developed in the 1960s by chemists working for DuPont and has been extensively studied for both industrial production and research purposes.[150−152] Olefin metathesis requires metal catalysts to occur quantitatively. An in-depth discussion on these catalysts is out of the scope of this article, but a rich literature and very relevant books are available.[150,152] At first glance, the overall reaction seems to be rather simple and can be summarized as a carbene exchange between two olefins. Nevertheless, the underlying mechanism involved is complex. Yves Chauvin, Richard Schrock, and Robert Grubbs were awarded the Nobel Prize in Chemistry in 2005 for elucidating this mechanism, developing the first catalysts, and synthesizing more convenient catalysts, respectively.[153−155] Their studies deepened the knowledge of this exchange reaction, which was useful to develop new catalysts. Indeed this reaction fully relies on metal−carbene catalysts.

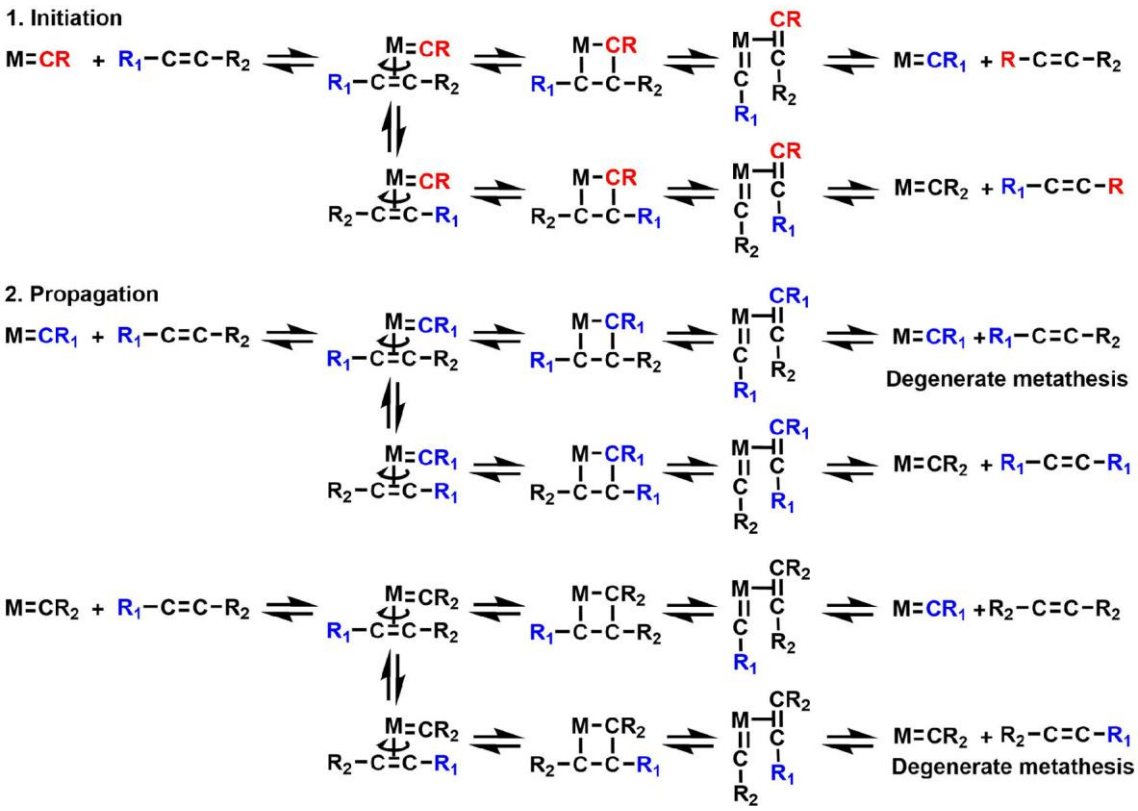

Scheme 14. Olefin Metathesis Mechanism[150]

The mechanism of olefin metathesis is detailed in Scheme 14.[150,156–159] All the steps for this reaction are equilibria, so if the reactants and desired exchanged products have a similar enthalpy, the reaction is degenerate. This property is convenient to make exchangeable cross-links in vitrimers. In contrast, when metathesis is used for organic synthesis, aiming at efficient synthesis of a desired exchanged olefin product, the equilibrium can be easily displaced by using a R−CH=CH2 olefin as the substrate. Thereby, the direct reaction yields the desired product, and easy removal of ethylene from the reaction vessel provides the necessary driving force for the reaction to happen preferentially in the desired direction. An example of polybutadiene vitrimers implementing olefin metathesis as the exchange reaction was reported.[160,161] These materials were made of cross-linked polybutadiene by reaction of butadiene with benzoyl peroxide. The interest of polybutadiene is the presence of insaturations in the network after cross-linking. These insaturations can undergo olefin metathesis in the presence of a Grubbs catalyst. Therefore, it is possible to make a vitrimer by adding a Grubbs second generation catalyst before the polymerization, but a much more original approach is to make a vitrimer out of a thermoset by swelling it with a solution of the catalyst after the cross-linking process. Such a strategy to make vitrimers has so far been specific to olefin metathesis vitrimers. These vitrimers exhibited self-healing at ambient temperature and below. Selfhealing behavior was also observed for thermoset materials after the catalyst was only applied on the surface where healing was required. When no catalyst was used, no effective selfhealing was observed. In summary, olefin metathesis allows original

strategies to make vitrimers, which is not possible with other chemistries. However, the use of a metal catalyst seems unavoidable and could be seen as the major drawback of this exchange reaction.

Imines.

Imines result from the condensation of an aldehyde or a ketone and a primary amine to obtain a C=N bond. Imines were investigated in the field of biochemistry, as their reversible covalent bond is known to be involved in enzymatic reactions,[162] and more recently in the field of materials chemistry,[163–175] with the growing interest in dynamic covalent networks. Actually three exchange reactions are known for imines: a dissociative hydrolysis followed by reaction with another amine; an associative exchange between an imine bond and a free amino moiety called transimination; and a direct associative imine−imine exchange termed imine metathesis.[166,170] Obviously, only the latter two associative reactions are interesting for associative CANs design. Although dissociative hydrolysis may happen in imine-based vitrimers, if the amount of water in the polymer matrix remains low, this reaction is unlikely to influence significantly the properties of the material. Therefore, the focus here is put on transimination, which requires residual amines, and on imine metathesis, which does not. Transimination has been known to occur through an equilibrated associative pathway for several decades.[176,177] Three successive steps were described. The first and rate-determining step consists in the attack of a free primary amine on the imine carbon atom to form a geminal diamine tetrahedral intermediate.[162,178–181] Then, two protons transfer from the nitrogen atom of the formerly attacking amino moiety to the nitrogen atom of the former imine moiety.[162,179,181] Finally the exchanged amino moiety dissociates and leads to the formation of the new imine[162] (Scheme 15a). The mechanism of imine metathesis is less extensively studied but is described as a nucleophilic addition of a neutral imine to a protonated one. The reaction proceeds through a 1,3-diazetidinium intermediate, yielding the exchanged imines or the initial reactants[179,182] (Scheme 15b). Transimination and imine metathesis have already been implemented in various polymeric materials to make vitrimers directly from polyimines[163,165,167,169] or by using imine bonds to cross-link polyesters,[166,172,173,175] polybutadienes,[164,168] polydimethylsiloxanes,[171] and polyethers.[174]

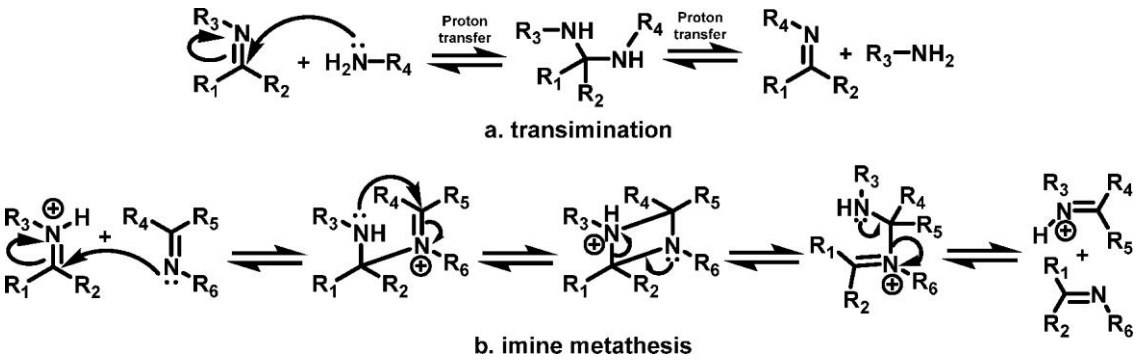

Scheme 15. (a) Transimination and (b) Imine Metathesis Mechanisms

Vinylogous Urethanes, Ureas, and Amides.

In the late 1970s, the exchange of amine moieties on enaminone structures was reported.[183] Later in the 1990s, similar exchanges between dialkylamine-derived enaminones and aromatic primary amines were discussed.[184,185] However, this exchangeable bond was not implemented in polymers until 2014.[186] Moreover, the mechanism involved in this first example was based on a reversible hydrolysis to the amine and carbonyl components, although a possible "component exchange" (amine direct exchange) was evoked by the authors. In this field of chemistry, enaminones are commonly termed vinylogous urethanes, vinylogous ureas, and vinylogous amides depending on their structure. These structures are easily prepared by acetoacetylation of polyols followed by reaction with a primary amine.[18] In 2015, Denissen et al.[18] reported the first vinylogous urethane vitrimer, exhibiting relaxation times as short as 85 s at 170 °C without the need of any catalyst. The exchange mechanism was later described by the same team[187] and depends on whether the medium is acidic, neutral, or basic. In neutral and acidic conditions, the free primary amine is protonated to form an ammonium, and the ammonium−enamine couple is in equilibrium with the amine−iminium couple. The latter couple can evolve by reaction of the nitrogen atom of the amine with the iminium to form a geminal amine−ammonium tetrahedral adduct similar to the intermediate described earlier for transimination. Then, dissociation occurs, yielding either the exchanged products or the reactants (Scheme 16a). The amine−iminium pathway written in Scheme 16a (bottom) for a Brønstedt acid can be extended to Lewis acids. Under these conditions, the reaction can proceed through a zwitterionic intermediate.

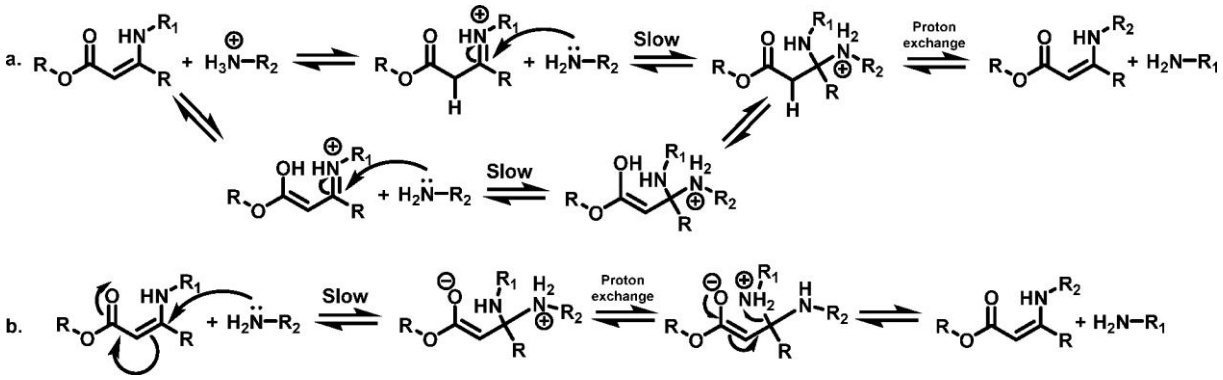

Scheme 16. Vinylogous Urethane Transamination Mechanism (a) in Acidic and Neutral Conditions and (b) in Basic Conditions

For instance, Friary et al.[184] studied the transamination of an enaminone bearing alkyl substituents with an aromatic primary amine in solution. The exchanged enaminone was then able to cyclize. When 1 equiv of toluenesulfonic acid was added, the overall yield increased from 29 to 56%. The authors suggested that the acid accelerated the enaminone transamination step (Scheme 17).

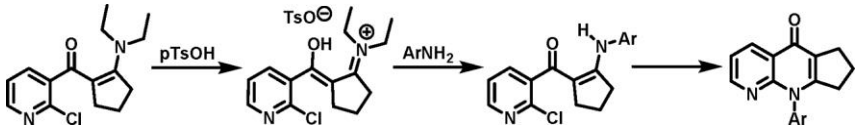

Scheme 17. Diketoenamine Transamination Catalyzed by p-Toluenesulfonic Acid (p-TsOH)

The catalyst protonates the oxygen atom of the enaminone and generates an iminium tosylate, more electrophilic toward the attack of the amine. The exchange kinetics can be tuned by using simple additives. Brønsted and Lewis acids such as sulfuric acid, dibultyltin dilaurate (DBTL), or zinc(II) accelerate the reaction. The use of 1 mol % p-toluenesulfonic acid was reported to reduce the time to reach equilibrium from >1 h to <10 min at 100 °C. On the contrary, non-nucleophilic bases such as triazabicyclodecene (TBD) were reported to increase the equilibration time.[187,188] In a basic environment the exchange reaction happens but is slower and involves a direct Michael-like addition of a neutral amine on a neutral vinylogous urethane (Scheme 16b).[187,189] These mechanisms are all associative and thus suitable to obtain vitrimer properties. Some vitrimers exhibit a dual temperature response.[189,190] Interestingly, their dual behavior was explained by possibly concomitant mechanisms a and b (Scheme 16), which are usually independent as they require different pH conditions. The iminium pathway would be dominant at low temperatures whereas the neutral Michael-type pathway would prevail at high temperatures. Catalysts also have an impact on the behavior of vitrimers. The relaxation time of vinylogous urethane materials was reported to decrease from 10 min at 120 °C in the absence of catalysts to 2 min with 0.5 mol % of p-TsOH.[187] A recent study by Haida and Abetz[191] studied the impact of p-TsOH in vinylogous urethane vitrimers with different stoichiometries. The networks were synthesized from hexane-1,6-diylbis(3- oxobutanoate) and tris(2-aminoethyl)amine

(TREN). When an excess of amine was used, the relaxation time decreased from 29 s without p-TsOH to 0.3 s with 0.05 wt % p-TsOH. Similarly, with an excess of the acetoacetate the relaxation time decreased from >46800 s to only 134 s (Figure 3).[191] DBTL and sulfuric acid were shown to be less effective. In the case of sulfuric acid, the sulfate anions probably form salts with the ammonium ions. In consequence, the ammonium species are less available and thus less reactive.

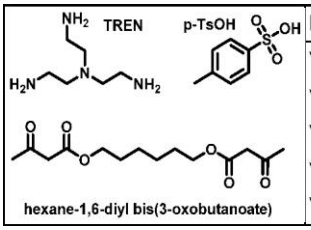

Reference	R (AA/N)[a]	T_g (°C)	p-TsOH	τ (s)[b]	E_a (kJ.mol^{-1})[c]
VU-E_{H+}	1.0	51		80	84.9
VU-A	0.7	13		29	75.9
VU-A_{H+}	0.7	17	✓	0.3	60.3
VU-NA	1.35	-8		> 46800	-
VU-NA_{H+}	1.35	29	✓	134	75.8

Figure 3. Impact of the stoichiometry and p-TsOH catalysis on vinylogous urethane properties. [a]Ratio acetoacetate/amine. [b]Relaxation time at 110 °C. [c]Activation energy (VU-E stands for an equal ratio of amines and acetoacetates, VU-A an excess of acetoacetates, and VU-NA an excess of amines).[191]

Similarly, carboxylate anions are also known to be proton scavengers for ammonium species in nonaqueous solutions, for instance.[187] When DBTL was used, the reaction activation energy dropped from 74 to 45 kJ mol^{-1}, suggesting a different mechanism, probably via the carbonyl moiety activation of the vinylogous urethane. On the contrary, TBD increased the activation energy up to 103 kJ mol^{-1} because of proton scavenging. Interestingly, Spiesschaert et al.[192] managed to incorporate acidic or basic functionalized fillers in PDMS-vinylogous urethane matrices. When 10 wt % kaolin bearing acidic groups was incorporated, the relaxation time of the resulting material decreased from 5725 to 4650 s at 150 °C, whereas nonfunctional fillers were shown to increase relaxation time. Acid, basic, or neutral alumina fillers were also studied. When the relaxation time for the matrix was 4000 s, the material containing neutral alumina or basic alumina displayed relaxation times of 4650 and 4500 s, respectively. On the contrary, the material made from acid alumina showed a shorter relaxation time (3600 s), in agreement with the results observed in solution (Figure 4).[192]

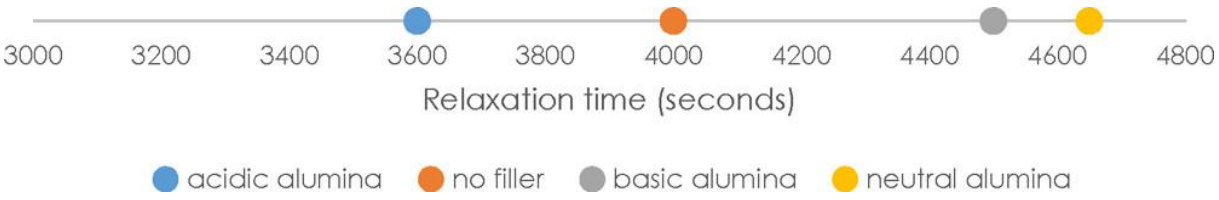

Figure 4. Effect of different functionalization of alumina fillers on vinylogous urethane vitrimer composites' relaxation time.

Other kinds of catalysis were also reported, and not surprisingly an excess of free primary amines in a vinylogous urethane vitrimer accelerates transamination.[189] Eventually, it is important to highlight the crucial role of the backbone and cross-linking density on the behavior of vitrimers, as already mentioned for imine vitrimers. Spiesschaert et al.[190] recently disclosed in a detailed study that the

relaxation rate of various vinylogous urethane-cross-linked polyether vitrimers decreased with increasing cross-linking density. An effect on the activation energy was also reported even if a clear trend was not identified. A dual temperature behavior was reported for polytetrahydrofuran, poly(propylene glycol), and poly(ethylene glycol) backbones, as reported previously in perfluoropolyether.[189,190] Nonetheless, this effect was not observed on a polypropanediol backbone, emphasizing the influence of both the matrix type and the molar mass of the spacers. The dual mechanism discussed earlier is probably the cause for this dual behavior.[190] Because they are versatile and they allow short reprocessing times, vinylogous urethanes have already been implemented in various polymers networks. Many examples were reported such as polysaccharide hydrogels,[193] polysiloxanes,[188,190,192,194,195] polybutadienes,[190,196] perfluoropolyethers,[189] methyl methacrylate-(2-acetoacetoxy)ethyl methacrylate copolymers,[197] polystyrenes,[198] polydimethylsiloxane (PDMS)−kaolin, PDMS−alumina and PDMS-aminated silica composites,[188,192] epoxy−amine copolymers,[199] polyethers,[190] and vinylogous urethane polymers bearing photodimerizable anthracene units.[200]

Diketoenamines.

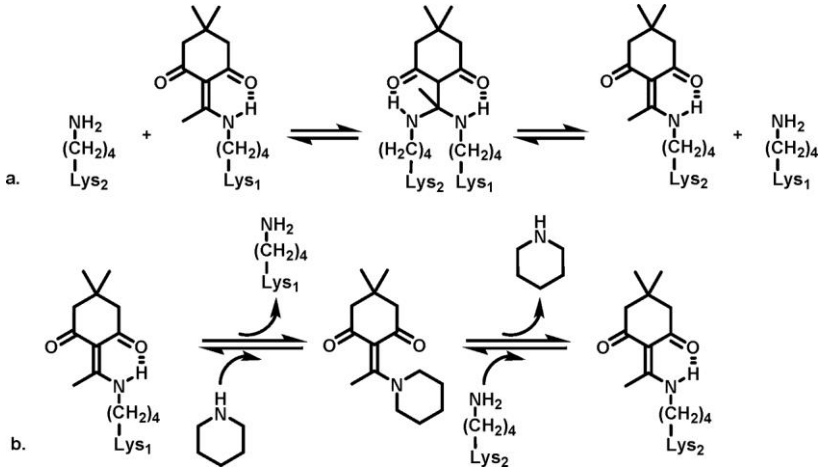

Scheme 18. Dde Protection Group Exchange on Amines (a) by Direct Electrophilic Attack and (b) Mediated by Piperidine[201]

Diketoenamines are known as a Dde protecting group for amines in peptide synthesis.[201,202] This protecting group is formed by reaction between 2-acetyl-5,5-dimethyl-1,3-cyclohexanedione (also known as 2-acetyldimedone) and primary amines.[203] In 2009, the behavior of Dde was studied in detail on lysine in solid-phase synthesis. Lysine is an interesting amino acid bearing two amino moieties in the α- and ε-positions.[201] This study reported the ability of ε-NH2 to attack a Dde-protected ε-NH2 or α-NH2, leading to an amine exchange. According to the authors,[201] the mechanism involves a direct nucleophilic attack of the free amine on the Dde group via a Michael addition, before a retro-Michael addition yielding either the original structure or the amine exchanged one (Schemes 18a and 19).

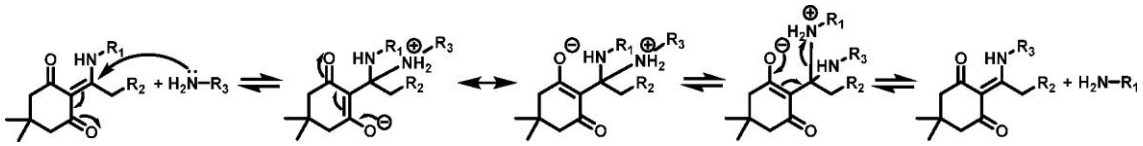

Scheme 19. Mechanism of Diketoenamine Exchange

Another mechanism involving piperidine as catalyst was also described. Piperidine acts as a mediator to pick up the Dde group from the originally protected amine before attack of another primary amino group. The overall reaction is composed of two successive exchanges: first between the originally protected amine and piperidine and then between the protected piperidine and a free amine (Scheme 18b). In all cases, the mechanism of amine exchange is associative. This chemistry was implemented in materials synthesis by Christensen et al. to make vitrimers;[204,205] they reported the synthesis of a network by click polycondensation between β-triketones and primary amines (Scheme 20).

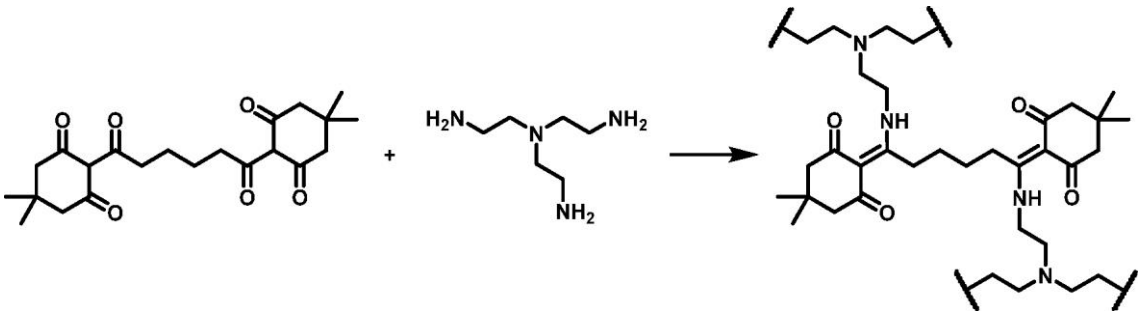

Scheme 20. Example of Synthesis of Diketoenamine Vitrimer; Alternatively, Various Diketones and Mixes of Primary Triamines and Diamines Were Also Used[204,205]

Triketones were synthesized from polytopic carboxylic acids and 1,3-diketones and the final materials simply by ball-milling of the reactants at room temperature. The materials obtained were reprocessable without requiring a catalyst and followed an Arrhenius behavior. These materials areeasily hydrolyzed. While this feature is often considered as a flaw, it can be beneficial for specific applications. In particular, as the materials are fully hydrolyzed in a few hours at room temperature in sulfuric acid (<12 h in 5 M H_2SO_4), the monomers can be easily recovered. Amines are separated from the triketones thanks to an ion exchange resin, with a recovery above 90%. The recovered monomers can be reused to make new poly(diketoenamines). This feature affords a convenient and efficient chemical recycling by hydrolysis at room temperature, while other hydrolyzable vitrimers require heating and more demanding conditions. The range of exchange reactions suitable for the design of vitrimers is already large (Figure 2), and new exchange chemistries occurring via associative pathways are still to be implemented in such materials,[206] although proving the associative character of an exchange reaction is often challenging and remains uncertain in some cases. In addition, a survey of the activation energies of the associative exchange reactions implemented in vitrimers (Figure 5)

shows that these energies can be distributed over relatively large ranges. This is certainly an asset for chemists and materials scientists who want to tune the reshaping ability of vitrimers.

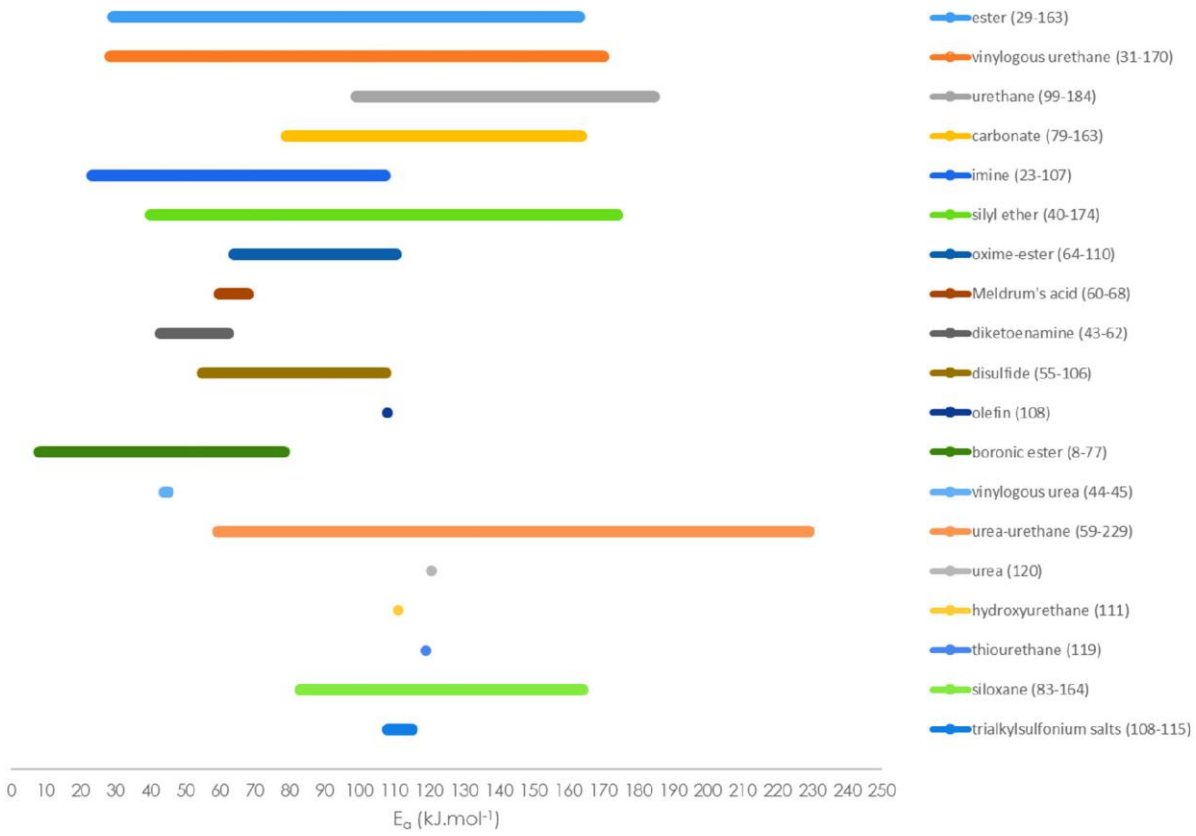

Figure 5. Activation energy ranges for exchangeable bonds implemented in vitrimers.

3. Internal Catalysis, Sterics, and Neighboring Groups Effects on Exchangeable Bonds

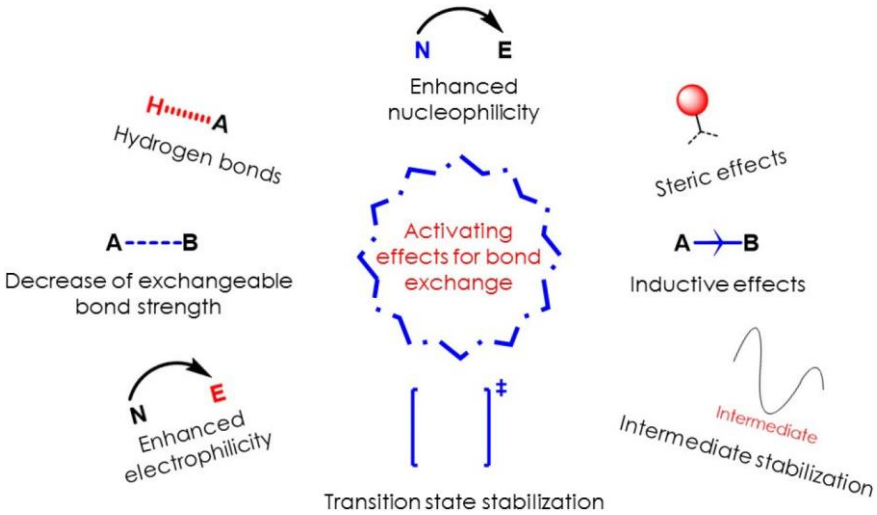

Figure 6. Examples of effects to activate bond exchanges.

Many parameters influence the properties of vitrimers: the cross-link density, the nature of the network backbone, and obviously the type of exchangeable bonds, for instance. For the exchange reaction to be efficient, many vitrimers rely on external catalysts. These compounds often come with some risks of leaching out of the material or premature aging limiting the recycling abilities of the materials. To address these problems, internal catalysis, steric effects, and neighboring group participation (NGP) are valuable. For a given exchange reaction, well-designed chemical modification of the exchangeable bonds surroundings is a way to accelerate the exchange, without resorting to any external catalyst. Different effects at the molecular scale are gathered in these three concepts (Figure 6). In light of the reaction mechanisms discussed, some relevant activating groups, either already implemented in bulk vitrimer networks or only in solution, are presented below. This should give new insights for further research in such dynamic materials.

Transesterification Enhancement by Neighboring Groups: Influence on the Exchange Mechanism and Vitrimer Properties.

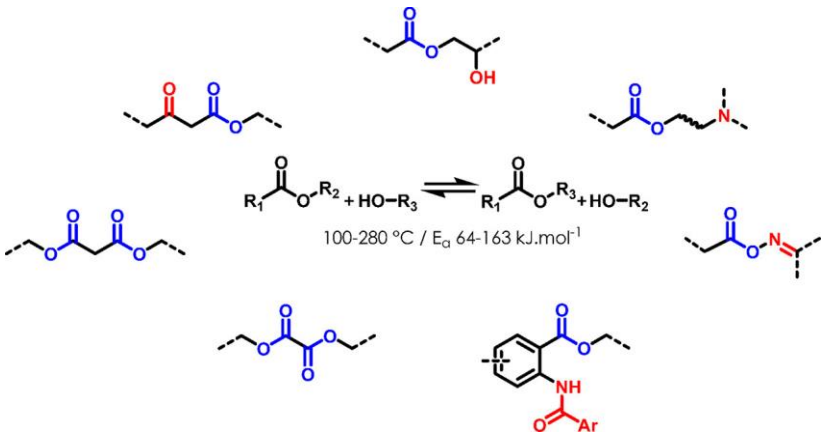

Figure 7. Main examples of activating groups activating transesterification. The temperature range[25] for stress–relaxation experiments and the range of calculated activation energies[24] of the exchange reaction in vitrimers are given.

A few activating groups have been reported to influence the reactivity of esters toward transesterification and/or hydrolysis in solution (Figure 7). For instance, on phenyl esters, a neighboring hydroxymethyl group on the ortho position increases the transesterification rate. However, the mechanism involves a cyclization after the attack on the ester by the −OH group, leading to a transient lactone (Scheme 21).[207]

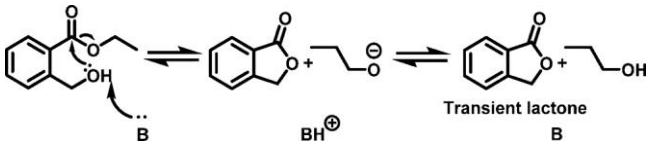

Scheme 21. Catalytic Effect of an Ortho Hydroxymethyl Group on Phenyl Ester Transesterification by Transient Lactone Formation

This chemistry if it were implemented in a CAN would proceed through a dissociative mechanism. A regioselectivity effect is also reported on pyridine triesters as one of the ester groups possesses an ortho hydroxyl group. Interestingly the transesterification reaction was reported to be regioselective on the ortho hydroxy ester, highlighting a reactivity increase (Scheme 22).[208]

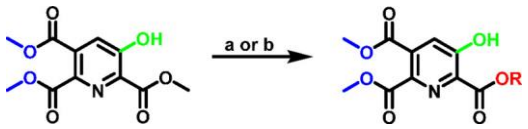

Scheme 22. Regioselective Transesterification: (a) 10 mol % $EtNiPr_2$, ROH, 60 °C; (b) 5 mol % $Sc(OTf)_3$, ROH, cat. H_2O, 60 °C[208]

Nevertheless, in this case the regioselectivity is due to the hydrogen-bonding ability of the hydroxyl group, and the mechanism is associative, contrary to the previous example. The same kind of regioselectivity was reported with 3-benzamidophthalates. The ester group located ortho to the amide moiety undergoes transesterification whereas that located in the meta position does not (Scheme 23).[209]

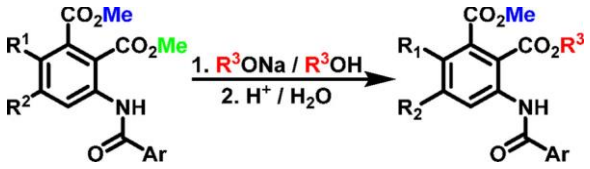

Scheme 23. Regioselectivity of 3-Benzamidophtalates Transesterification

Two mechanisms were discussed depending on the substituent: the first one is the regular attack of the alcohol on the ester groups activated by hydrogen bonding with the proton of the amide (Scheme 24a), and the second one is the formation of a more reactive 3,1-benzoxazin-4-one intermediate (Scheme 24b).

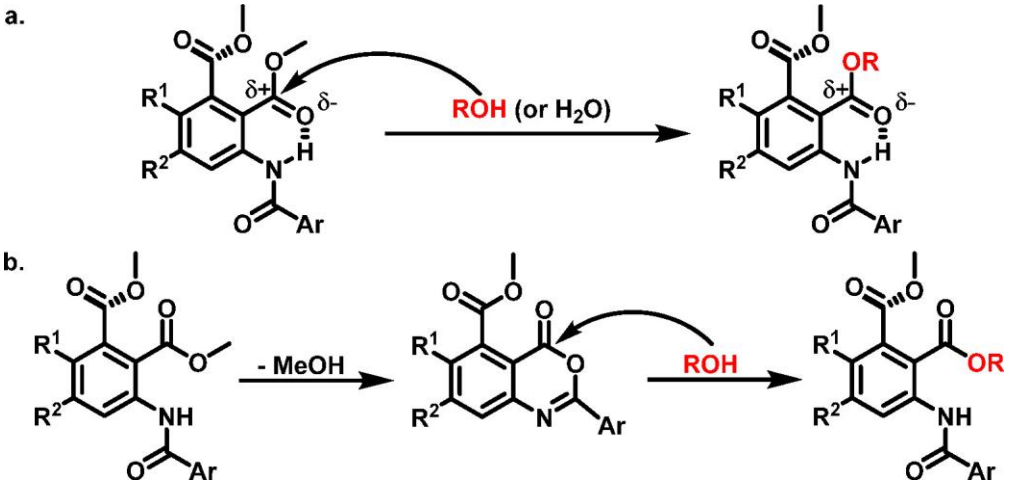

Scheme 24. Regioselective Transesterification of 3-Benzamidophtalates: (a) Direct Pathway and (b) Pathway with 3,1-Benzoxazin-4-one Intermediate

In contrast, neighboring thioether groups stabilize the ester bond,[210] hence decreasing its reactivity toward transesterification. Fluorene structures (Figure 8) bearing a methyl carboxylate substituent on the 1-position were studied. When one ethylthio group was present on the central five membered ring, the rate constant of transesterification (using methanol-d4) was 0.29 times the rate of the unsubstituted fluorene ester. Interestingly, on the fluorene ester bearing two ethylthio groups, the effect was shown to be opposite. This ester was more prone to transesterification.

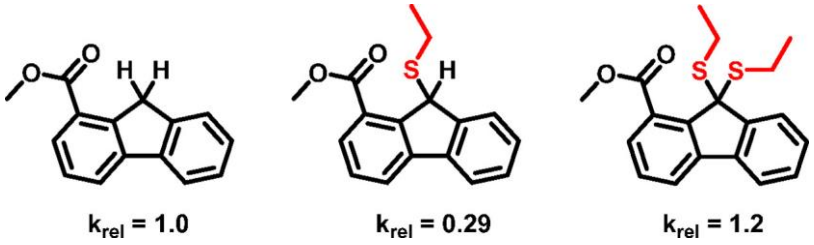

Figure 8. Effect of substitution by ethylsulfane groups on fluorene esters' transesterification rate.[210]

According to the authors of this study,[210] this phenomenon is likely due to at least two different causes, resulting in opposite effects on the transesterification rate. On one hand, the steric hindrance induced by one ethylthio group would decrease the transesterification rate, as the reactive site is less accessible. On the other hand, ethylthio groups induce a stabilizing electronic effect on the protonated ester intermediate (Scheme 25).

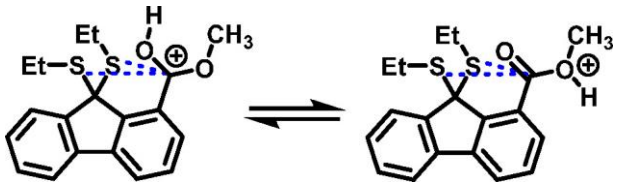

Scheme 25. Stabilizing Effect of Sulfur on Protonated Esters[210]

The authors hypothesized that the electronic effect were low compared to the steric effect when only one ethylthio substituent was present. On the contrary, when two ethylthio groups were present, the resulting electronic effect is significant and exceeds the steric effect, even though this effect is stronger than in the monosubstituted counterpart. β-Ketoesters as well as esters derived from malonates or oxalates, for example, are also more prone to transesterification reactions in solution.[211] Indeed, acetoacetic acid is 10 times stronger than acetic acid, so its conjugated base is more stable and the corresponding ester bond is weaker, leading to easier transesterification.[211] Oxalates' reactivity toward transesterification is explained exclusively by inductive effects. For β-ketoesters and malonates, a stabilized cyclic intermediate was proposed to explain the reactivity of the other aforementioned species, though inductive effects also play a significant role (Scheme 26).

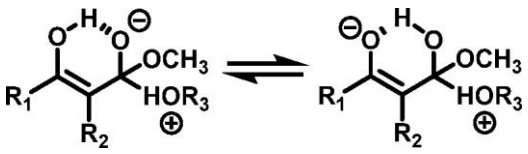

Scheme 26. Proposed Stabilization by Cyclic Intermediate for the Transesterification of β-Ketoesters[211]

Recently, diethylmalonate was used as cross-linker in a polyester vitrimer, disclosing the enhancing effect of β-activated esters.[212] Phthalate monoesters also displayed enhanced transesterification similarly to the previously discussed o-hydroxymethyl phenyl esters,[207] as demonstrated by Du Prez et al.[47] The neighboring carboxylic acid can indeed attack the carbonyl of the ester to yield a cyclic anhydride and an alcohol (Scheme 27a). Recently the same team enhanced this effect by using a β-aminodiol with a dianhydride to make networks (Scheme 27b).

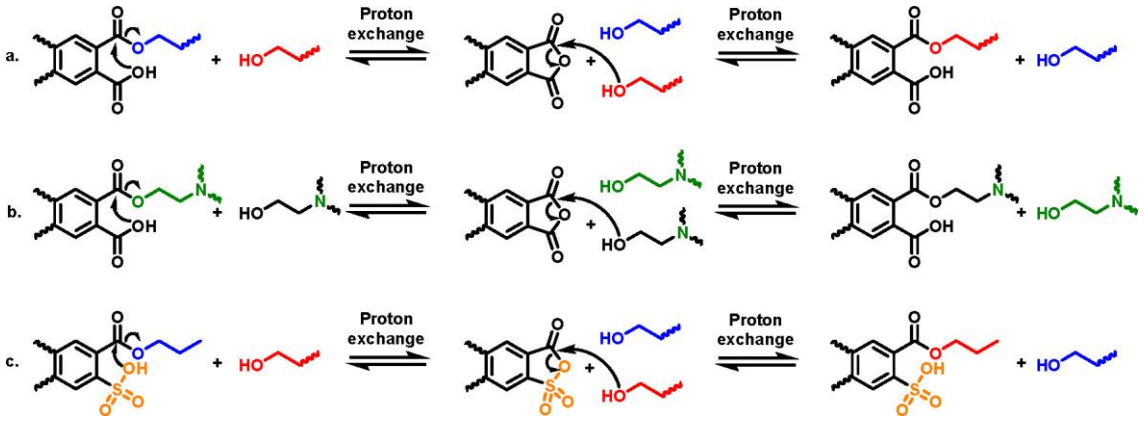

Scheme 27. Dissociative Transesterification Pathway Involving a Cyclization (a) by an o-Carboxylic Acid,[47] (b) by an o-Carboxylic Acid with an Inductive Effect of the β-Amino Alcohol,[214] and (c) by an o-Sulfonic Acid[48]

The enhancing effect of β-amines had already been described for ester hydrolysis in 1962.[213] The tertiary amine at the β-position of the hydroxyl groups induced a dual activation: the neighboring group participation of the dangling −COOH and the internal catalysis effect of the tertiary amine. The stress−relaxation times decreased by a factor 500 compared to the amine-free analogous network.[214] However, it should be noted that the mechanism was dissociative in these cases, highlighting that great care should be taken when considering neighboring groups participation as they potentially change the bond exchange mechanistic pathway.[47,214] The same mechanism was also recently reported with 2,5-bis(methoxycarbonyl)benzenesulfonic acid, a benzoester bearing an o-sulfonic acid moiety (Scheme 27c).[48] These materials showed a faster stress−relaxation than their carboxylic acid analogues. Amines were also shown to be efficient catalysts for transesterification vitrimers.[17] Triazabicyclodecene (TBD) in particular has often been used. Strategies have been designed to integrate tertiary amine groups into the polymer network. For example, bisphenol A diglycidyl ether (BADGE) was mixed with primary or secondary amines to generate epoxy terminated tertiary amines oligomers. In a second step, the oligomers were reacted with polyacids to obtain a network bearing

covalently bonded tertiary amines (Figure 9a).[38] The exchange reaction activation energy (Ea) for this network was 93.6 kJ mol^{-1}, very close to the 80−90 kJ mol^{-1} range observed for the Zn-catalyzed epoxy vitrimers.

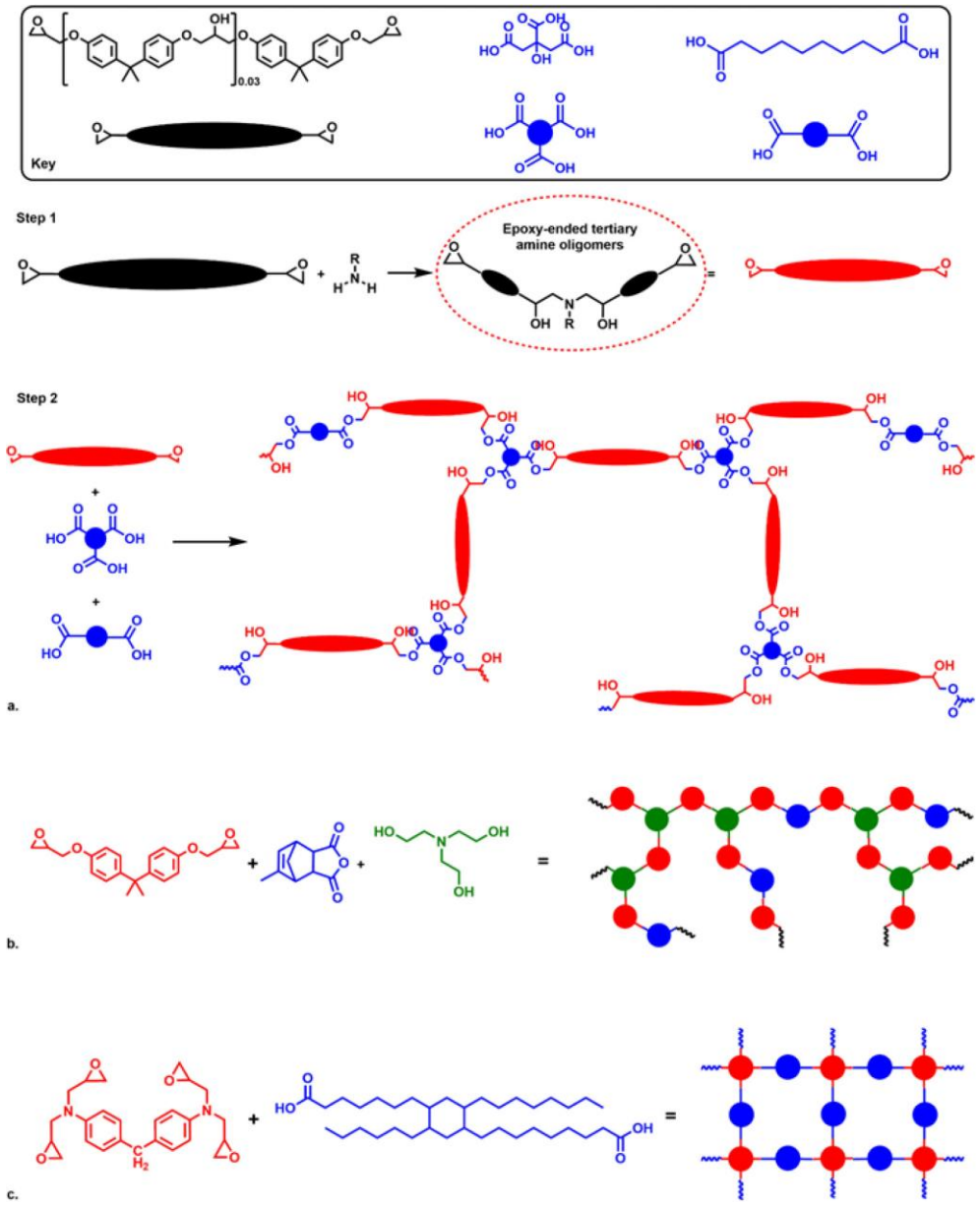

Figure 9. Strategies to embed tertiary amines in polyester networks using (a) epoxy-ended tertiary amines (two steps),[38] (b) ethanolamine as coreactant,[216] and (c) a commercial tetraepoxide bearing tertiary amines.[217]

Alternatively, triethanolamine was added as coreactant in a BADGE−(methyl nadic anhydride) system for the same purpose (Figure 9b).[216] The relaxation time at 190 °C decreased from 19460 to 4200 s when the triethanolamine content increased from 5 to 10 mol % (Figure 11).[216] Recently, catalyst-free transesterification vitrimers were synthesized from a hydrogenated dimerized acid derived from vegetable oil and tetraglycidyl-4,4'-diaminodiphenylmethane (TGDDM), a tetrafunctional epoxide bearing two tertiary amino groups (Figure 9c).[217] These tertiary amines were shown to act as internal

catalysts. The effect was reported to be enhanced by the flexibility induced by the vegetable oil structure. Instead of increasing monomers' flexibility, dangling chains which can plasticize the material were also shown to promote similar enhancement as tertiary amines' internal catalytic effect.[218] However, a similar internal catalysis was also reported in systems based on shorter, more rigid acids and which did not contain any plasticizer.[219] These examples of internal catalysis emphasize the role of tertiary amines as promising activating groups to increase the transesterification rate. Interestingly, a chemistry similar to the first vitrimer[1] featuring β-hydroxyesters pointed out the participation of the hydroxyl moiety in transesterification.[34,220,221] A six-membered ring with a hydrogen bond between the hydroxyl and the ester groups was hypothesized (Figure 10). The hydrogen bond is assumed to weaken the ester bond as previously discussed for the 3-benzamido group.

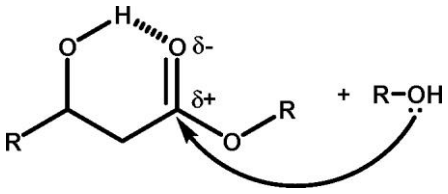

Figure 10. Hypothesized activating effect of the β-hydroxyl groups for transesterification. The hydrogen bond (dashed bond) increases the carbonyl C electrophilicity, facilitating the attack of an electrophile such as an alcohol (first step of the transesterification).

Besides, increasing the amount of free hydroxyl moieties was used to prepare catalyst-free transesterification vitrimers.[29,222] Although this effect cannot be considered as neighboring group activation or internal catalysis, it remains significant in transesterification vitrimers, was often reported in the vitrimer literature, and therefore deserves to be mentioned. The acceleration of the exchange reaction can be explained by the large amount of hydroxyl groups, facilitating the transesterification by a concentration effect.[33,219] In addition, a catalytic effect is also likely caused by hydrogen bonding, as in the case of oxime−esters (*vide infra*). Accordingly, the addition of glycerol to an epoxy−anhydride vitrimer matrix increases the concentration of free hydroxyl groups. The concentration effect is clear as the relaxation time of the materials at 180 °C dropped from 204 min to 86 and 66 min for 25, 50, and 75 mol % of glycerol, respectively (Figure 11).[33]

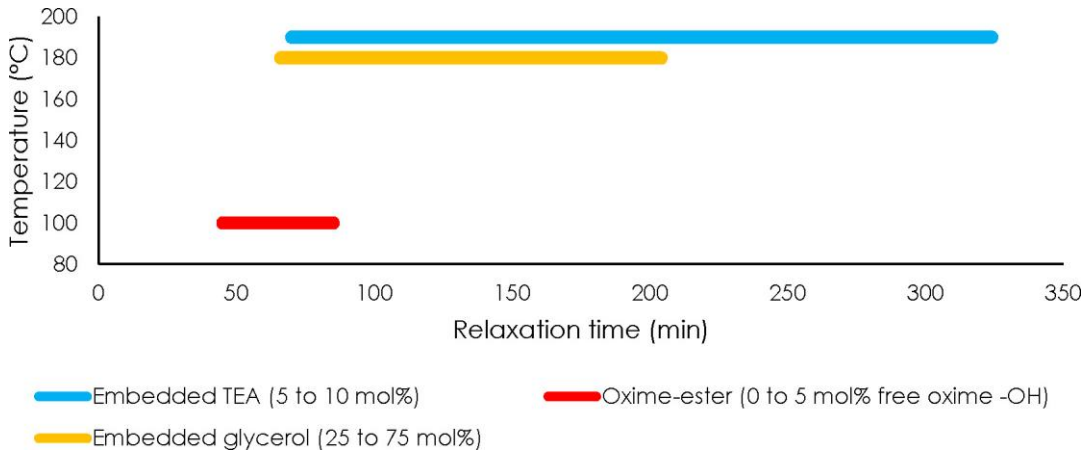

Figure 11. Effect of various enhancing strategies on stress–relaxation time: hyperbranched epoxy prepolymers (HBE), network-embedded triethanolamine (TEA), and free oxime hydroxyl group in the oxime–ester network.[33,216,233] Note that comparison between these three systems should be exerted with caution since structural parameters (backbone, cross-linking density, etc.) differ from one system to another.

The Case of Oxime–Esters.

Oxime–ester bonds can be considered as a subgroup of the ester family or as a specific type of bond. The most important difference between the oxime–ester and ester is the nucleophile (an oxime instead of an alcohol). Heat-induced transesterification of the oxime–ester enabled the synthesis of catalyst-free vitrimers (Scheme 28),[233] with relaxation times ranging from 5102 to 2725 s at only 100 °C, depending on the free oxime–OH available and their concentrations ranging from 0 to 5 mol % (Figure 11). The acceleration of the exchange reaction is caused mainly by the high concentration of exchangeable bonds. However, part of the enhancing effect can be explained by the higher nucleophilicity of the oxime (exchangeable moiety) compared to hydroxyl groups. This would allow to decrease relaxation temperatures and times. Nevertheless, considering the scarcity of reports dedicated to oxime–ester vitrimers, it would be unwary to compare the relaxation parameters with transesterification vitrimers, as many parameters are varying between the systems reported in the literature, such as the backbone or the cross-linking density, for example.

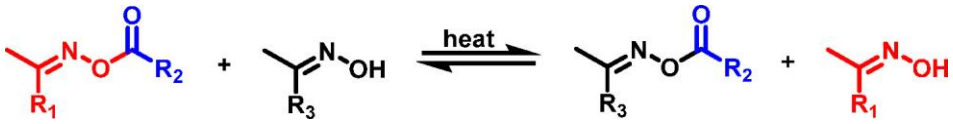

Scheme 28. Transesterification of Oxime–Ester Bonds[233]

Carbonate Activation by Electron-Withdrawing Groups.

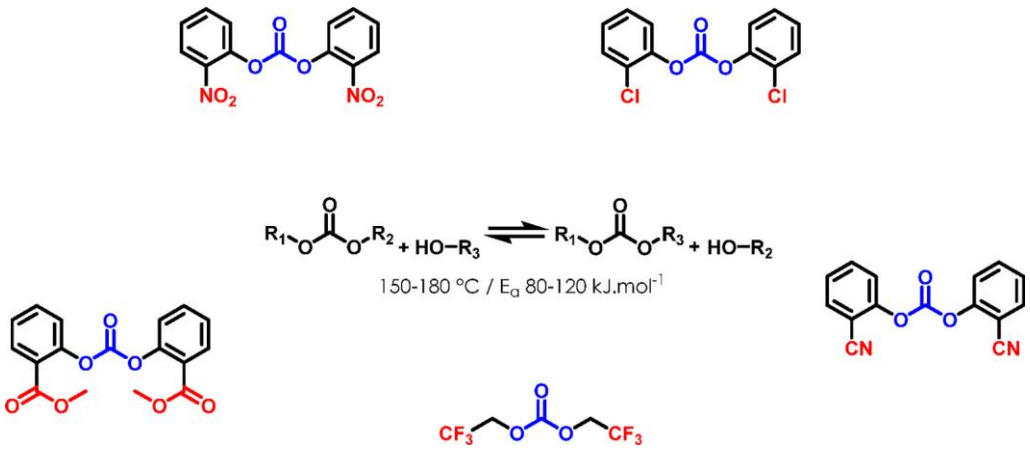

Figure 12. Examples of activating groups enhancing transcarbonation rate in solution and characteristics of reported transcarbonation vitrimers.[225–228]

Transcarbonation (Scheme 3) is used to synthesize polycarbonates, but this reaction requires a catalyst (Figure 12). Basic catalysts are probably the most used. Indeed, the generation of a more nucleophilic alkoxide increases the rate of addition onto the electrophilic carbon of the carbonate.[69,70,74,77–80] Activation of the carbonate with Lewis acids has also been reported but is less common.[74] Besides, some metal catalysts (such as tin or calcium salts, for instance) that may combine Lewis acid activation of the carbonate[67,71,73,76–78] and activation of the nucleophilic alcohol[71,73,75,77–79] have been also used. The formation of metal complexes coordinating both reacting partners increases the electrophilicity of the carbonyl[67,71,74,77–79] and also has a templating effect that accelerates the reaction. Nevertheless, neighboring group effects on transcarbonation are still relatively unknown (Figure 12). Inspired by a similar study on esters, Tillett and Wiggins investigated the effect of hydroxy- and methoxy-substituted phenylethylcarbonates on their hydrolysis rate (Figure 13a).[224]

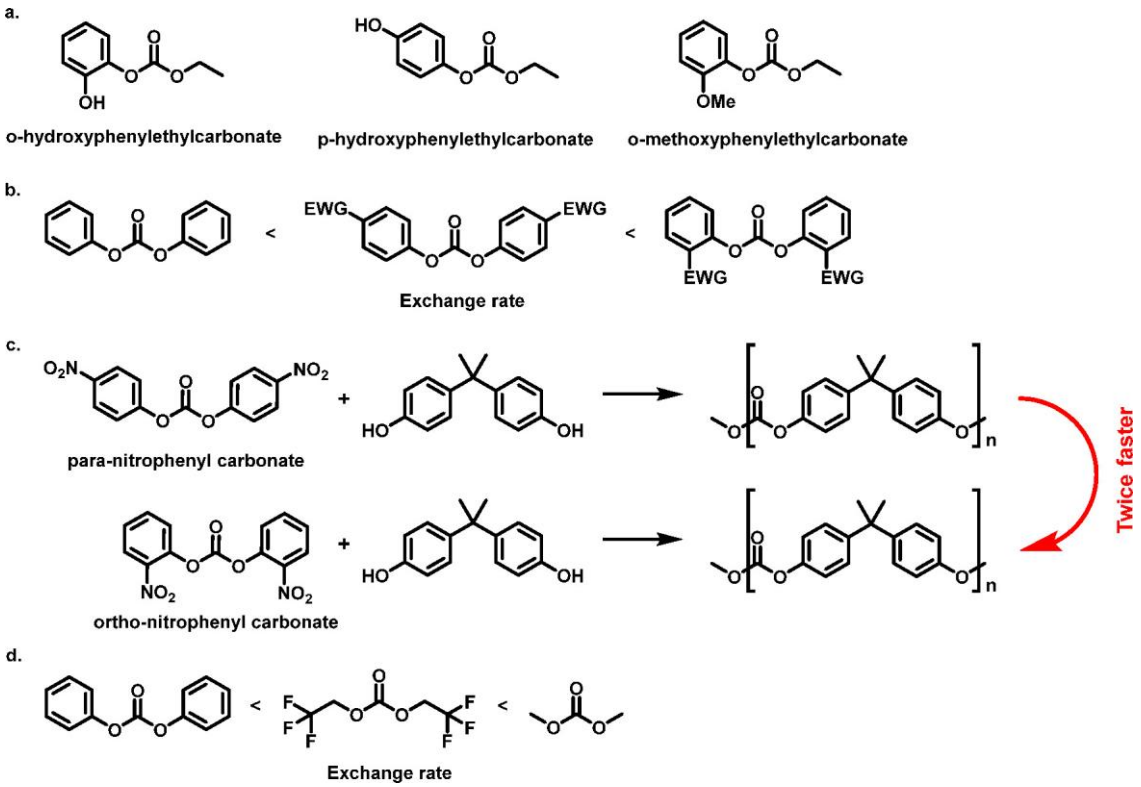

Figure 13. (a) Structures investigated by Tillett and Wiggins.[224] (b) Effect of the electron-withdrawing group (EWG) position on the exchange rate.[225] (c) Polymerization rate of nitrophenylcarbonates with bisphenol A depending on the substituent position.[226] (d) Effect of CF3 substituent on the exchange rate.[229]

An influence on the hydrolysis rate could be extrapolated to transcarbonation reactions due to the strong mechanistic similarities between these reactions. At high pH, the hydrolysis rates of o-hydroxy-, p-hydroxy-, and o-methoxy-substituted compounds were not significantly different. However, in neutral conditions the o-hydroxy-substituted phenylethylcarbonate was hydrolyzed 10 times faster than the two other compounds. General principles for transcarbonation were given in a very complete review on carbonates in 1996.[225] Generally, the more nucleophilic alcohol displaces the less nucleophilic one, and in the case of equal nucleophilicity, the less volatile alcohol displaces the more volatile one. This rule does not apply to phenols, as dialkylcarbonates react with phenols to make diarylcarbonates. In addition, alcohols bearing bulky groups or electron-withdrawing groups are poorly reactive. On the contrary, when the carbonate contains electron-withdrawing groups, the alcohol exchange is accelerated. For instance, fluorinated dialkylcarbonates and diarylcarbonates bearing $-NO_2$, −CN, or −Cl groups on the ortho position undergo much faster alcohol exchange (Figure 13b). The activation is less noticeable when the substituents are on the para position. Brunelle et al. harnessed this effect with the use of a catalyst. Hence, they successfully polymerized o-nitrophenylcarbonates with bisphenol A at room temperature and even below,[226] whereas high temperatures (up to 200−300 °C) are usually required to prepare polycarbonates.[227] The exchange between nitrophenylcarbonates and phenol was twice faster with the ortho-substituted carbonate

than with the parasubstituted homologue (Figure 13c). Similarly, bis-(trifluoroethyl)carbonates were shown to exchange with various alcohols and phenols in refluxing heptane or toluene (at 98 and 111 °C, respectively) in the presence of a base,[225,228] and their reactivity was reported to be between the very reactive dimethylcarbonate and the less reactive diphenylcarbonate (Figure 13d).[229] Kamps et al. studied bis(methylsalicyl)carbonate (BMSC, Figure 14) as an activated carbonate to lower the temperature for melt transcarbonation synthesis of polycarbonate.[227] BMSC was polymerized with bisphenol A (BPA), and this polymerization was compared to that of diphenylcarbonate (DPC) and BPA. DPC−BPA polymerization was achieved in 135 min, whereas for the BMSC−BPA system, 40 min was sufficient to reach similar molar masses (Figure 14).

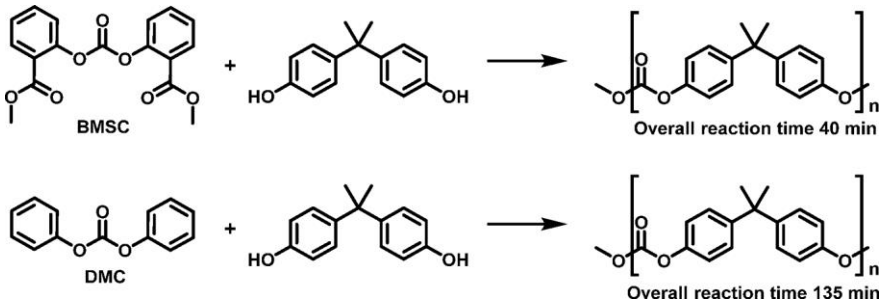

Figure 14. Polymerization of bis(methylsalicyl)carbonate (BMSC) and diphenylcarbonate (DPC) with bisphenol A (BPA).[227]

This polymerization is composed of two successive substitutions. The rates of the first and second substitutions were reported to be 30 and 9 times higher for the BMSC−BPA system, respectively. Although this study focused on the direct overall two-step reaction, the rate of the reverse reaction for the first substitution was determined for both BMSC and DPC. Indeed, the rate of the first step reverse reaction for DPC was half that of the direct reaction, whereas for BMSC it was 3 decades lower. The overall two-step reaction is an equilibrium. When this equilibrium was reached for the DPC−BPA system, the main product was the monosubstituted compound, and the same amounts of starting carbonate and disubstituted product were observed. In contrast, for the BMSC−BPA system, the disubstituted carbonate was the main product and the monosubstituted product was also present as byproduct, whereas no starting material remained, suggesting that the equilibrium was more displaced toward the products in this case. Such observation is significant for the design of vitrimers based on exchangeable carbonate bonds. Groups containing nitrogen seem to exert a significant activating group effect on carbonates. Amine-modified mesoporous silica prepared from amine-terminated silanes showed a catalytic effect on the transcarbonation between ethylene carbonate and methanol to produce dimethylcarbonate.[80] Thus, an amino neighboring group might have interesting effects on the transcarbonation reaction, too. Examples of vitrimers based on carbonate exchange are very scarce,[230,231] and they rely on Ti(IV) catalysts; they thus exhibit similar flaws to metal-catalyzed transesterification vitrimers discussed earlier. Smart molecular design based on the knowledge on

activating groups effects on transcarbonation might help the development of such transcarbonation vitrimers.

Dioxaborolane Transesterification Acceleration

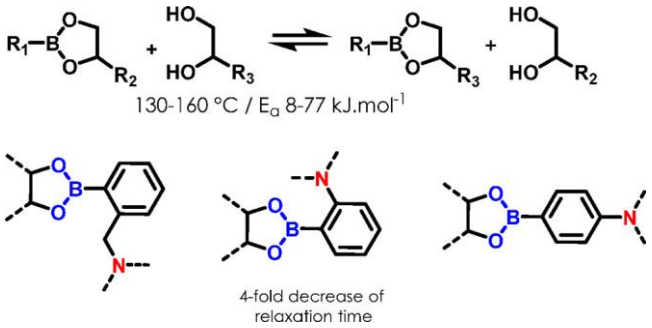

Figure 15. Reported activating groups enhancing dioxaborolanes' exchange rate and range of stress–relaxation experiment temperatures[25] and activation energies.[24]

As discussed previously, boronic esters were mainly used in aqueous media. Therefore, the effects of activating groups on boronic esters were mainly described under such conditions. Although the behavior of an exchangeable bond is very different in solution and in the bulk of a material, especially with a peculiar solvent such as water, it may still be possible to draw general conclusions on the effects of activating groups (Figure 15). In aqueous solution, there is an equilibrium between the dissociated boronic acid–diol couple and the corresponding boronic ester. The formation of a boronic ester by reaction between a boronic acid and a diol must be performed at a pH higher than the pKa of the acid.[232,233] Interestingly, the pKa of boronic acids can easily be tuned by chemical modification. For instance, compared to the pKa value of 8.8 of phenylboronic acid, the pKa of methylboronic acid is 10.4, whereas the pKa of the very electron-withdrawing 3-pyridylboronic acid is 4.0.[84] This shift of the esterification equilibrium gives a glimpse of the possible electronic and internal catalysis effects. An early study showed that arylboronic acids bearing ortho neighboring groups containing oxygen, sulfur, or fluorine do not enhance the esterification or the transesterification.[234] Nevertheless, electron-withdrawing groups decrease the boronic acid pKa, whereas electron-donating groups increase it[83,84] and destabilize the ester bond. For instance, the boron atom of phenylboronic acids is reported to be highly electron deficient, which reduces the pKa and facilitates ester formation.[84,233,235] Recently, benzoxaborole-cross-linked poly(ethylene glycol) (PEG) networks were synthesized out of 4-carboxy-3-fluorophenylboronic acid along with its non-fluorinated counterpart (Figure 16). Four-arm amine-terminated PEG was modified with 4-carboxy-3-fluorophenylboronic acid or 4-carboxyphenylboronic acid to afford tetrafunctional boronic acids. The same procedure was applied to d-glucolactone to obtain a tetrafunctional diol. Each tetrafunctional acid was then reacted with the tetrafunctional diol to make a network (Figure 16). This study showed that the resulting partially fluorinated material had a higher dynamic modulus and a faster relaxation time than the non-fluorinated analogue.[236]

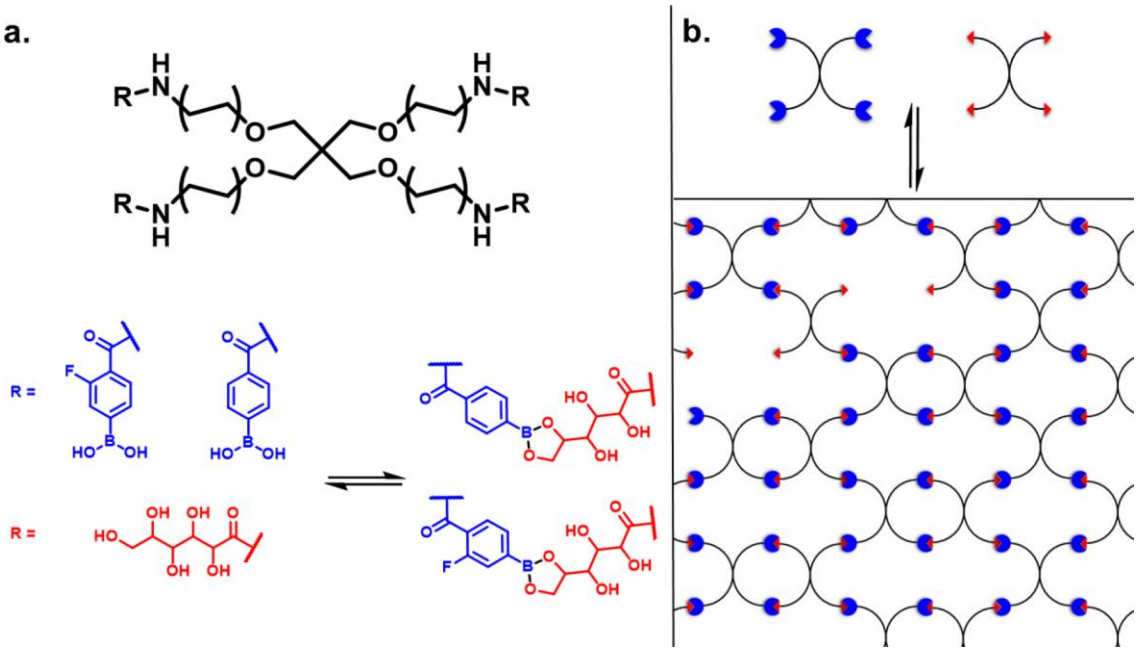

Figure 16. Synthesis of a network based on boronic esters: (a) poly(ethylene glycol) (PEG) monomers functionalized by boronic acids (blue) and diols (red) and their equilibrium with the boronic ester form; (b) schematic representation of the network.[236]

Nevertheless, the most studied and most promising activating groups so far are nitrogen-containing groups. Aminomethyl-substituted arylboronic acids were shown to be esterified several orders of magnitude faster than nonsubstituted phenylboronic acids.[237] Their transesterification was also accelerated compared to unsubstituted boronic acids or such acids bearing substituents containing oxygen, sulfur, or fluorine.[234,238] In solution, the addition of a dimethylaminomethyl group on a phenylboronic ester was shown to accelerate the rate of transesterification by 5 orders of magnitude.[44] The amino group on the ortho or para position decreases the pKa of phenylboronic acid[233] and facilitates the formation of the ester.[239] This is due to electronic substituent effects on the aromatic ring. Even when the amino moiety is not directly attached to the aromatic ring, the acceleration effect is noticeable. In this case, the effect is caused by the formation of B–N dative bonds (a proper example of neighboring group participation, Figure 17a).[83,85,233,239]

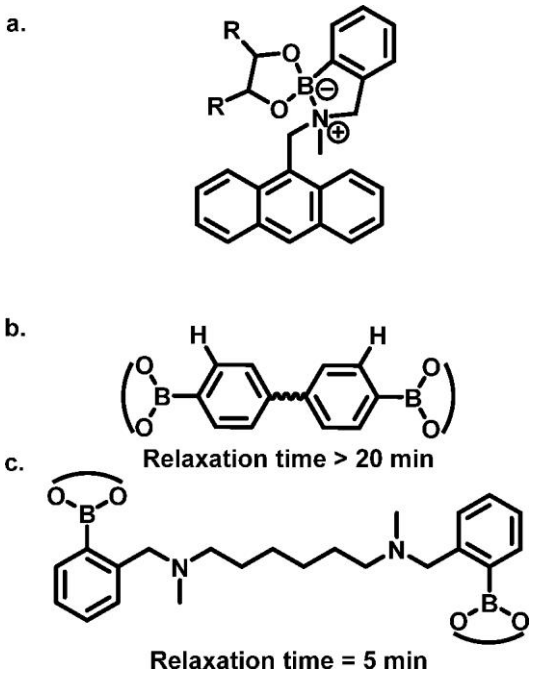

Figure 17. (a) Example of coordinative B–N bond.[239] (b) Slow exchange cross-linker and (c) fast exchange cross-linker (bottom) studied by Guan et al.[44]

Interestingly, amino activating groups have been implemented in vitrimers.[44] They demonstrated an accelerating effect on boronic esters transesterification in bulk, which enabled the tuning of the properties of dioxaborolane vitrimers. Indeed, materials containing amino activating groups relaxed stress within 5 min while the reference dioxaborolane material required more than 20 min (Figures 17b and 18).

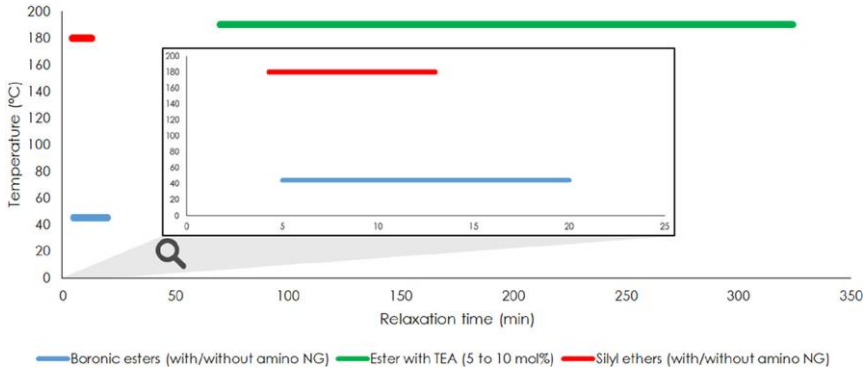

Figure 18. Effect of amine activating groups on the relaxation time of vitrimers with different kinds of exchangeable bonds (NG stands for neighboring group and TEA for triethanolamine).

Other kinds of effects such as steric interactions and ring strain also play a role in the ester stability, as functional groups attached or adjacent to the boron atom on a boronic acid decrease the association constant with diols.[83,232,240] Steric hindrance is particularly relevant in polymers. Sumerlin et al. reported higher pKa and lower binding affinity of boronic acid-containing polymers compared to small molecules. The monomer pKa was 7.2 whereas the polymer had a pKa of 8.2. In the polymer, the low

mobility of the chains limited the availability of the binding sites.[87,232] Great care should be taken in the design of the exchangeable bond as the effect obtained can be opposite to the expected one in some cases. For instance, in a recent study, vitrimers based on nitrogen-coordinating cyclic boronic diesters were synthesized, with a dative B → N bond embedded in the cyclic diester (Figure 19).[241] This particular structure not only offered an improved resistance to hydrolysis but also lowered the exchange rate compared to other cyclic boronic esters. In this particular case the effect on transesterification is somewhat counterintuitive. In summary, boronic esters in polymers allow the fine-tuning of materials properties thanks to activating groups[84] with electronic and/or steric effects. This feature is interesting for vitrimers design. However, the knowledge on these effects in bulk remains scarce and deserves further investigations.[236]

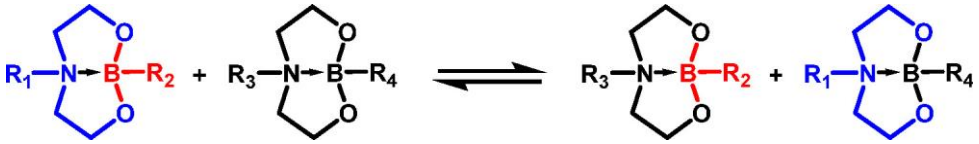

Figure 19. Nitrogen-coordinating cyclic boronic diester exchange.[241]

Disulfide Metathesis: Effect of Aromatic Substituents

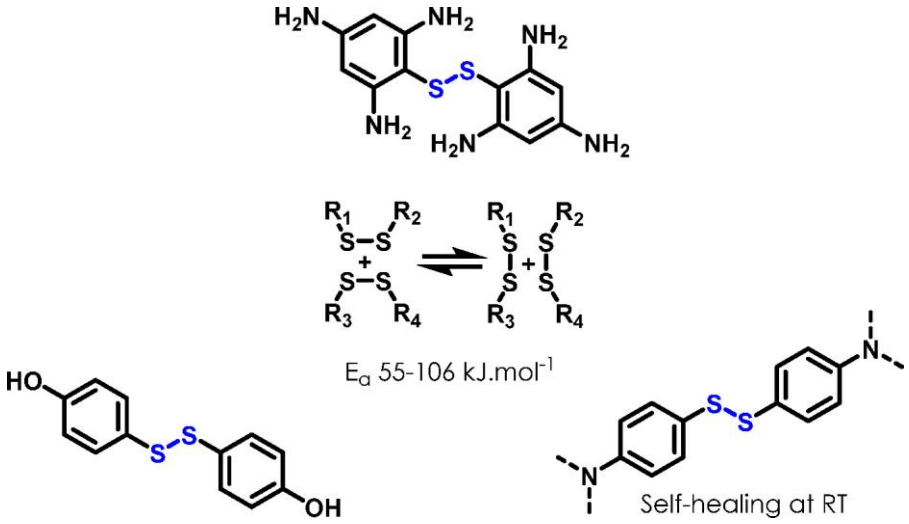

Figure 20. Disulfide exchange enhancement by activating groups (activation energy from Jourdain et al.[24]).

Neighboring group participation (NGP) in the exchange of disulfide bonds has hardly been probed yet, and the data readily available on this topic focus on the dissociative [2 + 1] radical assisted mechanism previously discussed in the Disulfides subsection (Figure 20). However, this general knowledge on disulfide bonds strength is useful to understand how to tune their dynamic behavior. Aromatic disulfides were mainly investigated, as the exchange reaction does not require the use of a catalyst to occur significantly contrary to exchange between alkyl disulfides usually catalyzed by triethylamine or

tributyl phosphate, for instance.[110-113,242,243] The metathesis of alkyl disulfides is a very slow reaction and even considered as not spontaneous in the absence of a catalyst, especially in solid state.[115] Adding 6% of triethylamine is, however, sufficient for the reaction to happen.[244] Phosphines are also good catalyst candidates, and 5 mol % tricyclohexylphosphine was reported to accelerate the reaction 240 times in solution at room temperature, whereas the same amount of tri(dimethylamino)phosphine accelerated it 520 times, although some degradation products were observed in that case.[245] Nevertheless, a catalyst-free self-healable hydrogel based on alkyl disulfide was reported.[246] The network was formed by harnessing the thiol–disulfide exchange reaction of a telechelic thiol-ended PEG with telechelic PEG bearing cyclic five-membered disulfide (Scheme 29). This network formation did not require any catalyst, as the tension of the five-membered disulfide ring favors its opening and enhances the exchange reaction. This design also allowed self-healing in slightly acidic condition, whereas such behavior is usually observed only in neutral and alkaline mediums, in the presence of nucleophilic thiolates.

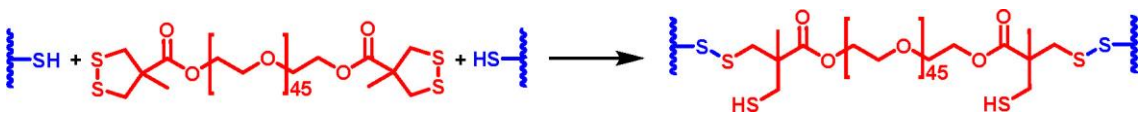

Scheme 29. Hydrogel Polymerization by Thiol–Disulfide Exchange on Strained Five-Membered Ring Disulfides[246]

Nitrogen has an enhancing effect[110] in different kinds of activating groups such as tertiary amines on phenyl disulfides,[111,247] thiuram disulfides,[248] or sulfenamides.[243] For instance aromatic sulfenamide-derived disulfides (Figure 21) exhibited a bond dissociation energy (BDE) of around 35 kcal mol^{-1}, whereas their nitrogen-free counterpart exhibited a BDE around 50 kcal mol^{-1}.[243] The lower is the BDE, the more radicals are generated, and the easier is the exchange reaction. Thanks to the enhancement of the exchange reaction, some catalyst-free materials based on aromatic disulfides exhibited self-healing at room temperature.[116] In those materials bis(4-aminophenyl) disulfides were used as dynamic cross-linkers to make poly(urethane–urea) systems.

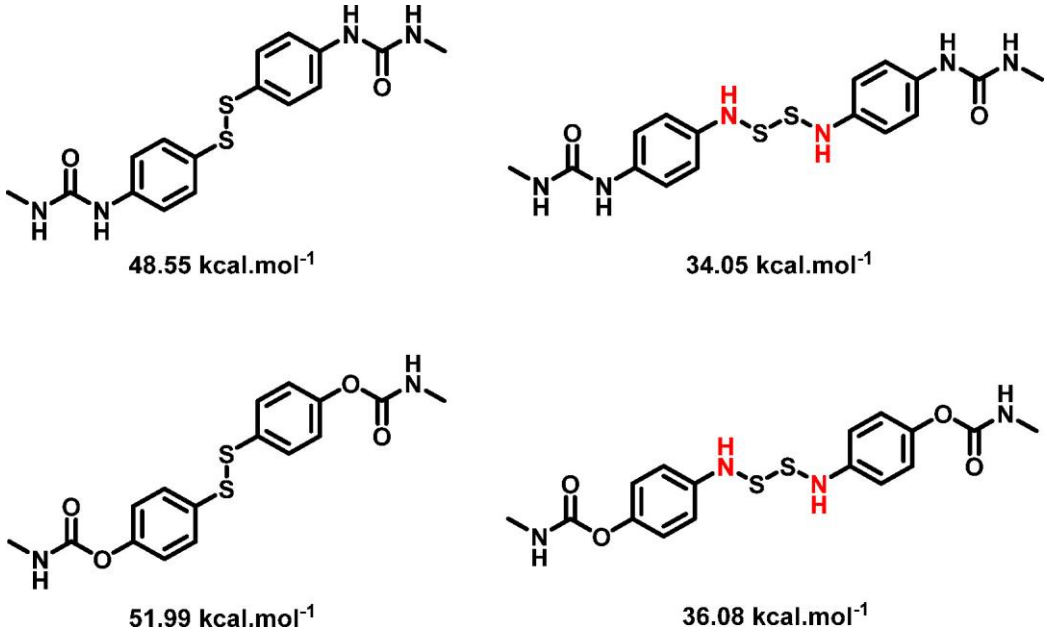

Figure 21. Structures of aromatic sulfenamide-derived disulfides and the associated bond dissociation energies (BDE) calculated by DFT.[243]

4-Hydroxyphenyl disulfides are known to undergo faster radical generation than their 4-aminophenyl homologues,[113] but this effect is still poorly documented. 4-Hydroxyphenyl disulfide exchange reaction with diphenyl disulfide reached 60% conversion in only 2 h, whereas 12 h was necessary for the 4-aminophenyl disulfide with diphenyl disulfide under UV radiation. Matxain et al. published a thorough computational reactivity study of the disulfide bonds dissociation energy.[110] They pointed out that electron-donating groups lower the disulfide BDE and that electron-withdrawing groups (EWG) increase this BDE. Compared to the 48 kcal mol^{-1} BDE value of unsubstituted aromatic disulfides, the p-sulfonic acid substituent increased this value to 55.6 kcal mol^{-1} whereas an amino derivative in the para position decreased the BDE to 41.3 kcal mol^{-1} and even to 30.1 kcal mol^{-1} with the trisubstituted bis(2,4,6-triaminephenyl) disulfide (Figure 22a). They also reported that dendralene and thiuram disulfides (Figures 22b and 22c) have a low BDE, which may allow self-healing at room temperature and provide a good alternative to aryl disulfides. Though disulfide bonds have been known for a long time, there is still much research needed to understand how to better tune the exchange reaction in materials, especially in the case of the associative thiol–disulfide reaction about which literature remains scarce.

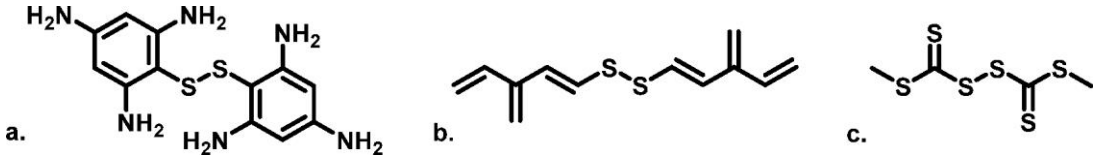

Figure 22. Structures of (a) bis(2,4,6-triaminephenyl) disulfide, (b) dendralene disulfide, and (c) thiuram disulfide.

Internal Catalysis of Silyl Ether Transalkoxylation by Amines, Urethanes, and Ureas

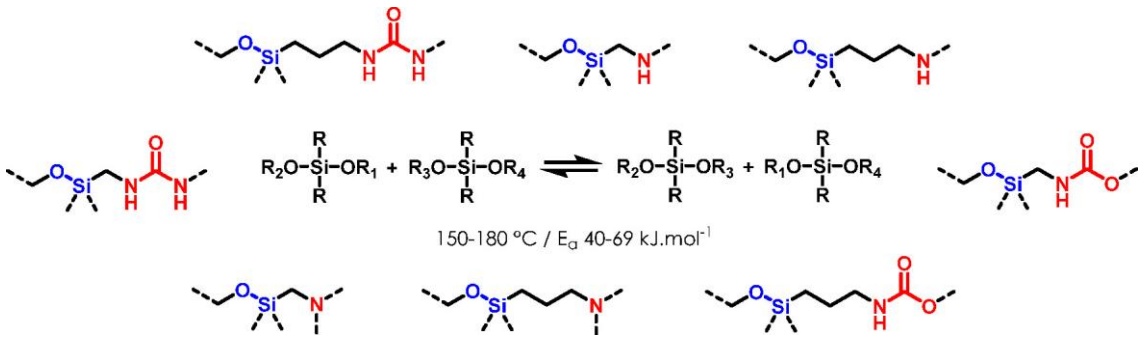

Figure 23. Examples of activating groups enhancing silyl ether exchange and range of stress–relaxation experiment temperatures[25] and activation energies.[24]

When implementing the previously discussed ion pair dissociation-triggered mechanism in silyl ethers, the main parameters to tune the exchange reactivity are obviously the nature[131] and concentration[130] of the ion pairs. The environment of the counterion influences its ability to dissociate and thus the rate of the exchange reaction (Figure 23). For instance, cation complexation by oxygen atoms on neighboring siloxane chains was reported to increase the electrophilic behavior of silicon atoms and the nucleophilic behavior of silanolate moieties, facilitating trans-siloxanation.[131] In 1970, Wright et al. studied the equilibrium between chains and rings in $[R(CH_3)SiO]_x$ structures, showing that for x = 2 or 4 bulkier R led to favored cyclization. However, the opposite effect was shown for x > 10.[249] Catalysis by triphenylphosphine (TPP) and triazabicyclodecene (TBD) in silicone materials was also reported. TPP led to materials with a temperature of plastic flow around 240 °C whereas the materials containing TBD flowed at 120 °C.[250] In 2014, tertiary and secondary amines, urea, and carbamate groups on α- and γ-silanes (Figure 24) were reported to interact with the alkoxy leaving group or the attacking nucleophile, thus increasing the hydrolysis rate of the alkoxy group. This study performed both in solution and in silico showed the significant influence of several activating groups. For instance, secondary amines accelerated the hydrolysis reaction from 5 to 50 times and tertiary amines at least 40 times. Carbamate groups accelerated the reaction from 6 to 80 times, depending on their position and structure.[251]

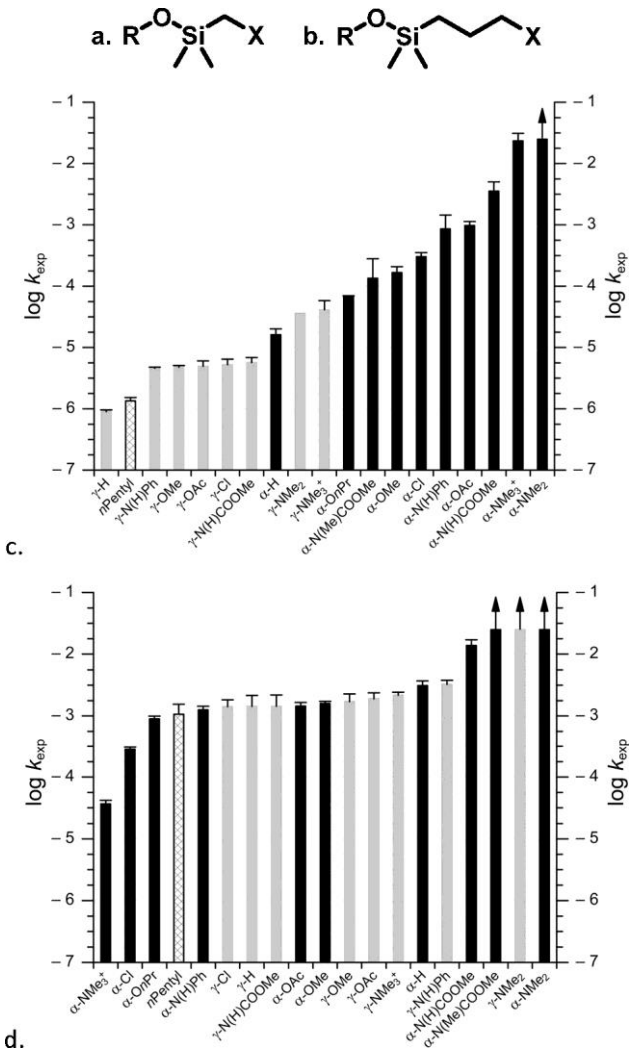

Figure 24. Structure of (a) α-silanes and (b) γ-silanes. The effects of various –X substituents on the hydrolysis rate of the alkoxy group were studied (c) in basic conditions and (d) in acidic conditions.[251]

This result was later successfully implemented in malleable materials with activating amino moieties accelerating the exchange rate of silyl ethers.[45,252] A copolymer of styrene and 2-((4-vinylbenzyl)oxy)ethan-1-ol was synthesized by free radical copolymerization. Then the resulting copolymer was cross-linked either with N,N'-bis(3-(trimethoxysilyl)propyl)ethane-1,2-diamine or with 1,10-bis(trichlorosilyl)decane (Scheme 30). Both cross-linked structures were similar, and the cross-linkers used had the same length. The relaxation time for the structure incorporating secondary amines was 260 s at 180 °C, 3 times less than the 779 s needed for the amine-free structure (Scheme 30).[45] Variations of the silyl ether bulkiness and the polymer backbone are suggested to tune the properties of these materials.[132]

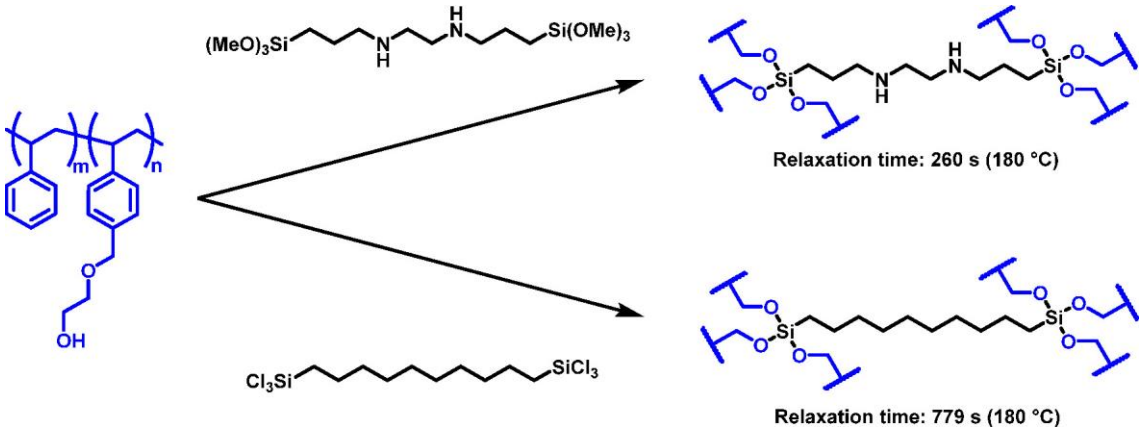

Scheme 30. Synthesis of Styrene-Derived Networks Cross-Linked by Silyl Ethers[a]

[a]Two cross-linkers were used, one bearing secondary amines (top) and the other not (bottom). The reprocessabilities of the obtained materials were compared.[45]

Case of Urethanes and Hydroxyurethanes

As discussed previously, the mechanism involved in polyhydroxyurethane exchange reaction remains uncertain. Hence, the determination of the effects of activating groups on transcarbamoylation is intricate as they were mainly studied for the dissociative decomposition reaction discussed in section I (Figure 25).[254-256] It should be mentioned that an important activation reported is the oxime-promoted transcarbamoylation, similar to the effect on esters previously discussed. It was implemented in dissociative covalent adaptable networks since the mechanism is purely dissociative in this case.[253]

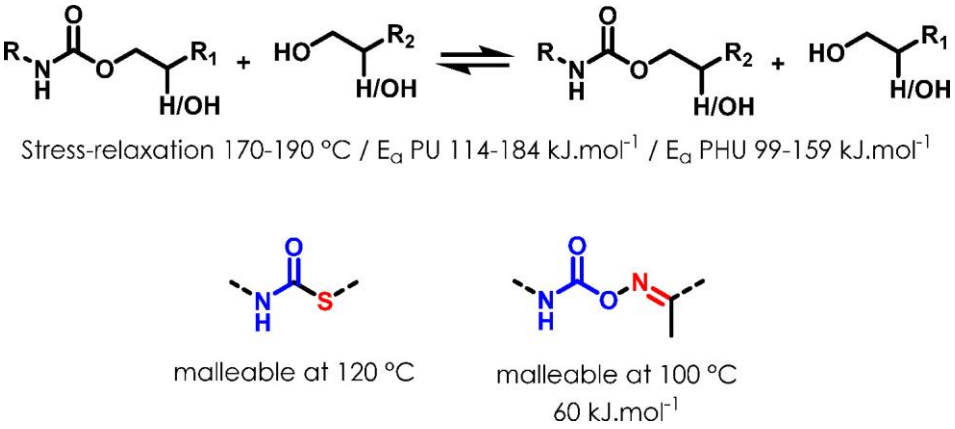

Figure 25. Characteristics of polyurethanes, polyhydroxyurethanes, polythiourethanes, and poly(oxime–urethanes): range of stress–relaxation experiments temperatures[25] or reprocessing temperatures and activation energies.[24,253]

For thiourethanes solvolysis by thiols, secondary amines or alcohols, the suggested reaction pathway was an associative addition/elimination mechanism[257] instead of the dissociative elimination/addition commonly accepted. Nonetheless, as previously pointed out, the recent implementation of thiourethane bonds in materials highlighted a dual associative and dissociative mechanism.[258] Knowledge on the effects of activating groups on hydroxyurethane-based vitrimers is very limited. Nevertheless, an excess of free exchanging dangling groups, namely alcohol groups for polyurethanes

and thiol groups for polythiourethanes, was shown to favor the associative pathway and decrease degradation reactions. Furthermore, this excess of dangling exchanging groups allows a better control over the reprocessing temperature and shorter reprocessing time.[144,258] After 70 min at 140 °C a PU network without free −OH group exhibited 83% recovery of cross-link density in the presence of 1 mol % dibutyltin dilaurate (DBTDL) as catalyst. In contrast, only 15 min at 120 °C was sufficient to reprocess a PU containing 20% of free −OH.[258] In contrast, an increase of the relaxation time was observed in the case of thiourethane-based networks (Scheme 11) containing free thiols compared to the thiol-free analogue. This counterintuitive result was explained by a change from a dissociative to a slower associative mechanism.[144] In conclusion, the chemistry of polyhydroxyurethanes is much more complex that it seems at first glance. Dissociative and associative exchange mechanisms compete and are influenced by many parameters such as the availability of exchangeable group, the presence of activating group or internal catalysts, or the temperature. Therefore, much caution should be taken when designing covalent adaptable networks out of polyhydroxyurethanes.

Ureas Exchange

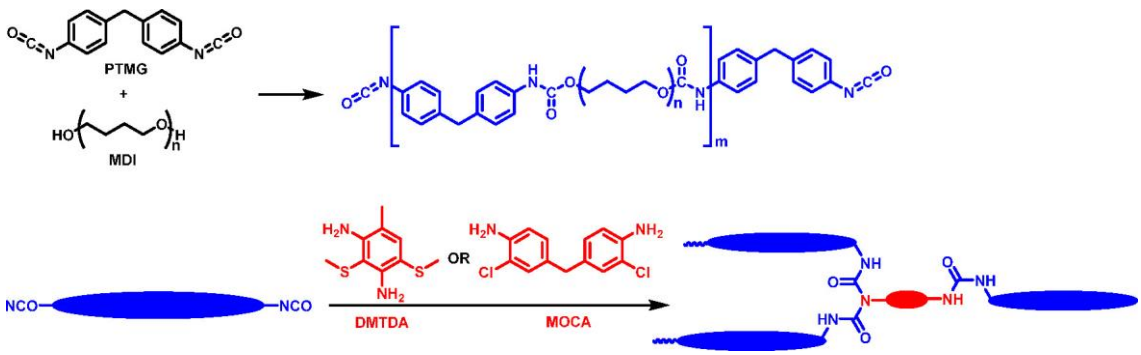

Scheme 31. Synthesis of Polyurethane–Urea Self-Healable Elastomers[259]

Recently, a polyurethane‑urea elastomer was claimed to be a vitrimer.[259] The authors first synthesized a PU prepolymer out of poly(oxatetramethylene) glycol (PTMG) and 4,4'-diphenylmethane diisocyanate (MDI). Then this prepolymer was mixed either with 3,5-dimethylthio-2,4-toluenediamine (DMTDA) or with 3,3'-dichloro-4,4'-diaminodiphenylmethane (MOCA) to form exchangeable biuret groups (N,N'-diarylurea) (Scheme 31). Because the diamines used are primary, each amine can react twice, thus ensuring the formation of a cross-linked materials (primary diamines can be considered as hidden tetrafunctional reactants). The amines used possessed either electron-donating methylthio substituents or electron-withdrawing chlorine atoms. The stress–relaxation time of the methylthio group-containing network was 3–4 times shorter than that of the chlorinated analogue, depending on the temperature (100–120 °C). The relaxation was assigned to urea–urea exchanges, and the mechanism was reported as associative.[259] Nevertheless, there is little proof to support this claim.

Transimination Acceleration by Activating Groups

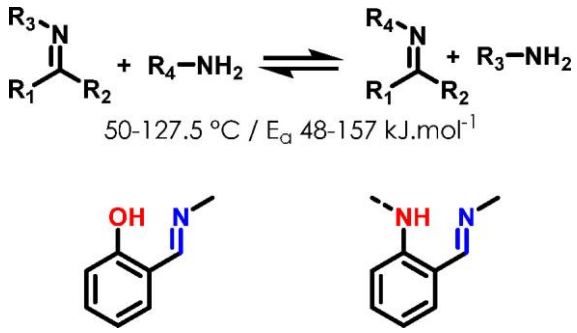

Figure 26. Characteristics of transimination: reported range of stress–relaxation experiments temperatures[25] and activation energies.[260] Two examples of potentially active neighboring groups are given.

The success of imine-derived vitrimers (Figure 26) may be explained by the versatility of this linkage but also because these vitrimers can be reprocessed without the need for a catalyst.[163-174] When used in organic chemistry or biochemistry, transimination was reported to be catalyzed by thiourea–metal complexes (2 orders of magnitude rate acceleration),[177] triflate salts of scandium, terbium, samarium, and other lanthanides (up to 5 orders of magnitude acceleration),[178,261] zinc bromide,[262] iron chloride, copper chloride, and magnesium chloride.[263] Besides, acidic and basic catalyses are known to be efficient as well in aqueous[175,264] or organic solutions.[175,265] In particular, interesting examples of internal basic catalysis in solution were reported in the 1980s by using primary amines featuring an internal tertiary amine function.[264,265] Ciaccia et al.[180] reported a study on aromatic imines in organic solvents at room temperature. Part of this work dealt with the exchange between N-benzylideneanilines and p-toluidine (Figure 27). The exchange reaction exhibited low equilibrium constants (Keq < 10); thus, the results could have been carefully extrapolated to degenerate system such as those encountered in vitrimers. The authors showed that the rate of the forward transimination reaction was almost unaffected by EWG and EDG on the imine aromatic ring but that the reverse reaction was mildly affected by these substituents. The electron-donating $-OCH_3$ group slightly increased the reverse reaction rate, whereas electron-withdrawing −CN and $-NO_2$ groups decreased this rate (Figure 27). Similarly, Schaufelberger et al.[262] studied the impact of substituents on the exchange of aromatic imines with benzylamines in the presence of zinc bromide as catalyst in acetonitrile. Nevertheless, in this system, two simultaneous reactions were involved: imine isomerization and transimination. Thus, it would be dubious to draw general conclusions on internal catalysis based on this study.

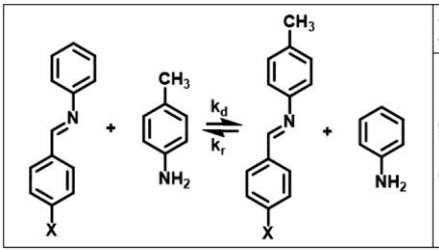

X	K	k_d ($M^{-1}s^{-1}$)	k_r ($M^{-1}s^{-1}$)
H	2.6	1.0×10^{-1}	3.8×10^{-2}
OCH_3	3.0	1.2×10^{-1}	4.0×10^{-2}
CN	4.5	1.1×10^{-1}	2.4×10^{-2}
NO_2	7.2	0.94×10^{-1}	1.3×10^{-2}

Figure 27. Transimination reaction between N-benzylideneanilines and p-toluidine and kinetic parameters studied by Ciaccia et al.[180]

Because the first step of the amine–imine exchange reaction is associative, it occurs at room temperature without catalyst in solvents only with unhindered reactants.[179] This idea underlines the fact that the environment of the exchangeable bond likely plays a major role in the reaction. For instance, the solvent used to make dynamic covalent gels had an influence—acetonitrile allowing faster imine exchange than toluene.[266] Additionally, imine metathesis is catalyzed by zirconium, molybdenum, rhenium, and niobium in organic solvents if the temperature reaches 100 °C[179] and by hafnium imido complexes at 80 °C as well.[267] An interesting strategy involving minute amounts of primary amines was also reported to accelerate this reaction in solution at room temperature.[179] The effect of primary amines on imine metathesis was investigated in terms of mechanism and thermodynamics. Mechanistically speaking, the overall reaction can be seen as two concomitant transimination reactions (Scheme 32). Thus, it is not *stricto sensu* an imine metathesis, but the overall result is the same. Minute amounts of an imine A bearing an isobutyl group exchange with the minute amount of n-butylamine, leading to the release of minute amounts of the exchanged imine C and isobutylamine. This amine then undergoes transimination with an imine B bearing a n-butyl group. This second step releases the exchanged imine D and n-butylamine able to react with A and so on. The overall reaction is an equilibrium between amines A and B, on one hand, and between C and D, on the other. Thermodynamically speaking, the overall reaction is an imine metathesis.[179] This effect was implemented in imine-cross-linked PEG networks. A slight excess of dangling primary amines enabled self-healing at 50 °C within 5 min.[266] Thus, choosing carefully the stoichiometry for the synthesis of imine-derived vitrimers would enable the tuning of their properties.

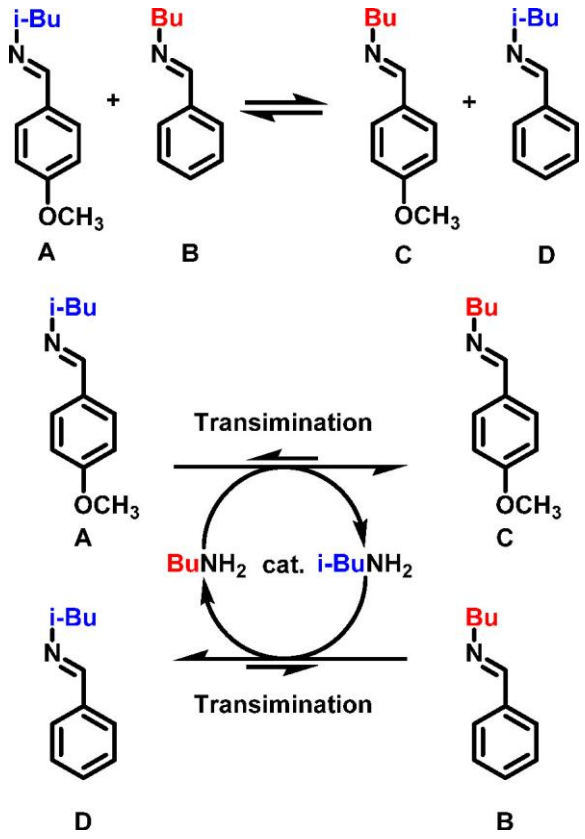

Scheme 32. Imine Metathesis Catalysis by Minute Amounts of Primary Amines[179]

Recently the effect of hydrogen bonds was also emphasized. Indeed, hydrogen bond donors such as thioureas and squaramides catalyzed both imine metathesis and transimination in solution and their efficiencies depended on their structures.[268] Similarly imines derived from salicylaldehyde were reported to be stabilized by hydrogen bonding with −OH or −NHR substituents on the ortho position.[269] Once again, this effect could be used in the molecular design of imines to tune the exchangeable bond properties.

Vinylogous Urethanes and Amides, an Efficient Exchange Chemistry without Catalyst

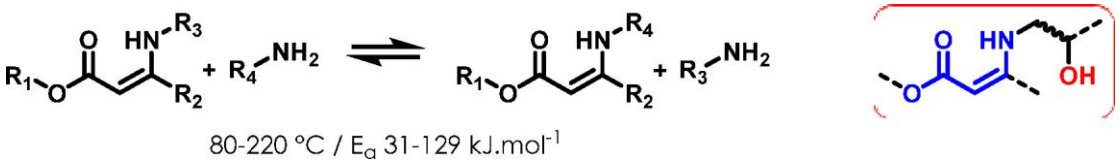

Scheme 33. Characteristics of Vinylogous Urethane Transamination: Reported Range of Stress–Relaxation Experiment Temperatures[25] *and Activation Energies;*[24] *Dangling Hydroxyl Groups Accelerate the Relaxation Time of VU Materials*

Transamination of vinylogous urethane is a very effective exchange reaction and enables chemists to design easily reprocessable catalyst-free vitrimers (Schemes 16 and 33). This observation might be the cause for the rarity of reports on such effects on vinylogous urethanes. Although the exchange is so efficient that many catalyst-free vitrimers were synthesized, vinylogous urethane-based CANs would still benefit from activating group participation or internal catalysis to lower reprocessing

temperatures. Actually, an example of internal catalysis was recently reported in vinylogous urethane-cross-linked epoxy–amine materials.[199] Tri- and difunctional amines were reacted with a bisacetoacetate to prepare a vinylogous urethane bond-containing hardener for an industrial epoxy resin. Two synthesis methods were compared. On the one hand, the amines, the bisacetoacetate, and the epoxy resin were mixed in one pot. On the other, the amines and the bisacetoacetate reacted in a first step to yield a vinylogous urethane curing agent bearing free primary amines. Then the curing agent was mixed with the epoxy resin in a second step (Figure 28). The difference lies in the water release when amines and the bisacetoacetate reacted together. In the one-pot strategy, this water was trapped in the material, whereas in the two-step strategy the water produced during the first step was removed prior to the second step to yield a water-free material. The materials exhibited a relaxation time at 160 °C of 3.5 s for the one-pot material and of 5.5 s for the two-step synthesis, showing no significant difference between the two preparation procedures. These values must be compared with the 25.5 s relaxation time observed in epoxy-free vinylogous urethanes vitrimers with a similar structure, although having a higher vinylogous urethane bond concentration. Certainly, the network structure influences the relaxation time, and thus direct comparison of these values might be adventurous, but an internal catalytic effect from the dangling hydroxyl groups is likely responsible for the shorter relaxation times.[199] To support this idea, the authors performed model reaction on small molecules. They studied the disappearance of propyl-3-(octylamino)but-2-enoate (octyl VU) with benzylamine in 2-hexanol or dodecane at 100 °C. The reaction was faster in 2-hexanol, showing the accelerating effect of hydroxyl moieties on the exchange reaction, independently of any matrix effect. As the study of vinylogous urethane vitrimers is popular, numerous tuning possibilities might emerge in the future not only by implementation of internal catalysis in these networks but also by variation of the backbones nature and length.

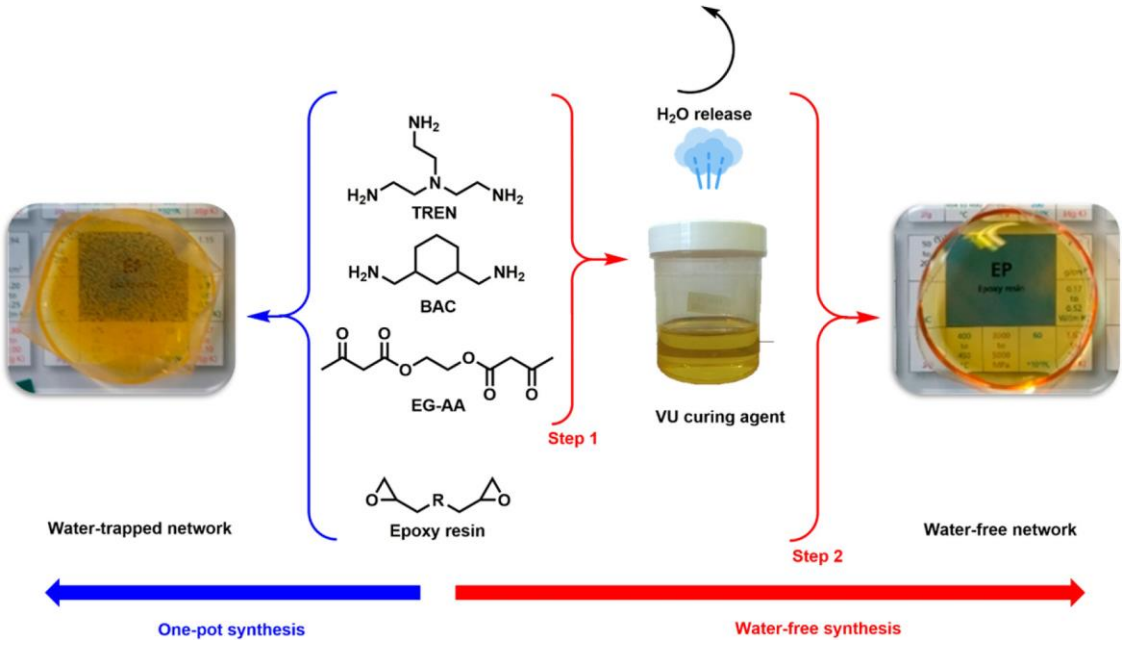

Scheme 34. Two strategies to synthesize VU networks were reported by Spiesschaert et al.[199] The one-pot strategy traps the water released by the reaction. The two-step strategy allows to remove water from the VU curing agent after the first step, allowing water-free network. TREN = tris(2-aminoethyl)amine; BAC = 1,3-bis(aminomethyl)cyclohexane; EG-AA = ethylene glycol–bisacetoacetate.

Hints for Diketoenamine Activation

As previously mentioned, diketoenamines were essentially studied as protecting groups, and there is no extensive knowledge on a potential effect of neighboring groups. Nevertheless, in the work of Augustyns et al.[201] already discussed earlier, a few interesting trends on reactivity were gathered. The two amino groups on lysine did not have the same reactivity toward the exchange of the Dde group. Unprotected ε-NH2 groups could exchange with protected ε-NH_2 and α-NH_2 groups, but free α-NH_2 groups could not exchange Dde with ε-NH_2. This was probably because α-NH_2 groups were too sterically hindered and not nucleophilic enough due to the neighboring electron-withdrawing carboxylic acid. In addition, when 2-acetyldimedone was reacted with polyamine, primary amines were selectively protected.[201] The use of diketoenamines in vitrimers is just starting to emerge, and there is undoubtedly a lot to discover on this chemistry based on the encouraging proof of concept recently disclosed.[204,205]

Effect of the Alkylating Agent on Trialkylsulfonium Salt Exchange

As mentioned before, the knowledge on trialkylsulfonium exchange with thioethers is poor except for the proof-of-concept disclosed by Du Prez's group.[40] Of course, the most obvious parameters to tune the material reprocessability are the nature and quantity of the alkylating agent. Without an alkylating agent, no stress–relaxation was observed in polythioether.[40] Conversely increasing the concentration of the butyl brosylate alkylating agent from 1 to 10 mol % decreased relaxation time at 150 °C from 75 to 10 min.[40] The same behavior was observed by using trimethylsulfonium iodide as an alkylating

agent.[124] Once again, there might be room for internal catalysis studies with this kind of chemistry. Indeed, this exchange reaction was studied on small arylalkyl sulfides in solution. If no change in the kinetics was observed with electron-rich aromatic groups, electron-poor aromatic groups slowed the conversion rate. The alkyl substituent bulkiness also played a role. Phenylalkyl sulfides bearing various alkyl groups were transalkylated with methyl iodide. tert-Butylphenyl sulfides reached full conversion in 25 h, whereas the butyl-, 3-pentyl- and 2,2-dimethylpropyl analogues only reached 70, 60, and 8% conversion, respectively. Diphenyl sulfide showed no conversion at all.[270] This effect has never been studied in materials but underlines the importance of the exchangeable group and might bring useful insights. These articles also underline the effect of the counteranions which nucleophilicity likely plays a role as seen in the transalkylation of triazolium salts.[271-273]

Conclusion and Outlook

Since the invention of vitrimers ten years ago, this class of organic materials has triggered an undeniable enthusiasm in the polymer scientists' community. These materials have not only aroused scientists' curiosity, but their implications for industrial applications are also potentially transformative. Indeed, the rheological behavior of these materials allows a precise control of the viscosity upon heating. This property is central to processing and reprocessing issues. One drawback of these materials is that many vitrimers require catalysts, sometimes at high loadings, which raise concerns for the risks of leaching and premature aging of the materials. Consequently, further work on vitrimers will likely focus on designing catalyst-free vitrimers and on the tuning of the vitrimers' properties, especially the reshaping ability, for the associative systems already known. Parameters such as the cross-linking density, the concentration and availability of exchanging moieties, or the structure and chemical groups of the backbone are already known to influence the behavior of vitrimers. A few studies on the effect of activating groups on the exchange reactions and consequently on materials reshaping are already available. Nonetheless, the use of this strategy to tune the rheologic profile of associative CANs is still in infancy. Beyond the sole tuning of the reshaping parameters, the study of activating group and internal catalysis would be significant progress for understanding how the exchange reactions in vitrimers works, and it would give access to the scientists' community to more intimate knowledge of this innovative class of polymer materials. At the moment knowledge on the phenomena occurring at the molecular scale in vitrimers is still poor. In addition, the mechanistic studies on the exchange mechanisms involved are sometimes only preliminary or even inexistent. Moreover, activating groups can have an influence on the exchange mechanism at work in CANs. They may change an associative exchange into a dissociative one. Mechanistic studies are thus fundamental for the development of CANs. A better comprehension of the phenomena at the molecular scale would indeed allow scientists to design materials with original properties by exploiting such mechanism

changes. Broadening the pool of techniques used to characterize CANs would also undoubtedly help to understand their behavior and contribute to a better and more purposeful design. For example, molecular mobility studies using dielectric spectroscopy or dynamic mechanical analysis could enrich knowledge on these fascinating materials.

References

(1) Montarnal, D.; Capelot, M.; Tournilhac, F.; Leibler, L. Silica-like malleable materials from permanent organic networks. Science (Washington, DC, U. S.) 2011, 334, 965−968.

(2) Pascault, J.-P.; Sautereau, H.; Verdu, J.; Williams, R. J. J. J. Thermosetting Polymers; Marcel Dekker, Inc.: New York, 2002.

(3) Thermal Characterization of Polymeric Materials; Tori, E. A., Ed.; Academic Press Inc.: New York, 1981.

(4) Craven, J. M. U.S. Patent 3435003, 1969.

(5) Bowman, C.; Du Prez, F.; Kalow, J. Introduction to chemistry for covalent adaptable networks. Polym. Chem. 2020, 11, 5295−5296.

(6) Kloxin, C. J.; Scott, T. F.; Adzima, B. J.; Bowman, C. N. Covalent adaptable networks (CANs): A unique paradigm in cross-linked polymers. Macromolecules 2010, 43, 2643−2653.

(7) Chujo, Y.; Sada, K.; Saegusa, T. Reversible Gelation of Polyoxazoline by Means of Diels-Alder Reaction. Macromolecules 1990, 23, 2636−2641.

(8) Goussé, C.; Gandini, A.; Hodge, P. Application of the DielsAlder reaction to polymers bearing furan moieties. 2. Diels-Alder and retro-Diels-Alder reactions involving furan rings in some styrene copolymers. Macromolecules 1998, 31, 314−321.

(9) Jones, J. R.; Liotta, C. L.; Collard, D. M.; Schiraldi, D. A. Crosslinking and modification of poly(ethylene terephthalate-co-2,6- anthracenedicarboxylate) by Diels-Alder reactions with maleimides. Macromolecules 1999, 32, 5786−5792.

(10) Imai, Y.; Itoh, H.; Naka, K.; Chujo, Y. Thermally reversible IPN organic-inorganic polymer hybrids utilizing the Diels-Alder reaction. Macromolecules 2000, 33, 4343−4346.

(11) McElhanon, J. R.; Wheeler, D. R. Thermally responsive dendrons and dendrimers based on reversible furan-maleimide dielsalder adducts. Org. Lett. 2001, 3, 2681−2683.

(12) Chen, X.; Dam, M. A.; Ono, K.; Mal, A.; Shen, H.; Nutt, S. R.; Sheran, K.; Wudl, F. A thermally re-mendable cross-linked polymeric material. Science (Washington, DC, U. S.) 2002, 295, 1698−1702.

(13) Oehlenschlaeger, K. K.; Mueller, J. O.; Brandt, J.; Hilf, S.; Lederer, A.; Wilhelm, M.; Graf, R.; Coote, M. L.; Schmidt, F. G.; Barner-Kowollik, C. Adaptable hetero Diels-Alder networks for fast self-healing under mild conditions. Adv. Mater. 2014, 26, 3561−3566.

(14) Scott, T. F.; Schneider, A. D.; Cook, W. D.; Bowman, C. N. Chemistry: Photoinduced plasticity in cross-linked polymers. Science (Washington, DC, U. S.) 2005, 308, 1615−1617.

(15) Breuillac, A.; Kassalias, A.; Nicolaÿ, R. Polybutadiene Vitrimers Based on Dioxaborolane Chemistry and Dual Networks with Static and Dynamic Cross-links. Macromolecules 2019, 52, 7102−7113.

(16) Taplan, C.; Guerre, M.; Winne, J. M.; Du Prez, F. E. Fast processing of highly crosslinked, low-viscosity vitrimers. Mater. Horiz. 2020, 7, 104−110.

(17) Capelot, M.; Unterlass, M. M.; Tournilhac, F.; Leibler, L. Catalytic control of the vitrimer glass transition. ACS Macro Lett. 2012, 1, 789−792.

(18) Denissen, W.; Rivero, G.; Nicolaÿ, R.; Leibler, L.; Winne, J. M.; Du Prez, F. E. Vinylogous Urethane Vitrimers. Adv. Funct. Mater. 2015, 25, 2451−2457.

(19) Denissen, W.; Winne, J. M.; Du Prez, F. E. Vitrimers: Permanent organic networks with glass-like fluidity. Chemical Science 2016, 7, 30−38.

(20) Obadia, M. M.; Jourdain, A.; Cassagnau, P.; Montarnal, D.; Drockenmuller, E. Tuning the Viscosity Profile of Ionic Vitrimers Incorporating 1,2,3-Triazolium Cross-Links. Adv. Funct. Mater. 2017, 27, 1703258.

(21) Chakma, P.; Morley, C. N.; Sparks, J. L.; Konkolewicz, D. Exploring How Vitrimer-like Properties Can Be Achieved from Dissociative Exchange in Anilinium Salts. Macromolecules 2020, 53, 1233−1244.

(22) Hayashi, M. Implantation of Recyclability and Healability into Cross-Linked Commercial Polymers by Applying the Vitrimer Concept. Polymers 2020, 12, 1322.

(23) Hayashi, M.; Chen, L. Functionalization of triblock copolymer elastomers by cross-linking the end blocks: via trans-N -alkylationbased exchangeable bonds. Polym. Chem. 2020, 11, 1713−1719.

(24) Jourdain, A.; Asbai, R.; Anaya, O.; Chehimi, M. M.; Drockenmuller, E.; Montarnal, D. Rheological Properties of Covalent Adaptable Networks with 1,2,3-Triazolium Cross-Links: The Missing Link between Vitrimers and Dissociative Networks. Macromolecules 2020, 53, 1884−1900.

(25) Elling, B. R.; Dichtel, W. R. Reprocessable Cross-Linked Polymer Networks: Are Associative Exchange Mechanisms Desirable? ACS Cent. Sci. 2020, 6, 1488.

(26) Zhang, L.; Rowan, S. J. Effect of Sterics and Degree of CrossLinking on the Mechanical Properties of Dynamic Poly(alkylureaurethane) Networks. Macromolecules 2017, 50, 5051−5060.

(27) Imbernon, L.; Norvez, S.; Leibler, L. Stress Relaxation and SelfAdhesion of Rubbers with Exchangeable Links. Macromolecules 2016, 49, 2172−2178.

(28) Alabiso, W.; Schlögl, S. The impact of vitrimers on the industry of the future: Chemistry, properties and sustainable forward-looking applications. Polymers 2020, 12, 1660.

(29) Liu, T.; Zhao, B.; Zhang, J. Recent development of repairable, malleable and recyclable thermosetting polymers through dynamic transesterification. Polymer 2020, 194, 122392.

(30) Yang, X.; Guo, L.; Xu, X.; Shang, S.; Liu, H. A fully bio-based epoxy vitrimer: Self-healing, triple-shape memory and reprocessing triggered by dynamic covalent bond exchange. Mater. Des. 2020, 186, 108248.

(31) Van Zee, N. J.; Nicolaÿ, R. Vitrimers: Permanently crosslinked polymers with dynamic network topology. Prog. Polym. Sci. 2020, 104, 101233.

(32) Han, J.; Liu, T.; Hao, C.; Zhang, S.; Guo, B.; Zhang, J. A Catalyst-Free Epoxy Vitrimer System Based on Multifunctional Hyperbranched Polymer. Macromolecules 2018, 51, 6789−6799.

(33) Liu, T.; Zhang, S.; Hao, C.; Verdi, C.; Liu, W.; Liu, H.; Zhang, J. Glycerol Induced Catalyst-Free Curing of Epoxy and Vitrimer Preparation. Macromol. Rapid Commun. 2019, 40, 1800889.

(34) Altuna, F. I.; Pettarin, V.; Williams, R. J. J. Self-healable polymer networks based on the cross-linking of epoxidised soybean oil by an aqueous citric acid solution. Green Chem. 2013, 15, 3360− 3366.

(35) Altuna, F. I.; Pettarin, V.; Williams, R. J. J. Self-healable polymer networks based on the cross-linking of epoxidised soybean oil by an aqueous citric acid solution. Green Chem. 2013, 15, 3360− 3366.

(36) Han, J.; Liu, T.; Hao, C.; Zhang, S.; Guo, B.; Zhang, J. A Catalyst-Free Epoxy Vitrimer System Based on Multifunctional Hyperbranched Polymer. Macromolecules 2018, 51, 6789−6799.

(37) Liu, T.; Zhang, S.; Hao, C.; Verdi, C.; Liu, W.; Liu, H.; Zhang, J. Glycerol Induced Catalyst-Free Curing of Epoxy and Vitrimer Preparation. Macromol. Rapid Commun. 2019, 40, 1800889.

(38) Altuna, F. I.; Hoppe, C. E.; Williams, R. J. J. Epoxy vitrimers with a covalently bonded tertiary amine as catalyst of the transesterification reaction. Eur. Polym. J. 2019, 113, 297−304.

(39) Guerre, M.; Taplan, C.; Nicolaÿ, R.; Winne, J. M.; Du Prez, F. E. Fluorinated Vitrimer Elastomers with a Dual Temperature Response. J. Am. Chem. Soc. 2018, 140, 13272−13284.

(40) Hendriks, B.; Waelkens, J.; Winne, J. M.; Du Prez, F. E. Poly(thioether) Vitrimers via Transalkylation of Trialkylsulfonium Salts. ACS Macro Lett. 2017, 6, 930−934.

(41) Li, Y.; Liu, T.; Zhang, S.; Shao, L.; Fei, M.; Yu, H.; Zhang, J. Catalyst-free vitrimer elastomers based on a dimer acid: robust mechanical performance, adaptability and hydrothermal recyclability. Green Chem. 2020, 22, 870−881.

(42) Wang, S.; Teng, N.; Dai, J.; Liu, J.; Cao, L.; Zhao, W.; Liu, X. Taking Advantages of Intramolecular Hydrogen Bonding to Prepare Mechanically Robust and Catalyst-free Vitrimer. Polymer 2020, 210, 123004.

(43) Guerre, M.; Taplan, C.; Winne, J. M.; Du Prez, F. E. Vitrimers: directing chemical reactivity to control material properties. Chemical Science 2020, 11, 4855−4870.

(44) Cromwell, O. R.; Chung, J.; Guan, Z. Malleable and SelfHealing Covalent Polymer Networks through Tunable Dynamic Boronic Ester Bonds. J. Am. Chem. Soc. 2015, 137, 6492−6495.

(45) Nishimura, Y.; Chung, J.; Muradyan, H.; Guan, Z. Silyl Ether as a Robust and Thermally Stable Dynamic Covalent Motif for Malleable Polymer Design. J. Am. Chem. Soc. 2017, 139, 14881−14884.

(46) Van Lijsebetten, F.; Holloway, J. O.; Winne, J. M.; Du Prez, F. E. Internal catalysis for dynamic covalent chemistry applications and polymer science. Chem. Soc. Rev. 2020, 49, 8425.

(47) Delahaye, M.; Winne, J. M.; Du Prez, F. E. Internal Catalysis in Covalent Adaptable Networks: Phthalate Monoester Transesterification As a Versatile Dynamic Cross-Linking Chemistry. J. Am. Chem. Soc. 2019, 141, 15277−15287.

(48) Zhang, H.; Majumdar, S.; Van Benthem, R. A. T. M.; Sijbesma, R. P.; Heuts, J. P. A. Intramolecularly Catalyzed Dynamic Polyester Networks Using Neighboring Carboxylic and Sulfonic Acid Groups. ACS Macro Lett. 2020, 9, 272−277.

(49) Ramjit, H. G.; Sedgwick, R. D. The Kinetics of Ester-Ester Exchange Reactions by Mass Spectrometry. J. Macromol. Sci., Chem. 1976, 10, 815−824.

(50) Talapatra, K. Studies in ester interchange reactions in glycerides. Doctoral dissertation, University of Calcutta, 1968.

(51) Otera, J. Transesterification. Chem. Rev. 1993, 93, 1449−1470.

(52) Kursanov, D. N.; Korshak, V. V.; Vinogradova, S. V. Investigation of the polyester exchange reaction by the use of deuterium. Bull. Acad. Sci. USSR, Div. Chem. Sci. 1953, 2, 125−128.

(53) Kotliar, A. M. Interchange reactions involving condensation polymers. Macromol. Rev. 1981, 16, 367−395.

(54) Riemenschneider, W.; Bolt, H. M. Esters, Organic. In Ullmann's Encyclopedia of Industrial Chemistry; Wiley-VCH Verlag GmbH & Co.: 2005; pp 645−266.

(55) McCullagh, C. M.; Blackwell, J. 10 - Structure and Properties of Aromatic Liquid Crystalline Copolyesters. In Comprehensive Polymer Science and Supplements; Allen, G., Bevington, J. C., Eds.; Pergamon: 1989; pp 389−410.

(56) Medina, R. M.; Likhatchev, D.; Alexandrova, L.; Sánchez-Solís, A.; Manero, O. Mechanism and kinetics of transesterification in poly(ethylene terephthalate) and poly(ethylene 2,6-naphthalene dicarboxylate) polymer blends. Polymer 2004, 45, 8517−8522.

(57) Parker, V. D.; Baker, A. W. The Mechanism of Ester Acidolysis. Chem. Commun. (London) 1968, 691.

(58) Li, T.; Zhang, X.; Zhang, C.; Li, R.; Liu, J.; Zhang, H.; et al. A Density Functional Theory Study on the Acid-Catalyzed Transesterification Mechanism for Biodiesel Production from Waste Cooking Oils. J. Am. Oil Chem. Soc. 2018, 96, 137−145.

(59) Li, X. Y.; Jiang, J. C.; Wang, K.; Li, K.; Gao, Y. W. Reaction Mechanism and Impact Factors Analysis of Transesterification Biodiesel Production. Adv. Mater. Res. 2011, 343−344, 222−226.

(60) Goodman, I.; Nesbitt, B. F. The structures and reversible polymerization of cyclic oligomers from poly(ethylene terephthalate). Polymer 1960, 1, 384−396.

(61) Lai, C.-L.; Lee, H. M.; Hu, C.-H. Theoretical study on the mechanism of N-heterocyclic carbene catalyzed transesterification reactions. Tetrahedron Lett. 2005, 46, 6265−6270.

(62) Liu, X.; He, H.; Wang, Y.; Zhu, S.; Piao, X. Transesterification of soybean oil to biodiesel using CaO as a solid base catalyst. Fuel 2008, 87, 216−221.

(63) Guo, F.; Wei, N.-N.; Xiu, Z.-L.; Fang, Z. Transesterification mechanism of soybean oil to biodiesel catalyzed by calcined sodium silicate. Fuel 2012, 93, 468−472.

(64) Lin, L.; Silva Gomes, E.; Payan, F.; Jaber, M.; Krafft, J.-M.; Laugel, G.; Lauron-Pernot, H. How the acido-basic properties of Mg silicates and clays govern the catalytic mechanism of transesterification reactions. Catal. Sci. Technol. 2019, 9, 6072−6084.

(65) Guan, Q.; Shang, H.; Liu, J.; Gu, J.; Li, B.; Miao, R.; Chen, Q.; Ning, P. Biodiesel from transesterification at low temperature by AlCl3 catalysis in ethanol and carbon dioxide as cosolvent: Process, mechanism and application. Appl. Energy 2016, 164, 380−386.

(66) Santacesaria, E.; Trulli, F.; Minervini, L.; Di Serio, M.; Tesser, R.; Contessa, S. Kinetic and catalytic aspects in melt transesterification of dimethyl terephthalate with ethylene glycol. J. Appl. Polym. Sci. 1994, 54, 1371−1384.

(67) Hsu, J.-P.; Wong, J.-J. Kinetic modeling of melt transesterification of diphenyl carbonate and bisphenol-A. Polymer 2003, 44, 5851−5857.

(68) Harris, R. F.; Lopez, K. M. Reactions of glycerol with poly(ethylene ether carbonate) polyols. J. Appl. Polym. Sci. 1992, 44, 1663−1670.

(69) Bi, F.-L.; Xi, Z.-H.; Zhao, L. Reaction Mechanisms and Kinetics of the Melt Transesterification of Bisphenol-A and Diphenyl Carbonate. Int. J. Chem. Kinet. 2018, 50, 188−203.

(70) Fan, M.; Zhang, P. Activated Carbon Supported K2CO3 Catalysts for Transesterification of Dimethyl Carbonate with Propyl Alcohol. Energy Fuels 2007, 21, 633−635.

(71) Shaikh, A. A. G.; Sivaram, S. Dialkyl and diaryl carbonates by carbonate interchange reaction with dimethyl carbonate. Ind. Eng. Chem. Res. 1992, 31, 1167−1170.

(72) Du, Z.; Xiao, Y.; Chen, T.; Wang, G. Catalytic study on the transesterification of dimethyl carbonate and phenol to diphenyl carbonate. Catal. Commun. 2008, 9, 239−243.

(73) Liang, Y.; Su, K.; Cao, L.; Gao, Y.; Li, Z. Study on the transesterification and mechanism of bisphenol A and dimethyl carbonate catalyzed by organotin oxide. Chem. Pap. 2019, 73, 2171− 2182.

(74) Samuilov, A. Y.; Samuilov, Y. D. Theoretical study of transesterification of diethyl carbonate with methanol catalyzed by base and Lewis acid. Theor. Chem. Acc. 2019, 138, 24.

(75) Song, Z.; Subramaniam, B.; Chaudhari, R. V. Kinetic modeling and mechanistic investigations of transesterification of propylene carbonate with methanol over an Fe−Mn double metal cyanide catalyst. React. Chem. Eng. 2020, 5, 101−111.

(76) Wang, Q.; Li, C.; Guo, M.; Luo, S.; Hu, C. Transesterification of dimethyl carbonate with phenol to diphenyl carbonate over hexagonal Mg(OH)2 nanoflakes. Inorg. Chem. Front. 2015, 2, 47−54.

(77) Song, Z.; Jin, X.; Hu, Y.; Subramaniam, B.; Chaudhari, R. V. Intriguing Catalyst (CaO) Pretreatment Effects and Mechanistic Insights during Propylene Carbonate Transesterification with Methanol. ACS Sustainable Chem. Eng. 2017, 5, 4718−4729.

(78) Song, Z.; Subramaniam, B.; Chaudhari, R. V. Kinetic Study of CaO-Catalyzed Transesterification of Cyclic Carbonates with Methanol. Ind. Eng. Chem. Res. 2018, 57, 14977−14987.

(79) Samuilov, A. Y.; Korshunov, M. V.; Samuilov, Y. D. Transesterification of Diethyl Carbonate with Methanol Catalyzed by Sodium Methoxide. Russ. J. Org. Chem. 2019, 55, 1338−1343.

(80) Crocella, V.; Tabanelli, T.; Vitillo, J. G.; Costenaro, D.; Bisio,` C.; Cavani, F.; Bordiga, S. A multi-technique approach to disclose the reaction mechanism of dimethyl carbonate synthesis over aminomodified SBA-15 catalysts. Appl. Catal., B 2017, 211, 323−336.

(81) Godard, P.; Dekoninck, J. M.; Devlesaver, V.; Devaux, J. Molten bisphenol-A polycarbonate ← poly(ethylene terephthalate) blends. II. Kinetics of the exchange reaction. J. Polym. Sci., Part A: Polym. Chem. 1986, 24, 3315−3324.

(82) Roettger, M. Associative exchange reactions of boron or nitrogen containing bonds and design of vitrimers. Doctoral dissertation, UniversitéPierre et Marie Curie, Paris VI, 2016.

(83) Fujita, N.; Shinkai, S.; James, T. D. Boronic Acids in Molecular Self-Assembly. Chem. - Asian J. 2008, 3, 1076−1091.

(84) Marco-Dufort, B.; Tibbitt, M. W. Design of moldable hydrogels for biomedical applications using dynamic covalent boronic esters. Mater. Today Chem. 2019, 12, 16−33.

(85) Hall, D. G. Structure, Properties, and Preparation of Boronic Acid Derivatives. Overview of Their Reactions and Applications. In Boronic Acids; Hall, D. G., Ed.; Wiley-VCH Verlag GmbH & Co.: Weinheim, 2005; pp 1−99.

(86) Mancini, R. S.; Lee, J. B.; Taylor, M. S. Boronic esters as protective groups in carbohydrate chemistry: processes for acylation, silylation and alkylation of glycoside-derived boronates. Org. Biomol. Chem. 2017, 15, 132−143.

(87) Roy, D.; Sumerlin, B. S. Glucose-Sensitivity of Boronic Acid Block Copolymers at Physiological pH. ACS Macro Lett. 2012, 1, 529−532.

(88) Wang, L.; Zhang, J.; Kim, B.; Peng, J.; Berry, S. N.; Ni, Y.; Su, D.; Lee, J.; Yuan, L.; Chang, Y.-T. Boronic Acid: A Bio-Inspired Strategy To Increase the Sensitivity and Selectivity of Fluorescent NADH Probe. J. Am. Chem. Soc. 2016, 138, 10394−10397.

(89) Liu, J.; Yang, K.; Shao, W.; Qu, Y.; Li, S.; Wu, Q.; Zhang, L.; Zhang, Y. Boronic Acid-Functionalized Particles with Flexible ThreeDimensional Polymer Branch for Highly Specific Recognition of Glycoproteins. ACS Appl. Mater. Interfaces 2016, 8, 9552−9556.

(90) Brooks, W. L. A.; Sumerlin, B. S. Synthesis and Applications of Boronic Acid-Containing Polymers: From Materials to Medicine. Chem. Rev. 2016, 116, 1375−1397.

(91) Zhao, Z.; Yao, X.; Zhang, Z.; Chen, L.; He, C.; Chen, X. Boronic Acid Shell-Crosslinked Dextran- b-PLA Micelles for AcidResponsive Drug Delivery. Macromol. Biosci. 2014, 14, 1609−1618.

(92) Yang, H.; Zhang, C.; Li, C.; Liu, Y.; An, Y.; Ma, R.; Shi, L. Glucose-Responsive Polymer Vesicles Templated by α-CD/PEG Inclusion Complex. Biomacromolecules 2015, 16, 1372−1381.

(93) Crane, B. C.; Barwell, N. P.; Gopal, P.; Gopichand, M.; Higgs, T.; James, T. D.; Jones, C. M.; Mackenzie, A.; Mulavisala, K. P.; Paterson, W. The Development of a Continuous Intravascular Glucose Monitoring Sensor. J. Diabetes Sci. Technol. 2015, 9, 751− 761.

(94) Sun, X.; James, T. D. Glucose Sensing in Supramolecular Chemistry. Chem. Rev. 2015, 115, 8001−8037.

(95) Bernardini, R.; Oliva, A.; Paganelli, A.; Menta, E.; Grugni, M.; De Munari, S.; Goldoni, L. Stability of Boronic Esters to Hydrolysis: A Comparative Study. Chem. Lett. 2009, 38, 750−751.

(96) Li, H.; Li, H.; Dai, Q.; Li, H.; Brédas, J.-L. Hydrolytic Stability of Boronate Ester-Linked Covalent Organic Frameworks. Adv. Theory Simulations 2018, 1, 1700015.

(97) Deng, C. C.; Brooks, W. L. A.; Abboud, K. A.; Sumerlin, B. S. Boronic Acid-Based Hydrogels Undergo Self-Healing at Neutral and Acidic pH. ACS Macro Lett. 2015, 4, 220−224.

(98) Dong, Y.; Wang, W.; Veiseh, O.; Appel, E. A.; Xue, K.; Webber, M. J.; Tang, B. C.; Yang, X.-W.; Weir, G. C.; Langer, R.; Anderson, D. G. Injectable and Glucose-Responsive Hydrogels Based on Boronic Acid−Glucose Complexation. Langmuir 2016, 32, 8743−8747.

(99) Pettignano, A.; Grijalvo, S.; Häring, M.; Eritja, R.; Tanchoux, N.; Quignard, F.; Díaz Díaz, D. Boronic acid-modified alginate enables direct formation of injectable, self-healing and multistimuliresponsive hydrogels. Chem. Commun. 2017, 53, 3350−3353.

(100) Cash, J. J.; Kubo, T.; Bapat, A. P.; Sumerlin, B. S. RoomTemperature Self-Healing Polymers Based on Dynamic-Covalent Boronic Esters. Macromolecules 2015, 48, 2098−2106.

(101) Cash, J. J.; Kubo, T.; Dobbins, D. J.; Sumerlin, B. S. Maximizing the symbiosis of static and dynamic bonds in self-healing boronic ester networks. Polym. Chem. 2018, 9, 2011−2020.

(102) Kasemsiri, P.; Lorwanishpaisarn, N.; Pongsa, U.; Ando, S. Reconfigurable Shape Memory and Self-Welding Properties of Epoxy Phenolic Novolac/Cashew Nut Shell Liquid Composites Reinforced with Carbon Nanotubes. Polymers 2018, 10, 482.

(103) Röttger, M.; Domenech, T.; Van Der Weegen, R.; Breuillac, A.; Nicolaÿ, R.; Leibler, L. High-performance vitrimers from commodity thermoplastics through dioxaborolane metathesis. Science (Washington, DC, U. S.) 2017, 356, 62−65.

(104) Winne, J. M.; Leibler, L.; Du Prez, F. E. Dynamic covalent chemistry in polymer networks: A mechanistic perspective. Polym. Chem. 2019, 10, 6091−6108.

(105) Brunet, J.; Collas, F.; Humbert, M.; Perrin, L.; Brunel, F.; Lacôte, E.; Montarnal, D.; Raynaud, J. High Glass-Transition Temperature Polymer Networks Harnessing the Dynamic Ring Opening of Pinacol Boronates. Angew. Chem., Int. Ed. 2019, 58, 12216−12222.

(106) Nessler, C. US Patent 1052167, 1913.

(107) Sastri, V. R.; Tesoro, G. C. Reversible crosslinking in epoxy resins. II. New approaches. J. Appl. Polym. Sci. 1990, 39, 1439−1457.

(108) Tesoro, G. C.; Sastri, V. Reversible crosslinking in epoxy resins. I. Feasibility studies. J. Appl. Polym. Sci. 1990, 39, 1425−1437.

(109) Stern, M. D.; Tobolsky, A. V. Stress-Time-Temperature Relations in Polysulfide Rubbers. Rubber Chem. Technol. 1946, 19, 1178−1192.

(110) Matxain, J. M.; Asua, J. M.; Ruipérez, F. Design of new disulfide-based organic compounds for the improvement of selfhealing materials. Phys. Chem. Chem. Phys. 2016, 18, 1758−1770.

(111) Azcune, I.; Odriozola, I. Aromatic disulfide crosslinks in polymer systems: Self-healing, reprocessability, recyclability and more. Eur. Polym. J. 2016, 84, 147−160.

(112) Martin, R.; Rekondo, A.; de Luzuriaga, A. R.; Casuso, P.; Dupin, D.; Cabañero, G.; Grande, H. J.; Odriozola, I. Dynamic sulfur chemistry as a key tool in the design of self-healing polymers. Smart Mater. Struct. 2016, 25, 084017.

(113) Nevejans, S.; Ballard, N.; Miranda, J. I.; Reck, B.; Asua, J. M. The underlying mechanisms for self-healing of poly(disulfide)s. Phys. Chem. Chem. Phys. 2016, 18, 27577−27583.

(114) Michal, B. T.; Jaye, C. A.; Spencer, E. J.; Rowan, S. J. Inherently photohealable and thermal shape-memory polydisulfide networks. ACS Macro Lett. 2013, 2, 694−699.

(115) Belenguer, A. M.; Friščič , T.; Day, G. M.; Sanders, J. K. M.́ Solid-state dynamic combinatorial chemistry: reversibility and thermodynamic product selection in covalent mechanosynthesis. Chem. Sci. 2011, 2, 696.

(116) Rekondo, A.; Martin, R.; Ruiz de Luzuriaga, A.; Cabañero, G.; Grande, H. J.; Odriozola, I. Catalyst-free room-temperature selfhealing elastomers based on aromatic disulfide metathesis. Mater. Horiz. 2014, 1, 237−240.

(117) Fernandes, P. A.; Ramos, M. J. Theoretical Insights into the Mechanism for Thiol/Disulfide Exchange. Chem. - Eur. J. 2004, 10, 257−266.

(118) Bowman, C. N.; Podgórski, M.; Mavila, S.; Huang, S.; Spurgin, N.; Sinha, J. Thiol-Anhydride Dynamic Reversible Networks. Angew. Chem., Int. Ed. 2020, 59, 9345.

(119) El-Zaatari, B. M.; Ishibashi, J. S. A.; Kalow, J. A. Cross-linker control of vitrimer flow. Polym. Chem. 2020, 11, 5339−5345.

(120) Simonds, R. P.; Goethals, E. J. Cationic degradation of poly(propylene sulfide). Makromol. Chem. 1978, 179, 1689−1697.

(121) Simonds, R. P.; Goethals, E. J.; Spassky, N. Cationic degradation of poly(propylene sulfide). Confirmation of the transalkylation reaction. Makromol. Chem. 1978, 179, 1851−1853.

(122) Vancraeynest, W. M.; Goethals, E. J. The formation of cyclic oligomers by cationic degradation of poly(phenylthiirane). Makromol. Chem. 1978, 179, 2613−2619.

(123) Liu, T.; Qiu, R.; Zhu, L.; Yin, S.-F.; Au, C.-T.; Kambe, N. Alkyl Sulfides as Promising Sulfur Sources: Metal-Free Synthesis of Aryl Alkyl Sulfides and Dialkyl Sulfides by Transalkylation of Simple Sulfides with Alkyl Halides. Chem. - Asian J. 2018, 13, 3833−3837.

(124) Tang, Z.; Liu, Y.; Huang, Q.; Zhao, J.; Guo, B.; Zhang, L. A real recycling loop of sulfur-cured rubber through transalkylation exchange of C−S bonds. Green Chem. 2018, 20, 5454−5458.

(125) Corden, C.; Tyrer, D.; Menadue, H.; Calero, J.; Dade, J.; Leferink, R. Global Silicones Council Socio-economic evaluation of the global silicones industry Final Report; Global Silicones Council; Amec Foster Wheeler Environment & Infrastructure UK Limited: 2016.

(126) Osthoff, R. C.; Bueche, A. M.; Grubb, W. T. Chemical StressRelaxation of Polydimethylsiloxane Elastomers. J. Am. Chem. Soc. 1954, 76, 4659−4663.

(127) Kantor, S. W.; Grubb, W. T.; Osthoff, R. C. The Mechanism of the Acid- and Base-catalyzed Equilibration of Siloxanes. J. Am. Chem. Soc. 1954, 76, 5190−5197.

(128) Buese, M. A.; Chang, P.-S. US Patent 5347028, 1994.

(129) Zheng, P.; McCarthy, T. J. A Surprise from 1954: Siloxane Equilibration Is a Simple, Robust, and Obvious Polymer Self-Healing Mechanism. J. Am. Chem. Soc. 2012, 134, 2024−2027.

(130) Schmolke, W.; Perner, N.; Seiffert, S. Dynamically CrossLinked Polydimethylsiloxane Networks with Ambient-Temperature Self-Healing. Macromolecules 2015, 48, 8781−8788.

(131) Angot, F. É lastomeres siloxanes a`liens dynamiques. Doctoral dissertation, UniversitéPierre et Marie Curie, Paris VI, 2016.

(132) Tretbar, C. A.; Neal, J. A.; Guan, Z. Direct Silyl Ether Metathesis for Vitrimers with Exceptional Thermal Stability. J. Am. Chem. Soc. 2019, 141, 16595−16599.

(133) Geyer, R.; Jambeck, J. R.; Law, K. L. Production, use, and fate of all plastics ever made. Sci. Adv. 2017, 3, No. e1700782.

(134) Offenbach, J. A.; Tobolsky, A. V. Chemical relaxation of stress in polyurethane elastomers. J. Colloid Sci. 1956, 11, 39−47.

(135) Colodny, P. C.; Tobolsky, A. V. Chemorheological Study of Polyurethan Elastomers. J. Am. Chem. Soc. 1957, 79, 4320−4323.

(136) Jiang, L.; Liu, Z.; Lei, Y.; Yuan, Y.; Wu, B.; Lei, J. Sustainable Thermosetting Polyurea Vitrimers Based on a Catalyst-Free Process with Reprocessability, Permanent Shape Reconfiguration and SelfHealing Performance. ACS Appl. Polym. Mater. 2019, 1, 3261−3268.

(137) Delebecq, E.; Pascault, J.-P.; Boutevin, B.; Ganachaud, F. On the Versatility of Urethane/Urea Bonds: Reversibility, Blocked Isocyanate, and Non-isocyanate Polyurethane. Chem. Rev. 2013, 113, 80−118.

(138) Fortman, D. J.; Brutman, J. P.; De Hoe, G. X.; Snyder, R. L.; Dichtel, W. R.; Hillmyer, M. A. Approaches to Sustainable and Continually Recyclable Cross-Linked Polymers. ACS Sustainable Chem. Eng. 2018, 6, 11145−11159.

(139) Brutman, J. P.; Fortman, D. J.; De Hoe, G. X.; Dichtel, W. R.; Hillmyer, M. A. Mechanistic Study of Stress Relaxation in UrethaneContaining Polymer Networks. J. Phys. Chem. B 2019, 123, 1432− 1441.

(140) Deshpande, S. R.; Likhite, A. P.; Rajappa, S. Transesterification of alkyl carbamate to aryl carbamate: Effect of varying the alkyl group. Tetrahedron 1994, 50, 10367−10370.

(141) Ying, H.; Zhang, Y.; Cheng, J. Dynamic urea bond for the design of reversible and self-healing polymers. Nat. Commun. 2014, 5, 3218.

(142) Ying, H.; Cheng, J. Hydrolyzable Polyureas Bearing Hindered Urea Bonds. J. Am. Chem. Soc. 2014, 136, 16974−16977.

(143) Zhang, Y.; Ying, H.; Hart, K. R.; Wu, Y.; Hsu, A. J.; Coppola, A. M.; Kim, T. A.; Yang, K.; Sottos, N. R.; White, S. R.; Cheng, J. Malleable and Recyclable Poly(urea-urethane) Thermosets bearing Hindered Urea Bonds. Adv. Mater. 2016, 28, 7646−7651.

(144) Gamardella, F.; De la Flor, S.; Ramis, X.; Serra, A. Recyclable poly(thiourethane) vitrimers with high Tg. Influence of the isocyanate structure. React. Funct. Polym. 2020, 151, 104574.

(145) Li, L.; Chen, X.; Torkelson, J. M. Reprocessable Polymer Networks via Thiourethane Dynamic Chemistry: Recovery of Crosslink Density after Recycling and Proof-of-Principle Solvolysis Leading to Monomer Recovery. Macromolecules 2019, 52, 8207−8216.

(146) Fortman, D. J.; Brutman, J. P.; Cramer, C. J.; Hillmyer, M. A.; Dichtel, W. R. Mechanically Activated, Catalyst-Free Polyhydroxyurethane Vitrimers. J. Am. Chem. Soc. 2015, 137, 14019−14022.

(147) Fortman, D. J.; Brutman, J. P.; Hillmyer, M. A.; Dichtel, W. R. Structural effects on the reprocessability and stress relaxation of crosslinked polyhydroxyurethanes. J. Appl. Polym. Sci. 2017, 134, 44984.

(148) Chen, X.; Li, L.; Jin, K.; Torkelson, J. M. Reprocessable polyhydroxyurethane networks exhibiting full property recovery and concurrent associative and dissociative dynamic chemistry via transcarbamoylation and reversible cyclic carbonate aminolysis. Polym. Chem. 2017, 8, 6349−6355.

(149) Schneider, V.; Frolich, P. K. Mechanism of Formation of Aromatics from Lower Paraffins 1,2. Ind. Eng. Chem. 1931, 23, 1405− 1410.

(150) Olefin Metathesis Theory and Practice; Grela, K., Ed.; John Wiley & Sons, Inc.: Hoboken, NJ, 2014.

(151) Calderon, N.; Chen, H. Y.; Scott, K. W. Olefin metathesis - A novel reaction for skeletal transformations of unsaturated hydrocarbons. Tetrahedron Lett. 1967, 8, 3327−3329.

(152) Handbook of Metathesis (3 Vol. Set); Grubbs, R. H., Ed.; WileyVCH Verlag GmbH & Co. KGaA: Weinheim, 2003; Vols. 1−3.

(153) Chauvin, Y. Olefin Metathesis: The Early Days (Nobel Lecture). Angew. Chem., Int. Ed. 2006, 45, 3740−3747.

(154) Schrock, R. R. Multiple Metal−Carbon Bonds for Catalytic Metathesis Reactions (Nobel Lecture). Angew. Chem., Int. Ed. 2006, 45, 3748−3759.

(155) Grubbs, R. H. Olefin-Metathesis Catalysts for the Preparation of Molecules and Materials (Nobel Lecture). Angew. Chem., Int. Ed. 2006, 45, 3760−3765.

(156) Jean-Louis Hérisson, P.; Chauvin, Y. Catalyse de transformation des olefines par les complexes du tungstène. II. Télomérisation des oléfines cycliques en présence d'oléfines acycliques. Makromol. Chem. 1971, 141, 161−176.

(157) Grubbs, R. H.; Brunck, T. K. Possible intermediate in the tungsten-catalyzed olefin metathesis reaction. J. Am. Chem. Soc. 1972, 94, 2538−2540.

(158) Grubbs, R. H.; Burk, P. L.; Carr, D. D. Mechanism of the olefin metathesis reaction. J. Am. Chem. Soc. 1975, 97, 3265−3267.

(159) Grubbs, R. H.; Carr, D. D.; Hoppin, C.; Burk, P. L. Consideration of the mechanism of the metal catalyzed olefin metathesis reaction. J. Am. Chem. Soc. 1976, 98, 3478−3483.

(160) Lu, Y.-X. X.; Tournilhac, F.; Leibler, L.; Guan, Z. Making insoluble polymer networks malleable via olefin metathesis. J. Am. Chem. Soc. 2012, 134, 8424−8427.

(161) Lu, Y.-X.; Guan, Z. Olefin Metathesis for Effective Polymer Healing via Dynamic Exchange of Strong Carbon−Carbon Double Bonds. J. Am. Chem. Soc. 2012, 134, 14226−14231.

(162) Cerqueira, N. M. F. S. A.; Fernandes, P. A.; Ramos, M. J. Computational Mechanistic Studies Addressed to the Transimination Reaction Present in All Pyridoxal 5′ -Phosphate-Requiring Enzymes. J. Chem. Theory Comput. 2011, 7, 1356−1368.

(163) Taynton, P.; Yu, K.; Shoemaker, R. K.; Jin, Y.; Qi, H. J.; Zhang, W. Heat- or Water-Driven Malleability in a Highly Recyclable Covalent Network Polymer. Adv. Mater. 2014, 26, 3938−3942.

(164) Zhang, H.; Wang, D.; Liu, W.; Li, P.; Liu, J.; Liu, C.; Zhang, J.; Zhao, N.; Xu, J. Recyclable polybutadiene elastomer based on dynamic imine bond. J. Polym. Sci., Part A: Polym. Chem. 2017, 55, 2011−2018.

(165) Liu, H.; Zhang, H.; Wang, H.; Huang, X.; Huang, G.; Wu, J. Weldable, malleable and programmable epoxy vitrimers with high mechanical properties and water insensitivity. Chem. Eng. J. 2019, 368, 61−70.

(166) Hajj, R.; Duval, A.; Dhers, S.; Avérous, L. Network Design to Control Polyimine Vitrimer Properties: Physical Versus Chemical Approach. Macromolecules 2020, 53, 3796−3805.

(167) Snyder, R. L.; Lidston, C. A. L.; De Hoe, G. X.; Parvulescu, M. J. S.; Hillmyer, M. A.; Coates, G. W. Mechanically robust and reprocessable imine exchange networks from modular polyester prepolymers. Polym. Chem. 2020, 11, 5346−5355.

(168) Wang, S.; Ma, S.; Li, Q.; Yuan, W.; Wang, B.; Zhu, J. Robust, Fire-Safe, Monomer-Recovery, Highly Malleable Thermosets from Renewable Bioresources. Macromolecules 2018, 51, 8001−8012.

(169) Zhao, S.; Abu-Omar, M. M. Recyclable and Malleable Epoxy Thermoset Bearing Aromatic Imine Bonds. Macromolecules 2018, 51, 9816−9824.

(170) Geng, H.; Wang, Y.; Yu, Q.; Gu, S.; Zhou, Y.; Xu, W.; Zhang, X.; Ye, D. Vanillin-Based Polyschiff Vitrimers: Reprocessability and Chemical Recyclability. ACS Sustainable Chem. Eng. 2018, 6, 15463−15470.

(171) Liu, Y.; Tang, Z.; Chen, Y.; Wu, S.; Guo, B. Programming dynamic imine bond into elastomer/graphene composite toward mechanically strong, malleable, and multi-stimuli responsive vitrimer. Compos. Sci. Technol. 2018, 168, 214−223.

(172) Zheng, H.; Liu, Q.; Lei, X.; Chen, Y.; Zhang, B.; Zhang, Q. A conjugation polyimine vitrimer: Fabrication and performance. J. Polym. Sci., Part A: Polym. Chem. 2018, 56, 2531−2538.

(173) Dhers, S.; Vantomme, G.; Avérous, L. A fully bio-based polyimine vitrimer derived from fructose. Green Chem. 2019, 21, 1596−1601.

(174) Feng, Z.; Yu, B.; Hu, J.; Zuo, H.; Li, J.; Sun, H.; Ning, N.; Tian, M.; Zhang, L. Multifunctional Vitrimer-Like Polydimethylsiloxane (PDMS): Recyclable, Self-Healable, and Water-Driven Malleable Covalent Networks Based on Dynamic Imine Bond. Ind. Eng. Chem. Res. 2019, 58, 1212−1221.

(175) Yu, Q.; Peng, X.; Wang, Y.; Geng, H.; Xu, A.; Zhang, X.; Xu, W.; Ye, D. Vanillin-based degradable epoxy vitrimers: Reprocessability and mechanical properties study. Eur. Polym. J. 2019, 117, 55−63.

(176) Hogg, J. L.; Jencks, D. A.; Jencks, W. P. Catalysis of transimination through trapping by acids and bases. J. Am. Chem. Soc. 1977, 99, 4772−4778.

(177) Boate, A. R.; Eaton, D. R. Metal complex catalyzed reactions of anils. II. Transimination. Can. J. Chem. 1977, 55, 2426−2431.

(178) Salva, A.; Donoso, J.; Frau, J.; Mun˜oz, F. Density Functional Theory Studies on Transimination of Vitamin B6 Analogues through Geminal Diamine Formation. J. Phys. Chem. A 2004, 108, 11709− 11714.

(179) Ciaccia, M.; Cacciapaglia, R.; Mencarelli, P.; Mandolini, L.; Di Stefano, S. Fast transimination in organic solvents in the absence of proton and metal catalysts. A key to imine metathesis catalyzed by primary amines under mild conditions. Chem. Sci. 2013, 4, 2253.

(180) Ciaccia, M.; Pilati, S.; Cacciapaglia, R.; Mandolini, L.; Di Stefano, S. Effective catalysis of imine metathesis by means of fast transiminations between aromatic−aromatic or aromatic−aliphatic amines. Org. Biomol. Chem. 2014, 12, 3282−3287.

(181) Ciaccia, M.; Di Stefano, S. Mechanisms of imine exchange reactions in organic solvents. Org. Biomol. Chem. 2015, 13, 646−654.

(182) Tóth, G.; Pintér, I.; Messmer, A. Mechanism of the exchange reaction of aromatic Schiff bases. Tetrahedron Lett. 1974, 15, 735− 738.

(183) Abdulla, R. F.; Emmick, T. L.; Taylor, H. M. A New Synthetic Approach to 4(1H)-Pyridone Derivatives. I. 1-Alkyl-3,5-diaryl-4(1H)- pyridones. Synth. Commun. 1977, 7, 305−312.

(184) Friary, R. J.; Seidl, V.; Schwerdt, J. H.; Chan, T.-M.; Cohen, M. P.; Conklin, E. R.; Duelfer, T.; Hou, D.; Nafissi, M.; Runkle, R. L.; Tahbaz, P.; Tiberi, R. L.; Mc Phail, A. T. Intermolecular transaminations of enaminones: a synthesis of fused, polycyclic, N-aryl pyridones. Tetrahedron 1993, 49, 7179−7192.

(185) Ostrowska, K.; Ciechanowicz-Rutkowska, M.; Pilati, T.; Zżuchowski, G. Synthesis and Transamination of Enaminones: Derivatives of 1-Phenyl-4-(phenylhydroxymethylidene)-pyrrolidine2,3,5-trione. Monatsh. Chem. 1999, 130, 555−562.

(186) Sanchez-Sanchez, A.; Fulton, D. A.; Pomposo, J. A. pHresponsive single-chain polymer nanoparticles utilising dynamic covalent enamine bonds. Chem. Commun. 2014, 50, 1871−1874.

(187) Denissen, W.; Droesbeke, M.; Nicolaÿ, R.; Leibler, L.; Winne, J. M.; Du Prez, F. E. Chemical control of the viscoelastic properties of vinylogous urethane vitrimers. Nat. Commun. 2017, 8, 14857.

(188) Bai, L.; Zheng, J. Robust, reprocessable and shape-memory vinylogous urethane vitrimer composites enhanced by sacrificial and self-catalysis Zn(II)−ligand bonds. Compos. Sci. Technol. 2020, 190, 108062.

(189) Guerre, M.; Taplan, C.; Nicolaÿ, R.; Winne, J. M.; Du Prez, F. E. Fluorinated Vitrimer Elastomers with a Dual Temperature Response. J. Am. Chem. Soc. 2018, 140, 13272−13284.

(190) Spiesschaert, Y.; Taplan, C.; Stricker, L.; Guerre, M.; Winne, J. M.; Du Prez, F. E. Influence of the polymer matrix on the viscoelastic behaviour of vitrimers. Polym. Chem. 2020, 11, 5377−5385.

(191) Haida, P.; Abetz, V. Acid-Mediated Autocatalysis in Vinylogous Urethane Vitrimers. Macromol. Rapid Commun. 2020, 41, 2000273.

(192) Spiesschaert, Y.; Guerre, M.; Imbernon, L.; Winne, J. M.; Du Prez, F. Filler reinforced polydimethylsiloxane-based vitrimers. Polymer 2019, 172, 239−246.

(193) Liu, H.; Sui, X.; Xu, H.; Zhang, L.; Zhong, Y.; Mao, Z. SelfHealing Polysaccharide Hydrogel Based on Dynamic Covalent Enamine Bonds. Macromol. Mater. Eng. 2016, 301, 725−732.

(194) Zhang, Y.; Yuan, L.; Guan, Q.; Liang, G.; Gu, A. Developing self-healable and antibacterial polyacrylate coatings with high mechanical strength through crosslinking by multi-amine hyperbranched polysiloxane via dynamic vinylogous urethane. J. Mater. Chem. A 2017, 5, 16889−16897.

(195) Stukenbroeker, T.; Wang, W.; Winne, J. M.; Du Prez, F. E.; Nicolaÿ, R.; Leibler, L. Polydimethylsiloxane quenchable vitrimers. Polym. Chem. 2017, 8, 6590−6593.

(196) Liu, Z.; Zhang, C.; Shi, Z.; Yin, J.; Tian, M. Tailoring vinylogous urethane chemistry for the cross-linked polybutadiene: Wide freedom design, multiple recycling methods, good shape memory behavior. Polymer 2018, 148, 202−210.

(197) Lessard, J. J.; Garcia, L. F.; Easterling, C. P.; Sims, M. B.; Bentz, K. C.; Arencibia, S.; Savin, D. A.; Sumerlin, B. S. Catalyst-Free Vitrimers from Vinyl Polymers. Macromolecules 2019, 52, 2105−2111.

(198) Lessard, J. J.; Scheutz, G. M.; Hughes, R. W.; Sumerlin, B. S. Polystyrene-Based Vitrimers: Inexpensive and Recyclable Thermosets. ACS Appl. Polym. Mater. 2020, 2 (8), 3044−3048.

(199) Spiesschaert, Y.; Guerre, M.; De Baere, I.; Van Paepegem, W.; Winne, J. M.; Du Prez, F. E. Dynamic Curing Agents for AmineHardened Epoxy Vitrimers with Short (Re)processing Times. Macromolecules 2020, 53, 2485−2495.

(200) Wright, T.; Tomkovic, T.; Hatzikiriakos, S. G.; Wolf, M. O. Photoactivated Healable Vitrimeric Copolymers. Macromolecules 2019, 52, 36−42.

(201) Augustyns, K.; Kraas, W.; Jung, G. Investigation on the stability of the Dde protecting group used in peptide synthesis: migration to an unprotected lysine1. J. Pept. Res. 1998, 51, 127−133.

(202) Rohwedder, B.; Mutti, Y.; Dumy, P.; Mutter, M. Hydrazinolysis of Dde: Complete orthogonality with Aloc protecting groups. Tetrahedron Lett. 1998, 39, 1175−1178.

(203) Kocienski, P. J Protecting Groups; Georg Thieme Verlag: Stuttgart, 2005.

(204) Christensen, P. R.; Scheuermann, A. M.; Loeffler, K. E.; Helms, B. A. Closed-loop recycling of plastics enabled by dynamic covalent diketoenamine bonds. Nat. Chem. 2019, 11, 442−448.

(205) He, C.; Christensen, P. R.; Seguin, T. J.; Dailing, E. A.; Wood, B. M.; Walde, R. K.; Persson, K. A.; Russell, T. P.; Helms, B. A. Conformational Entropy as a Means to Control the Behavior of Poly(diketoenamine) Vitrimers In and Out of Equilibrium. Angew. Chem., Int. Ed. 2020, 59, 735−739.

(206) Boucher, D.; Madsen, J.; Caussé, N.; Pébere, N.; Ladmiral, V.;` Negrell, C. Hemiacetal Ester Exchanges, Study of Reaction Conditions and Mechanistic Pathway. Reactions 2020, 1, 89−101.

(207) Fife, T. H.; Benjamin, B. M. General base catalyzed intramolecular transesterification. J. Am. Chem. Soc. 1973, 95, 2059−2061.

(208) Wojtas, K. P.; Lu, J.-Y.; Krahn, D.; Arndt, H.-D. Regioselective Functionalization of 3-Hydroxy-pyridine Carboxylates by Neighboring Group Assistance. Chem. - Asian J. 2016, 11, 2859−2862.

(209) Krivec, M.; Perdih, F.; Kosmrlj, J.; Kočevar, M. Regioselective Hydrolysis and Transesterification of Dimethyl 3-Benzamidophthalates Assisted by a Neighboring Amide Group. J. Org. Chem. 2016, 81, 5732−5739.

(210) Nakanishi, W.; Nakanishi, H.; Yanagawa, Y.; Ikeda, Y.; Oki, M. The effets of the neigboring methoxycarbonyl group and sulfur atom(s) in the carbon-sulfue bond cleavage and the ester exchange in fluorene systems. Chem. Lett. 1983, 12, 105−108.

(211) Bader, A. R.; Vogel, H. A. Transesterification. II. Esters of Strong Organic Acids. J. Am. Chem. Soc. 1952, 74, 3992−3994.

(212) Debnath, S.; Kaushal, S.; Ojha, U. Catalyst Free Partially BioBased Polyester Vitrimers. ACS Appl. Polym. Mater. 2020, 2, 1006− 1013.

(213) Shafer, J. A.; Morawetz, H. Hydrolysis of an Ester with a Neighboring Carboxyl and a Quaternary Ammonium Group. J. Org. Chem. 1962, 27, 2269−2270.

(214) Delahaye, M.; Tanini, F.; Holloway, J. O.; Winne, J. M.; Du Prez, F. E. Double neighbouring group participation for ultrafast exchange in phthalate monoester networks. Polym. Chem. 2020, 11, 5207−5215.

(215) Liu, Y.; Ma, S.; Li, Q.; Wang, S.; Huang, K.; Xu, X.; Wang, B.; Zhu, J. Dynamic transfer auto-catalysis of epoxy vitrimers enabled by the carboxylic acid/epoxy ratio based on facilely synthesized trifunctional monoesterified cyclic anhydrides. Eur. Polym. J. 2020, 135, 109881.

(216) Hao, C.; Liu, T.; Zhang, S.; Liu, W.; Shan, Y.; Zhang, J. Triethanolamine-Mediated Covalent Adaptable Epoxy Network: Excellent Mechanical Properties, Fast Repairing, and Easy Recycling. Macromolecules 2020, 53, 3110−3118.

(217) Li, Y.; Liu, T.; Zhang, S.; Shao, L.; Fei, M.; Yu, H.; Zhang, J. Catalyst-free vitrimer elastomers based on a dimer acid: robust mechanical performance, adaptability and hydrothermal recyclability. Green Chem. 2020, 22, 870−881.

(218) Altuna, F. I.; Casado, U.; Dell'Erba, I. E.; Luna, L.; Hoppe, C. E.; Williams, R. J. J. Epoxy vitrimers incorporating physical crosslinks produced by self-association of alkyl chains. Polym. Chem. 2020, 11, 1337−1347.

(219) Giebler, M.; Sperling, C.; Kaiser, S.; Duretek, I.; Schlögl, S. Epoxy-Anhydride Vitrimers from Aminoglycidyl Resins with High Glass Transition Temperature and Efficient Stress Relaxation. Polymers 2020, 12, 1148.

(220) Craun, G. P.; Sobek, S. M.; Berghoff, W. F. US Patent 4897450, 1990.

(221) Wang, S.; Teng, N.; Dai, J.; Liu, J.; Cao, L.; Zhao, W.; Liu, X. Taking Advantages of Intramolecular Hydrogen Bonding to Prepare Mechanically Robust and Catalyst-free Vitrimer. Polymer 2020, 210, 123004.

(222) Mu, S.; Zhang, Y.; Zhou, J.; Wang, B.; Wang, Z. Recyclable and Mechanically Robust Palm Oil-Derived Epoxy Resins with Reconfigurable Shape-Memory Properties. ACS Sustainable Chem. Eng. 2020, 8, 5296−5304.

(223) He, C.; Shi, S.; Wang, D.; Helms, B. A.; Russell, T. P. Poly(oxime−ester) Vitrimers with Catalyst-Free Bond Exchange. J. Am. Chem. Soc. 2019, 141, 13753−13757.

(224) Tillett, J. G.; Wiggins, D. E. Neighbouring hydroxyl group catalysis in the hydrolysis of carbonate esters. Tetrahedron Lett. 1971, 12, 911−914.

(225) Shaikh, A.-A. G.; Sivaram, S. Organic Carbonates. Chem. Rev. 1996, 96, 951−976.

(226) Brunelle, D. J. Transesterification Chemistry, Low Temperature Reactions of O-Nithophenyl Carbonates. J. Macromol. Sci., Chem. 1991, 28, 95−102.

(227) Kamps, J. H.; Hoeks, T.; Kung, E.; Lens, J. P.; McCloskey, P. J.; Noordover, B. A. J.; Heuts, J. P. A Activated carbonates: enabling the synthesis of differentiated polycarbonate resins via melt transcarbonation. Polym. Chem. 2016, 7, 5294−5303.

(228) Brunelle, D. J.; Smith, W. E. US Patent 4349486, 1982.

(229) Sugiyama, M.; Akiyama, M.; Nishiyama, K.; Okazoe, T.; Nozaki, K. Synthesis of Fluorinated Dialkyl Carbonates from Carbon Dioxide as a Carbonyl Source. ChemSusChem 2020, 13, 1775−1784.

(230) Snyder, R. L.; Fortman, D. J.; De Hoe, G. X.; Hillmyer, M. A.; Dichtel, W. R. Reprocessable Acid-Degradable Polycarbonate Vitrimers. Macromolecules 2018, 51, 389−397.

(231) Zhao, W.; Feng, Z.; Liang, Z.; Lv, Y.; Xiang, F.; Xiong, C.; Duan, C.; Dai, L.; Ni, Y. Vitrimer-Cellulose Paper Composites: A New Class of Strong, Smart, Green, and Sustainable Materials. ACS Appl. Mater. Interfaces 2019, 11, 36090−36099.

(232) Brooks, W. L. A.; Deng, C. C.; Sumerlin, B. S. Structure− Reactivity Relationships in Boronic Acid−Diol Complexation. ACS Omega 2018, 3, 17863−17870.

(233) Piest, M.; Zhang, X.; Trinidad, J.; Engbersen, J. F. J. pHresponsive, dynamically restructuring hydrogels formed by reversible crosslinking of PVA with phenylboronic acid functionalised PPO−PEO−PPO spacers (Jeffamines®). Soft Matter 2011, 7, 11111.

(234) Lauer, M.; Boehnke, H.; Grotstollen, R.; Salehnia, M.; Wulff, G. Chemistry of binding sites. IV. Unusual increase in reactivity of arylboronic acids through neighboring groups. Chem. Informationsdienst 1985, 16, 132−133.

(235) Martínez-Aguirre, M. A.; Villamil-Ramos, R.; GuerreroAlvarez, J. A.; Yatsimirsky, A. K. Substituent Effects and pH Profiles for Stability Constants of Arylboronic Acid Diol Esters. J. Org. Chem. 2013, 78, 4674−4684.

(236) Figueiredo, T.; Ogawa, Y.; Jing, J.; Cosenza, V.; Jeacomine, I.; Olsson, J. D. M.; Gerfaud, T.; Boiteau, J.-G.; Harris, C.; Auzély-Velty, R. Self-crosslinking smart hydrogels through direct complexation between benzoxaborole derivatives and diols from hyaluronic acid. Polym. Chem. 2020, 11, 3800−3811.

(237) Wulff, G.; Lauer, M.; Böhnke, H. Rapid Proton Transfer as Cause of an Unusually Large Neighboring Group Effect. Angew. Chem., Int. Ed. Engl. 1984, 23, 741−742.

(238) Zhu, L.; Shabbir, S. H.; Gray, M.; Lynch, V. M.; Sorey, S.; Anslyn, E. V. A Structural Investigation of the N-B Interaction in an o-(N,N-Dialkylaminomethyl)arylboronate System. J. Am. Chem. Soc. 2006, 128, 1222−1232.

(239) Collins, B. E.; Metola, P.; Anslyn, E. V. On the rate of boronate ester formation in ortho-aminomethyl-functionalised phenyl boronic acids. Supramol. Chem. 2013, 25, 79−86.

(240) Aoyagi, M.; Ushioda, M.; Seio, K.; Sekine, M. A new 2',3'-cis diol protecting group required for the solid-phase synthesis of capped oligonucleotide derivatives. Nucleic Acids Symp. Ser. 2003, 3, 149−150.

(241) Zhang, X.; Wang, S.; Jiang, Z.; Li, Y.; Jing, X. Boronic Ester Based Vitrimers with Enhanced Stability via Internal Boron-Nitrogen Coordination. J. Am. Chem. Soc. 2020, 142 (52), 21852−21860.

(242) Ohishi, T.; Iki, Y.; Imato, K.; Higaki, Y.; Takahara, A.; Otsuka, H. Insertion Metathesis Depolymerization of Aromatic Disulfidecontaining Dynamic Covalent Polymers under Weak Intensity Photoirradiation. Chem. Lett. 2013, 42, 1346−1348.

(243) Ruipérez, F.; Galdeano, M.; Gimenez, E.; Matxain, J. M. Sulfenamides as Building Blocks for Efficient Disulfide-Based SelfHealing Materials. A Quantum Chemical Study. ChemistryOpen 2018, 7, 248−255.

(244) Sarma, R. J.; Otto, S.; Nitschke, J. R. Disulfides, Imines, and Metal Coordination within a Single System: Interplay between Three Dynamic Equilibria. Chem. - Eur. J. 2007, 13, 9542−9546.

(245) Caraballo, R.; Rahm, M.; Vongvilai, P.; Brinck, T.; Ramström, O. Phosphine-catalyzed disulfide metathesis. Chem. Commun. 2008, 6603.

(246) Yu, H.; Wang, Y.; Yang, H.; Peng, K.; Zhang, X. Injectable self-healing hydrogels formed via thiol/disulfide exchange of thiol functionalized F127 and dithiolane modified PEG. J. Mater. Chem. B 2017, 5, 4121.

(247) Li, Z.-J.; Zhong, J.; Liu, M.-C.; Rong, J.-C.; Yang, K.; Zhou, J.- Y.; Shen, L.; Gao, F.; He, H.-F. Investigation on Self-healing Property of Epoxy Resins Based on Disulfide Dynamic Links. Chin. J. Polym. Sci. 2020, 38, 932−940.

(248) Amamoto, Y.; Otsuka, H.; Takahara, A.; Matyjaszewski, K. Self-Healing of Covalently Cross-Linked Polymers by Reshuffling Thiuram Disulfide Moieties in Air under Visible Light. Adv. Mater. 2012, 24, 3975−3980.

(249) Wright, P.; Semlyen, J. Equilibrium ring concentrations and the statistical conformations of polymer chains: Part 3. Substituent effects in polysiloxane systems. Polymer 1970, 11, 462−471.

(250) Saed, M. O.; Terentjev, E. M. Catalytic Control of Plastic Flow in Siloxane-Based Liquid Crystalline Elastomer Networks. ACS Macro Lett. 2020, 9, 749−755.

(251) Berkefeld, A.; Guerra, C. F.; Bertermann, R.; Troegel, D.; Daiß, J. O.; Stohrer, J.; Bickelhaupt, F. M.; Tacke, R. Silicon α-Effect: A Systematic Experimental and Computational Study of the Hydrolysis of C α- and C γ-Functionalized Alkoxytriorganylsilanes of the Formula Type ROSiMe2(CH2)nX (R = Me, Et; n = 1, 3; X = Functional Group). Organometallics 2014, 33, 2721−2737.

(252) Zych, A.; Pinalli, R.; Soliman, M.; Vachon, J.; Dalcanale, E. Polyethylene vitrimers via silyl ether exchange reaction. Polymer 2020, 199, 122567.

(253) Liu, W.-X.; Zhang, C.; Zhang, H.; Zhao, N.; Yu, Z.-X.; Xu, J. Oxime-Based and Catalyst-Free Dynamic Covalent Polyurethanes. J. Am. Chem. Soc. 2017, 139, 8678−8684.

(254) Subrayan, R. P.; Zhang, S.; Jones, F. N.; Swarup, V.; Yezrielev, A. I. Reactions of phenolic ester alcohol with aliphatic isocyanatesTranscarbamoylation of phenolic to aliphatic urethane: a 13C-NMR study. J. Appl. Polym. Sci. 2000, 77, 2212−2228.

(255) Mukaiyama, T.; Iwanami, M. On the Thermal Dissociation of Organic Compounds. XI. The Effects of the Substituents on the Thermal Dissociation of Urethans in Amine Solvent. J. Am. Chem. Soc. 1957, 79, 73−76.

(256) Young, Y. H.; Lin, H. M.; Lin, M. Y. Studies of Thermal Transesterification of Phenylurethane by High Pressure Liquid Chromatograph. J. Chin. Chem. Soc. 1978, 25, 225−229.

(257) Mormann, W.; Frank, P.; Schupp, T.; Seel, K. Reactions of Nacetylcysteine adducts of aromatic (di)isocyanates with functional groups of organic molecules: transcarbamoylation reactions in aqueous buffer and in an organic solvent. EXCLI J. 2008, 7, 19−43.

(258) Chen, X.; Hu, S.; Li, L.; Torkelson, J. M. Dynamic Covalent Polyurethane Networks with Excellent Property and Cross-Link Density Recovery after Recycling and Potential for Monomer Recovery. ACS Appl. Polym. Mater. 2020, 2, 2093−2101.

(259) Zhang, D.; Chen, H.; Dai, Q.; Xiang, C.; Li, Y.; Xiong, X.; Zhou, Y.; Zhang, J. Stimuli-Mild, Robust, Commercializable Polyurethane-Urea Vitrimer Elastomer via N,N′ -Diaryl Urea Crosslinking. Macromol. Chem. Phys. 2020, 221, 1900564.

(260) Liu, Y.; Tang, Z.; Chen, J.; Xiong, J.; Wang, D.; Wang, S.; Wu, S.; Guo, B. Tuning the mechanical and dynamic properties of imine bond crosslinked elastomeric vitrimers by manipulating the crosslinking degree. Polym. Chem. 2020, 11, 1348−1355.

(261) Giuseppone, N.; Schmitt, J.-L.; Schwartz, E.; Lehn, J.-M. Scandium(III) Catalysis of Transimination Reactions. Independent and Constitutionally Coupled Reversible Processes. J. Am. Chem. Soc. 2005, 127, 5528−5539.

(262) Schaufelberger, F.; Hu, L.; Ramström, O. trans -Symmetric Dynamic Covalent Systems: Connected Transamination and Transimination Reactions. Chem. - Eur. J. 2015, 21, 9776−9783.

(263) Wang, S.; Ma, S.; Li, Q.; Xu, X.; Wang, B.; Huang, K.; Liu, Y.; Zhu, J. Facile Preparation of Polyimine Vitrimers with Enhanced Creep Resistance and Thermal and Mechanical Properties via Metal Coordination. Macromolecules 2020, 53, 2919−2931.

(264) Okuyama, T.; Nagamatsu, H.; Kitano, M.; Fueno, T. Nucleophilic catalysis of hydrolysis of a Schiff base by amines. Intramolecular catalysis of transimination. J. Org. Chem. 1986, 51, 1516−1521.

(265) Toullec, J.; Razafindralambo, R. Intramolecular base catalysis in N-benzylideneaniline transimination by (dimethylamino)- alkylamines in methanol. J. Org. Chem. 1987, 52, 1646−1647.

(266) Chao, A.; Negulescu, I.; Zhang, D. Dynamic Covalent Polymer Networks Based on Degenerative Imine Bond Exchange: Tuning the Malleability and Self-Healing Properties by Solvent. Macromolecules 2016, 49, 6277−6284.

(267) Aljuhani, M. A.; Barman, S.; Abou-Hamad, E.; Gurinov, A.; Ould-Chikh, S.; Guan, E.; Jedidi, A.; Cavallo, L.; Gates, B. C.; Pelletier, J. D. A.; Basset, J.-M. Imine Metathesis Catalyzed by a SilicaSupported Hafnium Imido Complex. ACS Catal. 2018, 8, 9440− 9446.

(268) Schaufelberger, F.; Seigel, K.; Ramström, O. Hydrogen-Bond Catalysis of Imine Exchange in Dynamic Covalent Systems. Chem. - Eur. J. 2020, 26, 15581−15588.

(269) Feng, Z.; Jia, S.; Chen, H.; You, L. Modulation of imine chemistry with intramolecular hydrogen bonding: Effects from orthoOH to NH. Tetrahedron 2020, 76, 131128.

(270) Nawrot, D.; Kolenic, M.; Kuneš , J.; Kostelansky, F.; Miletin,̌ M.; Novakova, V.; Zimcik, P. Transalkylation of alkyl aryl sulfides with alkylating agents. Tetrahedron 2018, 74, 594−599.

(271) Obadia, M. M.; Mudraboyina, B. P.; Serghei, A.; Montarnal, D.; Drockenmuller, E. Reprocessing and Recycling of Highly CrossLinked Ion-Conducting Networks through Transalkylation Exchanges of C−N Bonds. J. Am. Chem. Soc. 2015, 137, 6078−6083.

(272) Chakma, P.; Digby, Z. A.; Shulman, M. D.; Kuhn, L. R.; Morley, C. N.; Sparks, J. L.; Konkolewicz, D. Anilinium Salts in Polymer Networks for Materials with Mechanical Stability and Mild Thermally Induced Dynamic Properties. ACS Macro Lett. 2019, 8, 95−100.

(273) Chakma, P.; Morley, C. N.; Sparks, J. L.; Konkolewicz, D. Exploring How Vitrimer-like Properties Can Be Achieved from Dissociative Exchange in Anilinium Salts. Macromolecules 2020, 53, 1233−1244.

Conclusion du chapitre I

Dans ce chapitre bibliographique, un état de l'art des réactions d'échange mises en œuvre dans des vitrimères a été dressé. Les mécanismes d'échanges ont été discutés, ainsi que leurs implications sur les propriétés du matériau, rhéologiques notamment. D'autre part, cette étude a permis de mettre en lumière les différentes manières d'activer ces réactions d'échange, pour chacune d'entre elles. En outre, ces stratégies n'ont pas été limitées à celles décrites dans la synthèse de matériaux activés, mais ont été élargies à des effets observés dans d'autres domaines de la chimie, organique notamment. L'objectif ne se limite pas à un catalogue de l'existant dans le domaine des vitrimères, il est de proposer des stratégies encore inutilisées, pour de futures études, afin d'approfondir la connaissance de ce type de matériaux et de leur caractère dynamique.

Les premiers vitrimères décrits étaient basés sur des réseaux polyesters. Bien que de nombreuses autres réactions aient été utilisées depuis, les polyesters présentent l'avantage d'être facilement produits en quantités importantes. En effet, ils peuvent être synthétisés à partir d'époxy et d'acides carboxyliques polyfonctionnels, et beaucoup de ces monomères existent dans le commerce pour des utilisations à l'échelle industrielle.

Cependant, l'utilisation de catalyseurs tels que le zinc (II) ou le triazabicyclodecene (TBD) en grande quantités pose un problème pour l'industrialisation de tels matériaux, et leur stabilité, en usage et au moment de leur recyclage.

La précédente étude bibliographique a permis également d'identifier des moyens d'activer les réactions d'échange. Dans le cas de la transestérification qui a lieu dans les vitrimères polyesters, les effets inductifs peuvent diminuer la force de la liaison ester et rendre le carbone du carbonyle plus électrophile vis-à-vis du –OH nucléophile à l'origine de l'échange.

Le fluor a été identifié comme un candidat prometteur afin de créer un effet inductif suffisamment intense pour transestérifier sans catalyseur. En effet, le fluor est l'atome le plus électronégatif, il devrait donc fortement augmenter le caractère électrophile du carbonyle. De plus, la chimie des polymères fluorés est une compétence historique de l'équipe polymères de l'ICGM, c'est donc tout naturellement que cette idée d'activation par le fluor a germé.

Dans la suite de ce manuscrit, nous détaillerons la stratégie définie en termes de structures de monomères et de position des atomes de fluor, afin d'obtenir un réseau tridimensionnel, de garantir l'effet d'activation escompté sur la liaison ester, et de veiller à former des fonctions –OH lors de la polymérisation, qui sont indispensables à la réaction de transestérification.

CHAPITRE II : SYNTHESE ET CARACTERISATION D'UN VITRIMERE DE TRANSESTERIFICATION SANS CATALYSEUR ACTIVE PAR DES α,α-DIFLUOROESTERS

Chapitre II : Synthèse et caractérisation d'un vitrimère de transestérification sans catalyseur activé par des α,α-difluoroesters

Introduction du chapitre 2

Dans le premier volet de ces travaux, l'objectif est de démontrer que l'effet inductif des atomes de fluor sur la liaison ester a pour effet de favoriser la transestérification dans des matériaux polyester. A cette fin, le système de monomères utilisé doit être conçu en respectant plusieurs contraintes, qui constituent le cahier des charges.

Tout d'abord, la question de la position de l'atome de fluor par rapport à la liaison ester s'est posée. La fonctionnalisation peut se faire du côté du groupe partant (R_1-COO-**R_2**) ou du côté du carbonyle (**R_1**-COO-R_2). Dans le premier cas, le groupement fluoré va diminuer la densité électronique de l'oxygène du groupe partant (HO-R_2). Ainsi, lorsque ce groupe se retrouvera à l'état « libre » (OH libre), le caractère nucléophile de l'oxygène sera diminué. Par suite, la réactivité du groupe hydroxyle vis-à-vis de la transestérification s'en trouvera diminuée. En revanche, sous la forme ester, le groupe partant sera meilleur. L'effet sur la vitesse de transestérification sera donc vraisemblablement limité. En revanche, si le groupement fluoré est placé du côté du carbonyle, la densité électronique sur l'atome de carbone va diminuer et le rendre plus nucléophile, favorisant la transestérification. La fonctionnalisation doit donc se faire du côté du carbonyle (Figure D). De plus, afin de maximiser l'effet inductif du fluor, et comme les effets inductifs sont très localisés, le choix de placer les atomes de fluor au plus prés du carbonyle a été fait. Ainsi, les travaux décrits porteront sur des α,α-difluoro esters.

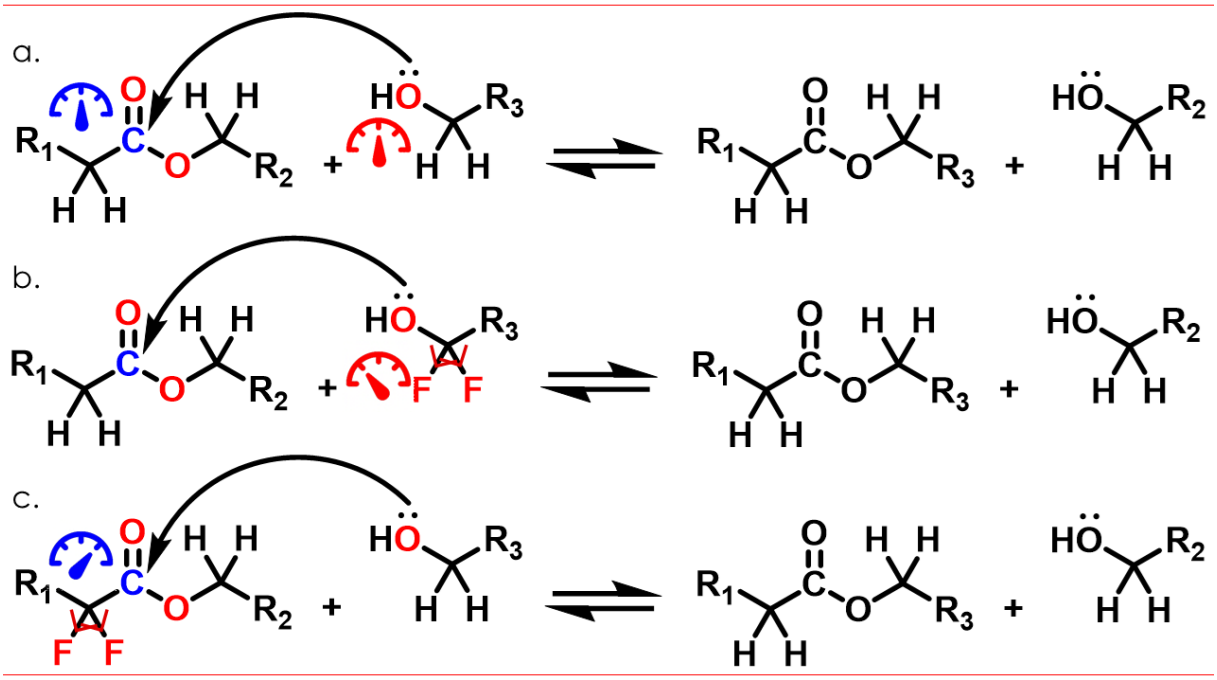

Figure D. a. réaction de transestérification b. désactivation par des atomes de fluor sur le nucléophile et c. activation par des atomes de fluor sur l'électrophile

Il convient de choisir les fonctions chimiques qui conduiront au matériau polyester. La synthèse peut impliquer la condensation d'acides carboxyliques et de polyols, la transestérification d'esters plurifonctionnels avec un polyol, ou encore l'ouverture de fonction époxyde avec des acides carboxyliques. La voie par condensation est souvent difficile à mettre en œuvre, requiert des températures élevées, au-delà de 200 °C, et un montage permettant une élimination efficace de l'eau. Cette voie est utilisée industriellement dans la synthèse de résines alkydes (ou glycéro-phtaliques) utilisées dans les peintures,[4] mais le contrôle de ces réactions est difficile et les polymères obtenus présentent généralement une importante variabilité (distribution de masses molaires, variabilité d'un lot à l'autre). La voie par transestérification est utilisée pour la synthèse industrielle du poly(éthylène téréphtalate) (PET) à partir de téréphtalate de diméthyle et de l'éthylène glycol.[5] Là encore, la réaction a lieu à haute température et nécessite l'élimination en continu du méthanol formé. La dernière voie envisagée semble la plus avantageuse. En effet, l'ouverture d'un cycle oxirane par un acide carboxylique conduit à la formation de β-hydroxyesters. Ces fonctions –OH formées sont d'un intérêt majeur, puisqu'elles sont à l'origine de la réaction de transestérification, qui ne peut avoir lieu en leur absence. De plus, beaucoup de prépolymères époxy sont disponibles dans le commerce. Cette dernière voie a donc été retenue pour ce projet.

Compte-tenu des choix de former des α,α-difluoro esters et de l'utilisation de la réaction époxy-acide pour former le réseau, il est nécessaire de synthétiser des α,α-difluoro acides carboxyliques. Les monomères utilisés doivent être de fonctionnalité moyenne supérieure à 2, afin de créer un réseau tridimensionnel et non des chaînes linéaires. La première voie envisagée a été la synthèse d'acides α,α-difluorés difonctionnels, et de les faire réagir sur des époxy commerciaux tri- ou tétrafonctionnels. Cependant, après étude du marché des époxy, plusieurs écueils potentiels ont été identifiés. Tout d'abord, beaucoup des prépolymères époxy commerciaux vendus sont solides, et la plupart des acides carboxyliques polyfonctionnels sont solides également, ce qui peut poser des problèmes au moment du mélange, et provoquer la formation de matériaux inhomogènes. D'autre part, ces références commerciales sont souvent des mélanges de structures chimiques différentes difficiles à distinguer, ce qui peut nuire à la rigueur nécessaire à l'obtention d'une preuve de concept solide et indiscutable. Enfin, du fait de ces mélanges, la fonctionnalité moyenne observée est souvent à peine supérieure à

[4] Chardon, F.; Denis, M.; Negrell, C.; Caillol, S. Hybrid Alkyds, the Glowing Route to Reach Cutting-Edge Properties? Prog. Org. Coatings 2021, 151, 106025.
[5] De Vos, L.; Van de Voorde, B.; Van Daele, L.; Dubruel, P.; Van Vlierberghe, S. Poly(Alkylene Terephthalate)s: From Current Developments in Synthetic Strategies towards Applications. Eur. Polym. J. 2021, 161, 110840.

2. Cette faible fonctionnalité peut remettre en cause la formation d'un réseau tridimensionnel, et le caractère vitrimère du matériau final peut être mis en doute.

Afin de palier ces préoccupations, une stratégie différente a finalement été adoptée. Le choix s'est porté sur la synthèse d'un acide α,α-difluoré trifonctionnel, qu'il est possible de faire réagir avec un époxy difonctionnel pour former un réseau covalent. L'intérêt est qu'il existe des époxy difonctionnels dont la pureté est suffisamment élevée pour ne pas nuire au caractère tridimensionnel du réseau. De plus, certains de ces époxy sont des liquides, ce qui simplifie le procédé de synthèse du polymère. Le diglycidyléther de butanediol (BDGE) a été identifié comme un candidat intéressant. En effet il est vendu avec une pureté supérieure à 95 %, il est liquide à température ambiante et présente une faible viscosité (16,65 mPa.s à 20 °C).

Ce chapitre décrit la synthèse d'un acide α,α-difluoré trifonctionnel, sa caractérisation, sa polymérisation avec le BDGE, et les caractérisations du matériau dynamique obtenu. Ces travaux ont été décrits dans une publication dans le journal *Polymer Chemistry*.[6]

[6] Cuminet, F.; Berne, D.; Lemouzy, S.; Dantras, E.; Joly-Duhamel, C.; Caillol, S.; Leclerc, E.; Ladmiral, V. Polym. Chem. 2022, 8, 5255–5446.

Catalyst-free transesterification vitrimers: activation via α-difluoroesters

Florian Cuminet,[a] Dimitri Berne,[a] Sébastien Lemouzy,[a] Éric Dantras,[b] Christine Joly-Duhamel,[a] Sylvain Caillol,[a] Éric Leclerc[a] and Vincent Ladmiral[a]

[a]ICGM, Univ Montpellier, CNRS, ENSCM, Montpellier, France
[b]CIRIMAT Physique des Polymères, Université de Toulouse, CNRS, Université Toulouse 3 - Paul Sabatier, 31062 Toulouse, France

1. Abstract

Transesterification vitrimers often require high catalyst loadings to achieve 3D networks reprocessable at moderately high temperature. The addition of an activating group close to the ester bonds allows to synthesize catalyst-free transesterification vitrimers. Here, we unveil the effect of the α-difluoromethylene group as a novel activating group for such materials. Fluorine features exceptional properties, in particular a strong electronegativity enabling CF_2 groups to activate the epoxy-acid polymerization, and more interestingly also the transesterification reaction on adjacent esters. Consequently, this fluorinated group affords the easy synthesis of a highly crosslinked reprocessable material that do not require any metallic or organic catalyst. This vitrimer is endowed with advantageous reprocessing abilities and underwent 10 consecutive cycles without loss of mechanical properties. In brief, the vitrimer combines durability, recyclability and is catalyst-free. This discovery is one step further towards recyclable greener polymers.

2. Introduction

For decades, polymer materials have been classified depending on their macromolecular structure. On the one hand are amorphous thermoplastics, composed of entangled linear chains. In these materials, polymer chains are not covalently bonded, and are able to slide on one another.[1] This translates, at the macroscopical scale, in their solubility in suitable solvents and in their ability to be reshaped upon heating. On the other hand are thermosets, composed of a 3D network. Theoretically, a thermoset is a single infinite macromolecule forming a covalently crosslinked network. This permanent structure leads to insolubility in solvents, and prevents recycling by simple thermal methods.[1,2] In the pursuit of greener, more sustainable polymers, thermosets remain a challenge for recycling.[3] Yet, they are assets in many applications for which thermal and chemical resistances are required. A third class of polymer materials consisting in a covalent crosslinked network in which the covalent bonds can be exchanged by reversible chemical reactions was proposed. They were called CANs, short for Covalent Adaptable

Networks. In 2005, Bowman *et al.*[4] synthesized a covalently bonded 3D network alike thermosets, endowed with covalent bonds able to exchange *via* an associative mechanism upon irradiation with visible light. This concept was further developed by Leibler *et al.*[5] in 2011 with a material based on transesterification activated upon heating. This material was insoluble in common organic solvents even at high temperature, but able to flow and to be reshaped upon heating. Interestingly, this new kind of material exhibited an Arrhenian viscosity decrease with increasing temperature, a feature usually observed for inorganic glasses, or more generally for "strong" glasses in accordance with the work of Angell.[6] This analogy inspired the name vitrimers for such materials. Since this discovery, other kinds of exchangeable bonds such as carbonates,[7] boronic esters,[8,9] disulfides,[10,11] silyl ethers,[12,13] urethanes,[14–18] olefins,[19] imines,[20–23] vinylogous urethanes,[24–26] diketoenamines,[27] acylated acetals,[28,29] and trialkylsulfonium salts[30,31] have been investigated. Despite the success of vitrimers in materials research, they have yet to be implemented in industrial and commercial applications as they are not adapted to the recycling processes existing for thermoplastics.[32] Moreover, long reprocessing times at high temperatures can trigger premature degradation of the vitrimer after repeated reshaping processes.[33] To accelerate the reshaping process, one solution is the use of catalysts. However, some exchange reactions such as transesterification are so slow that they often require high loadings.[5] Yet, the use of catalysts raise concerns about the materials ageing or the risk of leaching,[34,35] which is undesirable for application such as food-contact materials for example. The first catalyst-free vitrimer was based on vinylogous urethanes exchange. This reaction is fast enough to afford short reprocessing times without catalyst.[25] Since this seminal article, other examples of catalyst-free vitrimers based on fast exchange reactions were proposed, such as hydroxyurethanes,[16] hemiacetal esters,[28] trialkylsulfonium salts,[31] oxime-esters[33] and imines.[36] Lowering the crosslinking density and increasing the number of exchangeable moieties were proven to enhance the reshaping abilities of catalyst-free materials.[37–41] However, since these parameters also influence the materials mechanical properties, this strategy may not be suitable to a wide range of applications. To overcome the risk of catalyst leaching, some vitrimers were also synthesized with a catalyst (amines for instance) embedded in the network.[42–44]

In 2015, Guan *et al.* proposed to implement in vitrimers the concept of neighboring group participation (NGP), well-known in the field of organic chemistry but new to the field of vitrimers.[45] Materials crosslinked using difunctional dioxaborolane and possessing neighboring amino groups relaxed faster than the one deprived of such groups. The potential of internal catalysis or internal activation and neighboring group participation (NGP) to tune CANs has recently been reviewed.[46,47] In their review, Van Lijsebetten *et al.*[46] made a clear distinction between NGP for which the neighboring group is

involved with a covalent bond at some point of the reaction, and the broader concept of internal catalysis including effects such as inductive effects.

The present work focuses on transesterification vitrimers, as they usually require a catalyst. To address the concerns raised by the use of external catalysts, some functional groups were reported to be efficient for NGP, such as phthalate monoesters[48] or benzenesulfonic acid groups.[49] Such groups modify the transesterification mechanism and facilitate the exchange. Examples of activation by inductive effect were reported on Meldrum's acids in PDMS[50] or in polyimine vitrimers for instance.[51] In transesterification vitrimers, malonates were used to activate the exchange reaction.[52] Because of its high electronegativity, fluorine has a strong potential to activate bond exchanges. Indeed, the carbonyl group of fluorinated esters is known to be very electrophilic,[53] which facilitates hydrolysis and nucleophilic attack.[54,55] Fluorine substitution thus appear as a good strategy to activate transesterification reactions. Recently, a CF_3 group positionned on the α carbon of esters was demonstrated to have a significant activating effect on transesterification in polyester networks.[56] In the present work, fluorine atoms were added one atom closer to the ester bond and α-diflluoro esters are implemented for the first time to design a catalyst-free transesterification vitrimer. A trifunctional α-difluoro carboxylic acid was prepared and used in combination with a commercial diepoxide (butanediol diglycidyl ether, BDGE) to prepare an epoxy-acid network which displayed insolubility in organic solvents, but was able to be reshaped under relatively mild conditions without catalyst.

3. Results and discussion

α-Difluoro carboxylic acid monomer synthesis

Transesterification vitrimers require dangling hydroxy groups for the exchange reactions to happen. Fortunately, the epoxy opening by a carboxylic acid produces such groups in beta position to the ester. The strategy developed here therefore relies on the use of a trifunctional carboxylic acid monomer, and a commercial diepoxide to obtain a 3D network. To maximize the inductive effect of fluorine on the ester bond, the strongest fluorinated activating group (CF_2) should be positioned as close as possible to the exchangeable bond. A trifunctional monomer bearing three α-difluorocarboxylic acids was thus designed and synthesized in two steps from a commercial triphenol (1,1,1-tris(4-hydroxyphenyl)ethane, "TPE"). TPE was reacted with ethyl bromodifluoroacetate at 70 °C for 40 hours to obtain by nucleophilic substitution a mixture of the di- and trisubstituted esters (15 and 60 mol% respectively). After column chromatography, the resulting α-difluoro triester then underwent facile saponification to yield, after appropriate workup, the desired α-difluoro triacid (TPE-TAF) as a white waxy solid with an overall yield of 50% (Scheme 1).

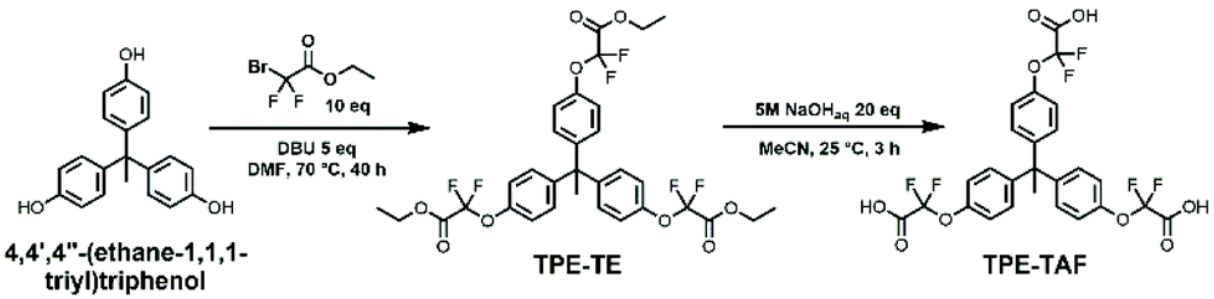

Scheme 1. 2-Step synthesis of the trifunctional α-difluoro carboxylic acid TPE-TAF.

Polymerization and curing

Butanediol diglycidyl ether (BDGE, Annexes A Figures S14, S15 and sections A, B) was identified as a promising commercial epoxy resin, as its viscosity is very low and because it can dissolve TPE-TAF before gelation happens. In addition, its structure advantageously adds flexibility to the network, may counterbalance the rigidity of the TPE-TAF structure, and might prevent a high T_g which would make the reprocessability of the material more difficult (Scheme 2).

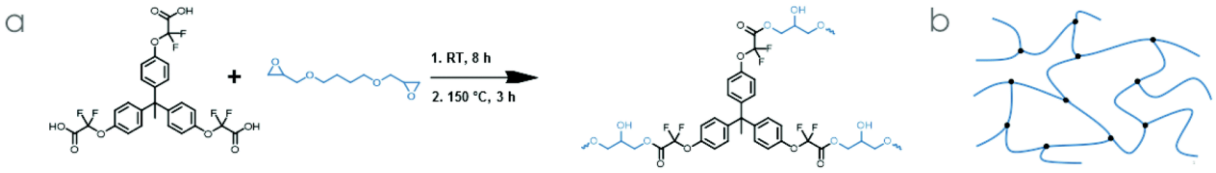

Scheme 2. (a) Network synthesis from TPE-TAF and BDGE and (b) schematic representation of the network.

TPE-TAF was dissolved in BDGE at room temperature (*ca*. 20 °C). The mixing time needed to be reduced to a few minutes only, to avoid the gelation caused by the fast reaction between the α-difluoro acids and the epoxides (even at room temperature) and ensure the homogeneity of the mixture. The mixture was then left at room temperature for at least 8 h, resulting into a brittle gel, which was then cured at 150 °C.

The gel time observed visually was consistent with the gel time determined by rheological analysis (Annexes A Figure S17). At 20 °C, a gel time of 1.3 h was estimated at the crossover of loss and storage moduli, confirming that the epoxy opening by the α-difluoro carboxylic acid readily happens at room temperature. This behavior is highly unusual for epoxy-acid systems, which usually require catalysis and relatively high temperatures (80–120 °C).[57] For catalyst-free systems, even higher temperatures (around 200 °C) are required.[58] This fast polymerization reaction at low temperature strongly suggests the activating inductive effect of fluorine atoms on the carboxylic acid towards the epoxy-opening reaction.

The polymerization kinetics at room temperature were monitored *via* FTIR. The disappearance of the epoxy band at 908 cm^{-1} was clearly observed but the conversion of acid functions at 1758 cm^{-1} into

esters at 1761 cm^{-1} could not be determined, because the acid and ester bands overlapped too much (Annexes A Figure S22). The epoxy band decreased significantly for the first 6 h of reaction, and then decreased at a much lower rate until the end of the acquisition after 64 h (Figure 1). This rate change was probably due to the gelation of the mixture which slowed down the reaction between the remaining reactive species.

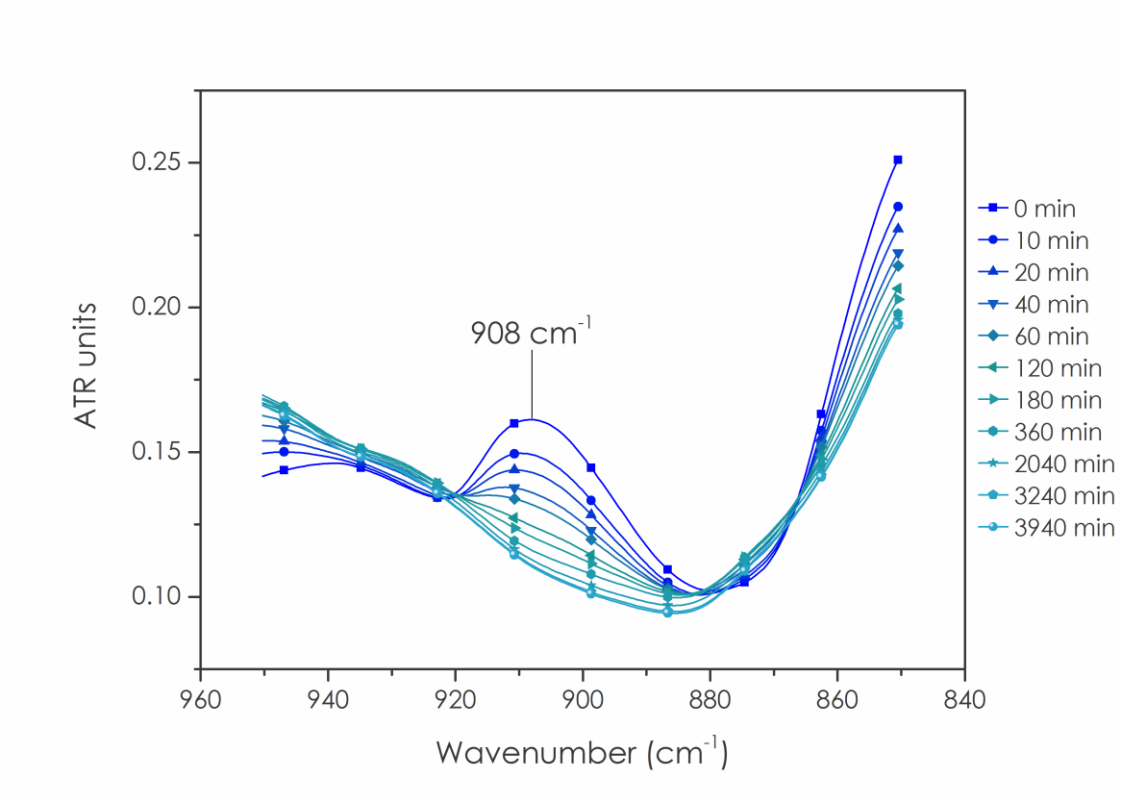

Figure 1. Evolution of the epoxy FTIR band at 908 cm^{-1} of the TPE-TAF/BDGE binary mixture versus time at room temperature (ca. 20 °C).

The material obtained after 4 days at room temperature was left for 3 h in an oven at 150 °C to ensure complete polymerization. Three consecutive DSC ramps were carried out on the resulting material. The thermograms overlaid perfectly, did not show any residual exotherm and revealed a T_g of 47 °C which did not evolve after any of these heating ramps (Annexes A Figure S18). The curing of the material was thus deemed complete.

Solubility tests were performed in acetone, THF, toluene, cyclohexane, DMSO, DCM and acetonitrile (Annexes A Table S1). The highest values were found for acetone and THF. In particular, after 24 h under agitation, an insoluble fraction of 94 ± 2% was measured in acetone (the best solvent for BDGE and TPE-TAF), thus proving that the curing process led to the formation of a 3D crosslinked material, as expected.

Vitrimer characterization

TGA under air showed that no significant mass loss was observed up to 200 °C, with a 2% and 5% degradation temperatures $T_{d2\%}$ and $T_{d5\%}$ of 205 °C and 262 °C respectively (Annexes A Figure S20 and Table 1). The T_g of the TPE-TAF/BDGE material was determined to be 47 °C (Annexes A Figure S18 and Table 1). TPE-TAF contains three aromatic cycles which bring rigidity to the polymer structure, whereas the linear structure of BDGE adds flexibility. This balance explains the moderate T_g value observed.

Table 1. Table of the vitrimer properties

Gel content[a] (%)	**$T_{d2\%}$ (°C)**	**Mass loss[b] (4 h, %)**	**Mass loss[b] (16 h, %)**	**T_g (°C)**	**T_α (°C)**	**E'_G[c] (GPa)**	**E'_R[d] (MPa)**
94 ± 2	205	4.3	4.4	47	39	3.7	18.1

[a] Gel content in acetone at 20 °C for 24 h. [b] T = 100 °C. [c] Value at T_α −50 °C. [d] Value at T_α +50 °C.

A few preliminary reshaping trials allowed to set the reshaping temperature value at 100 °C. The material stability to reprocessing cycles was then determined by isothermal TGA experiments performed at 100 °C for 16 h under air, to simulate the oxidative environment during reprocessing (Figure 2 and Table 1). After 4 h, a mass loss of 4.3% was observed. The value stabilized to 4.4% after 5 h and did not evolve afterwards. This loss might be due to the evaporation of remaining unreacted monomers trapped in the TPE-TAF after synthesis.

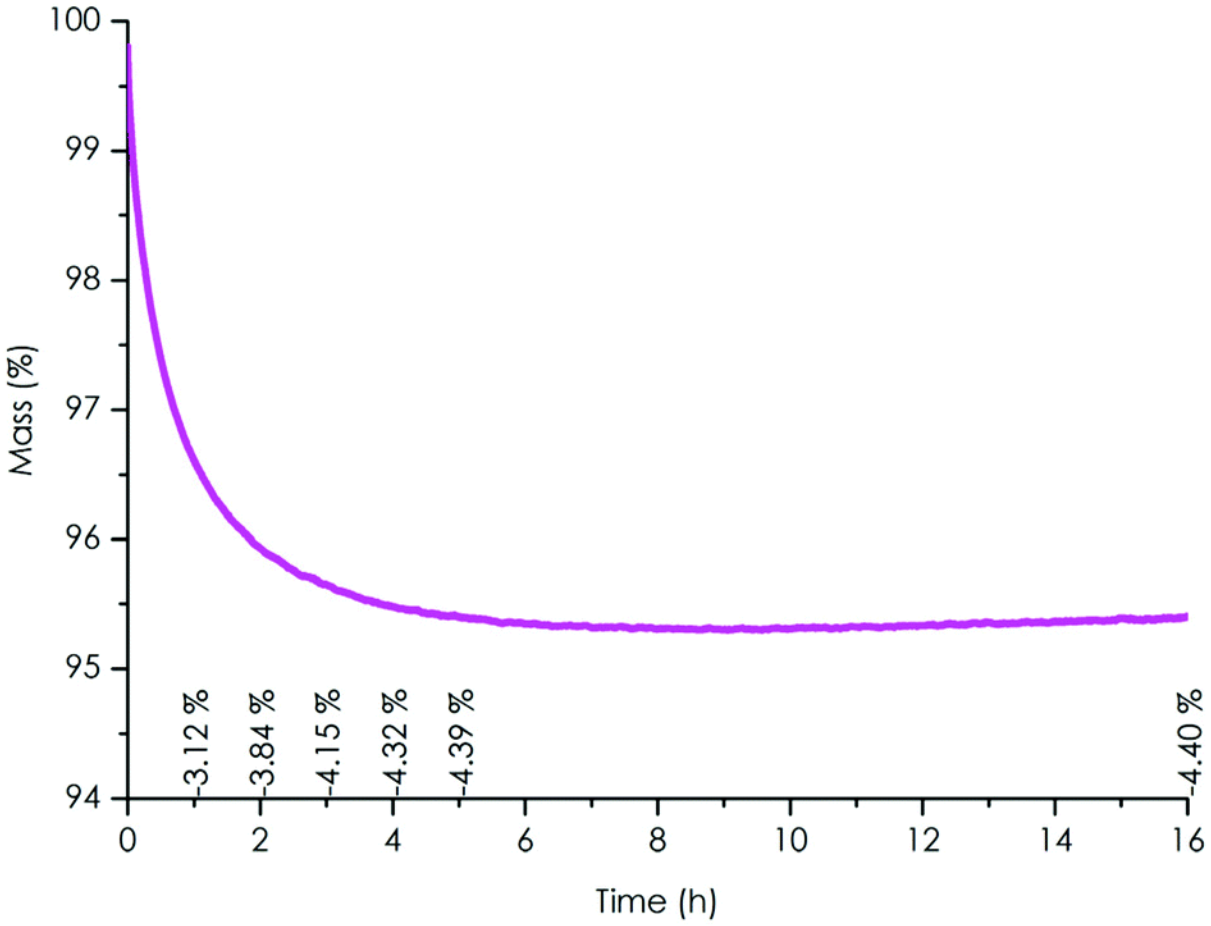

Figure 2. Isothermal TGA thermogram of TPE-TAF/BDGE material under air at 100 °C (% mass loss).

The kinetics of the flow behavior of the material was studied using stress-relaxation experiments. The relaxation modulus was monitored with time between 170 and 210 °C with 10 °C steps (Figure 3). It is important to state here that analogous non fluorinated polyester epoxy network prepared using 0.1 mol% Zn catalyst by Leibler *et al.* did not show vitrimer properties.[5]

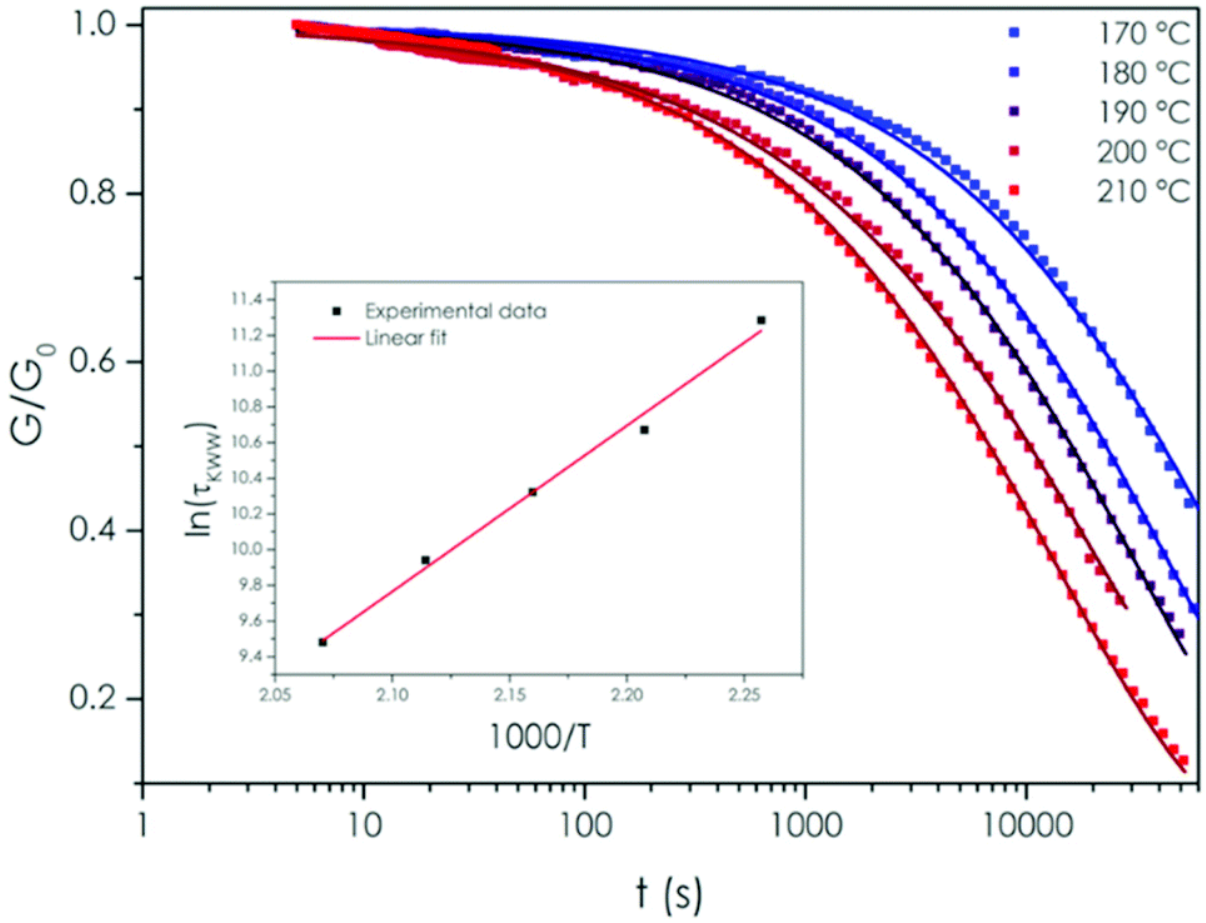

Figure 3. Normalized stress–relaxation curves from 170 to 210 °C with 10 °C steps fitted with the Kohlrausch–Williams–Watts equation (KWW) and τ_{KWW} relaxation times reported in the Arrhenius diagram (inset, R^2 = 0.98985).

Normalized stress-relaxation experimental curves shown in Figure 3 reveal that, in the 170 °C–210 °C temperature range, the TPE-TAF/BDGE network relaxed the stress applied. This behavior is expected only if the network is able to reorganise. The fact that this material flowed on the rubbery plateau proves that fluorine atoms activated the transesterification. A contribution from minute amounts of unreacted carboxylic acid function might as well favor the transesterification.[60] Furthermore, the relaxation rate depended on the temperature, as expected for a vitrimer.

The usual fitting model for such experiments is the exponential decay (Maxwell model). Nevertheless, this model did not fit well the experimental data obtained in the logarithmic time scale (R^2 between 0.934 and 0.989). A Kohlrausch–Williams–Watts "stretched exponential" equation was found to better fit (see Annexes A Table S2 for the equation and the fitting parameters) the stress relaxation dataset[1] (R^2 between 0.995 and 0.99975, depending on the temperature). In KWW model, a stretch parameter β is added to the exponential decay. The closer to 1 is β, the closer to the Maxwell model are the data. From 170 °C to 210 °C, the value of β was about 0.56 ± 0.02, indicating that the flow

kinetics was associated with a distribution of relaxations rather than with a single relaxation time kinetics.[1]

The relaxation time values obtained from the KWW fitting equations were plotted in an Arrhenius diagram (Figure 3 inset) to determine the value of the flow activation energy E_a. This E_a was determined to be 77 kJ mol^{-1}, in good agreement with the 29–163 kJ mol^{-1} range reported so far for transesterification vitrimers,[47] especially for catalyst-free vitrimers activated by neighboring groups for which the activation energy values are ranging from 78 to 94 kJ mol^{-1}.[42,59–61]

The material relaxation observed in the absence of external catalyst demonstrated the activating effect on the transesterification of the two fluorine atoms located on the α-carbon of the esters, as non-catalyzed epoxy-acid networks usually exhibit no relaxation on a measurable time scale. As previously mentioned, tiny amounts of unreacted carboxylic acid, if present, could also add a contribution on this effect. A slight contribution from the phenoxy group is plausible, but would be much weaker than the contributions of the two fluorine atoms given the relative electronegativities of these elements (χ_F = 4.2, χ_O = 3.6). This is well illustrated by the pK_as of acetic acid 4.7, glycolic acid 3.8, phenoxyacetic acid 3.2 and difluoroacetic acid 1.2.[63,64] This range stresses out the difference in electron-withdrawing ability of two fluorine *vs*. one oxygen atom. The material behavior in temperature followed an Arrhenius law, as expected for a vitrimer. α-Difluoro esters are thus efficient activated esters for the design of catalyst-free transesterification vitrimers.

The discrepancy between the sluggishness in stress-relaxation experiments and the mild reprocessing conditions observed is striking. This difference can be explained by the pressure applied to the material,[65,66] which is an important and often overlooked parameter. The force applied onto the material during reprocessing is 8.8 times the force applied during relaxation experiments. The reprocessing experiments are thus carried out at high pressure value in compression, which explains the difference in the behavior observed.

Reprocessing classical thermosets by compression molding is impossible, in contrast to vitrimers which possess exchangeable bonds. The TPE-TAF/BDGE material was successfully reprocessed using compression-molding further demonstrating its vitrimer character. 1 mm^3 pieces of the material were reassembled into a small ribbon after 1.5 h at 100 °C under a 6 ton load. The required reprocessing conditions were relatively mild compared to transesterification vitrimers reported in literature, whether they are catalyzed or not (Figure 4).[5,37,40,44,48,52,62,67–72]

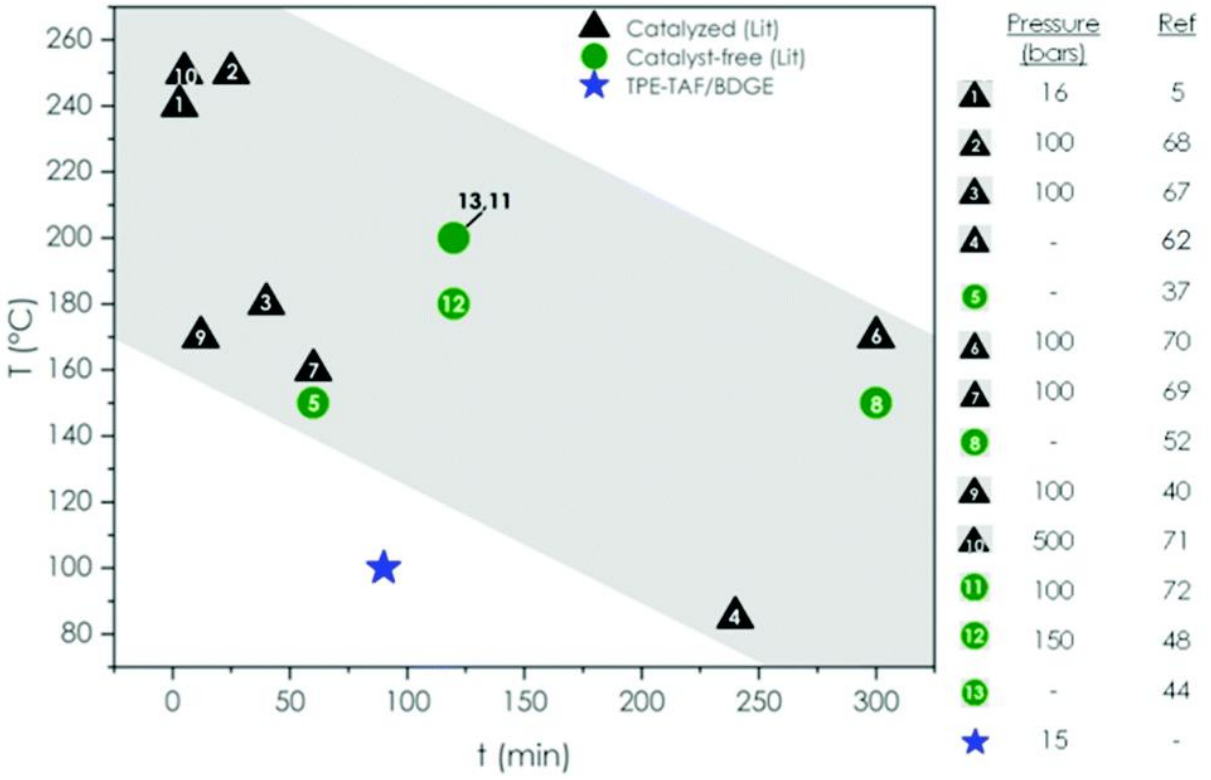

Figure 4. Comparison of TPE-TAF/BDGE reprocessing temperature, pressure and time with various catalyzed and catalyst-free transesterification vitrimers reported so far.[5,37,40,44,48,52,62,67–72]

Ten successive reprocessing cycles were successfully performed and each time homogeneous transparent samples were recovered. The color of the material did not significantly change with the successive reshaping cycles (Figure 5). To quantitatively assess the material evolution with reprocessing, thermomechanical analyses were performed.

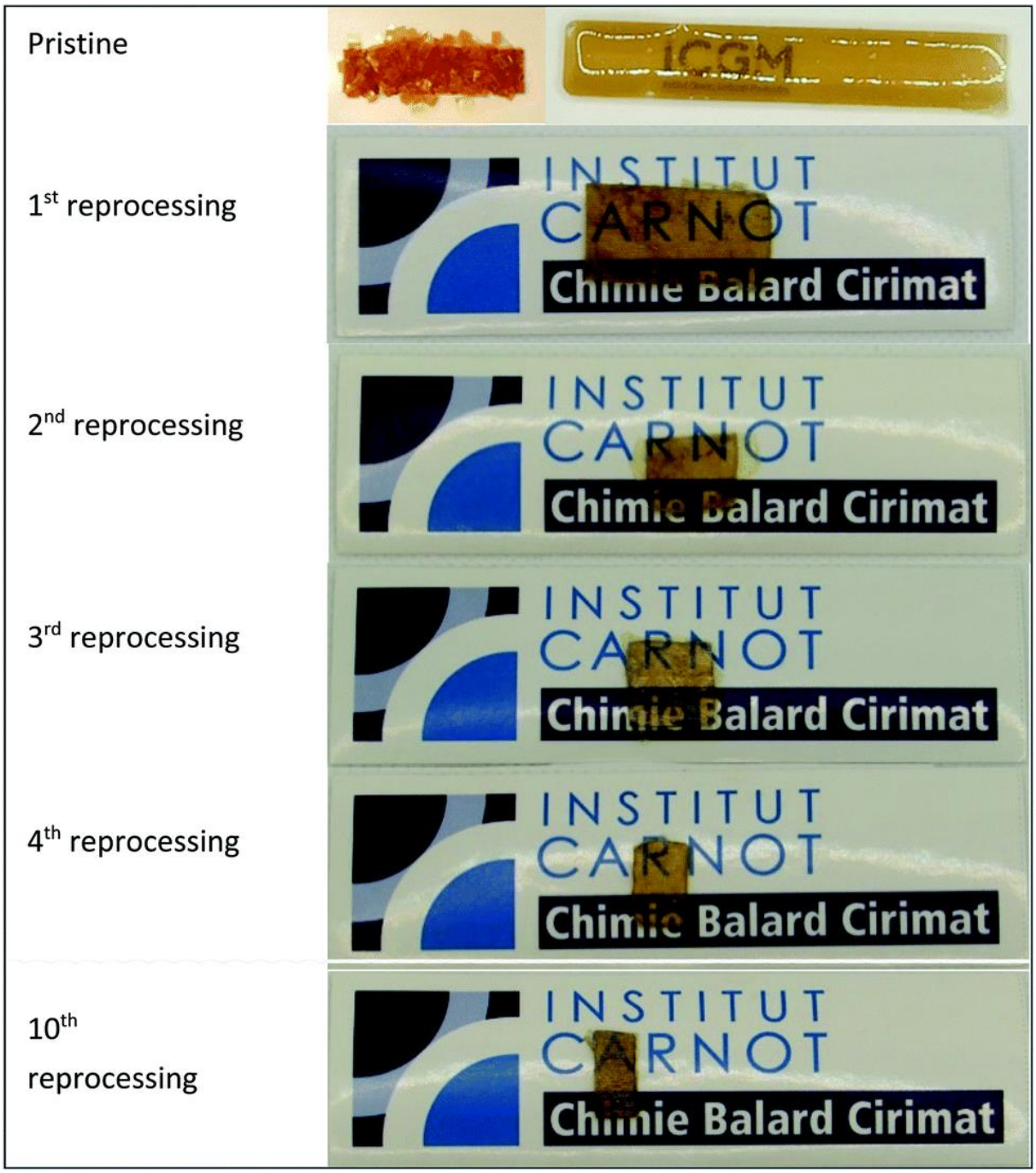

Figure 5. TPE-TAF/BDGE aspect after several reprocessing cycles.

The TPE-TAF/BDGE material evolution with reprocessing was studied using DMA experiments. The values of the storage modulus *E'* in the glassy plateau and in the rubbery plateau regions, and the evolution of T_α allow to detect whether the TPE-TAF/BDGE material mechanical properties decrease after several reprocessing cycles. A ramp from −100 to +150 °C was performed after each reprocessing cycle to check whether the mechanical properties were fully recovered.

The pristine material exhibited a glassy plateau storage modulus E'_G = 3.7 GPa, a rubbery plateau storage modulus E'_R = 18 MPa and a T_α = 39 °C, which is consistent with the values reported in the literature[37,70,72–74] for epoxy-acid and epoxy-anhydride vitrimers (Table 2 and Annexes A Figure S19).

Table 2. Evolution of DMA characteristic values before and after 10 reprocessing cycles

Reprocessing cycle	T_α (°C)	E'_G[a] (GPa)	E'_R[b] (MPa)
Pristine	39	3.7	18.1
10	49	3.9	18.7

[a] Value at T_α −50 °C. [b] Value at T_α +50 °C.

Upon the first three reprocessing cycles, the T_α increased from 39 °C to 41, 47 and 49 °C respectively, suggesting that the crosslink density slightly increased after each reshaping step, which is consistent with the increase of the rubbery plateau modulus (Table 2). After this 3rd reshaping process, the T_α value did not change with further reprocessing cycles up to the tenth cycle (Table 3).

Table 3. Evolution of T_α with the successive reprocessing cycles

Reprocessing cycle	Pristine	1	2	3–10
T_α (°C)	39	41	47	49

The storage modulus (E') value in the glassy plateau region slightly changed from 3.7 to 3.9 GPa for the pristine network and after the tenth reprocessing respectively. Similarly, the value of E' in the rubbery plateau region increased by a mere 0.6 MPa (Table 2) (from 18.1 to 18.7 MPa for the pristine and 10th reprocessing cycle). These results show that there is no significant evolution of the network after 10 cycles.

Conclusion

In summary, polyester vitrimers were prepared out of a synthesized trifunctional α-difluoroacid and a commercially available difunctional epoxy resin. Thanks to the activation of the acid by the fluorine atoms, the epoxy-acid polymerization reaction happened readily at room temperature, whereas catalysts and high temperatures are usually needed for non-fluorinated systems. The resulting TPE-TAF/BDGE material was insoluble yet able to be reprocessed under mild conditions (100 °C, 1.5 h, 6 t). As expected, α-difluoro ester underwent significantly accelerated transesterification. This activation was such that no external catalyst was needed, in contrast to most other transesterification vitrimers. The flow activation energy E_a was evaluated to be 77 kJ mol^{-1} which is consistent with the values reported for transesterification vitrimers catalysed by internal amines for instance, but also very close to the value (67–72 kJ mol^{-1}) obtained for α-CF_3 activation.[56] This polymer proved highly stable over

repeated reprocessing cycles, with very little degradation of the mechanical properties observed after 10 cycles. The proof-of-concept based on the high electron withdrawing effect of fluorinated groups and exposed here is very promising to tune vitrimers properties and address the concerns related to the use of external catalysts, such as premature ageing, leaching of the catalyst or limited reprocessing abilities.[34,35,75]

Experimental section

Materials

1,4-Butanediol diglycidyl ether (BDGE, Aldrich, ≥95%, NMR spectra, FTIR spectrum and EEW calculations in Annexes A Figures S14, S15 and sections A, B), 1,1,1-Tris(4-hydroxyphenyl)ethane ("TPE", Sigma-Aldrich, 99%), 1,8-Diazabicyclo(5.4.0)undec-7-ene (DBU, Fluorochem, 98%), ethyl bromodifluoroacetate (Fluorochem, 98%), benzophenone (Avocado Research Chemicals Ltd, 99%), succinic acid (ABCR, 99%) were used as received. Solvents were supplied by VWR Chemicals. Deuterated solvents were supplied by Eurisotop (99.8%).

Synthetic procedures

"TPE-TE" compound: 1,1,1-Tris(4-hydroxyphenyl) ethane (6.13 g, 20 mmol, 1 equiv.) was dissolved in dry DMF (120 mL, 0.16 M). 1,8-Diazabicyclo [5.4.0] undec-7-ene (DBU, 15 mL, 100 mmol, 5 equiv.) was added in one portion and the reaction was heated to 70 °C. Ethyl bromodifluoroacetate (12.8 mL, 100 mmol, 5 equiv.) was then added *via* a syringe pump at a rate of 5.0 mL h^{-1} and the reaction was stirred at 70 °C for 40 h. The resulting reaction mixture was very dark due to the probable oxidation of some of the phenol reagents, which could not be prevented even under argon atmosphere or protection from light. The crude mixture was cooled to room temperature, diluted with H_2O (600 mL), and extracted 5 times with Et_2O (5 × 100 mL). The combined organic layers were washed with 2 × 150 mL water and with 150 mL of brine, dried with Na_2SO_4, filtered, and concentrated under reduced pressure. The dark-brown crude mixture was purified by column chromatography on silica gel using pentane/ethyl acetate mixtures (5/1, 3/1 and finally 1/1) as eluent to afford the pure triester (F1: 8.2 g, 61%, white solid) and diester (F2: 1.8 g, 16%, off-yellow viscous oil).

Triester TPE-TE characterizations (NMR spectra in Annexes A Figures S1 to S3): **^{1}H NMR 400MHz $CDCl_3$**: δ 7.15–7.10 (m, 6H, aromatic protons, *m*-OCF_2), 7.07–7.02 (m, 6H, aromatic protons, *o*-OCF_2), 4.39 (q, ^3J = 7.2 Hz, 6H, O$CH_2$$CH_3$), 2.15 (s, 3H, Ar_3C-CH_3), 1.36 (t, ^3J = 7.1 Hz, 9H, OCH_2CH_3). **^{19}F NMR 377 MHz, $CDCl_3$**: δ −76.41. **^{13}C NMR 101 MHz, $CDCl_3$**: δ 159.9 (CO_2Et, t, $^2J_{C-F}$ = 41.5 Hz), 148.0 (*ipso*-^{Ar}*C*-O, t, $^3J_{C-F}$ = 2.0 Hz), 146.5 (*ortho*-^{Ar}*C*-O, t, $^4J_{C-F}$ = 2.0 Hz), 129.9 (*ipso*-^{Ar}*C*-C-CH_3), 121.2 (*ortho*-^{Ar}*C*-C-CH_3), 114.1 (OCF_2, t, $^1J_{C-F}$ = 272.5 Hz), 63.8 (O-CH_2CH_3), 51.7 (Ar-*C*-CH_3), 30.9 (Ar-C-CH_3), 14.0 (O-

CH_2CH_3). R_f (petroleum ether : ethyl acetate 5 : 1) = 0.42. **HRMS (ESI+)** Calc. for $[M + Na]^+$ 695.1686, found 695.1677.

Disubstituted ester characterizations (NMR spectra in Annexes A Figures S4 to S8): **^{1}H NMR 400MHz $CDCl_3$**: δ 7.14–7.08 (m, 4H, aromatic protons, *m*-OCF_2), 7.07–7.03 (m, 4H aromatic protons, *o*-OCF_2), 6.95–6.89 (m, 2H aromatic protons, *m*-OH), 6.79–6.72 (m, 2H, aromatic protons, *o*-OH), 5.06 (s, 1H, O*H*), 4.39 (q, ^3J = 7.1 Hz, 4H, OCH_2CH_3), 2.12 (s, 3H, Ar_3C-CH_3), 1.36 (t, ^3J = 7.2 Hz, 6H, OCH_2CH_3). **^{19}F NMR 377 MHz, $CDCl_3$**: δ −76.34. **^{13}C NMR 101 MHz, $CDCl_3$**: δ 160.0 (CO_2Et, t, $^2J_{C–F}$ = 41.2 Hz), 154.1, 147.7 (*ipso*-^{Ar}*C*-O, t, $^3J_{C–F}$ = 2.0 Hz), 147.2, 140.6, 129.9, 129.9, 121.1 (*ortho*-^{Ar}*C*-O t, $^4J_{C–F}$ = 0.7 Hz), 115.0, 114.1 (OCF_2, t, $^1J_{C–F}$ = 272.4 Hz), 63.8 (O-CH_2CH_3), 51.4 (Ar-*C*-CH_3), 30.9 (Ar-C-CH_3), 14.0 (O-CH_2CH_3). R_f (petroleum ether : ethyl acetate 5 : 1) = 0.30.

"TPE-TAF" compound: In a 250 mL round bottom flask, 7 g of triester were dissolved in acetonitrile (90 mL). Then, a 5 M aqueous solution of NaOH (12.5 g in 62 mL) was added slowly at room temperature, and the mixture was stirred for 3 h. 200 mL of a saturated $NaHCO_3$ solution was added to the mixture and the aqueous layer was washed with 100 mL of diethyl ether. The organic layer was extracted with 50 mL of saturated $NaHCO_3$ solution, and the gathered aqueous layers were acidified to pH = 1 using 2 M HCl. Finally, the acidified aqueous layer was extracted with 3 × 100 ml of diethyl ether, and the solvent was removed under high vacuum to afford the desired triacid as a white waxy solid (yield over the two steps η = 50%, purity >98% estimated from ^{1}H NMR spectrum). Up to 9 grams per batch could be obtained.

Trifunctional acid TPE-TAF characterizations (NMR spectra, FTIR spectrum and TGA thermogram in Annexes A Figures S9 to S13): **^{1}H NMR 400MHz d_6-acetone**: δ 7.89 (br s, 3H, COO*H*), 7.20 (m, 12H, aromatic protons), 2.22 (s, 3H, C-CH_3). **^{19}F NMR 377 MHz, d_6-acetone**: δ −77.50. **^{13}C NMR 101 MHz, d_6-acetone**: δ 160.9 (*C*OOH, t, $^2J_{C–F}$ = 40.7 Hz), 148.9 (*ipso*-^{Ar}*C*-O, t, $^3J_{C–F}$ = 2.0 Hz), 147.6, 130.8, 121.8, 115.3 (OCF_2, t, $^1J_{C–F}$ = 270.9 Hz), 52.4 (C-CH_3), 30.9 (*C*-CH_3). **HRMS (ESI+)** Calc. for $[M + Na]^+$ 611.0747, found 611.0750.

Determination of the epoxy equivalent weight (EEW)

The EEW of the BDGE was evaluated by NMR titration using benzophenone as standard in deuterated chloroform (experimental details are given in Annexes A section A). This value was confirmed by DSC studies using succinic acid as the curing agent (experimental details are given in Annexes A section B). The procedure was described in a previous article.[76] Several BDGE/succinic acid ratios were used to make a series of thermosets. The highest T_g was achieved for a 1 : 1 stoichiometry, from which the EEW was calculated.

"TPE-TAF/BDGE" vitrimer

Typically, 1.156 g (5.90 meq COOH) of TPE-TAF was quickly mixed manually in a 10 mL beaker with 0.682 g (5.93 meq epoxy) of BDGE at room temperature (*ca*. 20 °C) until the acid was fully dissolved. A clear yellowish viscous liquid was obtained and quickly cast in PTFE molds. The mixture was left at least 8 h at room temperature for gelation. The resulting material (TPE-TAF/BDGE) was then removed from the molds and cured 3 h at 150 °C.

Instrumentation

NMR: ^{1}H, ^{13}C and ^{19}F were acquired on a Bruker Avance 400 MHz spectrometer at 23 °C. External reference was tetramethylsilane (TMS) with chemical shifts given in ppm. Samples were diluted in 0.5 mL of $CDCl_3$ or DMSO-d_6 depending on their solubility.

FTIR: FTIR spectra and single wavenumber measurements were acquired on a ThermoScientific Nicolet iS50 FT-IR equipped with an attenuated total reflectance cell (ATR). The data were analyzed using the software OMNIC Series 8.2 from Thermo Scientific.

Mechanical characterizations: Gel time experiment was performed at 1 Hz with a 20 mm plane-plane geometry on a ThermoScientific Haake Mars 60 rheometer equipped with a Peltier heating cell. A 30 mL h^{-1} nitrogen flux was applied. Stress relaxation experiments were performed on the same apparatus equipped with a textured 8 mm plane-plane geometry. A 10% torsional strain was applied on 8 mm diameter and 2 mm thickness circular samples, and the rubbery modulus evolution with time was monitored.

DMA: Dynamic Mechanical Analyses were carried out on Metravib DMA 25 with Dynatest 6.8 software. Uniaxial stretching of samples ($1 \times 5 \times 12$ mm^3) was performed while heating at a rate of 3 °C min^{-1} from −90 °C to 150 °C, keeping the frequency at 1 Hz.

TGA: Thermogravimetric thermograms were recorded on a TA TGA G50 instrument using a 40 mL min^{-1} flux of synthetic air as purge gas. Approximately 10 mg of sample were used for each analysis. Ramps from 20 to 500 °C were applied at a rate of 20 °C min^{-1}.

DSC: Analyses were carried out using a NETZSCH DSC200F3 calorimeter. The calibration was performed using adamantane, biphenyl, indium, tin, bismuth and zinc standards. Nitrogen was used as purge gas. Approximately 10 mg of sample were placed in perforated aluminum pans and the thermal properties were recorded between −100 °C and the temperature of 2% degradation $T_{d2\%}$ at 20 °C min^{-1}. The reported values are the values measured during the second heating ramp.

Reprocessing: the material was cut into 1 × 1 × 1 mm^3 pieces and then pressed in a PTFE mold for 1.5 h at 100 °C under a 6 tons load using a Carver 3960 manual heating press.

Notes and references

(1) G. M. Scheutz, J. J. Lessard, M. B. Sims and B. S. Sumerlin, J. Am. Chem. Soc. 2019, 141, 16181–16196.

(2) J.-P. Pascault, H. Sautereau, J. Verdu and R. J. J. Williams, Thermosetting Polymers, Marcel Dekker, Inc., New York, 2002.

(3) S. J. Pickering, in Wiley Encyclopedia of Composites, John Wiley & Sons, Inc., Hoboken, New Jersey, 2012.

(4) T. F. Scott, A. D. Schneider, W. D. Cook and C. N. Bowman, Science 2005, 308, 1615–1617.

(5) D. Montarnal, M. Capelot, F. Tournilhac and L. Leibler, Science 2011, 334, 965–968.

(6) C. A. Angell, J. Non-Cryst. Solids 1991, 131–133, 13–31.

(7) R. L. Snyder, D. J. Fortman, G. X. De Hoe, M. A. Hillmyer and W. R. Dichtel, Macromolecules 2018, 51, 389–397.

(8) M. Röttger, T. Domenech, R. Van Der Weegen, A. Breuillac, R. Nicolaÿ and L. Leibler, Science 2017, 356, 62–65.

(9) F. Caffy and R. Nicolaÿ, Polym. Chem. 2019, 10, 3107–3115.

(10) A. Ruiz de Luzuriaga, R. Martin, N. Markaide, A. Rekondo, G. Cabañero, J. Rodríguez and I. Odriozola, Mater. Horiz. 2016, 3, 241–247.

(11) Z. Ma, Y. Wang, J. Zhu, J. Yu and Z. Hu, J. Polym. Sci., Part A: Polym. Chem. 2017, 55, 1790–1799.

(12) Y. Nishimura, J. Chung, H. Muradyan and Z. Guan, J. Am. Chem. Soc. 2017, 139, 14881–14884.

(13) X. Wu, X. Yang, R. Yu, X. J. Zhao, Y. Zhang and W. Huang, J. Mater. Chem. A 2018, 6, 10184–10188.

(14) N. Zheng, Z. Fang, W. Zou, Q. Zhao and T. Xie, Angew. Chem., Int. Ed. 2016, 55, 11421–11425.

(15) N. Zheng, J. Hou, Y. Xu, Z. Fang, W. Zou, Q. Zhao and T. Xie, ACS Macro Lett. 2017, 6, 326–330.

(16) D. J. Fortman, J. P. Brutman, C. J. Cramer, M. A. Hillmyer and W. R. Dichtel, J. Am. Chem. Soc. 2015, 137, 14019–14022.

(17) D. J. Fortman, J. P. Brutman, M. A. Hillmyer and W. R. Dichtel, J. Appl. Polym. Sci. 2017, 134, 44984.

(18) X. Chen, L. Li, K. Jin and J. M. Torkelson, Polym. Chem. 2017, 8, 6349–6355.

(19) Y.-X. Lu and Z. Guan, J. Am. Chem. Soc. 2012, 134, 14226–14231.

(20) H. Zhang, D. Wang, W. Liu, P. Li, J. Liu, C. Liu, J. Zhang, N. Zhao and J. Xu, J. Polym. Sci., Part A: Polym. Chem. 2017, 55, 2011–2018.

(21) S. Wang, S. Ma, Q. Li, X. Xu, B. Wang, K. Huang, Y. Liu and J. Zhu, Macromolecules 2020, 53, 2919–2931.

(22) H. Zheng, Q. Liu, X. Lei, Y. Chen, B. Zhang and Q. Zhang, J. Mater. Sci. 2019, 54, 2690–2698.

(23) R. Hajj, A. Duval, S. Dhers and L. Avérous, Macromolecules 2020, 53, 3796–3805.

(24) W. Denissen, M. Droesbeke, R. Nicolaÿ, L. Leibler, J. M. Winne and F. E. Du Prez, Nat. Commun. 2017, 8, 14857.

(25) W. Denissen, G. Rivero, R. Nicolaÿ, L. Leibler, J. M. Winne and F. E. Du Prez, Adv. Funct. Mater. 2015, 25, 2451–2457.

(26) M. Guerre, C. Taplan, R. Nicolaÿ, J. M. Winne and F. E. Du Prez, J. Am. Chem. Soc. 2018, 140, 13272–13284.

(27) P. R. Christensen, A. M. Scheuermann, K. E. Loeffler and B. A. Helms, Nat. Chem. 2019, 11, 442–448.

(28) D. Boucher, J. Madsen, N. Caussé, N. Pébère, V. Ladmiral and C. Negrell, Reactions 2020, 1, 89–101.

(29) D. Boucher, J. Madsen, L. Yu, Q. Huang, N. Caussé, N. Pébère, V. Ladmiral and C. Negrell, Macromolecules 2021, 54, 6772–6779.

(30) Z. Tang, Y. Liu, Q. Huang, J. Zhao, B. Guo and L. Zhang, Green Chem. 2018, 20, 5454–5458.

(31) B. Hendriks, J. Waelkens, J. M. Winne and F. E. Du Prez, ACS Macro Lett. 2017, 6, 930–934.

(32) W. Alabiso and S. Schlögl, Polymers 2020, 12, 1660.

(33) C. He, S. Shi, D. Wang, B. A. Helms and T. P. Russell, J. Am. Chem. Soc. 2019, 141, 13753–13757.

(34) J. Wang, S. Chen, T. Lin, J. Ke, T. Chen, X. Wu and C. Lin, RSC Adv. 2020, 10, 39271–39276.

(35) J. J. Lessard, L. F. Garcia, C. P. Easterling, M. B. Sims, K. C. Bentz, S. Arencibia, D. A. Savin and B. S. Sumerlin, Macromolecules 2019, 52, 2105–2111.

(36) S. Dhers, G. Vantomme and L. Avérous, Green Chem. 2019, 21, 1596–1601.

(37) J. Han, T. Liu, C. Hao, S. Zhang, B. Guo and J. Zhang, Macromolecules 2018, 51, 6789–6799.

(38) F. I. Altuna, V. Pettarin and R. J. J. Williams, Green Chem. 2013, 15, 3360–3366.

(39) C. Hao, T. Liu, S. Zhang, L. Brown, R. Li, J. Xin, T. Zhong, L. Jiang and J. Zhang, ChemSusChem, 2019, 12, 1049–1058.

(40) S. Mu, Y. Zhang, J. Zhou, B. Wang and Z. Wang, ACS Sustainable Chem. Eng. 2020, 8, 5296–5304.

(41) T. Liu, B. Zhao and J. Zhang, Polymer 2020, 194, 122392.

(42) F. I. Altuna, C. E. Hoppe and R. J. J. Williams, Eur. Polym. J. 2019, 113, 297–304.

(43) C. Hao, T. Liu, S. Zhang, W. Liu, Y. Shan and J. Zhang, Macromolecules 2020, 53, 3110–3118.

(44) Y. Li, T. Liu, S. Zhang, L. Shao, M. Fei, H. Yu and J. Zhang, Green Chem. 2020, 22, 870–881.

(45) O. R. Cromwell, J. Chung and Z. Guan, J. Am. Chem. Soc. 2015, 137, 6492–6495.

(46) F. Van Lijsebetten, J. O. Holloway, J. M. Winne and F. E. Du Prez, Chem. Soc. Rev. 2020, 49, 8425–8438.

(47) F. Cuminet, S. Caillol, E. Dantras, E. Leclerc and V. Ladmiral, Macromolecules 2021, 54, 3927–3961.

(48) S. Wang, N. Teng, J. Dai, J. Liu, L. Cao, W. Zhao and X. Liu, Polymer 2020, 210, 123004.

(49) H. Zhang, S. Majumdar, R. A. T. M. Van Benthem, R. P. Sijbesma and J. P. A. Heuts, ACS Macro Lett. 2020, 9, 272–277.

(50) B. M. El-Zaatari, J. S. A. Ishibashi and J. A. Kalow, Polym. Chem. 2020, 8, 1–3.

(51) S. K. Schoustra, J. A. Dijksman, H. Zuilhof and M. M. J. Smulders, Chem. Sci. 2021, 12, 293–302.

(52) S. Debnath, S. Kaushal and U. Ojha, ACS Appl. Polym. Mater. 2020, 2, 1006–1013.

(53) P. G. Blake and B. F. Shraydeh, Int. J. Chem. Kinet. 1981, 13, 463–471.

(54) G. Schmeer and P. Sturm, Phys. Chem. Chem. Phys. 1999, 1, 1025–1030.

(55) J.-P. Brégué and D. Bonnet-Delpont, in Bioorganic and Medicinal Chemistry of Fluorine, John Wiley & Sons Inc., Hoboken, 2008.

(56) D. Berne, F. Cuminet, S. Lemouzy, C. Joly-Duhamel, R. Poli, S. Caillol, E. Leclerc and V. Ladmiral, Macromolecules 2022, 55, 5, 1669–1679.

(57) P.-J. Madec and E. Maréchal, Adv. Polym. Sci. 1985, 71, 153–228.

(58) L. Shechter, J. Wynstra and R. P. Kurkjy, Ind. Eng. Chem. 1957, 49, 1107–1109.

(59) M. Hayashi, ACS Appl. Polym. Mater. 2020, 2, 5365–5370.

(60) A. Adjaoud, A. Trejo-Machin, L. Puchot and P. Verge, Polym. Chem. 2021, 12, 3276–3289.

(61) T. Liu, C. Hao, L. Shao, W. Kuang, L. Cosimbescu, K. L. Simmons and J. Zhang, Macromol. Rapid Commun. 2020, 2000458.

(62) J. L. Self, N. D. Dolinski, M. S. Zayas, J. R. de Alaniz and C. M. Bates, ACS Macro Lett. 2018, 7, 817–821.

(63) K. U. Goss, Environ. Sci. Technol. 2008, 42, 456–458.

(64) N. V. Hayes and G. E. K. Branch, J. Am. Chem. Soc. 1943, 65, 1555–1564.

(65) A. M. Hubbard, Y. Ren, D. Konkolewicz, A. Sarvestani, C. R. Picu, G. S. Kedziora, A. Roy, V. Varshney and D. Nepal, ACS Appl. Polym. Mater. 2021, 3, 1756–1766.

(66) H. Fang, W. Ye, Y. Ding and H. H. Winter, Macromolecules 2020, 53, 4855–4862.

(67) H. Zhang, C. Cai, W. Liu, D. Li, J. Zhang, N. Zhao and J. Xu, Sci. Rep. 2017, 7, 11833.

(68) Y. Zhou, J. G. P. Goossens, R. P. Sijbesma and J. P. A. Heuts, Macromolecules 2017, 50, 6742–6751.

(69) X. Yang, L. Guo, X. Xu, S. Shang and H. Liu, Mater. Des. 2020, 186, 108248.

(70) T. Liu, S. Zhang, C. Hao, C. Verdi, W. Liu, H. Liu and J. Zhang, Macromol. Rapid Commun. 2019, 40, 1800889.

(71) M. Giebler, C. Sperling, S. Kaiser, I. Duretek and S. Schlögl, Polymers 2020, 12, 1148.

(72) Y. Liu, S. Ma, Q. Li, S. Wang, K. Huang, X. Xu, B. Wang and J. Zhu, Eur. Polym. J. 2020, 135, 109881.

(73) F. I. Altuna, C. E. Hoppe and R. J. J. Williams, Eur. Polym. J. 2019, 113, 297–304.

(74) J. Han, T. Liu, S. Zhang, C. Hao, J. Xin, B. Guo and J. Zhang, Ind. Eng. Chem. Res. 2019, 58, 6466–6475.

(75) W. Denissen, J. M. Winne and F. E. Du Prez, Chem. Sci. 2016, 7, 30–38.

(76) F. Jaillet, M. Desroches, R. Auvergne, B. Boutevin and S. Caillol, Eur. J. Lipid Sci. Technol. 2013, 115, 698–708.

Conclusion du chapitre II

Le premier volet des travaux décrits dans ce chapitre a conduit à la synthèse d'un acide carboxylique α,α-difluoré trifonctionnel (TPE-TAF) dont la structure était inédite dans la littérature au moment de la publication de ces travaux. Ce monomère a été engagé dans une réaction de polymérisation par ouverture de cycle avec le BDGE, afin de former un matériau à la structure tridimensionnelle. Le matériau obtenu TPE-TAF/ BDGE possède de très bonnes propriétés de remise en forme, dans des conditions douces comparées à celles décrites dans la littérature sur les vitrimères de transestérification avec catalyse interne par des céto-esters,[7] des amines tertiaires[8] ou encore des hydroxyles surnuméraires.[9,10,11] (1,5 h à 100 °C sous 15 bars). Après 10 cycles de remise en oeuvre, l'aspect du matériau et ses propriétés mécaniques ont très peu varié, ce qui montre sa très bonne tenue au recyclage.

Les propriétés rhéologiques du matériau ont été étudiées. L'écoulement depuis le plateau caoutchoutique, un comportement associé aux CAN, a été démontré. De plus, le temps de relaxation, temps caractéristique associé à cet écoulement, évolue avec la température en suivant la loi d'Arrhénius, un comportement observé en général pour les CAN associatifs, aussi appelés vitrimères.

En résumé, ce premier monomère a conduit à la synthèse d'un vitrimère de transestérification sans catalyseur grâce à l'effet inductif des atomes de fluor qui active les liaisons ester. La preuve de concept sur l'idée originale de ce projet a donc été validée.

Néanmoins, le système décrit présente des imperfections. En particulier, la voie de synthèse du monomère TPE-TAF nécessite une purification sur colonne de silice. Cette opération, très courante en synthèse organique, présente des inconvénients : elle est fastidieuse, et ne permet pas de traiter des quantités importantes de monomère. Ces limitations ont déjà engendré des difficultés pour les travaux décrits dans ce chapitre. En effet, l'analyse mécanique des polymères nécessite des échantillons de taille suffisante, avec des géométries contrôlées, et suffisamment de matière afin d'établir des protocoles optimisés et vérifier la répétabilité des analyses sur plusieurs échantillons d'un même matériau. Une voie de synthèse et une purification plus simples permettraient de faciliter les expériences d'analyse mécanique.

[7] Debnath, S.; Kaushal, S.; Ojha, U. ACS Appl. Polym. Mater. 2020, 2, 1006-1013.
[8] Li, Y.; Liu, T.; Zhang, S.; Shao, L.; Fei, M.; Yu, H.; Zhang, J. Green Chem. 2020, 22 (3), 870–881.
[9] Wang, S.; Teng, N.; Dai, J.; Liu, J.; Cao, L.; Zhao, W.; Liu, X. Polymer 2020, 210, 123004.
[10] Liu, Y.; Ma, S.; Li, Q.; Wang, S.; Huang, K.; Xu, X.; Wang, B.; Zhu, J. Eur. Polym. J. 2020, 135, 109881.
[11] Han, J.; Liu, T.; Hao, C.; Zhang, S.; Guo, B.; Zhang, J. Macromolecules, 2018, 51, 6789–6799.

Dans la suite de ces travaux, l'objectif a été de simplifier la synthèse de monomères acides carboxyliques α,α-difluorés, pour pouvoir la mener sur de plus grandes échelles (de quelques grammes par lot à quelques dizaines de grammes par lot). De plus, des méthodes de purifications adaptées à des lots de plus grande échelle ont été testées et développées.

CHAPITRE III : SYNTHESE D'UN VITRIMERE A PARTIR D'EPOXY ET D'α,α-DIFLUOROACIDES DIFONCTIONNELS

Introduction du chapitre III

L'objectif de ce deuxième volet de travaux est de faciliter l'obtention de monomères α,α-difluoro acides carboxyliques, notamment à une échelle supérieure à la synthèse du TPE-TAF, qui a permis la validation de la preuve de concept. La purification éventuelle du monomère devra également être adaptée à des lots de l'ordre de la dizaine de grammes, ceci dans le but d'obtenir des quantités d'échantillons suffisants afin de faciliter les études mécaniques.

La voie de synthèse décrite au chapitre précédent à partir d'un triphénol conduit à un mélange des composés trisubstitués, disubstitués, monosubstitués et probablement de produits d'oxydation au regard de la couleur très sombre et de l'opacité du mélange réactionnel, caractéristiques de l'oxydation de phénols. Ce mélange ne peut pas être utilisé en l'état et nécessite une purification par chromatographie sur silice. Bien que ce procédé soit usuel au laboratoire, il ne permet pas de purifier de grandes quantités de matière.

Afin d'éviter ces problèmes d'oxydation et de limiter les produits de substitution partielle, une autre voie de synthèse à partir de iodoaryles a été identifiée.[12,13] Cette synthèse a été décrite sur des aryles monoiodés, mais jamais sur des di- ou tri-iodés. L'autre inconvénient est que le triiodobenzene, bien que disponible commercialement, est vendu à des tarifs prohibitifs pour des applications industrielles. En revanche le diiodobenzene est accessible mais implique l'utilisation d'un époxy de fonctionnalité bien supérieure à 2, avec les limitations discutées au chapitre précédent.

Cependant, dans le cas de systèmes époxy-acide carboxylique, la réaction d'ouverture de l'époxy par l'acide n'est pas la seule mise en jeu dans la formation du réseau.[14] La transestérification peut être concomitante à la polymérisation par ouverture de cycle, ce qui conduit à des chaînes liées entre elles, c'est-à-dire un réseau tridimensionnel, et à la formation d'oligomères libres au sein du réseau macromoléculaire, mais non liés à cette structure. La transestérification est liée à la présence de catalyseur (TBD) dans les matériaux décrits. Ces considérations, ainsi que les travaux de Poutrel et al.[15] publiés en juin 2020 sur des vitrimères époxy-acide carboxylique ont amené à reconsidérer cette voie de synthèse.

[12] Eto, H.; Kaneko, Y.; Sakamoto, T. Chem. Pharm. Bull. 2000, 48 (7), 982–990.
[13] Mizuta, S.; Stenhagen, I. S. R.; O'Duill, M.; Wolstenhulme, J.; Kirjavainen, A. K.; Forsback, S. J.; Tredwell, M.; Sandford, G.; Moore, P. R.; Huiban, M.; Luthra, S. K.; Passchier, J.; Solin, O.; Gouverneur, V. Org. Lett. 2013, 15 (11), 2648–2651.
[14] Steinmann, B. Polym. Bull. 1989, 22 (5–6), 637–644.
[15] Poutrel, Q.-A.; Blaker, J. J.; Soutis, C.; Tournilhac, F.; Gresil, M. Polym. Chem. 2020, 11 (33), 5327–5338.

Dans le cas de polyesters sans catalyseur activés par le fluor, la question de la formation ou non d'un réseau tridimensionnel se pose. En effet, les conditions de polymérisation sont différentes, avec un traitement à 150 °C pendant 3 h après une polymérisationà température ambiante pendant 8 h dans le cas des acides fluorés,[16] contre un traitement de 8 h à 145 °C suivi de 8 h à 160 °C pour les vitrimères avec catalyseur.[17] Ce traitement thermique dans des conditions plus douces dans le cas des matériaux fluorés peut avoir des conséquences différentes sur les réactions mises en jeu au moment de la polymérisation, et donc sur la structure macromoléculaire des matériaux formés.

Afin de vérifier la faisabilité d'une telle structure, un monomère difonctionnel α,α-difluoro acide carboxylique a été synthétisé à partir de 1,4-diiodobenzene. La purification de ce monomère a pu été optimisée pour pouvoir être adaptée à grande échelle. Un échantillon a été synthétisé par réaction avec le BDGE. Ce matériau présente une structure tridimensionnelle, et des propriétés vitrimères à l'instar du premier système étudié (Figure E).

Cette étude inédite a été rédigée sous la forme d'une publication qui sera prochainement soumise dans le journal *European Polymer Journal*.

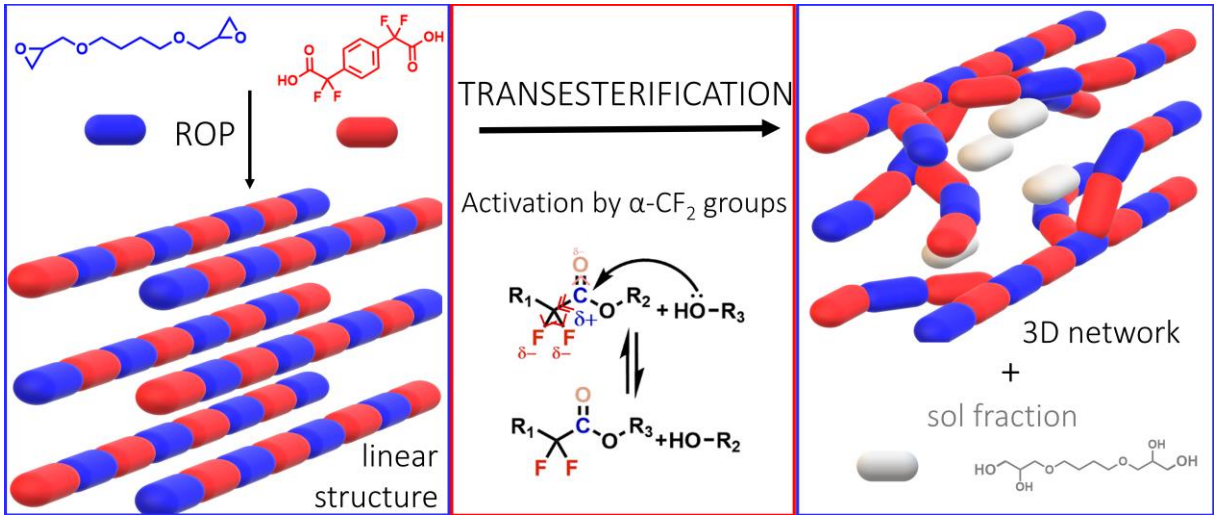

Figure E. Synthèse d'une macromolécule tridimensionnelle à partir d'un diacide fluoré et d'un diépoxy par transestérification activée par des groupements α-CF_2

[16] Cuminet, F.; Berne, D.; Lemouzy, S.; Dantras, E.; Joly-Duhamel, C.; Caillol, S.; Leclerc, E.; Ladmiral, V. Polym. Chem. 2022, 8, 5255–5446.
[17] Poutrel, Q.-A.; Blaker, J. J.; Soutis, C.; Tournilhac, F.; Gresil, M. Polym. Chem. 2020, 11 (33), 5327–5338.

Synthesis of a transesterification vitrimer activated by fluorine from an α,α-difluoro carboxylic acid and a diepoxy

Florian Cuminet,[a] Sylvain Caillol,[a] Éric Dantras,[b] Éric Leclerc,[a] Cédric Totée,[c] Olivier Guille,[d] and Vincent Ladmiral[a]

a ICGM, Univ Montpellier, CNRS, ENSCM, Montpellier, France
b CIRIMAT, Université Toulouse 3 Paul Sabatier, Physique des Polymères, 118 Route de Narbonne, 31062 Toulouse, France
c ICGM, PAC, Univ Montpellier, CNRS, ENSCM, Montpellier, France
d Institut d'Electronique et Systèmes (IES) UMR 5214, Université de Montpellier/CNRS, 34095, Montpellier, France

Abstract

An α,α-difluorodicarboxylic acid (P-DAF) was easily synthesized in two steps from diiodobenzene and reacted with a commercial diepoxy (BDGE). The electron-withdrawing effect of the fluorinated group activated the polymerization and gelation readily happened at room temperature. After curing at 150 °C a novel dynamic material was obtained. The P-DAF/BDGE material exhibited a high gel content (94 %) and was able to flow when heated. This material could be successfully reshaped by compression molding under mild conditions (1.5 h at 150 °C). This new material demonstrates that catalyst-free transesterification vitrimers can be prepared from difunctional monomers.

Introduction

Thermosets are polymers made of a network of covalent bonds. Thanks to this structure, they are endowed with high chemical resistance, as they do not solubilize in organic solvents, and high thermal resistance, as they do not flow upon heating.[1] In the current context of pursuit for greener and more sustainable polymers, thermosets are raising concerns as they cannot be easily recycled.[2] An answer to this issue is the use of reversible covalent bonds to prepare the network, since such bonds can be broken into reactive species able to re-associate with similar partners elsewhere in the network and form new bonds of the same nature.[3–7] At low temperatures, the bonds are unreactive and the network is permanent, whereas upon heating exchange reactions between reversible bonds can take place. This feature allows the polymer chains to rearrange at the local scale, and the material to flow at the macroscopic scale and be recycled. The most extensively studied chemistry for such materials is probably the Diels-Alder and retro-Diels-Alder reactions.[8,9] However, the dissociative nature of this reaction often induces a dramatic loss of the network integrity during the reprocessing steps.[10] In 2005, Bowman et al. introduced a dynamic network in which covalent bonds exchanges proceeded via an associative mechanism triggered by visible light.[11] In such exchange mechanisms the crosslinking

density does not decrease, as a new bond is formed when another is broken, simultaneously. Thereby, the number of crosslinks remains the same even when the network rearranges. Later, in 2011, the same idea was implemented in polyester networks, using transesterification reactions triggered by heat.[12] The exchange reaction was promoted by a Zn^{II} catalyst so that the rearrangements at high temperature were fast enough to induce a flow of the material. Because the viscosity of these polymers evolves linearly with temperature as silica glasses, and because they can be shaped the same way, they were called vitrimers. This discovery generated a strong emulation within the polymer scientists community, leading to the discovery of many other exchange reactions and their implementation in vitrimers: carbonates,[13] dioxaborolanes,[14,15] olefins,[16] vinylogous urethanes[17–19] and imines[20–23] are just a few examples of exchangeable functions that have been reported in vitrimers thus far. The major drawback of the polyester vitrimers is the use of an external catalyst, usually Zn^{2+}, triazabicyclodecene or phosphines.[24] However, these catalysts are suspected to leach out of the material or to induce premature ageing upon reprocessing.[25–27] To overcome this issue, some strategies were developed to synthesize catalyst-free transesterification vitrimers. Hyperbranched epoxy monomers were synthesized from BADGE and a trifunctional alcohol before curing with succinic anhydride. The resulting relatively loose network and the high content of free hydroxy groups favored the mobility and the catalyst-free transesterification.[28] The effect of high hydroxy group concentration alone was also reported.[29,30] Another strategy is to embed a catalytic function in the network. For example, tertiary amines integrated in a polyester network were proved to act as an internal catalyst and activate the material flow.[31] Finally, the addition of activating groups in the direct vicinity of the ester links can also promote the transesterification reaction.[32] Oxime-esters are a representative example of this strategy.[27] Recently, the activation of the transesterification reaction thanks to vicinal fluorinated groups was demonstrated.[33] In particular, the careful design of β,β,β-trifluoro and α,α-difluoro polycarboxylic acids, from a tetrathiol and a triphenol respectively, allowed the synthesis of catalyst-free polyester vitrimers.[34,35] The present work aimed at the diversification of such fluorinated monomers and of the properties of the materials obtained thereof. Inspired by the work of Poutrel et al. on the synthesis of crosslinked vitrimers from a mix of diepoxides and sebacic acid,[10] a catalyst-free transesterification vitrimer was synthesized from a simple difunctional α,α-difluorodicarboxylic acid and a commercially available difunctional epoxy. The gelation of diepoxy-diacid "2+2" systems for classical thermosets is well known[36] and was also reported for vitrimers.[10] In 2+2 systems, the ring opening of the epoxy by the acid cannot explain the gelation alone. Side reactions, such as direct esterification and epoxy homopolymerization also occur as the curing is done at high temperatures, thus inducing the crosslinking.[1] The goal of this work is to study the feasibility of a crosslinked network at lower temperature with fluorinated dicarboxylic acids. The activation of the transesterification by fluorine is expected to be beneficial for the crosslinking density. In this context, a novel

α,α-difluorodiacid (P-DAF) was synthesized in two scalable steps from 1,4-diiodobenzene. P-DAF was reacted with commercial butanediol diglycidylether (BDGE) to obtain an insoluble crosslinked material which resistance to solvents, mechanical properties and flow properties were studied. The P-DAF/BDGE vitrimer ability to be reprocessed was also assessed.

Results and Discussion

Monomer Synthesis

A novel α,α-difluorinated *bis*-carboxylic acid (P-DAF, Figure 1) was synthesized for the first time, following procedures described for monofunctional analogues.[37,38] The conditions for this reaction feature several advantages. First, the corresponding diester is synthetized in DMSO, which is a non-toxic solvent. The temperature of the reaction is 60 °C, which is relatively mild. In addition, the purification procedure is much easier and more convenient than the silica gel chromatography previously reported, especially for large-scale syntheses.[34] Indeed, the reaction conditions used to prepare α,α-difluorinated carboxylic acids from a tri-phenol induce a partial oxidation of the latter, thus requiring a purification on silica gel to obtain the pure target monomer. Here, the purification of the crude product is easily scalable, as the desired compound is isolated by a simple recrystallization in ethanol. The overall yield after the first recrystallization was 42 %. Nevertheless, this yield was improved by removing the solvent and performing a second recrystallization to reach an overall yield of 54 %. Finally, a straightforward saponification using a potassium carbonate aqueous solution in methanol led to the pure desired diacid P-DAF as a white powder, without further purification (Scheme 1).

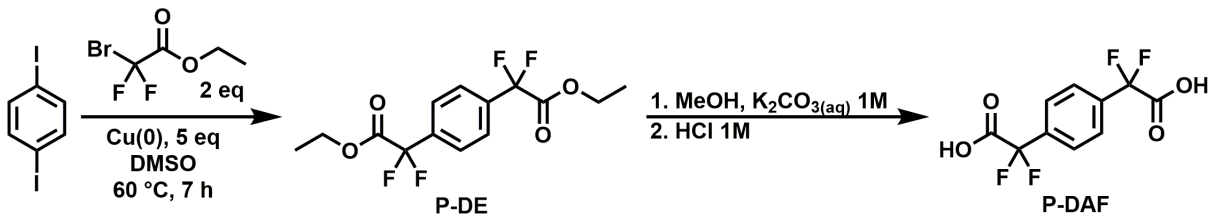

Scheme 1. 2-step synthesis of P-DAF from 1,4-diiodobenzene

Vitrimer Network Synthesis

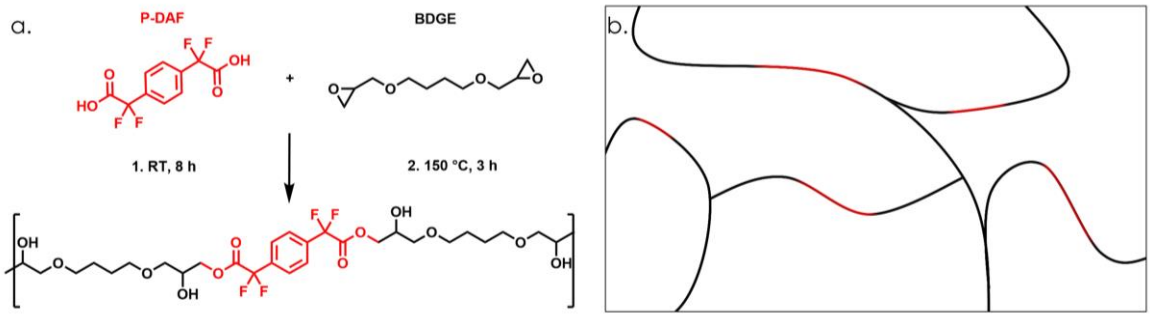

Figure 1. a. Vitrimer synthesis from P-DAF and BDGE and b. schematic representation of the structure

P-DAF was mixed with BDGE at room temperature (ca. 20°C) and a gel formed after after 8 h. The resulting gel was then cured at 150 °C for 3 h (Figure 1 and 3a). As previously described,[34,35] fluorine atoms enhance the acid reactivity towards the epoxy, allowing the ring opening to happen significantly at room temperature (RT). A FTIR monitoring was performed over the first two hours of reaction at RT (Annexes B Figure S1). The shift of the acid C=O band to the ester around 1761 cm^{-1} was too narrow to follow the conversion of these functions. Nevertheless, the intensity of the epoxy band at 914 cm^{-1} clearly decreased over time, which indicates that the opening of the epoxy by the acid occurs at RT (Annexes B Figure S2). Additionally, this reaction could also be observed using ^{13}C high resolution magic angle spinning (HRMAS) NMR spectroscopy. No deuterated solvent was used, which is common in solid state NMR, but rather uncommon for HRMAS NMR experiments. The high resolution obtained in ^{13}C allowed to acquire spectra without lock, and calibrate them using the peaks at 26 and 71 ppm of the butanediol core of BDGE. In addition, the outstandingly fast acquisition (256 scans, 0.1 s per scan) of these ^{13}C spectra allowed to qualitatively monitor the reaction by this technique. The progressive disappearance of the epoxy signals at 44 ppm (R-CH-O-C**H**$_2$) and 51 ppm (R-C**H**-O-CH$_2$) was easily followed over the course of 6 h, when they completely disappeared (Figure 2 and Annexes B Figure S3). Attempts to follow the reaction by ^{1}H HRMAS NMR failed because the signal resolution was too poor. ^{19}F HRMAS NMR could not be used either to follow the ester formation. Indeed the difference in chemical shifts of the α-difluoroacids and α-difluoroesters was too small (-102.1 ppm for P-DE and -103.0 ppm for P-DAF in solution ^{19}F NMR, Annexes B Figures S4 and S5).

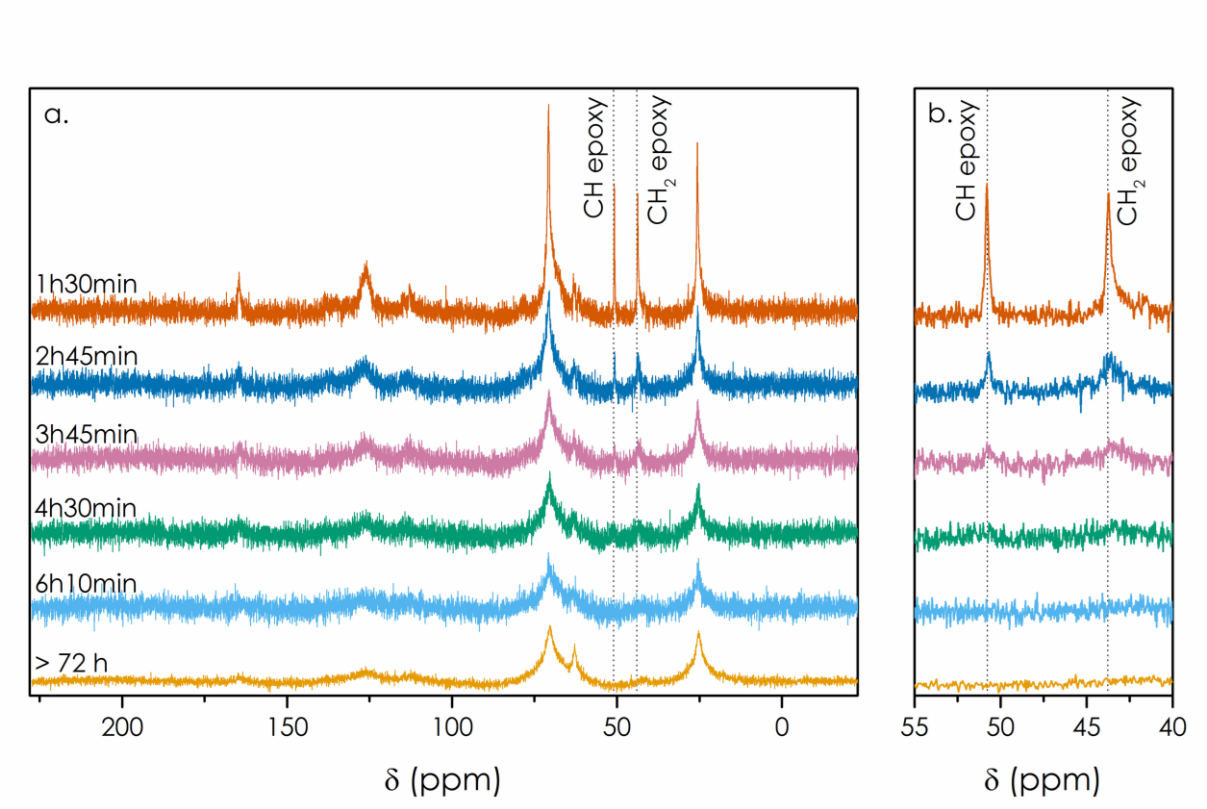

Figure 2. Monitoring of the P-DAF / BDGE polymerization reaction by ^{13}C HRMAS NMR over time a. full spectrum and b. zoom on the 55-40 ppm zone.

After gelation at room temperature, a DSC of the resulting material was performed to check whether the polymerization was complete. Two consecutive heating ramp from -100 °C to +250 °C were applied (Annexes B Figure S6). On the first heating ramp a T_g is visible at 13 °C, and a small endothermic peak can be observed between the T_g and the maximum temperature. On the second heating ramp, this endothermic phenomenon is absent and the T_g increased to 27 °C. This result suggests that a curing step at higher temperature is necessary to finish the polymerization reaction. This was confirmed by the relatively low gel content observed after the polymerization at room temperature (50-60 % in polar solvents, Annexes B Table S1). The end of the polymerization was also followed by monitoring the evolution of the dynamic storage modulus E' of the material with time, first at 150 °C (Annexes B Figure S7) and then at 170 °C (Annexes B Figure S8). At 150 °C, the storage modulus increased during 80 minutes from 0.5 to 3.7 MPa, before reaching a plateau. The analysis was stopped after 100 min. Then, a second step at 170 °C was applied, to check whether the polymerization was over or if a higher temperature would extend it again. No significant evolution of the modulus (which ranged between 4.0 and 4.5 MPa at this temperature) was observed. This result suggested that a curing step of 80 min at 150 °C was sufficient to finish the polymerization. This curing time was nonetheless doubled to ensure a complete curing; and the BDGE/P-DAF gel obtained at room temperature was cured for 3 h at 150 °C. This treatment produced a flexible light brown material (Figure 3b).

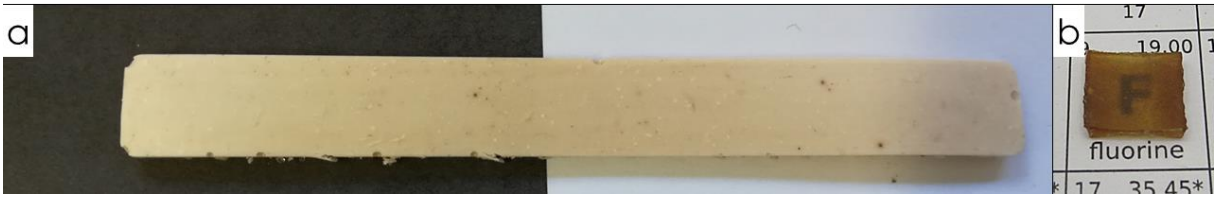

Figure 3. a. Crosslinked material after 8 h at room temperature (ca.20 °C); and b. after 3 h at 150 °C

The swelling index (SI) and gel content (GC) of the BDGE/P-DAF material were determined in a series of solvents (Annexes B Table S2). Polar solvents showed the highest affinity with the polymer, as the swelling index was 237, 148, 159 and 136 % in dimethylsulfoxide (DMSO), dichloromethane (DCM), water and tetrahydrofuran (THF), respectively. This is not surprising since the network contains many polar functions such as esters, hydroxyl and -CF_2 groups. The material exhibited a gel content of 96 % in THF, the best solvent for both monomers, thus confirming the crosslinked structure of the material. The morphology of the C=O FTIR band in the 1780-1710 cm^{-1} area (Annexes B Figure S9) did change form a single band at 1760 cm^{-1} with a shoulder towards low wavenumbers, to two bands at 1765 and 1730 cm^{-1} after the curing step at 150 °C. Unfortunately, the bands of the acid and of the ester are hardly distinguishable. Nevertheless, a very weak band centered on 2631 cm^{-1} which can be ascribed to the O-H stretching of carboxylic acid disappeared after the curing at 150 °C (Annexes B Figure S10). This confirmed that a small amount of unreacted carboxylic acid remained in the material after the polymerization at room temperature. This residual unreacted –COOH groups are probably due to the lack of mobility of the reactive species after the gelation occurred.

Obtaining a crosslinked network from a difunctional epoxy and a difunctional carboxylic acid seems counterintuitive if only the reaction of epoxide opening by acids is considered. In this case, the polymerization would indeed lead to linear polymer chains and the material would be a thermoplastic. However, if other reactions happen concomitantly to the epoxy ring-opening, in particular transesterification, then 3D network can be formed.[36] The epoxy opening by a carboxylic acid leads to primary and secondary β-hydroxyl esters (Scheme 1).

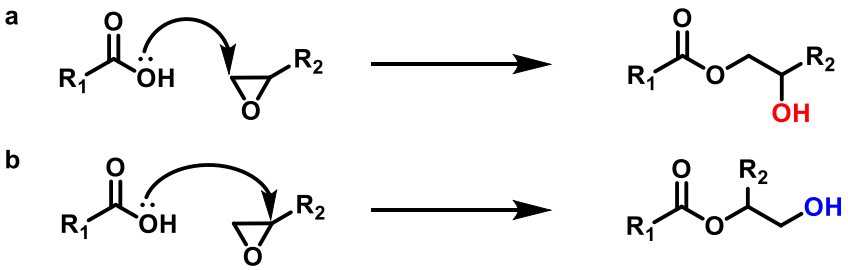

Scheme 1. Epoxide opening by a carboxylic acid leads to a. secondary or b. primary β-hydroxyl ester.

Then, the dangling hydroxy groups can undergo transesterification with an ester of another chain/segment. This leads to crosslinks and to the formation of free polyol oligomers, disconnected from the network, in the sol fraction (Figure 4). This mechanism was clearly explained and theorized recently for non-fluorinated epoxy-acid vitrimers made from difunctional acids and is represented for the present system in Figure 4.[10]

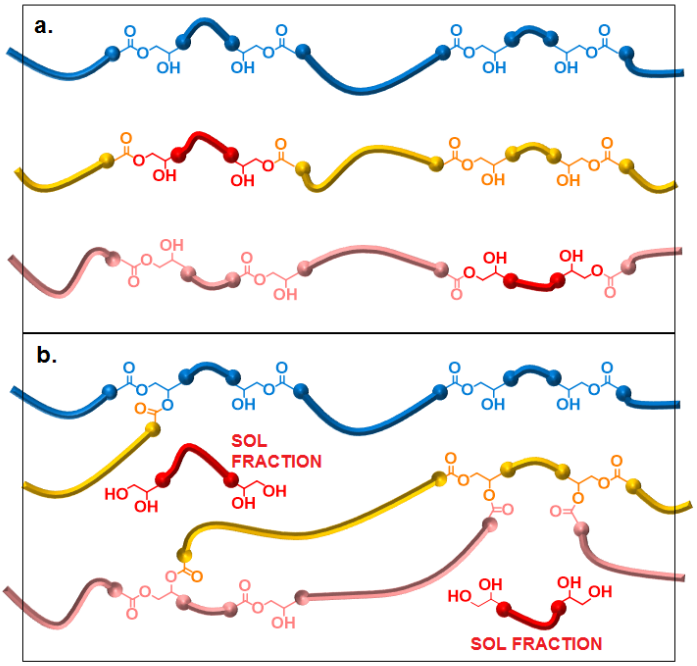

Figure 4. Expected structures of a diepoxy-diacid "2+2" polymer (a). if only epoxy opening by the acid is considered (b). if transesterification and Fisher esterification are taken into account (crosslinked network: blue, orange and pink segments and oligomers in the sol fraction in red).

In addition, other minor side reactions could increase the degree of crosslinking of the network: 1) Fisher esterification with the remaining traces of carboxylic acid groups (Figure 5a), and 2) irreversible formation of ether bonds (Figure 5b).[1,10]Although these reactions only happen to a small extent, they generate crosslinks which can be beneficial to the formation of 3D network.

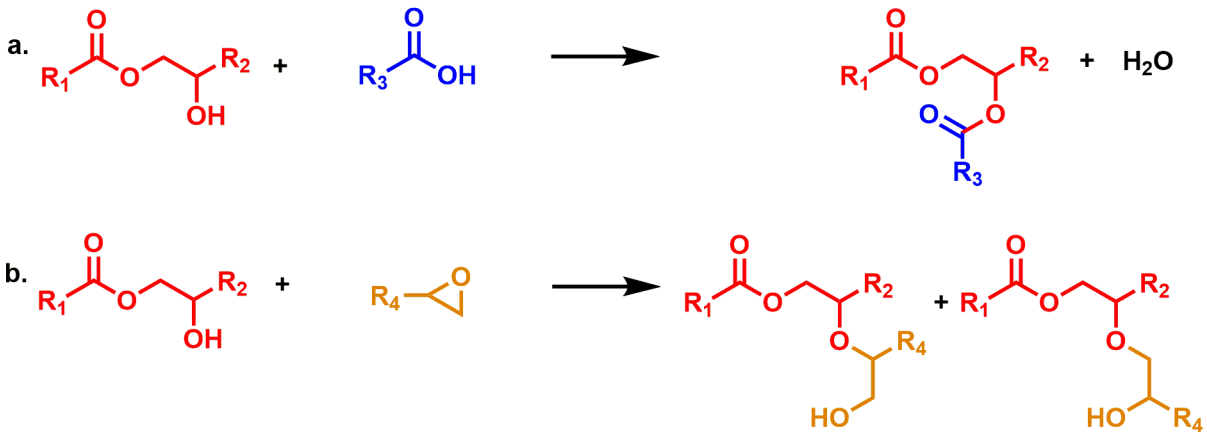

Figure 5. Possible side reactions during the curing step at 150 °C a. Fisher esterification, b. etherification by epoxy opening by an alcohol

Vitrimer Characterization

The thermal stability of the BDGE/P-DAF vitrimer was assessed by TGA under air. The temperature of 2 % mass loss was 262 °C whereas 5 % mass loss was attained at 321 °C (Annexes B Figure S11, Table 1). The T_g measured by DSC was 27 °C (Annexes B Figure S6). This value is rather low considering the aromatic nature of the diacid, and shows that BDGE brings flexibility to the network, as expected. This feature also translates on the DMA experiment, with T_α = 47 °C. The values of the storage modulus were E'_G = 1.9 GPa and E'_R = 11 MPa on the glassy plateau and on the rubbery plateau respectively (Annexes B Figure S12, Table 1), which is consistent with similar networks reported previously.[28,29,34,39,40]

Table 4. Thermal properties of the BDGE/P-DAF vitrimer

$T_{2\% \text{ loss}}$ (°C)	$T_{5\% \text{ loss}}$ (°C)	T_g (°C)	T_α (°C)	E'_G (GPa)[a]	E'_R (MPa)[b]	SI (%)[c]	GC (%)[c]
262	321	27	47	1.9	11	136	96±1

[a] at T_α–50 °C | [b] at T_α+50 °C | [c] in THF

The flow properties of the BDGE/P-DAF vitrimer were studied by stress-relaxation in the time domain. To assess the role of fluorine in the flow properties, a non-fluorinated counterpart called BDGE/P-DA was prepared by reaction of 1,4-phenylenediacetic acid and BDGE at 120 °C overnight and at 180 °C for 1 h. As no catalyst was used the polymerization of the non-fluorinated system required higher temperatures and longer polyùerization times, which might have an influence on the macromolecular structure. Nevertheless, this material is useful for the direct comparison of the dynamic properties of two uncatalysed systems, fluorinated and non-fluorinated. A 10 % torsionnal strain was applied and full stress relaxation was observed for the fluorinated BDGE/P-DAF material at 210 °C after 45900 s (12 h 45 min, the end of the curve is noisy because of the apparatus technical limitations to keep the

applied strain constant at low torque). The same experiment was performed on the non-fluorinated BDGE/P-DA counterpart. The relaxation was much slower, as only 37 % of the applied stress was relaxed after the same duration. This proves the significant effect of the α,α-difluoro group to activate transesterification and allow the material to flow (Figure 6).

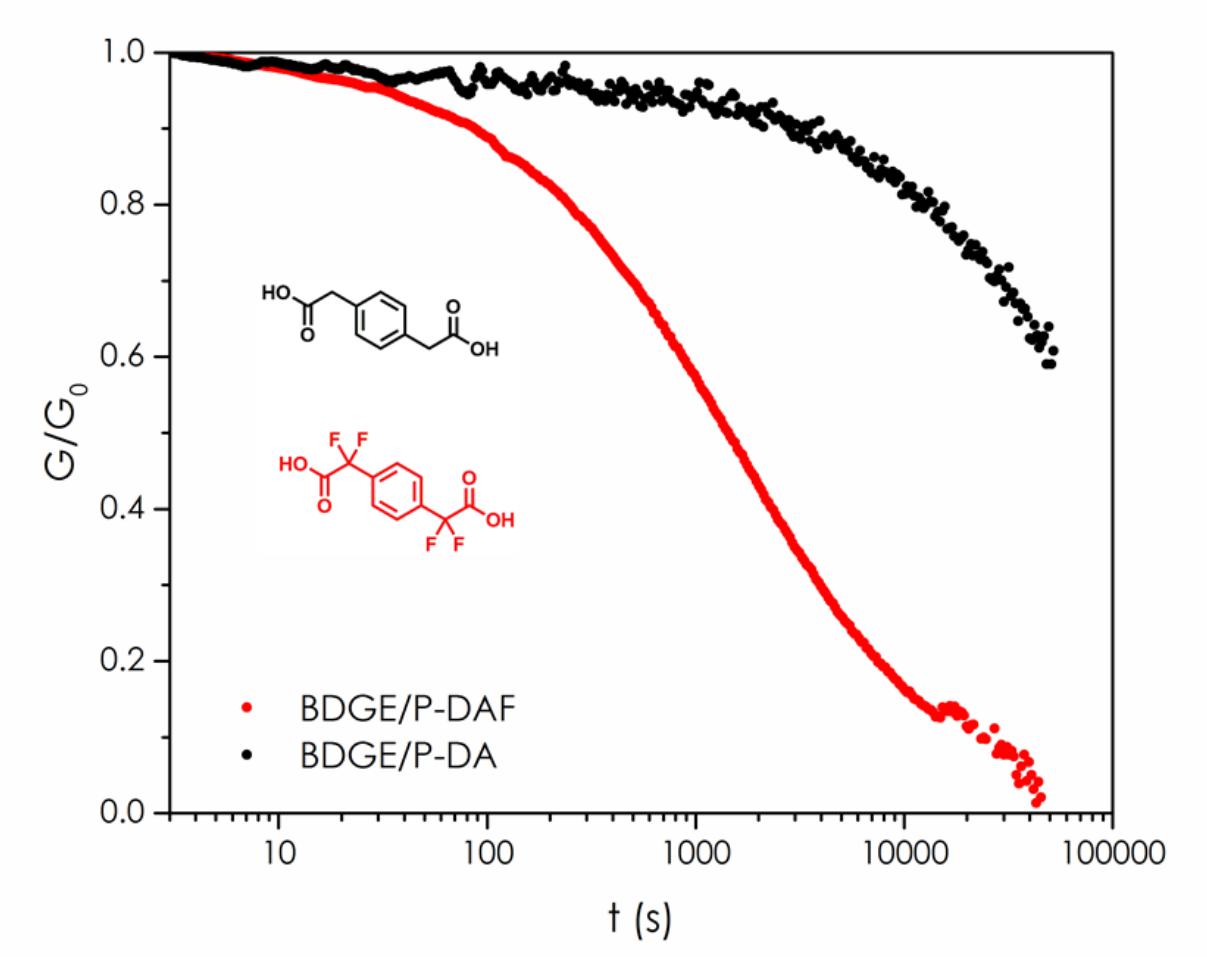

Figure 6. Stress relaxation experiments on fluorinated P-DAF/BDGE and non-fluorinated P-DA/BDGE at 210 °C with a 10 % strain.

The modulus behavior was monitored for isotherms ranging from 170 to 210 °C (Figure 7). The stress relaxation data were fitted with a Kohlraush-Williams-Watts equation and the obtained relaxation times τ_{kww} were plotted in an Arrhenius diagram (Figure 7 inset). The value obtained from the curve at 170 °C was discarded, because the data at this temperature was considered inaccurate. Indeed, the relaxation seemed faster than expected compared to the other isotherms. This is likely due to a slow slipping of the sample at lower temperatures for long experiment times, in spite of the experimental efforts implemented to overcome this issue. This translates clearly on the Arrhenius plot when the 5 isotherms values are plotted. Thus, only the isotherms from 180 °C to 210 °C were considered. The τ_{kww} values followed a linear fit, proving the vitrimer follows the Arrhenius law, and the activation energy was determined to be $E_a = 118 \pm 8$ kJ mol^{-1} (Figure 7 inset).

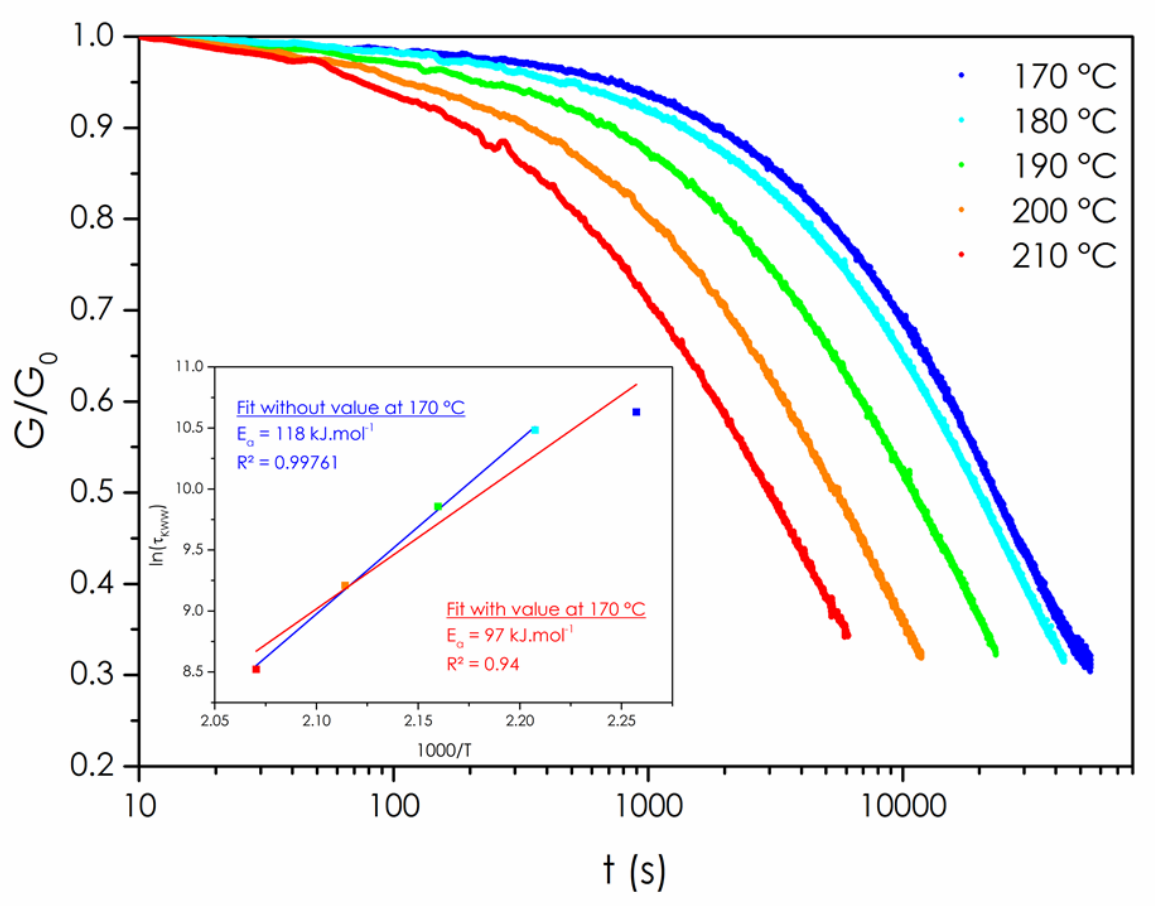

Figure 7. Normalized stress-relaxation experiments from 170 to 210 °C for BDGE/P-DAF vitrimer fitted with the Kohlraush-Williams-Watts equation (KWW) and Arrhenius plot of the τ_{KWW} relaxation times obtained.

The reprocessing ability of the vitrimer was successfully assessed by compression molding. Samples were diced into ≈ 1 mm^3 pieces and reprocessed by compression molding for 1.5 h at 150 °C under a 6 ton load (Figure 8).

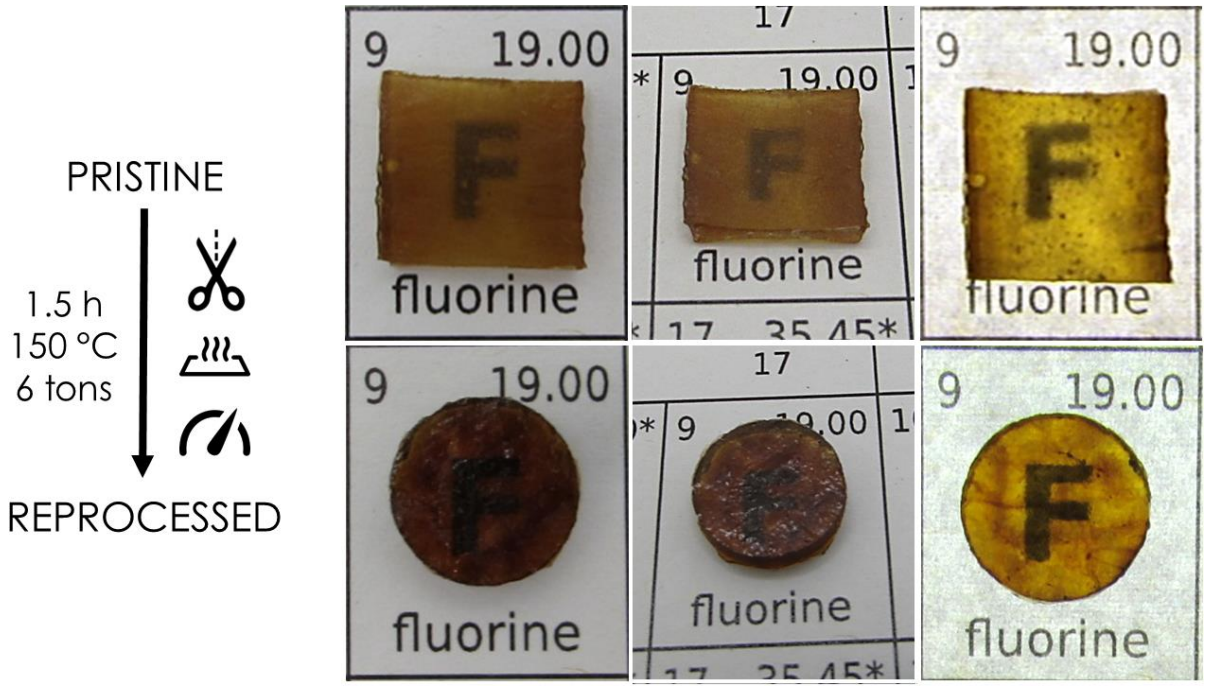

Figure 8. P-DAF/BDGE vitrimer before and after reprocessing by compression molding, front lighting (center) and backlit (right)

Table 5. Properties of P-DAF/BDGE vitrimer pristine, after reprocessing and after subsequent annealing

	Pristine	Reprocessed[b]	Annealed[c]
T_g (°C)	27	-2	20
T_α (°C)	47	30	40
SI (%)[a]	136	308	-
GC (%)[a]	96±1	93±1	-
E'_R (MPa)	11	7	6

[a] in THF | [b]1.5 h, 150 °C, 6 tons in press | [c]3 h, 150 °C in oven

The vitrimer chemical stability upon reshaping was checked by FTIR (Figure 9). A slight increase of the –OH band and the appearance of a weak band at 1630 cm^{-1} were observed. These may be caused by a slight water intake of the material from ambient moisture before reprocessing. The value of T_g obtained by DSC dropped from 27 °C for the pristine material to -2 °C for the reprocessed material (Table 2 and Annexes B Figure S13). The swelling index of 136 % before reprocessing increased to 308 % after reprocessing, whereas the gel content slightly decreased from 96±1 % to 93±1 % (Table 2). The water intake could lead to plasticization, or to some hydrolysis at high temperature in the heating press. By DMA the T_α shifted from 47 °C to 30 °C before and after reprocessing, respectively and the modulus on the rubbery plateau decreased from 11 to 7 MPa (Table 2 and Annexes B Figure S14). The T_α ascribes for the effects of both plasticization and possible hydrolysis, whereas the modulus on the rubbery plateau depends only on the crosslinking density, thus the decrease observed can be ascribed to hydrolysis during reprocessing. This hypothesis of a plasticization effect after hot pressing remains plausible, as the sample is constrained between two plates which hinder water evaporation. When a

reprocessed sample underwent an annealing treatment in an oven for 3 h at 150 °C, in which water is free to escape from the material, the T_g and the T_α reached values (T_g = 20 °C, T_α = 40 °C) close to those of the material before reprocessing. This results are consistent with a water plasticizing effect. Nevertheless, the modulus on the rubbery plateau was not recovered (6 MPa) which suggests partial hydrolysis. The change in the gel content, though very limited, also supports this hypothesis. Therefore, the behaviour of the material is most likely due to a combination of both plasticization and hydrolysis (Table 2).

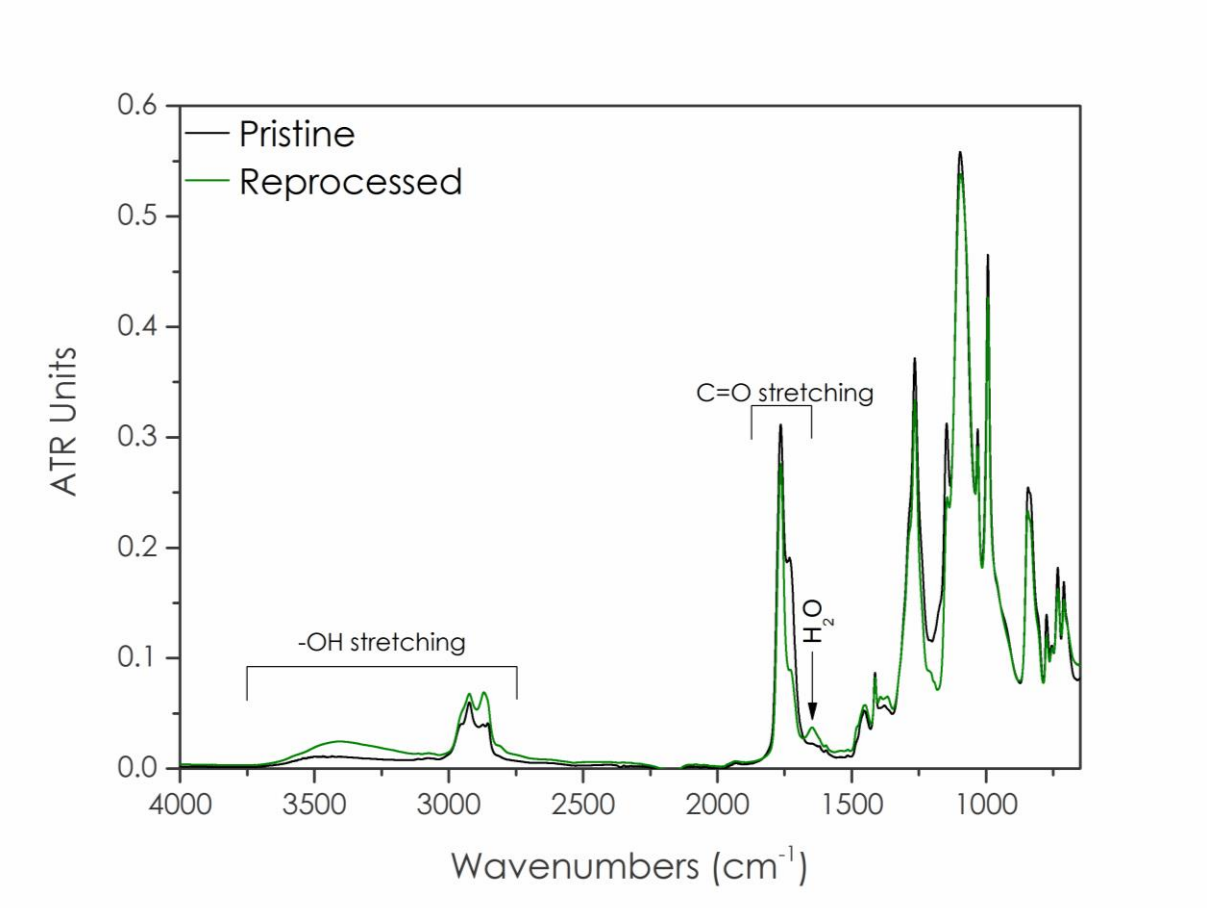

Figure 9. FTIR spectra of the P-DAF/BDGE vitrimer before and after reprocessing by compression molding

Conclusion

Catalyst-free transesterification vitrimers were synthesized from P-DAF, an α,α-difluorodicarboxylic acid and a commercially available diepoxy. P-DAF was easily synthesized in two steps and purified by recrystallization. The α,α-difluoro groups proved to activate P-DAF reactivity towards epoxy ring opening, as the reaction with the diepoxy BDGE readily happened at room temperature. This bulk polymerization resulted in a gelled material. After completion of the curing at 150 °C for 3 h, an

insoluble thermosetting material was obtained. Transesterification concomitant to the epoxy-acid reaction during the curing was responsible for the crosslinking of the network. The P-DAF/BDGE material relaxed stress when a constant strain was applied at temperatures ranging from 170 to 210 °C. The dynamic properties of this material are due to bond exchanges by transesterification activated by the inductive effect of the α-CF_2 groups to the ester bonds. The relaxation times at different isotherms followed the Arrhenius equation, which is consistent with the behavior of a vitrimer. The P-DAF/BDGE vitrimer was then successfully reprocessed by compression molding for 1.5 h at 150 °C under a 6-ton load to give homogeneous reshaped samples, without the need for any added catalyst. The feasibility of such α,α-difluoro activated vitrimers from difunctional monomers will simplify the synthesis of other similar materials, as difunctional species are more available than tri- or tetra-functional ones. This could benefit in the future to a better understanding of the structure/properties relationship in such materials, but also to their potential synthesis on larger scales.

Experimental Section

Materials

Copper powder (Aldrich, 99 %), 1,4-diiodobenzene (Fluorochem, 98 %), 1,4-butanediol diglycidyl ether (BDGE, Aldrich, ≥ 95 %, 1,1,1-Tris(4-hydroxyphenyl)ethane ("TPE", Sigma-Aldrich, 99 %), 1,8-Diazabicyclo(5.4.0)undec-7-ene (DBU, Fluorochem, 98 %), ethyl bromodifluoroacetate (Fluorochem, 98 %), 1,4-phenylenediacetic acid (ABCR, 97 %) were used as received. Solvents were supplied by VWR Chemicals. Deuterated solvents were supplied by Eurisotop (99.8 %).

Synthetic Procedures

Synthesis of diethyl 2,2'-(1,4-phenylene)bis(2,2-difluoroacetate) (P-DE): 1,4-diiodobenzene (41.3 g, 125 mmol, 1 equiv.) was dissolved in DMSO (300 mL) in a 500-mL round-bottom flask. Copper powder (42.17 g, 664 mmol, 5.3 equiv.) was added under vigorous stirring to obtain a suspension. Ethyl bromodifluoroacetate (51.0 g, 251 mmol, 2 equiv.) was then added. The flask was sealed with a septum and heated to 60 °C for 7 hours. The crude mixture was cooled to room temperature, poured in a mixture of ice and saturated ammonium chloride aqueous solution (1.5 L) under vigorous magnetic stirring. The aqueous solution was extracted 4 times with ethyl acetate (4 x 500 mL). The combined organic layers were washed 4 times with saturated aqueous ammonium chloride (4 x 400 mL) and twice with brine (2 x 400 mL), dried with $MgSO_4$ and concentrated under reduced pressure. The solvent was removed under high vacuum to afford 38 grams of an orange solid-and-oil mixture. The crude product was taken in a minimum of cold ethanol, inducing a crystallization of 17 grams of the pure diester (white solid, 42 %). The filtrate was concentrated under reduced pressure and the same operation was repeated to afford another 4.9 grams of the diester (off white solid, 12 %). **^{1}H NMR**

400MHz DMSO-d_6 (Annexes B Figure S15): δ (ppm) 7.80 (s, 4 H, aromatic protons), 4.31 (quad, 4 H, CH_2), 2.50 (DMSO), 1.21 (t, 6 H, CH_3). **^{19}F NMR 377 MHz, DMSO-d_6 (Annexes B Figure S16):** δ (ppm) -102.1. **^{13}C NMR 101 MHz, DMSO-d_6 (Annexes B Figure S17):** δ (ppm) 163.2 (RCOOR, J_{C-F} = 36 Hz), 135.4 (C^{IV} aromatic, J_{C-F} = 26 Hz), 126.6 (CH aromatic, J_{C-F} = 6 Hz), 113.3 (CF_2, J_{C-F} = 252 Hz), 64.2 (CH_2), 40.0 (DMSO), 14.0 (CH_3). **HRMS (ESI+)** Calc. for $[M+H]^+$ 323.0901, found 323.0902. **FTIR spectrum:** Annexes B Figure S18.

Synthesis of 2,2'-(1,4-phenylene)bis(2,2-difluoroacetic acid) (P-DAF): In a 250-mL round-bottom flask, 9.4 g of diester P-DE were dissolved in 80 mL of methanol. Then, 80 mL of a 1M potassium carbonate aqueous solution was added under magnetic stirring and the reaction was left to proceed overnight at room temperature. The crude mixture was then precipitated in 300 mL of 1M HCl, extracted with ethyl acetate (3 x 200 mL), washed twice with brine (2 x 150 mL), dried over Na_2SO_4 and the solvent was removed under reduced pressure to afford 7.7 g of the pure diacid (white solid). **^{1}H NMR 400MHz DMSO-d_6 (Annexes B Figure S19):** δ (ppm) 7.76 (s, 4 H, aromatic protons). **^{19}F NMR 377 MHz, DMSO-d_6 (Annexes B Figure S20):** δ (ppm) -103.0. **^{13}C NMR 101 MHz, DMSO-d_6 (Annexes B Figure S21) :** δ (ppm) 165.1 (RCOOR, J_{C-F} = 33 Hz), 135.9 (C^{IV} aromatic, J_{C-F} = 27 Hz), 125.6 (CH aromatic, J_{C-F} = 168 Hz), 113.5 (CF_2, J_{C-F} = 250 Hz), 40.0 (DMSO). **HRMS (ESI-)** Calc. for $[M-H]^-$ 265.0129, found 265.0135. **FTIR spectrum:** Annexes B Figure S22.

Synthesis of BDGE/P-DA reference material: 0.97 g (10 meq ; EEW=97 g/eq) of 1,4-phenylenediacetic acid was mixed with 1.19 g of BDGE at 90 °C to obtain a homogeneous light brown mixture. The mixture was cast in aluminum molds and left overnight in an oven at 120 °C. The mixture was not cured and a subsequent 1 h step at 180 °C was applied. The curing was checked by DSC and no remaining exothermic phenomenon was observed.

Synthesis of BDGE/P-DAF vitrimer: 1 g (7.5 meq COOH, HEW=133) of P-DAF and 1.067 g (7.5 meq epoxy, EEW=142) of butanediol diglycidyl ether (BDGE) were mixed together manually at room temperature until P-DAF was totally dissolved. A viscous clear yellowish solution was obtained and quickly cast in PTFE molds. The solution was left to gel at room temperature, typically for 8 hours. Then, a brittle gel was obtained, unmolded and left for 3 h in an oven at 150 °C.

Instrumentation

NMR: ^{1}H, ^{13}C and ^{19}F were acquired on a Bruker Avance 400 MHz spectrometer at 23 °C. External reference was tetramethylsilane (TMS) with chemical shifts given in ppm. Samples were dissolved or diluted in 0.5mL of $CDCl_3$ or DMSO-d_6 depending on their solubility.

FTIR: FTIR spectra were acquired on a ThermoScientific Nicolet iS50 FT-IR equipped with an attenuated total reflectance cell (ATR). The data were analyzed using the software OMNIC Series 8.2 from Thermo Scientific.

HRMAS: High resolution MAS NMR experiments were carried out on a Varian VNMRS 600 MHz spectrometer equipped with a wide bore magnet (B0 = 14.1 T). Prior to HRMAS NMR experiments, the BDGE and the P-DAF were manually mixed together in a beaker, and injected in a 4 mm quartz zirconia HRMAS rotor insert with a 1 mL syringe. No solvent was added and the calibration was made using the peaks at 72 and 26 ppm of the BDGE, as observed in liquid NMR. Experiments were performed at room temperature. The sample spinning rate was 5 kHz. ^{13}C NMR spectra were recorded at 20 °C, 38 kHz for spectral width, 15 kHz for transmitter frequency offset, 0.1 s for acquisition time, 256 scans (NS) with a 45 ° pulse (5.5 µs) and a relaxation delay at 1 s . ^{1}H decoupling was applied during the whole sequence. The outstandingly short overall acquisition time compared to usual ^{13}C experiments allowed to obtain spectra within a few minutes and to monitor qualitatively the polymerization reaction for several hours.

Mechanical analysis: Dynamic Mechanical Analyses were carried out on Metravib DMA 25 with Dynatest 6.8 software. Uniaxial stretching of samples ($1 \times 2 \times 6$ mm^3) was performed while heating at a rate of 3 °C min^{-1} from −90 °C to 150 °C, at a f=1 Hz frequency. Relaxation experiments were performed on a ThermoScientific Haake Mars 60 rheometer equipped with a electric heating cell and a textured 8-mm plane-plane geometry. A 10 % torsional strain was applied on 8 mm diameter and 2 mm thickness circular samples, and the relaxation modulus evolution with time was monitored. The curing checking experiment was performed on a TA Ares G2 at a given temperature (150 or 170 °C) by applying a 0.1 % deformation at $\omega = 1$ rad.s^{-1} under a normal force of 100 grams every 2 minutes, and monitoring G'.

TGA: Thermogravimetric thermograms were recorded on a TA TGA G50 appliance using a 40 mL min^{-1} flux of synthetic air as purge gas. Approximately 10 mg of sample were used for each analysis. Ramps from 20 to 500 °C were applied at a rate of 20 °C min^{-1}.

DSC: Analyses were carried out using a NETZSCH DSC200F3 calorimeter. The calibration was performed using adamantane, biphenyl, indium, tin, bismuth and zinc standards. Nitrogen was used as purge gas. Approximately 10 mg of sample were placed in perforated aluminum pans and the thermal properties were recorded between -100 °C and the temperature of 2% mass loss $T_{d2\%}$ at 20 °C min^{-1}. The reported values are the values measured during the second heating ramp.

Reprocessing: the material was cut into 1 x 1 x 1 mm^3 pieces and then pressed in a PTFE mold for 1.5 h at 150 °C under a 6 tons load using a Carver 3960 manual heating press.

Acknowledgements

This work was funded by the Institut Carnot Chimie Balard CIRIMAT (16CARN000801). The authors would like to thank Dr. Marc Guerre and Dr. François Tournilhac for fruitful discussions.

References

(1) J.-P. Pascault, H. Sautereau, J. Verdu and R. J. J. J. Williams, *Thermosetting Polymers*, Marcel Dekker, Inc., New York, 2002.

(2) S. J. Pickering, in *Wiley Encyclopedia of Composites*, John Wiley & Sons, Inc., Hoboken, New Jersey, 2012.

(3) L. Leibler, M. Rubinstein and R. H. Colby, *Macromolecules*, 2002, **24**, 4701–4707.

(4) C. J. Kloxin, T. F. Scott, B. J. Adzima and C. N. Bowman, *Macromolecules*, 2010, **43**, 2643–2653.

(5) C. N. Bowman and C. J. Kloxin, *Angew. Chemie - Int. Ed.*, 2012, **51**, 4272–4274.

(6) C. J. Kloxin and C. N. Bowman, *Chem. Soc. Rev.*, 2013, **42**, 7161–7173.

(7) X. Chen, M. A. Dam, K. Ono, A. Mal, H. Shen, S. R. Nutt, K. Sheran and F. Wudl, *Science*, 2002, **295**, 1698–1702.

(8) V. Froidevaux, M. Borne, E. Laborbe, R. Auvergne, A. Gandini and B. Boutevin, *RSC Adv.*, 2015, **5**, 37742–37754.

(9) A. Gandini, *Prog. Polym. Sci.*, 2013, **38**, 1–29.

(10) Q.-A. Poutrel, J. J. Blaker, C. Soutis, F. Tournilhac and M. Gresil, *Polym. Chem.*, 2020, **11**, 5327–5338.

(11) T. F. Scott, A. D. Schneider, W. D. Cook and C. N. Bowman, *Science*, 2005, **308**, 1615–1617.

(12) D. Montarnal, M. Capelot, F. Tournilhac and L. Leibler, *Science*, 2011, **334**, 965–968.

(13) R. L. Snyder, D. J. Fortman, G. X. De Hoe, M. A. Hillmyer and W. R. Dichtel, *Macromolecules*, 2018, **51**, 389–397.

(14) M. Röttger, T. Domenech, R. Van Der Weegen, A. Breuillac, R. Nicolaÿ and L. Leibler, *Science*, 2017, **356**, 62–65.

(15) F. Caffy and R. Nicolaÿ, *Polym. Chem.*, 2019, **10**, 3107–3115.

(16) Y.-X. Lu and Z. Guan, *J. Am. Chem. Soc.*, 2012, **134**, 14226–14231.

(17) W. Denissen, M. Droesbeke, R. Nicolaÿ, L. Leibler, J. M. Winne and F. E. Du Prez, *Nat. Commun.*, 2017, **8**, 14857.

(18) W. Denissen, G. Rivero, R. Nicolaÿ, L. Leibler, J. M. Winne and F. E. Du Prez, *Adv. Funct. Mater.*, 2015, **25**, 2451–2457.

(19) M. Guerre, C. Taplan, R. Nicolaÿ, J. M. Winne and F. E. Du Prez, *J. Am. Chem. Soc.*, 2018, **140**, 13272–13284.

(20) H. Zhang, D. Wang, W. Liu, P. Li, J. Liu, C. Liu, J. Zhang, N. Zhao and J. Xu, *J. Polym. Sci. Part A Polym. Chem.*, 2017, **55**, 2011–2018.

(21) S. Wang, S. Ma, Q. Li, X. Xu, B. Wang, K. Huang, Y. Liu and J. Zhu, *Macromolecules*, 2020, **53**, 2919–2931.

(22) H. Zheng, Q. Liu, X. Lei, Y. Chen, B. Zhang and Q. Zhang, *J. Mater. Sci.*, 2019, **54**, 2690–2698.

(23) R. Hajj, A. Duval, S. Dhers and L. Avérous, *Macromolecules*, 2020, **53**, 3796–3805.

(24) M. Capelot, M. M. Unterlass, F. Tournilhac and L. Leibler, *ACS Macro Lett.*, 2012, **1**, 789–792.

(25) J. Wang, S. Chen, T. Lin, J. Ke, T. Chen, X. Wu and C. Lin, *RSC Adv.*, 2020, **10**, 39271–39276.

(26) J. J. Lessard, L. F. Garcia, C. P. Easterling, M. B. Sims, K. C. Bentz, S. Arencibia, D. A. Savin and B. S. Sumerlin, *Macromolecules*, 2019, **52**, 2105–2111.

(27) C. He, S. Shi, D. Wang, B. A. Helms and T. P. Russell, *J. Am. Chem. Soc.*, 2019, **141**, 13753–13757.

(28) J. Han, T. Liu, C. Hao, S. Zhang, B. Guo and J. Zhang, *Macromolecules*, 2018, **51**, 6789–6799.

(29) T. Liu, S. Zhang, C. Hao, C. Verdi, W. Liu, H. Liu and J. Zhang, *Macromol. Rapid Commun.*, 2019, **40**, 1800889.

(30) F. I. Altuna, V. Pettarin and R. J. J. Williams, *Green Chem.*, 2013, **15**, 3360–3366.

(31) F. I. Altuna, C. E. Hoppe and R. J. J. Williams, *Eur. Polym. J.*, 2019, **113**, 297–304.

(32) F. Cuminet, S. Caillol, É. Dantras, É. Leclerc and V. Ladmiral, *Macromolecules*, 2021, **54**, 3927–3961.

(33) S. Lemouzy, F. Cuminet, D. Berne, S. Caillol, V. Ladmiral, R. Poli, E. Leclerc, S. Lemouzy, F. Cuminet, D. Berne, S. Caillol, V. Ladmiral, E. Leclerc and R. Poli, *Chem. – A Eur. J.*, , DOI:10.1002/CHEM.202201135.

(34) F. Cuminet, D. Berne, S. Lemouzy, E. Dantras, C. Joly-Duhamel, S. Caillol, E. Leclerc and V. Ladmiral, *Polym. Chem.*, 2022, **8**, 5255–5446.

(35) D. Berne, F. Cuminet, S. Lemouzy, C. Joly-Duhamel, R. Poli, S. Caillol, E. Leclerc and V. Ladmiral, *Macromolecules*, 2022, **55**, 1669–1679.

(36) B. Steinmann, *Polym. Bull.*, 1989, **22**, 637–644.

(37) H. Eto, Y. Kaneko and T. Sakamoto, *Chem. Pharm. Bull.*, 2000, **48**, 982–990.

(38) S. Mizuta, I. S. R. Stenhagen, M. O'Duill, J. Wolstenhulme, A. K. Kirjavainen, S. J. Forsback, M. Tredwell, G. Sandford, P. R. Moore, M. Huiban, S. K. Luthra, J. Passchier, O. Solin and V. Gouverneur, *Org. Lett.*, 2013, **15**, 2648–2651.

(39) Y. Liu, S. Ma, Q. Li, S. Wang, K. Huang, X. Xu, B. Wang and J. Zhu, *Eur. Polym. J.*, 2020, **135**, 109881.

(40) J. Han, T. Liu, S. Zhang, C. Hao, J. Xin, B. Guo and J. Zhang, *Ind. Eng. Chem. Res.*, 2019, **58**, 6466–6475.

Conclusion du chapitre III

Dans ce chapitre, un vitrimère de transestérification activé par le fluor a été synthétisé à partir d'un acide carboxylique difonctionnel et d'un époxy commercial difonctionnel. La formation d'un réseau macromoléculaire tridimensionnel est liée à la réaction de transestérification, qui a lieu en même temps que la polymérisation par ouverture de cycle de l'époxy par l'acide carboxylique. Grâce à la transestérification, les macromolécules théoriquement linéaires se lient entre elles en libérant des oligomères diglycol (tetraol) qui ne sont plus liés au réseau, que nous avons nommés « oligomères sacrificiels ». Si la formation d'un tel réseau a déjà été décrite pour des thermodurcissables[18] et pour des vitrimères polyester catalysés,[19] leur faisabilité à partir d'acides α,α-difluorés a été démontrée dans ces travaux.

D'une part, un des intérêts majeurs de la synthèse du diacide α,α-difluorés P-DAF décrite est sa facilité à être adaptée sur de plus grandes échelles. Cette synthèse permet déjà d'obtenir plusieurs dizaines de grammes par lot (environ 40 g) à l'échelle du laboratoire, et les conditions de synthèse employées ne présentent pas d'obstacle *a priori* à une montée en échelle pour produire de plus grandes quantités. De plus, la méthode de purification par cristallisations et lavages successifs est également adaptée à une production à grande échelle : elle est peu énergivore et est économe en solvants, en comparaison d'une chromatographie sur colonne de silice par exemple.

D'autre part, la réaction mise en jeu présente des conditions de réaction plus vertueuses. En particulier, le solvant employé est le DMSO, qui est non-toxique contrairement au DMF utilisé précédemment (voir Chapitre II). Le temps et la température de réaction sont aussi plus faibles, 7 h à 60 °C, contre 40 h à 70 °C, ce qui permet un gain d'énergie. De plus, la réaction est plus robuste, les réactifs sont introduits en même temps dans le réacteur et la réaction ne nécessite pas de précaution particulière, contrairement à la synthèse du TPE-TAF (voir Chapitre II) qui nécessite un ajout progressif du bromodifluoroacétate d'éthyle pour limiter les réactions secondaires. Toutefois, l'utilisation de cuivre (0) en grande quantité reste un inconvénient majeur pour envisager une éventuelle production industrielle. En effet, le cuivre utilisé lors de la réaction n'est pas totalement récupéré en fin de réaction, ce qui entraîne un coût important en matières premières. De plus, les sels formés peuvent être toxiques.[20] Des travaux d'optimisation pourraient être envisagés afin de réduire la quantité de

[18] Steinmann, B. Polym. Bull. 1989, 22 (5–6), 637–644.
[19] Poutrel, Q.-A.; Blaker, J. J.; Soutis, C.; Tournilhac, F.; Gresil, M. Polym. Chem. 2020, 11 (33), 5327–5338.
[20] Bisson, M.; Boulevert, E.; Marliere, M.; Oberson Geneste, D. Cuivre et Ses Composés - Fiche de Données Toxicologiques et Environnementales Des Substances Chimiques; INERIS 2019.

cuivre nécessaire pour cette réaction et de réutiliser au maximum les effluents de cette réaction. Le recours à d'autres métaux en quantités catalytique peut aussi être envisagé.

Pour finir, la disponibilité et la diversité des synthons difonctionnels est plus importante que celle des synthons trifonctionnels ou de fonctionnalité supérieure. La possibilité de former des structures tridimensionnelles à partir d'acides α,α-difluorés difonctionnels permet d'envisager l'utilisation de ces synthons difonctionnels voire le recours à d'autres voies de synthèse, ce qui permettrait de diversifier les structures des monomères accessibles et d'étudier leur influence sur les propriétés des matériaux qui en sont issus.

CHAPITRE IV : TRANSPOSITION DE LA SYNTHESE D'α,α-DIFLUOROACIDES AU RESVERATROL POUR LA SYNTHESE DE VITRIMERES BIOSOURCES SANS CATALYSEUR

Introduction du chapitre IV

Dans le contexte actuel d'intérêt croissant pour la préservation de l'environnement, l'utilisation de matériaux polymères soulève de plus en plus d'inquiétudes quant à la gestion de leur fin de vie. Les vitrimères présentent un élément de réponse original au problème de recyclage des matériaux thermodurcissables, puisque leur remise en œuvre est possible par certaines techniques de recyclage mécanique. En revanche, l'utilisation de catalyseurs dans ces matériaux n'est pas souhaitable. L'utilisation de groupements activants α,α-difluorés a permis de synthétiser un vitrimère de transestérification sans catalyseur, capable d'être remodelé plusieurs fois (voir Chapitre II). Par la suite, des monomères acide difonctionnel et époxy difonctionnel ont également permis d'obtenir un matériau de type vitrimère sans catalyseur, et d'ouvrir la voie à d'autres structures potentielles.

Si l'anticipation de la fin de vie des matériaux polymères est extrêmement importante, la question des ressources utilisées dans leur fabrication n'en demeure pas moins primordiale. Aujourd'hui, 99 % des polymères sont fabriqués à partir de matières premières d'origine fossile, en particulier du pétrole.[21] Cette dépendance au pétrole pose deux problèmes majeurs. D'une part, les filières de production de polymères sont dépendantes du prix du pétrole, qui fluctue en fonction de l'offre et de la demande, mais aussi d'évènements géopolitiques. D'autre part, les réserves fossiles sont par définition finies, ce qui implique que d'autres sources de matières premières devront être trouvées à échéance. Par conséquent, la recherche dans le domaine des polymères synthétisés à partir de synthons biosourcés s'est fortement développée ces dernières années.[22,23] Les vitrimères n'échappent pas à cette tendance, et de nombreux exemples de vitrimères biosourcés ont été décrits et publiés dans des articles scientifiques, dans le but de synthétiser des polymères toujours plus vertueux, de la matière première utilisée jusqu'à leur fin de vie.[24]

Un des enjeux actuels des vitrimères est d'obtenir de hautes T_g avec des propriétés mécaniques adaptées à des applications structurales, tout en conservant la capacité de ces matériaux à être remis en œuvre.[12] Ce contexte a amené l'idée de réutiliser la réaction de synthèse du TPE-TAF et de l'adapter à un polyphénol biosourcé. Le resvératrol, un triphénol extrait de la vigne, a été choisi pour ses similitudes structurales avec le TPE, et pour sa disponibilité. La forte densité en cycle aromatique a été mise à profit afin d'obtenir un matériau avec une haute T_g. Pour favoriser encore plus cette propriété, l'époxy utilisé a lui aussi été synthétisé à partir du resvératrol, pour obtenir un monomère

[21] Avérous, L. ; Caillol, S. L'Actualité Chimique, Société chimique de France, 2021, 95-100.
[22] Avérous, L. L'Actualité Chimique, Société chimique de France, 2013, 375-376, 83-90.
[23] Nakajima, H.; Dijkstra, P.; Loos, K. Polymers 2017, 9, 523.
[24] Vidil, T.; Llevot, A. Macromol. Chem. Phys. 2022, 223, 2100494.

trifonctionnel. La haute fonctionnalité moyenne des deux monomères, de l'ordre de 3, a permis la formation d'un réseau dense et d'un matériau rigide, qui pourrait être adapté à des applications telles que les composites par exemple (Figure F).

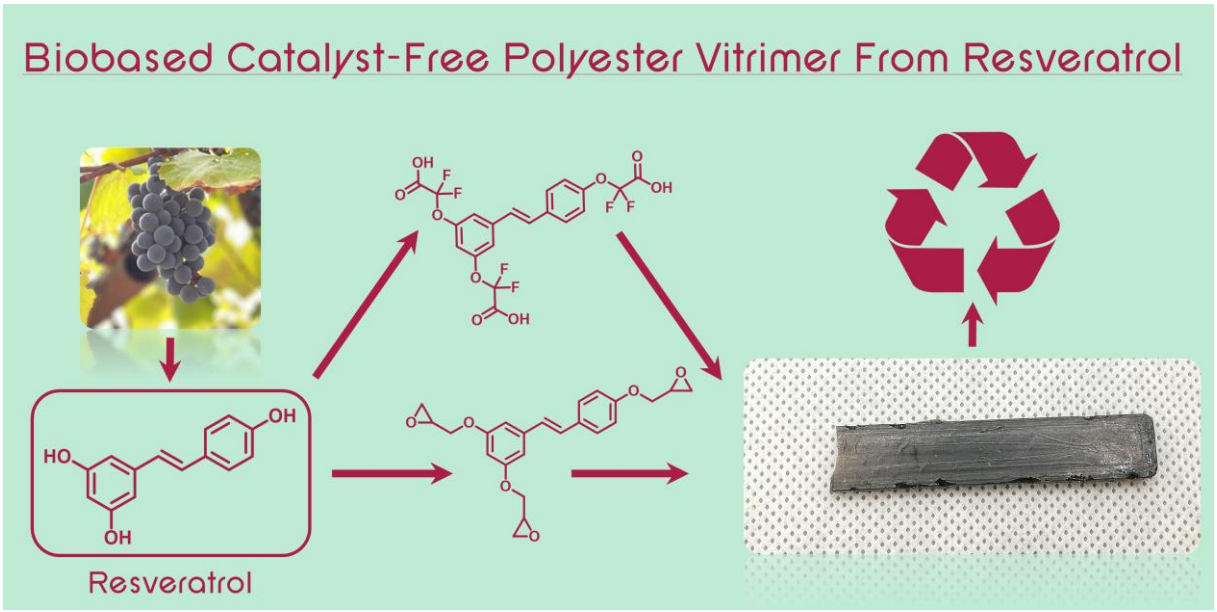

Figure F. Synthèse d'un vitrimère de transestérification sans catalyseur à base de resvératrol

From vineyards to 100 % resveratrol materials: α-CF_2 activation in biobased catalyst-free vitrimers

Florian Cuminet,[a,b] Sébastien Lemouzy,[a] Éric Dantras,[b] Sylvain Caillol,[a] Éric Leclerc[a] and Vincent Ladmiral*[a]

[a]ICGM, Univ Montpellier, CNRS, ENSCM, Montpellier, France
[b]CIRIMAT, Université Toulouse 3 Paul Sabatier, Physique des Polymères, 118 Route de Narbonne, 31062 Toulouse, France

Abstract

Vitrimers are a class of polymers bridging the gap between resistant crosslinked thermosets and recyclable linear thermoplastics. The first vitrimer was a polyester network requiring relatively high catalyst loadings to be reshaped. This feature raises concerns about catalyst potentially leaching out of the materials and accelerated ageing upon reprocessing cycles. Recently, strategies such as activation of the exchange reaction by inductive effects or neighboring group participation were implemented in vitrimers allowing to produce reshapable materials which do not require catalysts. Hence, α,α-difluoro esters proved to be very prone to transesterification thanks to fluorine exceptional properties, in particular its very high electronegativity. This feature implemented in polyester vitrimers permitted to synthesize reshapable catalyst-free highly crosslinked networks. Moreover, this principle initially designed on petrosourced monomers is here successfully adapted to resveratrol, a biobased polyphenol found in particular in grapes. The material presented here is fully bio-based, catalyst-free, durable and recyclable and features a high T_g.

Introduction

Vitrimers are a class of polymer materials which exhibits excellent mechanical properties and the ability to be recycled mechanically.[1,2] Ideally, they combine the best of thermoplastics, which are often easily recyclable, and thermosets, which are endowed with very good mechanical properties and resistance at high temperature. These exceptional properties come from their structure. While thermoplastics are essentially a network of entangled linear chains which cohesion is due to weak bonds, thermosets are a tridimensional network made of strong covalent bonds.[3] Vitrimers are also 3D networks made of covalent bonds, but these bonds feature a singular property: they can exchange with each other, or with free reactive groups on the polymer segments, by a degenerate chemical equilibrium.[4–7] These exchanges usually activated by heat are accountable for the vitrimers flow and recyclability at high temperature. Vitrimers were invented a decade ago, and first illustrated with

polyesters able to flow thanks to a transesterification reaction.[8] They are of particular interest in the field of composites, in which the polymer matrix needs high mechanical performances and thermal resistance.[9,10] Indeed, composites are difficult to recycle, in particular for thermoset-based composites, but the recovery of the valuable fibers without destroying them remains a challenge.[11,12] Vitrimers, because they can be reshaped, or in some cases, can undergo solvolysis, bring a solution to this issue.[13–15] However, one of the main obstacles to the implementation of vitrimers in composites is the difficulty to obtain rigid materials with high T_g, which remain reprocessable on reasonable time and temperature scales.[16–18] Such materials with excellent mechanical properties are desirable in structural application, for instance in aerospace, automotive or engineering applications.[19] Epoxy-anhydride vitrimers catalyzed by zinc (II) with T_g values upto 140 °C were described, but they required hard reprocessing conditions, at 250 °C under 500 bars.[20] A epoxy-acid system catalyzed by Sn(II) with 2 equivalent of epoxy compared to the acid allowed to reach a T_g at 231 °C thanks to the homopolymerization of the epoxy.[21] However, the resulting ether bonds are permanent and might decrease the material reprocessability. Furthermore, in the case of transesterification vitrimers, an external catalyst is usually required to accelerate the transesterification reaction, so that the material may flow at a measurable timescale and be recycled.[22] The use of catalysts such as zinc(II) and triazabicyclodecene (TBD) raises concerns about potential leaching of the catalyst out of the material, and premature ageing of the vitrimer after several recycling/reshaping cycles.[23–25] For these reasons, the use of catalyst-free vitrimers is preferable. A first strategy is to use other exchange reactions. For instance, vinylogous urethanes were used to make vinyl-based vitrimers with a T_g at 110 °C.[26] Gamardella et al. synthesized vitrimers based on polythiourethanes transcarbamoylation, with a T_g at 130 °C. Disulfides were used to make vitrimers with Tg at 129 °C[27] and recently at 175 °C for aerospace applications.[28] However, the dynamic behaviour of this last material was low, as a plateau at 20 % is visible at the end of stress relaxation experiments. Imine bonds were also used to make catalyst-free vitrimers with high T_g, between 100 and 150 °C[29–31] and even upto 274 °C with high thermal resistance.[32] Nishimura et al. reached a T_g at 125 °C with a silyl ether-based vitrimer.[33] Dynamic Si-O-Ph bonds were also used in a polybenzoxazine vitrimer with a T_α around 280-300 °C. Several other strategies were described to make catalyst-free vitrimers, in particular in the case of transesterification vitrimers. Hyperbranched vitrimers featuring a loose network allowed catalyst-free reprocessing, but their mechanical properties were fairly limited.[34] A high concentration of free hydroxyl groups in the network also accelerates the transesterification, but it implies limitations in terms of accessible monomers and network structures and properties, and may increase the water intake of such materials.[35,36] The kinetics of the exchange reaction can also be increased by an activating group, linked to the network, in proximity to the exchangeable bonds.[37,38] In particular, fluorinated esters were recently proven to undergo fast transesterification without the recourse to an external catalyst, both in solution[39] and in vitrimers.[40,41]

Furthermore, in a context of increasing tension on crude oil supply and price volatility, the pursuit of biobased materials is of booming interest to increase polymers sustainability.[42–44] The first vitrimer was partly biobased as the polyfunctional carboxylic acid used was made from dimers and trimers of fatty acids.[8] Many naturally occurring building blocks can be used in the synthesis of vitrimers, such as lignins, phenols, furans, oils, polysaccharides, carboxylic acids or natural rubber.[45] In particular, several examples of biobased vitrimers based on natural phenols such as vanillin,[46–48] eugenol[49,50] or cardanol[51] for instance have been reported. However, only few of them exhibit a T_g over 100 °C and high thermal stability, two precious properties for biobased vitrimers.[52] Liu et al. reported a biobased vitrimer synthesized from succinic acid and a trifunctional epoxy based on vanillin and guaiacol.[53] This transesterification vitrimer was catalyzed by Zn(II). Protocatechuic acid, was used as an alternative to BADGE to make a Zn(II)-catalyzed vitrimer by reaction with succinic anhydride, with a T_g of 157 °C. Finally, two examples of high-T_g catalyst-free biobased vitrimers were reported. The first example is based on acetal exchange, with a T_g up to 121 °C.[54] The other example is based on transesterification activated by tertiary amines in polybenzoxazines, with T_g ranging from 143 to 193 °C. Many of the high-T_g vitrimers reported so far are based on monomers featuring aromatic structures. Biobased phenols and furans,[45] thanks to their aromatic cycles and often compact structures, can provide high crosslinking density, rigidity, high T_g and thermal resistance to vitrimers.

In the work presented here, a catalyst-free, high T_g biobased transesterification vitrimer was synthesized from resveratrol, a biobased triphenol mainly found in grapes, peanuts and a plant called *Japanese knotweed (Reynoutria japonica)*.[55,56] The goal was to achieve high mechanical properties and reach high T_g thanks to the high aromatic carbon content of this bioresource. Resveratrol was functionalized to prepare two building blocks: a trifunctional epoxy, and a trifunctional α,α-difluorocarboxylic acid. The rationale was that the ring-opening polyaddition of these building blocks would lead to a dense network, endowed with high T_g and transesterification capability via fluorine group activation.

Results and Discussion

α,α-Difluoro Carboxylic Acid Monomer Synthesis

α,α-Difluoro carboxylic acids were proven to activate the transesterification reaction in polyester networks, without the need for any catalyst, thus enabling the synthesis of catalyst-free transesterification vitrimers.[39,41] A biobased tris α,α-difluoro carboxylic acid was synthesized from resveratrol (a biobased compound extracted from grapes). Starting from the triphenol, a 2-step synthesis lead to the desired monomer. Resveratrol underwent nucleophilic substitution with ethyl bromodifluoroacetate at 70 °C for 40 hours. After a filtration on silica gel, the expected α,α-difluoro

triester (RvOEt) was obtained in 87 % yield. The isolated product then underwent facile saponification to yield, after appropriate workup, the desired α,α-difluoro triacid (RvOH-TAF) as a brown waxy solid with an overall yield of 85 % and a biobased carbon content of 70 % (Scheme).

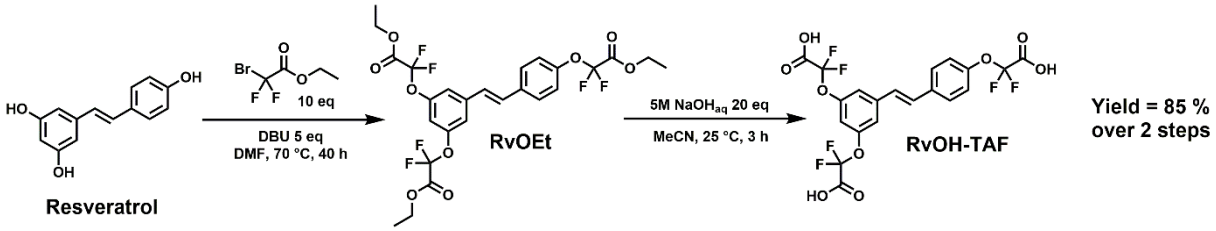

Scheme 1. 2-step synthesis of RvOH-TAF from resveratrol

Trifunctional Epoxy Synthesis

In parallel to the modification of resveratrol into an activated trifunctional acid, the triphenol was functionalized with epichlorohydrin to yield a trifunctional epoxy (Scheme 2). The glycidylation of phenols is very efficient, easily scalable and was extensively described already on biobased phenols including resveratrol.[57–60] The targeted building block RvOGly was prepared in large quantities (> 40g) by simple reaction of resveratrol with epichlorohydrin and tetrabutylammonium bromide (TBAB). RvOGly features high functionality (EEW = 185 g/eq) and a 52 % aromatic carbon content, close to the 57 % value of bisphenol A diglycidyl ether (BADGE). These properties are interesting to obtain materials with high T_g.

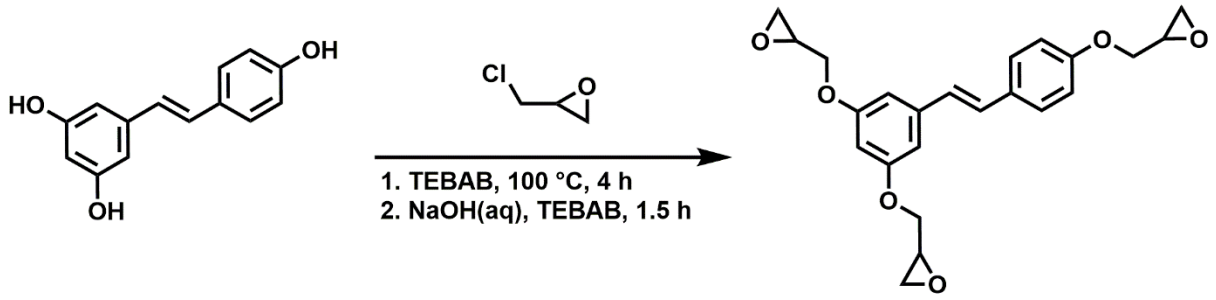

Scheme 2. Synthesis of epoxydized resveratrol RvOGly

Polymerization and Curing

RvOGly and RvOH-TAF were mixed at room temperature (ca. 20 °C) in PTFE molds to avoid any transfer step, because of the fast gelation of the mixture even at room temperature (ca. 20°C). The reaction between both monomers was exothermic and the mixing step needed to be performed on small scale, typically 1-2 g, to better control the heat transfer and to avoid gelation before complete mixing. This fast gelation is caused by the strong activation of the carboxylic acids toward the epoxy opening by the fluorine atoms. A reaction on larger scales may benefit from the addition of a solvent to control the heat release. This pathway was not explored in this study though, to avoid the plasticizing effect of

potential residual solvent and its effect on mechanical properties. The mixture formed a material within a few minutes, and was left at room temperature for 3 h.

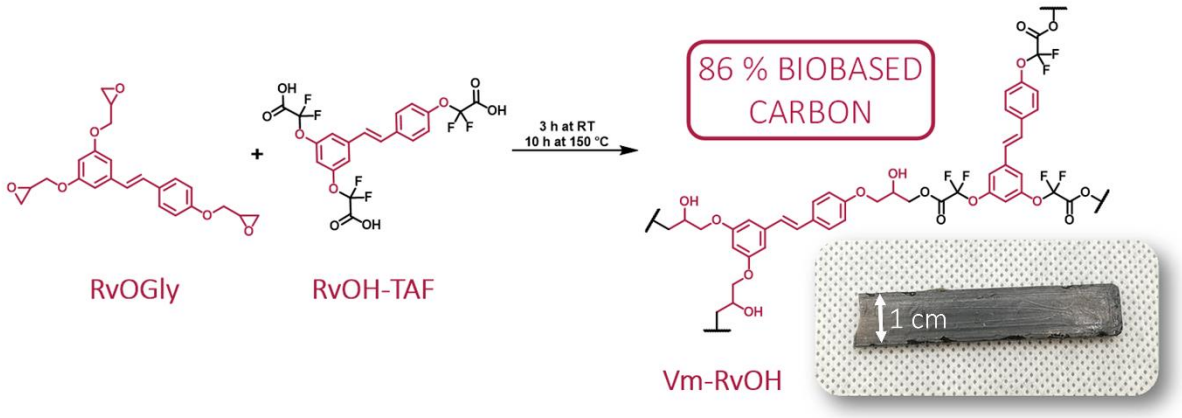

Figure 1. Polymerization of RvOGly and RvOH-TAF resulting into the Vm-RvOH material, insert : optical image of Vm-RvOH (1 cm x 4.5 cm x 0.3 cm)

The curing was checked by DSC (Annexes C Figure S9). On the first heating ramp, an exothermic enthalpy is visible starting from 150 °C. On the second ramp this phenomenon does not appear and a T_g is visible in the 100-130 °C range. The exothermic phenomenon was attributed to a residual polymerization occuring when the material is heated higher than 150 °C. Thus, a 1 h curing step at 150 °C was applied and the DSC analysis was repeated (Annexes C Figure S10). After this curing step, two consecutive heating ramps overlaid almost perfectly. There was no sign of ongoing polymerization by DSC. The curing was also checked by mechanical analysis. The evolution of the modulus was monitored with time at 150 °C. The stabilization of the value happened after 7 h (Annexes C Figure S11). Therefore, the materials were left 10 h at 150 °C to ensure complete polymerization, resulting into a hard brittle dark brown material (Vm-RvOH, Figure 1). The resulting material exhibits a 85 % biobased carbon content.

Vitrimer Characterization

After complete polymerization three consecutive DSC ramps were carried out on the resulting material. The first ramp was meant to erase the thermal history of the material, then the thermograms of the second and third ramps overlaid perfectly, and no residual exotherm was observed. The T_g is visible in the 92-125 °C range, but the transition is broad and the ΔCp is low (0.241 $J.g^{-1}.K^{-1}$). Therefore, the T_g was determined as the minimum of the heat flow derivative, at 117 °C (Annexes C Figure S12 and Table 1). The high T_g compared to previously reported covalent adaptable networks[40,41] was expected because of the high aromatic carbon content of the polymer (52 % aromatic carbon content). This value of T_g is comparable to the value of the catalyst-free biobased vitrimer synthesized from lignin by Moreno et al.[54] (T_g = 121 °C), but lower than the value of the catalyst-free biobased polybenzoxazine

vitrimers recently reported by Adjaoud et al. (T_g from 143 to 193 °C).[17] This last case benefits from a 50 % aromatic carbon content, close to the 52 % value reported here, but also a 17 % cycloaliphatic carbon content caused by the isosorbide core of its monomer, which brings additional rigidity. Thus, the performance of Vm-RvOH in term of T_g is consistent with its structure.

A DMA analysis was also performed to confirm the results observed by DSC, and to characterize the mechanical properties of the material (Annexes C Figure S13). T_α was determined as the maximum of the loss modulus E" at 94 °C. As observed by DSC, the mechanical relaxation was broad and the temperature of the maximum of tan(δ) was 117 °C, which is consistent with the T_g measured by DSC. The moduli on the glassy plateau and on the rubbery plateau were respectively E'_G = 2.1 GPa and E'_R = 46 MPa. The modulus on the glassy plateau is comparable to values reported for a material made from epoxydized resveratrol and 4,4'-diaminodicyclohexylmethane (PACM),[60] and with the value of a lignin-based catalyst-free vitrimer.[54] For the modulus on the rubbery plateau, the value for Vm-RvOH is 14 times lower than the epoxydized resveratrol-PACM thermoset,[60] but still in the 11-73 MPa range reported for other high-T_g vitrimers,[18,21] included for aerospace applications.[28] Additionally, this value is 2.5 times higher than the value reported on the similar α,α-difluoro vitrimer previously reported.[41] At temperatures over 200 °C, the modulus decreases from the rubbery plateau. This could be the mechanical manifestation of a beginning of flow.

The thermal stability of Vm-RvOH was assessed by TGA under nitrogen. The 2 % and 5 % degradation temperatures $T_{d2\%}$ and $T_{d5\%}$ were 237 °C and 275 °C respectively (Annexes C Figure S14 and Table). The residue at 900 °C under nitrogen was 28.9 % of the initial weight. The $T_{d5\%}$ value is low compared to the values superior to 300 °C reported for other high-T_g vitrimers,[18,31,32,61–63] but still higher than the value at 224 °C for a lignin-based catalyst-free vitrimer.[54]. The residue (char yield) was comparable with an epoxy vitrimer in the same range of T_g.[30] The relatively high char yields depends essentially on the monomers structures, thanks to the high aromatic carbon content (52 %).

Solubility tests were performed in THF (a good solvent for both resveratrol-based precursors). After 24 h under agitation, a swelling of 278 % and an insoluble fraction of 73 ± 2 % were measured (Table 1). These results prove the formation of a 3D crosslinked material.

Table 1. Physicochemical main properties of Vm-RvOH

T_g (°C)	**T_α** (°C)[a]	**Max tan(δ)** (°C)	**E'_G** (GPa)[b]	**E'_R** (MPa)[c]	**Gel content** (%)[d]	**Swelling index** (%)[d]	**$T_{d\,2\%}$** (°C)[e]	**$T_{d\,5\%}$** (°C)[e]	**Residue (char)** (%)[f]	**Weight loss** (%)[g]
117	94	117	2.1	46	73±2	278	237	275	28.9	2.9

[a] determined as the maximum of E" | [b] at T_α – 50 °C | [c] at T_α + 50 °C | [d] in THF | [e] N_2 atmosphere | [f] at 900 °C, N_2 atmosphere | [g] after 6 h at 170 °C, air atmosphere

Reprocessing trials were performed on Vm-RvOH by compression molding. In a previous study on a similar system, the reprocessing temperature was set at 100 °C, 50 °C above the T_g, under 16 bars.[41] At 170 °C, the material could be reprocessed in 2 h under 80 bars (Figure 3). The reprocessing temperature is 50 °C above the T_g, like the previous system. The pressure applied is lower than for many high-T_g vitrimers, which often require a pressure of at least 100 bars.[27,31,62–64]

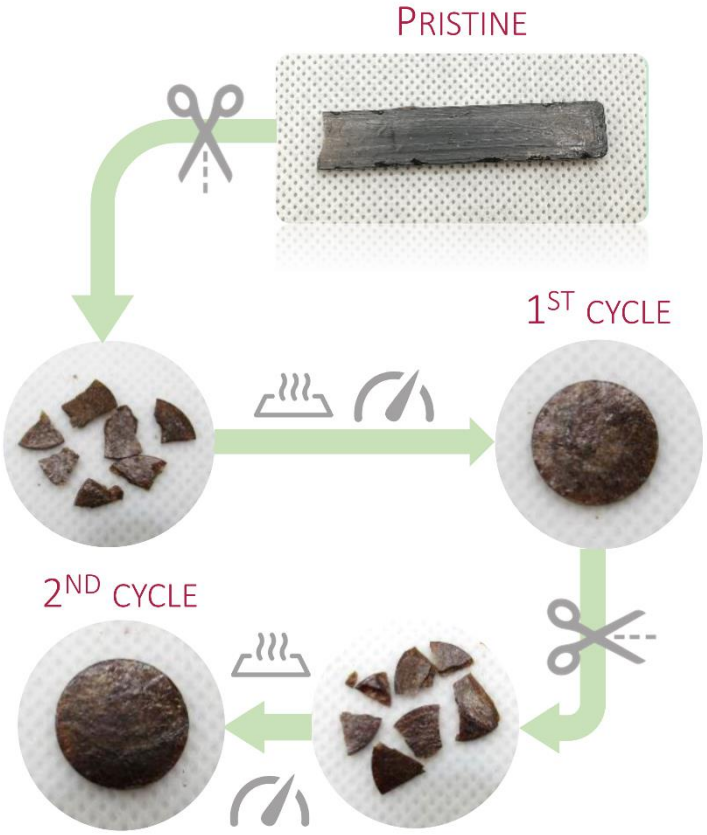

Figure 2. Vm-RvOH reprocessing for 2 h at 170 °C under 80 bars (scale of pristine material: 1 cm x 4.5 cm x 0.3 cm, diameter of recycled materials: 1 cm)

The thermal stability of the material at this reprocessing temperature was assessed. An isothermal experiment at 170 °C was performed in air atmosphere, to simulate the reprocessing conditions (Annexes C Figure S15). After 2 h, the relative mass loss was 2.48 %. Between 2 h and 4 h the additional mass loss was 0.29 % and between 4 h and 6 h, 0.47 % to attain an overall mass loss after 6 h around 3 %. This value is small, but cannot be ignored. Reprocessing trials were made at 150 °C under 80 bars to lower the risk of potential degradation, but the resulting materials remained very inhomogeneous after 4 h. Therefore, the DMA analysis of the material need to be assessed and compared before and after reprocessing at 170 °C, to monitor a possible degradation. Two consecutive reprocessing cycles at 170 °C were made, and the mechanical properties after each cycle were studied by DMA (Figure 3).

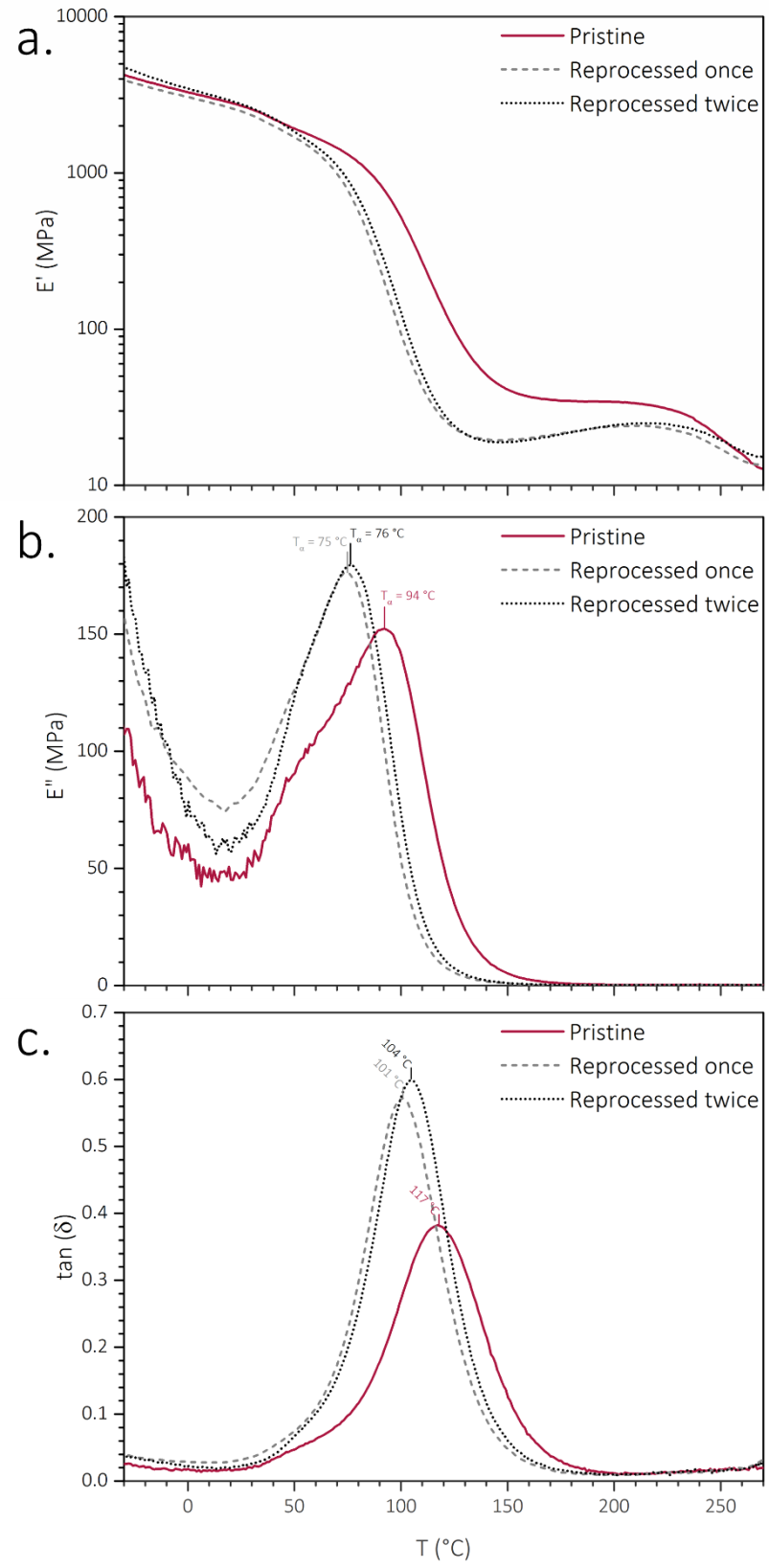

Figure 3. DMA thermograms (a) E', (b) E'' and (c) tan (δ) of Vm-RvOH pristine, after one reprocessing cycle and after two reprocessing cycles

The value of the modulus on the glassy plateau remains quasi-constant. The value of T_α decreased from 94 to 75 °C after the first reprocessing cycle, and remained at 76 °C after the second cycle (Table 2). Similarly, the values of the modulus on the rubbery plateau E'_R decreased from 46 to 23 MPa with the first reprocessing, and then remained the same after the second cycle. These results suggest a decrease of the crosslinking density upon the first cycle, which might be due to a slight hydrolysis at the reprocessing temperature. Then the crosslinking density remains constant for the subsequent cycle, thus the hydrolysis remains very limited. This is likely due to the aromatic carbon content (56 % aromatic carbon) which brings a hydrophobic behavior to the material and balances the hydrophilic behavior brought by the esters and hydroxyl groups. Moreover, the high T_g probably plays an important role, as the water uptake is very limited when the material is in the glassy state, but much easier in the rubbery state. Indeed, in the rubbery state, the mobility of the polymer makes easier the penetration of water in the network. Finally, the results obtained by DMA were confirmed by DSC, with a T_g of 117 °C for the pristine material, 97 °C after the first reprocessing and 91 °C after the second cycle.

Table 2. Evolution of the thermomechanical properties of Vm-RvOH with reprocessing cycles.

Reprocessing Cycle	**T_g** (°C)	**T_α** (°C)[a]	**Max tan(δ)** (°C)	**E'_G** (GPa)[b]	**E'_R** (MPa)[c]
Pristine	117	94	117	2.1	46
Reprocessed once	97	75	101	2.4	23
Reprocessed twice	91	76	104	2.7	23

[a] determined as the maximum of E" | [b] at T_α – 50 °C | [c] at T_α + 50 °C

The flow from the rubbery plateau was studied by isothermal stress-relaxation experiments to evaluate the kinetics of this phenomenon (Annexes C Figure S16). The modulus of the material was monitored under a 0.3 % strain between 170 and 210 °C. For all temperatures, a plateau around 5 % was reached at the end of the relaxation experiment. This is likely due to a proportion of non-exchangeable crosslinks in the network. The presence of such permanent crosslinks can be explained by a minor homopolymerization of the epoxy.[21] Indeed, the strong acidity of α,α-difluoro acids may favor this reaction.[21]

The stress-relaxation experiments were normalized, and a Kohlrausch-Williams-Watts "stretched exponential" equation with an added constant y_0 was used to fit the experimental data (Figure 4 and Annexes C Table S1). The constant y_0 shifts the final plateau of the relaxation, and the stretch parameter β describes the width of the distribution around the value of the relaxation time τ_{KWW}. The closer to 1 β is, the narrower the distribution is. This parameter describes the heterogeneity in the vicinity of the exchangeable bond. Here, the values of β ranged between 0.486 at 170 °C and 0.797 at 210 °C and increased with the temperature. With the increase of the temperature, the environment is

more homogeneous, the values of beta tend towards 1.The constant added y_0 allowed a better accuracy on the fitting, with $0.99264 \leq R^2 \leq 0.99639$ without constant and $R^2 = 0.99937$ to 0.99979 with a constant. The mean value of this constant y_0 (Annexes C Table S1) is 0.054 (values between 0.043 and 0.064). Thus, a mere 5 % of the applied stress is not relaxed because of the permanent crosslinks, which does not impede the reprocessing of the material.

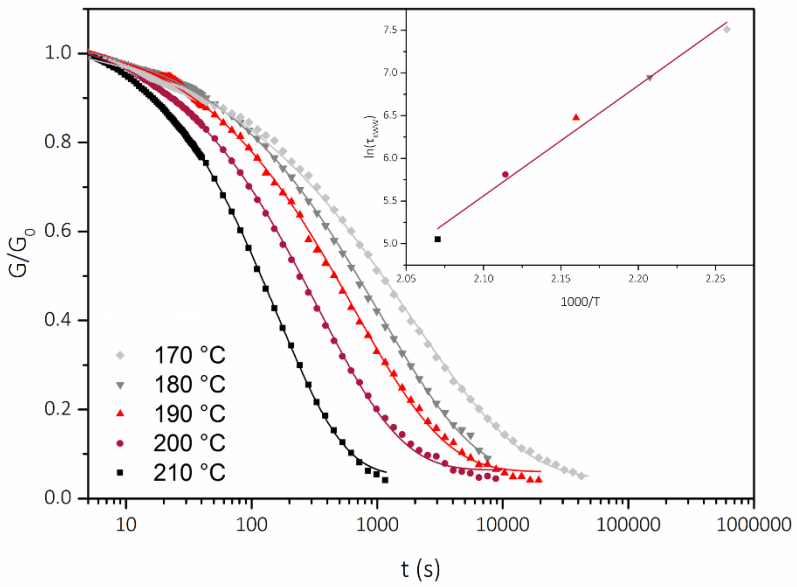

Figure 4. Normalized stress–relaxation curves from 170 to 210 °C with 10 °C steps fitted with the Kohlrausch–Williams–Watts equation (KWW) and τ_{KWW} relaxation times reported in the Arrhenius diagram (inset, $R^2 = 0.983$)

The relaxation times τ_{KWW} obtained for each temperature were plotted in an Arrhenius diagram (Figure 4 inset). A linear fit was obtained ($R^2 = 0.983$) and the flow activation was calculated from the slope E_a = 107 kJ mol^{-1}, in accordance with the 29-163 kJ mol^{-1} range reported for transesterification vitrimers.[38] This E_a is higher than that reported in previous studies of transesterification vitrimers activated by fluorinated groups (67-77 kJ mol^{-1}).[40,41] It is likely caused by the higher crosslinking density and lower mobility at the local scale of Vm-RvOH.

Conclusion

A catalyst-free polyester vitrimer was synthesized from resveratrol, a biobased triphenol found mainly in grapes. This material exhibits a high biobased carbon content of 85 %. A trifunctional epoxy and a trifunctional α,α-difluoro carboxylic acid were synthesized by functionalization of resveratrol with epichlorohydrin and ethyl bromodifluoroacetate, respectively. When these two resveratrol derivatives were mixed together, the ring opening polymerization of the epoxy by the acid occurred at room temperature due the activation of the acid by the fluorine atoms. After a curing step at 150 °C, a rigid

slightly brittle material was obtained. This material exhibited a high T_g (117 °C), comparabled to other high-T_g vitrimers,[27,30,65,66] which makes it relevant for composite application for instance. The synthesis described could be adapted to other biobased compounds with similar structures and higher functionality, such as quercetin, to reach even higher T_g values. Moreover, the α,α-difluoro esters can exchange with free hydroxyl groups without any added catalyst. This feature allows the efficient reprocessing of the material at 170 °C for 2 h by compression molding. Two recycling cycles were achieved and the mechanical performance remained worthwhile for structural applications This material is one of the first high-T_g catalyst-free biobased vitrimers.[17,54]

Experimental section

Materials

Trans-Resveratrol (Fluorochem, 98 %), 1,8-Diazabicyclo(5.4.0)undec-7-ene (DBU, Fluorochem, 98 %), ethyl bromodifluoroacetate (Fluorochem, 98 %), epichlorohydrin (Sigma-Aldrich, ≥ 99 %), tetrabutylammonium bromide (TCI, > 98 %), benzophenone (Avocado Research Chemicals Ltd, 99 %), were used as received. Dimethylformamide (DMF), tetrahydrofuran (THF) and $NaHCO_3$ were supplied by VWR Chemicals, diethyl ether and pentane were supplied by Carlo Erba, ethyl acetate was supplied by Fisher Chemicals, acetonitrile was supplied by Acros Organics, sodium hydroxide and chlorhydric acid ≥ 37 % were supplied by Honeywell Fluka. Deuterated solvents were supplied by Eurisotop (99.8 %).

Synthetic Procedures

"RvOEt" compound: Trans-Resveratrol (3,5,4'-trihydroxy-trans-stilbene, 2.3 g, 10 mmol, 1 eq) was dissolved in dry DMF (60 mL, 0.16 M). 1,8-Diazabicyclo [5.4.0] undec-7-ene (DBU, 7.5 mL, 50 mmol, 5 eq) was added in one portion and the reaction was heated to 70 °C. Ethyl bromodifluoroacetate (6.4 mL, 50 mmol, 5 eq) was then added via a syringe pump at a rate of 5.0 $mL.h^{-1}$ and the reaction was stirred at 70 °C for 40 h. The crude mixture was cooled to room temperature, diluted with H_2O (300 mL), and extracted 5 times with Et_2O (5 x 50 mL). The combined organic layers were washed twice with water and once with brine, dried with Na_2SO_4, filtered, and concentrated under reduced pressure to obtain a dark red oil. The crude mixture was purified by filtration on silica gel using pentane/ethyl acetate (1:1) to afford the pure triester (6 g, 87 %, clear brown viscous liquid).

Triester RvOEt characterizations (NMR spectra in Annexes C Figures S1 to S3: ^{1}H NMR 400MHz $CDCl_3$: δ 7.50 (m, 2H, aromatic protons), 7.25 – 7.21 (m, 4H, aromatic protons and C=C), 7.11 – 6.95 (m, 3H, aromatic protons), 4.40 (2q, ^{3}J = 8 Hz, 6H, OC**H$_2$**CH_3), 1.37 (2t, ^{3}J = 8 Hz, 9H, OCH_2C**H$_3$**). **^{19}F NMR 377 MHz, $CDCl_3$:** δ -76.30, -76.53. **^{13}C NMR 101 MHz, $CDCl_3$:** δ 159.9 (m, **C**O_2Et), 150.3 (m), 150.2 (m), 140.1, 134.7, 130.3, 128.1, 127.1, 122.0, 117.4, 114.1 (t, $^1J_{C-F}$ = 1021 Hz, OCF_2),), 114.0 (t, $^1J_{C-F}$ = 1025 Hz, OCF_2),

64.0 (O-**<u>CH$_2$</u>**CH$_3$), 63.9 (O-**<u>CH$_2$</u>**CH$_3$), 14.0 (O-CH$_2$**<u>CH$_3$</u>**), 14.0 (O-CH$_2$**<u>CH$_3$</u>**). **HRMS (ESI+)** Calc. for $[M+H]^+$ 595.1397, found 595.1394.

"RvOH-TAF" compound: In a 250 mL round bottom flask, 6 g of triester were dissolved in acetonitrile (90 mL). Then, a 5M aqueous solution of NaOH (12.5 g in 62 mL) was added slowly at room temperature, and the mixture was stirred for 3 h. 200 mL of a saturated $NaHCO_3$ solution was added to the mixture and the aqueous layer was washed with 100 mL of diethyl ether. The organic layer was extracted with 50 mL of saturated $NaHCO_3$ solution, and the gathered aqueous layers were acidified to pH=1 using 2M HCl. Finally, the acidified aqueous layer was extracted with 3 x 100 mL of diethyl ether, and the solvent was removed under high vacuum to afford 5 g of the desired triacid as a brown waxy solid (yield 98 %, yield over the two steps η = 85 %, purity > 98 % estimated from ^{1}H NMR spectrum).

Trifunctional acid TPE-TAF characterizations (NMR spectra in Annexes C Figures S4 to S6): ^{1}H NMR 400MHz d$_6$-DMSO: δ 7.72 (d, 2H), 7.59-7.13 (m, 5H, aromatic protons and C=C), 7.00 (s, 1H). **^{19}F NMR 377 MHz, d$_6$-DMSO:** δ -76.16, -76.50. **^{13}C NMR 101 MHz, d$_6$-DMSO:** δ 161.0 (COOH, t, $^2J_{C-F}$ = 39.0 Hz), 160.7 (COOH, t, $^2J_{C-F}$ = 39.0 Hz), 150.4 (ipso-ArC-O), 149.4, 140.8, 135.0, 130.6, 128.7, 127.1, 121.8, 117.3, 114.64 (OCF_2, t, $^1J_{C-F}$ = 272 Hz), 114.56 (OCF_2, t, $^1J_{C-F}$ = 274 Hz), 113.4. **HRMS (ESI+)** Calc. for $[M+H]^+$ 511.0458, found 511.0468. HRMS (ESI-) Calc. for $[M-H]^-$ 509.0313, found 509.0319.

"RvOGly" compound (glycidylation of resveratrol): In a 500 mL round bottom flask, 20.56 g (90 mmol, 1 eq) of resveratrol was dissolved in 82 mL (96 g, 1.04 mol, 12 eq) epichlorohydrin at room temperature under magnetic stirring. The flask was then equipped with a condenser and heated to 100 °C. 1.56 g (4.8 mmol, 0.05 eq) of tetrabutylammonium bromide "TEBAB" was added and the reaction was left to proceed under stirring at 100 °C for 4 h. Then, the reaction medium was cooled to room temperature and 20 wt% aqueous solution of NaOH and TEBAB was added (21 g NaOH + 1.56 g TEBAB in 106 mL deionized water). The mixture was left 1.5 h under vigorous stirring. The mixture was then diluted with 600 mL of water and extracted with 3 x 300 mL ethyl acetate. The organic layers were gathered, washed with 2 x 200 mL brine, dried on magnesium sulfate. The solvent was evaporated under reduced pressure to afford 42.3 g of a clear yellow viscous oil.

Epoxydized resveratrol RvOGly characterizations (NMR spectra in Annexes C Figures S7 and S8): ^{1}H NMR 400MHz d$_6$-acetone: δ 7.52 (d, 2H), 7.29-6.99 (dd, 2H, C=C), 6.97 (m, 2H), 6.81 (d, 2H), 6.51 (t, 1H), 4.34 and 3.86 (3+3H), 3.33 (3H), 2.86 and 2.73 (3+3H). **^{13}C NMR 101 MHz, d$_6$-acetone:** δ 160.9, 159.3, 140.7, 131.0, 129.5, 128.6, 127.1, 115.5, 106.0, 101.3, 70.1, 50.6, 44.4.

Determination of the Epoxy Equivalent Weight (EEW): The EEW of the RvOGly was evaluated by NMR titration using benzophenone as standard in deuterated chloroform (experimental details are given in Annexes C Section A).

"TPE-TAF/BDGE" vitrimer: Typically, 1 g (2.0 mmol, 5.9 meq COOH, HEW = 170 g/eq) of RvOH-TAF was quickly mixed manually directly in a PTFE mold with 1.07 g (5.9 meq epoxy, EEW = 185 g/eq) of RvOGly at room temperature (ca. 20 °C) until a light brown viscous homogeneous mixture was obtained. The mixture was left at least 3 h at room temperature for gelation. The resulting material (TPE-TAF/BDGE) was then removed from the molds and cured 10 h at 150 °C.

Instrumentation

NMR: ^{1}H, ^{13}C and ^{19}F were acquired on a Bruker Avance 400 MHz spectrometer at 23 °C. External reference was tetramethylsilane (TMS) with chemical shifts given in ppm. Samples were diluted in 0.5 mL of $CDCl_3$, DMSO-d_6 or acetone-d_6 depending on their solubility.

Mechanical characterizations: temperature ramps in elongation mode were carried out on Netzsch DMA 242 E Artemis cooled by liquid nitrogen. Uniaxial stretching of samples (1 × 3.5 × 12 mm^3) was applied while heating at a rate of 3 °C min^{-1} from −50 °C to 270 °C, keeping the frequency at 1 Hz. Curing monitoring experiments were performed on a ThermoScientific Haake Mars 60 rheometer equipped with a Peltier heating cell and a 8-mm plane-plane geometry. A 0.1 % deformation was applied to 8 mm diameter and 2 mm thickness circular samples at ω = 1 $rad.s^{-1}$ under a normal force of 100 grams every 2 minutes, and G' evolution over time was monitored. Stress relaxation experiments were performed with a 0.3 % torsional strain applied on 8 mm diameter and 2 mm thickness circular samples, and the rubbery modulus evolution with time was monitored.

TGA: thermogravimetric thermograms were recorded on a TA TGA G50 instrument using a 40 mL min^{-1} flux of nitrogen or synthetic air as purge gas. Approximately 10 mg of sample were used for each analysis. Ramps were applied at a rate of 20 °C min^{-1}.

DSC: analyses were carried out using a NETZSCH DSC200F3 calorimeter. The calibration was performed using adamantane, biphenyl, indium, tin, bismuth and zinc standards. Nitrogen was used as purge gas. Approximately 10 mg of sample were placed in perforated aluminum pans and the thermal properties were recorded at 20 °C min^{-1}. The reported values are the values measured during the second heating ramp.

Reprocessing: the material was grinded with a manual stainless steel coffee grinder (for DSC and DMA) or cut into 6 to 9 mm^3 pieces (for pictures) and then pressed in stainless steel molds for 2 h at 170 °C under 200 bars of pressure using a manual heating press.

Acknowledgements

This work was funded by the Institut Carnot Chimie Balard CIRIMAT (16CARN000801).

References

(1) Denissen, W.; Winne, J. M.; Du Prez, F. E. Vitrimers: Permanent Organic Networks with Glass-like Fluidity. *Chemical Science* 2016, 7, 30–38.

(2) Van Zee, N. J.; Nicolaÿ, R. Vitrimers: Permanently Crosslinked Polymers with Dynamic Network Topology. *Prog. Polym. Sci.* 2020, 104, 101233.

(3) Pascault, J.-P.; Sautereau, H.; Verdu, J.; Williams, R. J. J. *Thermosetting Polymers*; Marcel Dekker, Inc.: New York, 2002.

(4) Capelot, M.; Montarnal, D.; Tournilhac, F.; Leibler, L. Metal-Catalyzed Transesterification for Healing and Assembling of Thermosets. *J. Am. Chem. Soc* 2012, 134, 7664-7667.

(5) Leibler, L.; Rubinstein, M.; Colby, R. H. Dynamics of Reversible Networks. *Macromolecules* 2002, 24 (16), 4701–4707.

(6) Kloxin, C. J.; Scott, T. F.; Adzima, B. J.; Bowman, C. N. Covalent Adaptable Networks (CANs): A Unique Paradigm in Cross-Linked Polymers. *Macromolecules* 2010, 43 (6), 2643–2653.

(7) Kloxin, C. J.; Bowman, C. N. Covalent Adaptable Networks: Smart, Reconfigurable and Responsive Network Systems. *Chem. Soc. Rev.* 2013, 42 (17), 7161–7173.

(8) Montarnal, D.; Capelot, M.; Tournilhac, F.; Leibler, L. Silica-like Malleable Materials from Permanent Organic Networks. *Science* 2011, 334 (6058), 965–968.

(9) Hsissou, R.; Seghiri, R.; Benzekri, Z.; Hilali, M.; Rafik, M.; Elharfi, A. Polymer Composite Materials: A Comprehensive Review. *Compos. Struct.* 2021, 262, 113640.

(10) Zheng, J.; Png, Z. M.; Ng, S. H.; Tham, G. X.; Ye, E.; Goh, S. S.; Loh, X. J.; Li, Z. Vitrimers: Current Research Trends and Their Emerging Applications. *Mater. Today* 2021, 51, 586–625.

(11) Yang, Y.; Boom, R.; Irion, B.; van Heerden, D. J.; Kuiper, P.; de Wit, H. Recycling of Composite Materials. *Chem. Eng. Process. Process Intensif.* 2012, 51, 53–68.

(12) Krauklis, A. E.; Karl, C. W.; Gagani, A. I.; Jørgensen, J. K.; Krauklis, C. :; Karl, A. E. ; Gagani, C. W. ;; Jørgensen, A. I. ; Composite Material Recycling Technology—State-of-the-Art and Sustainable Development for the 2020s. *J. Compos. Sci.* 2021, 5 (1), 28.

(13) Kissounko, D. A.; Taynton, P.; Kaffer, C. New Material: Vitrimers Promise to Impact Composites. *Reinforced Plastics* 2017, 62.

(14) Yang, Y.; Xu, Y.; Ji, Y.; Wei, Y. Functional Epoxy Vitrimers and Composites. *Prog. Mater. Sci.* 2021, 120, 100710.

(15) Alabiso, W.; Schlögl, S. The Impact of Vitrimers on the Industry of the Future: Chemistry, Properties and Sustainable Forward-Looking Applications. *Polymers*. 2020, 12, 1660.

(16) Yang, Y.; Urban, M. W. Self-Healing Polymeric Materials. *Chem. Soc. Rev.* 2013, 42 (17), 7446–7467.

(17) Adjaoud, A.; Puchot, L.; Verge, P. High-Tgand Degradable Isosorbide-Based Polybenzoxazine

Vitrimer. *ACS Sustain. Chem. Eng.* 2022, 10 (1), 594–602.

(18) Liu, T.; Hao, C.; Zhang, S.; Yang, X.; Wang, L.; Han, J.; Li, Y.; Xin, J.; Zhang, J. A Self-Healable High Glass Transition Temperature Bioepoxy Material Based on Vitrimer Chemistry. *Macromolecules* 2018, 51 (15), 5577–5585.

(19) Chang, B. P.; Mohanty, A. K.; Misra, M. Studies on Durability of Sustainable Biobased Composites: A Review. *RSC Adv.* 2020, 10 (31), 17955–17999.

(20) Giebler, M.; Sperling, C.; Kaiser, S.; Duretek, I.; Schlögl, S. Epoxy-Anhydride Vitrimers from Aminoglycidyl Resins with High Glass Transition Temperature and Efficient Stress Relaxation. *Polymers* 2020, 12 (5), 1148.

(21) Tangthana-Umrung, K.; Poutrel, Q. A.; Gresil, M. Epoxy Homopolymerization as a Tool to Tune the Thermo-Mechanical Properties and Fracture Toughness of Vitrimers. *Macromolecules* 2021, 54 (18), 8393–8406.

(22) Capelot, M.; Unterlass, M. M.; Tournilhac, F.; Leibler, L. Catalytic Control of the Vitrimer Glass Transition. *ACS Macro Lett.* 2012, 1 (7), 789–792..

(23) Wang, J.; Chen, S.; Lin, T.; Ke, J.; Chen, T.; Wu, X.; Lin, C. A Catalyst-Free and Recycle-Reinforcing Elastomer Vitrimer with Exchangeable Links. *RSC Adv.* 2020, 10 (64), 39271–39276.

(24) Lessard, J. J.; Garcia, L. F.; Easterling, C. P.; Sims, M. B.; Bentz, K. C.; Arencibia, S.; Savin, D. A.; Sumerlin, B. S. Catalyst-Free Vitrimers from Vinyl Polymers. *Macromolecules* 2019, 52 (5), 2105–2111.

(25) He, C.; Shi, S.; Wang, D.; Helms, B. A.; Russell, T. P. Poly(Oxime–Ester) Vitrimers with Catalyst-Free Bond Exchange. *J. Am. Chem. Soc.* 2019, 141 (35), 13753–13757.

(26) Lessard, J. J.; Garcia, L. F.; Easterling, C. P.; Sims, M. B.; Bentz, K. C.; Arencibia, S.; Savin, D. A.; Sumerlin, B. S. Catalyst-Free Vitrimers from Vinyl Polymers. *Macromolecules* 2019, 52 (5), 2105–2111.

(27) Zhou, L.; Zhang, G.; Feng, Y.; Zhang, H.; Li, J.; Shi, X. Design of a Self-Healing and Flame-Retardant Cyclotriphosphazene-Based Epoxy Vitrimer. *J. Mater. Sci.* 2018, 53 (9), 7030–7047.

(28) Luzuriaga, A. R. de; Markaide, N.; Salaberria, A. M.; Azcune, I.; Rekondo, A.; Grande, H. J. Aero Grade Epoxy Vitrimer towards Commercialization. *Polymers* 2022, 14 (15), 3180.

(29) Zheng, H.; Liu, Q.; Lei, X.; Chen, Y.; Zhang, B.; Zhang, Q. A Conjugation Polyimine Vitrimer: Fabrication and Performance. *J. Polym. Sci. Part A Polym. Chem.* 2018, 56 (22), 2531–2538.

(30) Liu, H.; Zhang, H.; Wang, H.; Huang, X.; Huang, G.; Wu, J. Weldable, Malleable and Programmable Epoxy Vitrimers with High Mechanical Properties and Water Insensitivity. *Chem. Eng. J.* 2019, 368, 61–70.

(31) Zhang, X.; Eichen, Y.; Miao, Z.; Zhang, S.; Cai, Q.; Liu, W.; Zhao, J.; Wu, Z. Novel Phosphazene-Based Flame Retardant Polyimine Vitrimers with Monomer-Recovery and High Performances. *Chem. Eng. J.* 2022, 440, 135806.

(32) Lei, X.; Jin, Y.; Sun, H.; Zhang, W. Rehealable Imide–Imine Hybrid Polymers with Full Recyclability. *J. Mater. Chem. A* 2017, 5 (40), 21140–21145.

(33) Nishimura, Y.; Chung, J.; Muradyan, H.; Guan, Z. Silyl Ether as a Robust and Thermally Stable Dynamic Covalent Motif for Malleable Polymer Design. *J. Am. Chem. Soc.* 2017, 139 (42),

14881–14884.

(34) Han, J.; Liu, T.; Hao, C.; Zhang, S.; Guo, B.; Zhang, J. A Catalyst-Free Epoxy Vitrimer System Based on Multifunctional Hyperbranched Polymer. *Macromolecules* 2018, 51 (17), 6789–6799.

(35) Liu, T.; Zhang, S.; Hao, C.; Verdi, C.; Liu, W.; Liu, H.; Zhang, J. Glycerol Induced Catalyst-Free Curing of Epoxy and Vitrimer Preparation. *Macromol. Rapid Commun.* 2019, 40 (7), 1800889.

(36) Altuna, F. I.; Pettarin, V.; Williams, R. J. J. Self-Healable Polymer Networks Based on the Cross-Linking of Epoxidised Soybean Oil by an Aqueous Citric Acid Solution. *Green Chem.* 2013, 15 (12), 3360–3366.

(37) Altuna, F. I.; Hoppe, C. E.; Williams, R. J. J. Epoxy Vitrimers with a Covalently Bonded Tertiary Amine as Catalyst of the Transesterification Reaction. *Eur. Polym. J.* 2019, 113, 297–304.

(38) Cuminet, F.; Caillol, S.; Dantras, É.; Leclerc, É.; Ladmiral, V. Neighboring Group Participation and Internal Catalysis Effects on Exchangeable Covalent Bonds: Application to the Thriving Field of Vitrimer Chemistry. *Macromolecules* 2021, 54 (9), 3927–3961.

(39) Lemouzy, S.; Cuminet, F.; Berne, D.; Caillol, S.; Ladmiral, V.; Poli, R.; Leclerc, E. Understanding the Reshaping of Fluorinated Polyester Vitrimers by Kinetic and DFT Studies of the Transesterification Reaction. *Chem. – A Eur. J.* 2022. https://doi.org/10.1002/CHEM.202201135.

(40) Berne, D.; Cuminet, F.; Lemouzy, S.; Joly-Duhamel, C.; Poli, R.; Caillol, S.; Leclerc, E.; Ladmiral, V. Catalyst-Free Epoxy Vitrimers Based on Transesterification Internally Activated by an α–CF 3 Group . *Macromolecules* 2022, 55 (5), 1669–1679.

(41) Cuminet, F.; Berne, D.; Lemouzy, S.; Dantras, E.; Joly-Duhamel, C.; Caillol, S.; Leclerc, E.; Ladmiral, V. Catalyst-Free Transesterification Vitrimers: Activation via α -Difluoroesters. *Polym. Chem.* 2022, 8, 5255–5446.

(42) Babu, R. P.; O'Connor, K.; Seeram, R. Current Progress on Bio-Based Polymers and Their Future Trends. *Prog. Biomater.* 2013, 2 (1), 8.

(43) Nakajima, H.; Dijkstra, P.; Loos, K. The Recent Developments in Biobased Polymers toward General and Engineering Applications: Polymers That Are Upgraded from Biodegradable Polymers, Analogous to Petroleum-Derived Polymers, and Newly Developed. *Polymers* 2017, 9(10), 523

(44) Caillol, S. Natural Polymers and Biopolymers II. *Nat. Polym. Biopolym. II* 2021.

(45) Lucherelli, M. A.; Duval, A.; Avérous, L. Biobased Vitrimers: Towards Sustainable and Adaptable Performing Polymer Materials. *Prog. Polym. Sci.* 2022, 127, 101515.

(46) Engelen, S.; Wróblewska, A. A.; De Bruycker, K.; Aksakal, R.; Ladmiral, V.; Caillol, S.; Du Prez, F. E. Sustainable Design of Vanillin-Based Vitrimers Using Vinylogous Urethane Chemistry. *Polym. Chem.* 2022, 13 (18), 2665–2673.

(47) Genua, A.; Montes, S.; Azcune, I.; Rekondo, A.; Malburet, S.; Daydé-Cazals, B.; Graillot, A. Build-To-Specification Vanillin and Phloroglucinol Derived Biobased Epoxy-Amine Vitrimers. *Polymers* 2020, 12 (11), 2645.

(48) Liu, Y. Y.; He, J.; Li, Y. D.; Zhao, X. L.; Zeng, J. B. Biobased Epoxy Vitrimer from Epoxidized Soybean Oil for Reprocessable and Recyclable Carbon Fiber Reinforced Composite. *Compos. Commun.*

2020, 22, 100445.

(49) Ocando, C.; Ecochard, Y.; Decostanzi, M.; Caillol, S.; Avérous, L. Dynamic Network Based on Eugenol-Derived Epoxy as Promising Sustainable Thermoset Materials. *Eur. Polym. J.* 2020, 135, 109860.

(50) Liu, T.; Hao, C.; Wang, L.; Li, Y.; Liu, W.; Xin, J.; Zhang, J. Eugenol-Derived Biobased Epoxy: Shape Memory, Repairing, and Recyclability. *Macromolecules* 2017, 50 (21), 8588–8597..

(51) Chen, F.; Gao, F.; Zhong, J.; Shen, L.; Lin, Y. Fusion of Biobased Vinylogous Urethane Vitrimers with Distinct Mechanical Properties. *Mater. Chem. Front.* 2020, 4 (9), 2723–2730.

(52) Vidil, T.; Llevot, A. Fully Biobased Vitrimers: Future Direction toward Sustainable Cross-Linked Polymers. *Macromol. Chem. Phys.* 2022, 223 (13), 2100494.

(53) Liu, T.; Hao, C.; Zhang, S.; Yang, X.; Wang, L.; Han, J.; Li, Y.; Xin, J.; Zhang, J. A Self-Healable High Glass Transition Temperature Bioepoxy Material Based on Vitrimer Chemistry. *Macromolecules* 2018, 51 (15), 5577–5585.

(54) Moreno, A.; Morsali, M.; Sipponen, M. H. Catalyst-Free Synthesis of Lignin Vitrimers with Tunable Mechanical Properties: Circular Polymers and Recoverable Adhesives. *ACS Appl. Mater. Interfaces* 2021, 13 (48), 57952–57961.

(55) Jasiński, M.; Jasińska, L.; Ogrodowczyk, M. Resveratrol in Prostate Diseases – a Short Review. *Cent. Eur. J. Urol.* 2013, 66 (2), 144.

(56) Sales, J. M.; Resurreccion, A. V. A. Resveratrol in Peanuts. 2013, 54 (6), 734–770.

(57) Aouf, C.; Le Guernevé, C.; Caillol, S.; Fulcrand, H. Study of the O-Glycidylation of Natural Phenolic Compounds. the Relationship between the Phenolic Structure and the Reaction Mechanism. *Tetrahedron* 2013, 69 (4), 1345–1353.

(58) Tian, Y.; Wang, Q.; Shen, L.; Cui, Z.; Kou, L.; Cheng, J.; Zhang, J. A Renewable Resveratrol-Based Epoxy Resin with High Tg, Excellent Mechanical Properties and Low Flammability. *Chem. Eng. J.* 2020, 383, 123124.

(59) Garrison, M. D.; Savolainen, M. A.; Chafin, A. P.; Baca, J. E.; Bons, A. M.; Harvey, B. G. Synthesis and Characterization of High-Performance, Bio-Based Epoxy-Amine Networks Derived from Resveratrol. *ACS Sustain. Chem. Eng.* 2020, 8 (37), 14137–14149.

(60) Tian, Y.; Ke, M.; Wang, X.; Wu, G.; Zhang, J.; Cheng, J. A Resveratrol-Based Epoxy Resin with Ultrahigh Tg and Good Processability. *Eur. Polym. J.* 2021, 147, 110282.

(61) Liu, H.; Zhang, H.; Wang, H.; Huang, X.; Huang, G.; Wu, J. Weldable, Malleable and Programmable Epoxy Vitrimers with High Mechanical Properties and Water Insensitivity. *Chem. Eng. J.* 2019, 368, 61–70.

(62) Tao, Y.; Fang, L.; Dai, M.; Wang, C.; Sun, J.; Fang, Q. Sustainable Alternative to Bisphenol A Epoxy Resin: High-Performance Recyclable Epoxy Vitrimers Derived from Protocatechuic Acid. *Polym. Chem.* 2020, 11 (27), 4500–4506.

(63) Gao, S.; Liu, Y.; Feng, S.; Lu, Z. Reprocessable and Degradable Thermoset with High Tg Cross-Linked via Si–O–Ph Bonds. *J. Mater. Chem. A* 2019, 7 (29), 17498–17504.

(64) Giebler, M.; Sperling, C.; Kaiser, S.; Duretek, I.; Schlögl, S. Epoxy-Anhydride Vitrimers from Aminoglycidyl Resins with High Glass Transition Temperature and Efficient Stress Relaxation.

Polymers 2020, 12 (5), 1148.

(65) Gamardella, F.; Guerrero, F.; De la Flor, S.; Ramis, X.; Serra, A. A New Class of Vitrimers Based on Aliphatic Poly(Thiourethane) Networks with Shape Memory and Permanent Shape Reconfiguration. *Eur. Polym. J.* 2020, 122, 109361.

(66) Nishimura, Y.; Chung, J.; Muradyan, H.; Guan, Z. Silyl Ether as a Robust and Thermally Stable Dynamic Covalent Motif for Malleable Polymer Design. *J. Am. Chem. Soc.* 2017, 139 (42), 14881–14884.

Conclusion du chapitre IV

L'étude décrite dans ce chapitre porte sur la fonctionnalisation du resvératrol, un triphénol naturel extrait de la vigne. D'une part, ce triphénol a été transformé en acide α,α-difluoré trifonctionnel par réaction avec le bromodifluoroacétate d'éthyle. D'autre part, le resvératrol a également été transformé en époxy trifonctionnel par réaction avec l'épichlorhydrine, qui peut être biosourcée. La réaction de ces deux composés à température ambiante a conduit à la formation d'un matériau brun, fragile et rigide après cuisson à 150 °C pendant 10 h. L'utilisation de monomères avec une forte densité en carbones aromatiques et d'une fonctionnalité moyenne élevée a permis l'obtention d'une T_g élevée de l'ordre de 100 à 120 °C.

L'obtention d'une T_g élevée permet d'envisager une utilisation dans des applications telles que des composites plus structuraux, pour lesquelles le recyclage reste un défi à l'heure actuelle. Les atomes de fluor en position alpha de l'ester on encore une fois montré leur capacité d'activation pour rendre ce matériau dynamique. En effet, deux cycles de remise en œuvre ont été effectués. Si le premier cycle engendre une légère diminution des propriétés mécaniques, notamment de la T_α, celle-ci reste contenue et ne semble pas affecter le matériau après un deuxième cycle de remise en œuvre. Une telle capacité de remise en œuvre permettrait d'envisager le recyclage de composites par des techniques jusqu'ici réservées aux thermoplastiques, comme par exemple le moulage par compression.

Le resvératrol représente 50 % de la masse du matériau Vm-RvOH. Dans le cas où l'épichlorhydrine employée est biosourcée, le taux de carbone renouvelable dans ce matériau atteint 86 %. Ce matériau est donc hautement biosourcé, peut être remis en œuvre, ne contient pas de catalyseur externe, et présente des propriétés mécaniques intéressantes.

La structure du matériau Vm-RvOH peut également apporter des avantages en termes de vieillissement des matériaux. En effet, après plusieurs mois, les matériaux TPE-TAF/BDGE (Chapitre II) et dans une moindre mesure P-DAF/BDGE (Chapitre III) montrent une nette sensibilité à l'humidité ambiante, voire à l'hydrolyse. La structure de ces matériaux est riche en groupements hydrophiles (esters, éthers et hydroxyles), et le diépoxy employé présente une structure aliphatique très courte, qui favorise l'hydrophilie, à l'instar du polyéthylène glycol (PEG). Cette propriété entraîne une pénétration d'eau dans le matériau, limitée à l'état vitreux, mais importante à l'état caoutchoutique. De plus, l'activation recherchée de l'ester vis-à-vis de l'attaque nucléophile d'un alcool le rend également plus vulnérable à l'attaque nucléophile non souhaitée de l'eau, donc à l'hydrolyse du matériau. Bien qu'une étude approfondie soit nécessaire pour caractériser et quantifier ces

phénomènes de prise en eau, le matériau Vm-RvOH semble moins sensible à ce phénomène. En effet, la pénétration d'eau étant plus rapide à l'état caoutchoutique, une T_g supérieure à 100 °C limite fortement cette pénétration. De plus, le taux élevé de carbones aromatiques dans le réseau macromoléculaire augmente vraisemblablement son caractère hydrophobe, et limite également la pénétration de l'eau et, par conséquent l'hydrolyse.

CONCLUSION GENERALE

Les vitrimères, à l'interface entre les thermoplastiques et les thermodurcissables, présentent de nombreux intérêts par leurs propriétés originales. Ces matériaux sont résistants aux solvants et permettent d'obtenir des propriétés mécaniques parfois comparables aux thermodurcissables, ce qui peut être utile pour des applications structurales, par exemple dans des composites. De plus, leur caractère dynamique peut permettre une mise en œuvre par des techniques habituellement réservées aux thermoplastiques, par exemple le moulage par compression ou l'extrusion. Enfin, toujours grâce à leur caractère dynamique, ils peuvent être remis en œuvre en fin de vie, pour être réutilisés. Ainsi, leur durée de vie est accrue. Cependant, plusieurs facteurs limitants entravent leur développement dans des applications industrielles. En particulier, les vitrimères les plus étudiés, basés sur la réaction de transestérification, nécessitent la plupart du temps l'emploi de catalyseurs incorporés en quantité importante au sein même du réseau macromoléculaire. Les vitrimères encourent plusieurs risques liés à l'utilisation de catalyseurs. Au cours de leur utilisation, les catalyseurs peuvent s'échapper du polymère par lixiviation. Ce phénomène peut poser des risques pour la santé selon le catalyseur employé, mais il peut également réduire la capacité des matériaux à se remettre en forme. De plus, les catalyseurs externes peuvent induire un vieillissement prématuré qui limite également leur capacité de remise en œuvre. Ainsi, l'obtention de vitrimères sans catalyseur est devenue un des objectifs majeurs de la recherche dans ce domaine.

Plusieurs stratégies sont possibles pour éviter l'utilisation d'un catalyseur. La première est d'utiliser d'autres réactions d'échange, dont la vitesse de réaction intrinsèque est suffisamment rapide à la température de remise en œuvre. L'autre stratégie est de placer à proximité de la liaison échangeable un groupement activant, par des effets inductifs, stériques ou par assistance anchimérique.

Le premier chapitre de ce manuscrit passe en revue les différentes réactions d'échange qui ont été décrites dans la littérature sur les vitrimères. Les mécanismes mis en jeu ont été discutés, en particulier leur caractère associatif ou dissociatif. En effet, le caractère associatif d'une réaction est une condition suffisante (bien que pas toujours nécessaire) pour s'assurer que la vitesse d'écoulement du matériau suive une loi d'Arrhénius en fonction de la température. Cette propriété traduit la capacité de ces matériaux à être mis en forme par des techniques utilisées pour les verres inorganique, grâce à une diminution progressive de la viscosité, ce qui a inspiré le terme vitrimère. Ces considérations sur les différents mécanismes d'échange permettent de comprendre par quels leviers il est possible de les activer, et donc quels groupements utiliser à quelles positions. C'est l'objet de la deuxième partie de cette étude bibliographique. Pour chaque réaction décrite auparavant, les stratégies d'activation existantes dans la littérature sur les vitrimères ont été décrites. De plus, certaines stratégies et certains groupements utilisés dans d'autres domaines de la chimie, la chimie organique notamment, ont

également été rapportés. L'objectif est de donner des pistes de stratégies d'activation innovantes pour les futures études sur les vitrimères, en particulier les vitrimères sans catalyseur.

Suite à l'inventaire des stratégies d'activation connues, le choix de la réaction d'échange s'est porté sur la transestérification. En effet, les premiers vitrimères décrits sont basés sur cette réaction,[25] et les travaux sur les vitrimères de transestérification sont les plus nombreux, bien que beaucoup reste à faire sur la compréhension de ces systèmes. De plus, le mécanisme de transestérification a été largement étudié et il est aujourd'hui bien connu. La stratégie adoptée pour activer la liaison ester est basée sur des effets inductifs électroattracteurs pour diminuer la densité électronique sur le carbonyle, et le rendre plus réactif vis-à-vis d'une attaque nucléophile par une fonction alcool. Afin d'obtenir l'effet inductif le plus intense possible, le choix s'est porté sur l'atome de fluor, puisqu'il est l'élément le plus électronégatif (3.96 sur l'échelle de Pauling). De même, toujours dans le même but de maximiser l'effet inductif, le choix a été fait de placer les atomes de fluor au plus près de la liaison ester, en position α, tout en ayant le maximum de substituants fluor à cette position, donc un groupe α-CF_2.

Le premier volet de travaux expérimentaux, décrits dans le chapitre II, a un objectif double. Il est d'une part d'obtenir une preuve de concept sur la possibilité d'activer la transestérification par des groupements α-CF_2 à proximité des liaisons ester, et d'autre part de montrer son efficacité pour former des matériaux polyester dynamiques sans catalyseur. A partir d'un triphénol, un composé α,α-difluoro acide carboxylique trifonctionnel original a été synthétisé. Ce composé a été utilisé dans la polymérisation par ouverture de cycle d'un époxy difonctionnel, le BDGE, afin de former un matériau dont la structure est un réseau macromoléculaire tridimensionnel. Ce matériau est insoluble dans les solvants organiques aprotiques, et il peut être remis en forme jusqu'à 10 fois, dans des conditions modérées (100 °C, 1h30min, 15 bars), tout en conservant ses propriétés mécaniques. De plus, l'écoulement du matériau depuis le plateau caoutchoutique a été mis en évidence, et la vitesse de cet écoulement suit une loi d'Arrhénius en fonction de la température. Le matériau TPE-TAF/BDGE se comporte donc comme un vitrimère polyester, et son caractère dynamique ne nécessite pas d'ajout de catalyseur. Suite à cette étude, la preuve de concept sur la faisabilité d'un vitrimère sans catalyseur activé par le fluor a donc été validée.

Dans la continuité de ces travaux, l'objectif a été de se rapprocher d'éventuelles applications pratiques. Pour cela, il est nécessaire de simplifier la synthèse des monomères α,α-difluoro acides. En effet, la synthèse du TPE-TAF semble difficile à réaliser à grande échelle, et sa purification sur colonne de silice peu adaptée pour d'éventuelles applications industrielles. Un deuxième monomère, le P-DAF, a été

[25] Montarnal, D.; Capelot, M.; Tournilhac, F.; Leibler, L. Science 2011, 334 (6058), 965–968.

synthétisé à partir du diiodobenzène. La synthèse de ce composé est plus rapide, plus robuste et le solvant utilisé est le DMSO, moins dangereux que le DMF utilisé précédemment. Cependant le monomère obtenu est difonctionnel, ce qui ne garantit pas l'obtention d'un réseau tridimensionnel par réaction avec un époxy difonctionnel. La possibilité d'utiliser des époxy de plus haute fonctionnalité a été envisagée, mais présente de nombreuses limites. En effet, beaucoup de ces résines époxy sont solides, et pour celles qui se présentent sous forme liquide leur faible miscibilité avec le P-DAF pose problème. Une autre stratégie inspirée de la littérature a donc été choisie, dans laquelle le P-DAF réagit avec un époxy difonctionnel, et la réticulation est permise par la réaction de transestérification, conduisant à des liens entre les chaînes macromoléculaires, et à la formation d'oligomères sacrificiels. Ce phénomène bien connu pour les thermodurcissables époxy-acide[26] et décrit pour des vitrimères de transestérification catalysés, [27] implique que la réaction de transestérification a une cinétique dont l'ordre de grandeur est comparable à celle de la polymérisation par ouverture de cycle de l'époxy par l'acide. Dans le cas des acides fluorés, sans catalyseur, les conditions de polymérisation sont plus douces, puisque la réaction a lieu essentiellement à température ambiante. Bien qu'une étape en température à 150 °C soit nécessaire pour finir la polymérisation, la formation d'un réseau macromoléculaire ne semblait pas assurée. Le P-DAF a donc été engagé avec le BDGE afin de former un matériau. Après l'étape de réticulation en température, ce matériau s'est montré lui aussi insoluble dans les solvants aprotiques. Sa capacité à se remettre en forme a également été étudiée, ainsi que son caractère dynamique, par analyse mécanique.

Le développement de vitrimères sans catalyseur s'inscrit dans une démarche pour inventer des matériaux polymères plus durables et plus respectueux de l'environnement. Le sujet des additifs est au cœur des préoccupations qui ont amené à la réalisation de ces travaux. Le problème de la fin de vie des matériaux polymères est l'essence même du concept de vitrimère. Cependant, la question de la provenance des matières premières utilisées n'a pas encore été posée dans les travaux décrits aux chapitres précédents. En effet, la grande majorité des polymères produits sont issus de matières premières fossiles, dont les réserves sont finies. Afin d'anticiper de futures tensions croissantes pour l'accès aux ressources fossiles, des polymères sont développés à partir de matière première d'origine renouvelable. Cette tendance se confirme également dans le domaine des vitrimères.[28] Une autre limite des vitrimères développés jusqu'à présent concerne leurs propriétés mécaniques souvent insuffisantes pour certaines applications telles que les composites. En particulier les valeurs de T_g

[26] Steinmann, B. Polym. Bull. 1989, 22 (5–6), 637–644.
[27] Poutrel, Q.-A.; Blaker, J. J.; Soutis, C.; Tournilhac, F.; Gresil, M. Polym. Chem. 2020, 11 (33), 5327–5338.
[28] Vidil, T.; Llevot, A. Macromol. Chem. Phys. 2022, 223 (13), 2100494.

rapportées sont généralement en-dessous de 100 °C. C'est également le cas des deux vitrimères décrits précédemment. L'objectif de ce dernier volet de travaux a été d'obtenir un matériau avec une T_g supérieure à 100 °C. Pour cela, un polyphénol biosourcé a été mis à profit, le resvératrol. Ce composé est extrait de la vigne et comporte trois fonctions phénol qui peuvent être modifiées. De plus, il est riche en carbones aromatiques, ce qui lui confère de la rigidité, qui est favorable à l'obtention de T_g élévée. Le resvératrol a été fonctionnalisé de deux manières différentes. D'une part, les fonctions phénol ont été modifiées pour obtenir un α,α-difluoro acide trifonctionnel. D'autre part, le resvératrol a été transformé en époxy trifonctionnel par réaction avec l'épichlorhydrine. Le mélange des deux monomères a une fonctionnalité moyenne de 3, ce qui permet d'obtenir un réseau plus dense et d'augmenter la T_g du Vm-RvOH par rapport aux matériaux précédents. Ainsi, le Vm-RvOH a une T_g de 120 °C, tout en conservant sa capacité à être remis en œuvre, à 170 °C pendant 2 h. Ce matériau présente un taux de carbone renouvelable de 86 %.

En conclusion, ces travaux de thèse ont permis de démontrer l'efficacité de groupements α-CF_2 pour activer la liaison ester vis-à-vis de la transestérification, et d'utiliser cet effet pour former des vitrimères de transestérification sans catalyseur inédits, activés par le fluor. Des pistes ont été trouvées afin de simplifier la synthèse de composés α,α-difluoro acides pour obtenir de tels matériaux. En particulier, la faisabilité d'une structure macromoléculaire tridimensionnelle à partir de monomères acide et époxy difonctionnels a été montrée. De plus, la synthèse de monomères α,α-difluoro acides a été adaptée à un triphénol biosourcé, le resvératrol. Cette synthèse a permis d'obtenir un vitrimère biosourcé, sans catalyseur, avec une T_g élevée.

Néanmoins de nombreuses pistes d'améliorations peuvent être envisagées pour la poursuite de ces travaux. En termes de montée en échelle, la synthèse du TPE-TAF n'est pas adaptée, car impossible à purifier avec des procédés industriels. Une optimisation des conditions de réactions pourrait être envisagée afin de réduire la formation de composés disubstitués et monosubstitués. La synthèse du P-DAF utilise des procédés beaucoup plus simples, et la purification par cristallisation-lavage est adaptée à la production à grande échelle. Cependant, cette réaction fait intervenir du cuivre métallique en grande quantité. Une partie de ce cuivre n'est pas récupéré après la réaction. Le cuivre consommé doit donc être renouvelé, et les effluents, qui présentent un risque pour l'environnement et la santé, doivent être traités, ce qui rend l'utilisation du cuivre très coûteuse. Là encore, une optimisation des conditions de réaction pourrait permettre de réduire les quantités de cuivre utilisées. La synthèse du RvOH-TAF semble finalement plus prometteuse, bien que proche de celle du TPE-TAF, car la purification se fait par une simple filtration sur silice, et les rendements sont meilleurs.

Les propriétés mécaniques du Vm-RvOH le rendent intéressant pour des applications composites plus structuraux. L'étude de divers procédés de mise en œuvre de ce matériau dans la fabrication de composites pourrait être une suite intéressante à donner à ces travaux, par exemple par moulage par compression ou par infusion d'une solution des deux monomères dans des fibres.

De plus, le phénomène d'hydrolyse des matériaux, qui n'avait pas été anticipé, mérite d'être étudié afin de trouver des solutions à ce problème. En effet, le carbone du carbonyle de l'ester est activé vis-à-vis de l'attaque nucléophile d'un alcool, mais cet effet a pour conséquence de l'activer également vis-à-vis de l'attaque nucléophile néfaste d'eau. Ce phénomène se traduit par une hydrolyse des matériaux après plusieurs mois, le TPE-TAF/BDGE étant le plus sujet à l'hydrolyse. Le matériau Vm-RvOH semble moins sensible à l'hydrolyse, probablement du fait de sa haute T_g. En effet la pénétration d'humidité au sein du matériau est plus importante à l'état caoutchoutique. Une T_g élevée et des monomères plus hydrophobes limitent donc cette pénétration d'eau et par suite les risques d'hydrolyse. Toutefois, ce phénomène d'hydrolyse nécessite d'être étudié en détail pour chacun des matériaux formés. Bien que ce ne soit pas le but initial, l'activation de l'hydrolyse par le fluor pourrait avoir une utilité, par exemple pour fabriquer des matériaux thermodurcissables dégradables.

Outre l'hydrolyse, les vitrimères subissent d'autres phénomènes de vieillissement, notamment le vieillissement thermique au moment de la remise en œuvre. Ce phénomène n'est pas décrit dans la littérature. Une étude approfondie du vieillissement des vitrimères avec catalyseur et sans catalyseur activés par le fluor pourrait permettre de mettre en évidence et de quantifier l'effet bénéfique d'une activation interne par rapport à un catalyseur externe sur la durée de vie du matériau.

Pour finir, les esters de phosphate présentent l'intérêt de s'échanger sans catalyseur, et quelques vitrimères basés sur cet échange ont été décrits.[29,30,31,32] Dans ce cas, la stratégie est différente puisqu'il s'agit d'utiliser une réaction qui ne nécessite pas de catalyseur, et non plus de l'activer par des groupes à proximité. Cependant ce type d'esters présente des avantages. Pour commencer, ils limitent les étapes de synthèse car ils n'ont pas besoin d'être activés. De plus, ils peuvent être synthétisés à partir d'acide phosphorique et d'époxy, de façon similaire aux esters d'acides carboxyliques. Quelques travaux préliminaires ont été menés sur ces esters, qui ont permis de mettre en évidence deux limites sur lesquelles travailler : la forte exothermie de la réaction d'ouverture de cycle des époxy par l'acide

[29] Majumdar, S.; Zhang, H.; Soleimani, M.; A. T. M. van Benthem, R.; P. A. Heuts, J.; P. Sijbesma, R. ACS Macro Lett. 2020, 9 (12), 1753–1758.
[30] Feng, X.; Li, G. Chem. Eng. J. 2021, 417, 129132.
[31] Huang, L.; Yang, Y.; Niu, Z.; Wu, R.; Fan, W.; Dai, Q.; He, J.; Bai, C. Macromol. Rapid Commun. 2021, 2100432.
[32] Liu, Y.; Wang, B.; Ma, S.; Xu, X.; Qiu, J.; Li, Q.; Wang, S.; Lu, N.; Ye, J.; Zhu, J. Eur. Polym. J. 2021, 144, 110236.

phosphorique, qui doit être contenue, et la sensibilité importante de ces matériaux à l'hydrolyse. Ces matériaux ont été peu étudiés à l'heure actuelle et semblent dignes d'intérêt pour de futurs travaux

ANNEXES A : ANNEXES AU CHAPITRE II

Catalyst-Free Transesterification Vitrimers: α-CF_2 group activation of the ester linkages: Supporting Information

Florian Cuminet,[a] Dimitri Berne,[a] Sébastien Lemouzy,[a] Éric Dantras,[b] Christine Joly-Duhamel,[a] Sylvain Caillol,[a] Éric Leclerc[a] and Vincent Ladmiral[a]

[a] ICGM, Univ Montpellier, CNRS, ENSCM, Montpellier, France
[b] CIRIMAT, Université Toulouse 3 Paul Sabatier, Physique des Polymères, 118 Route de Narbonne, 31062 Toulouse, France

TPE-TE characterizations

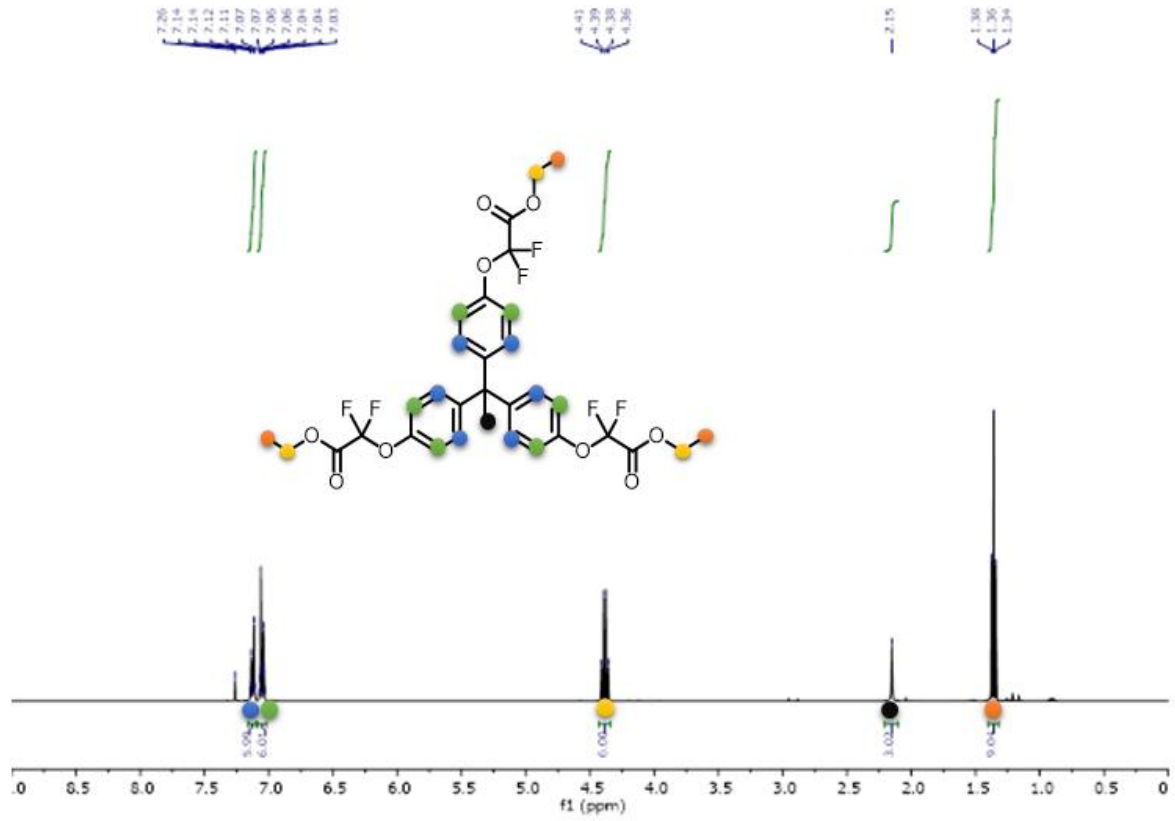

Figure S1. ^{1}H NMR spectrum of the triester TPE-TE in $CDCl_3$

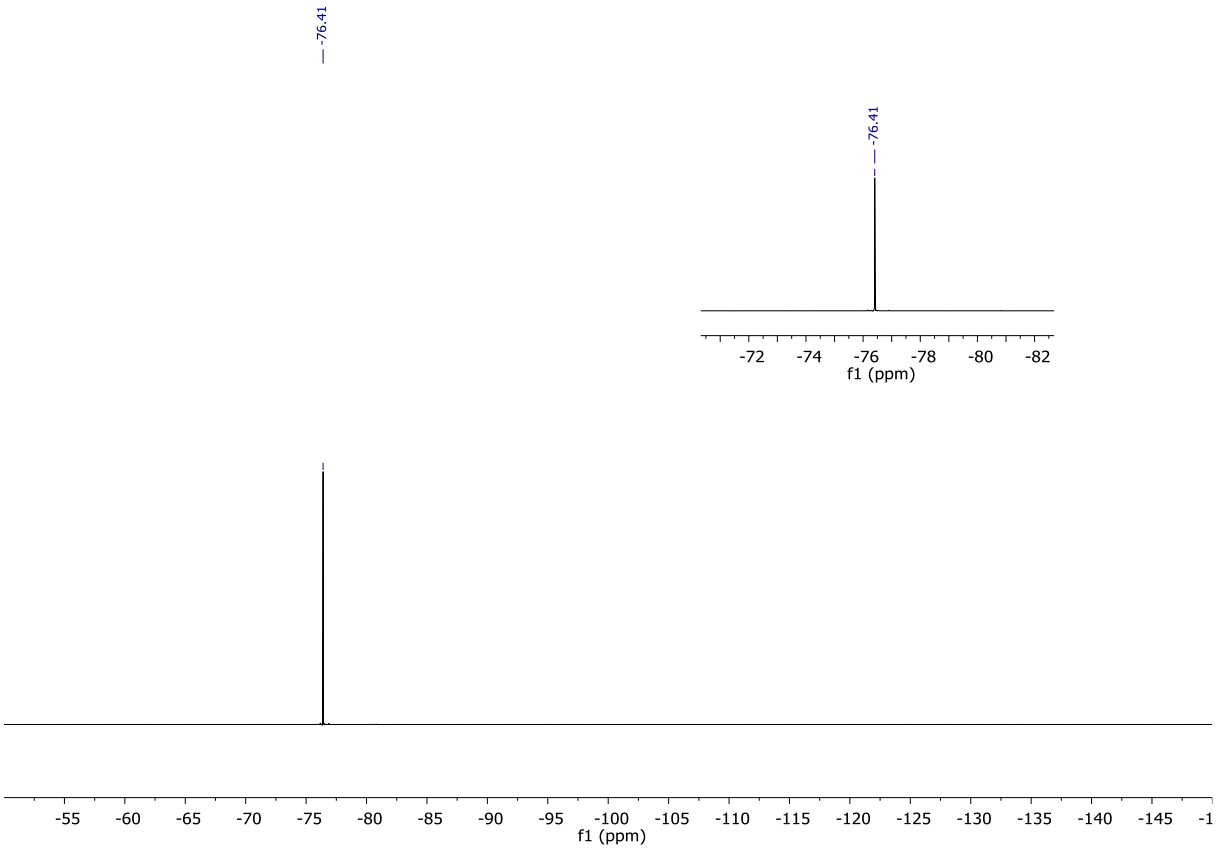

Figure S2. ^{19}F NMR spectrum of the triester TPE-TE in $CDCl_3$

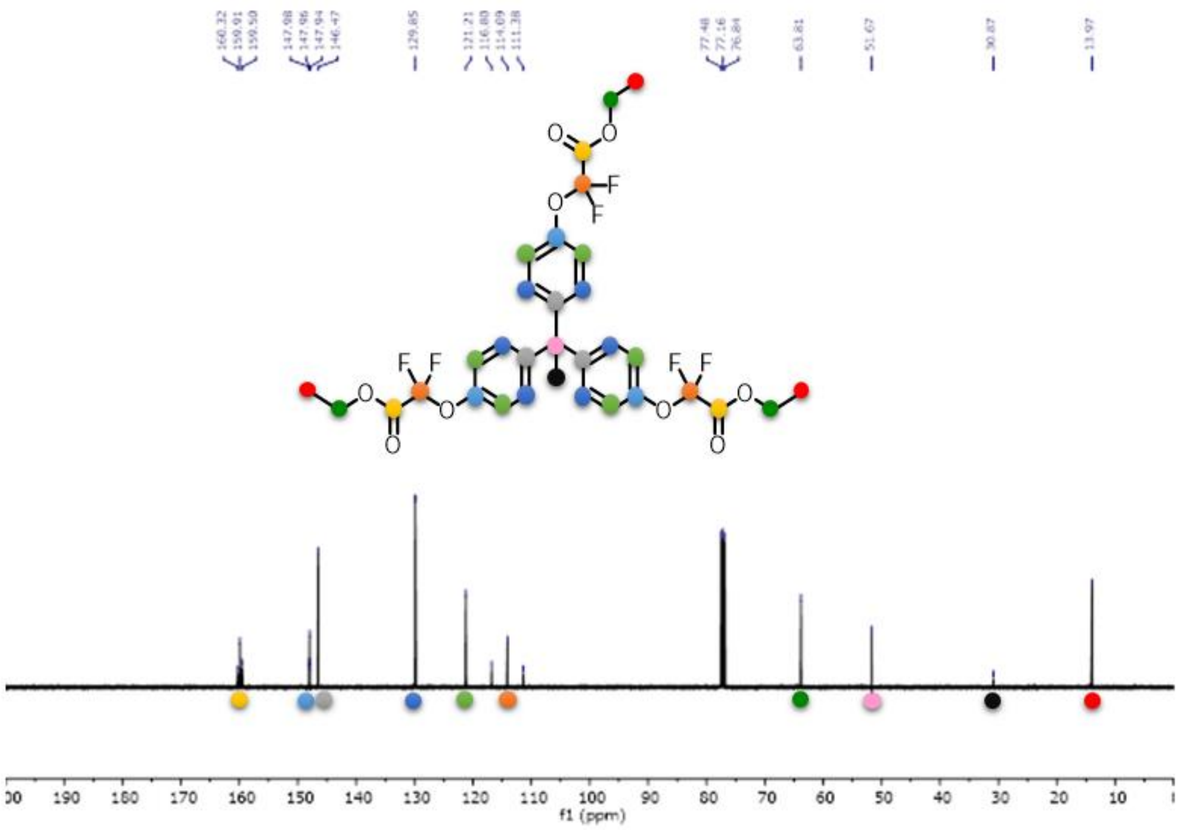

Figure S3. ^{13}C NMR spectrum of the triester TPE-TE in $CDCl_3$

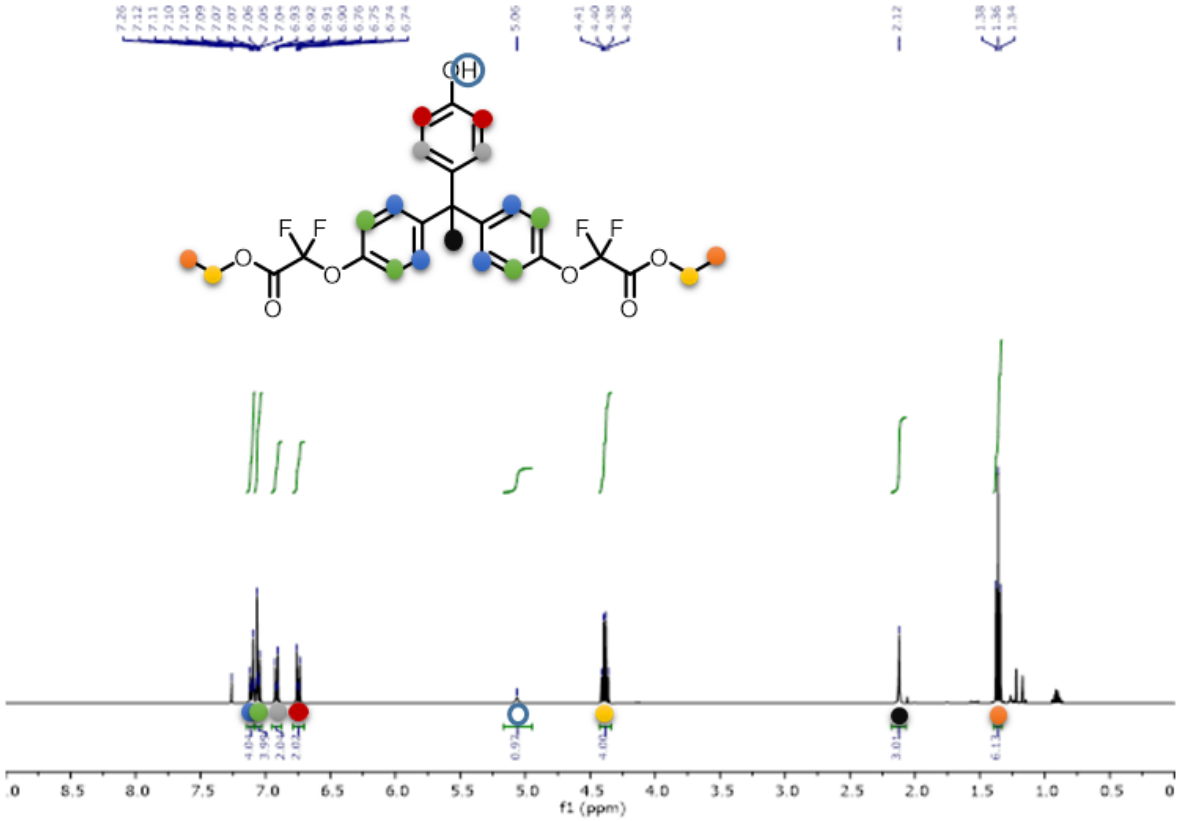

Figure S4. ^{1}H NMR spectrum of the disubstituted byproduct in $CDCl_3$

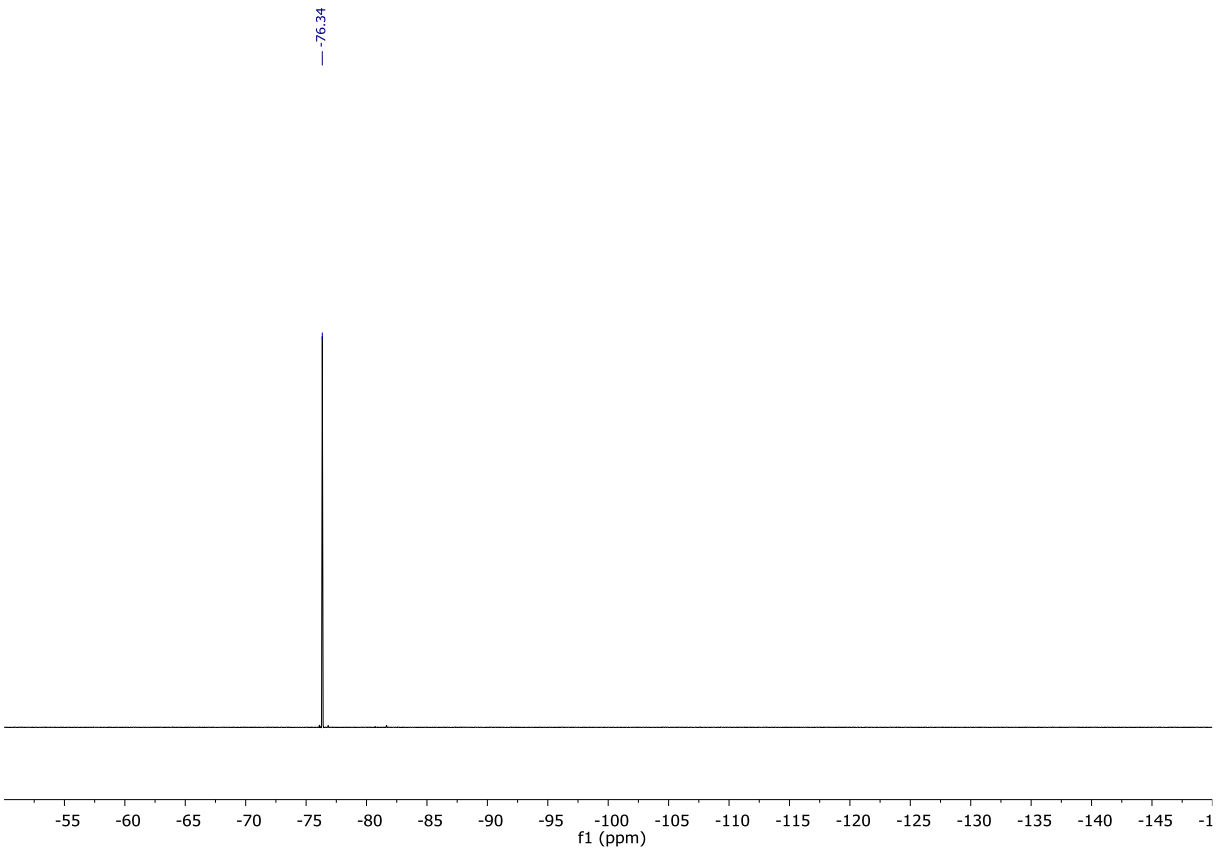

Figure S5. ^{19}F NMR spectrum of the disubstituted byproduct in $CDCl_3$

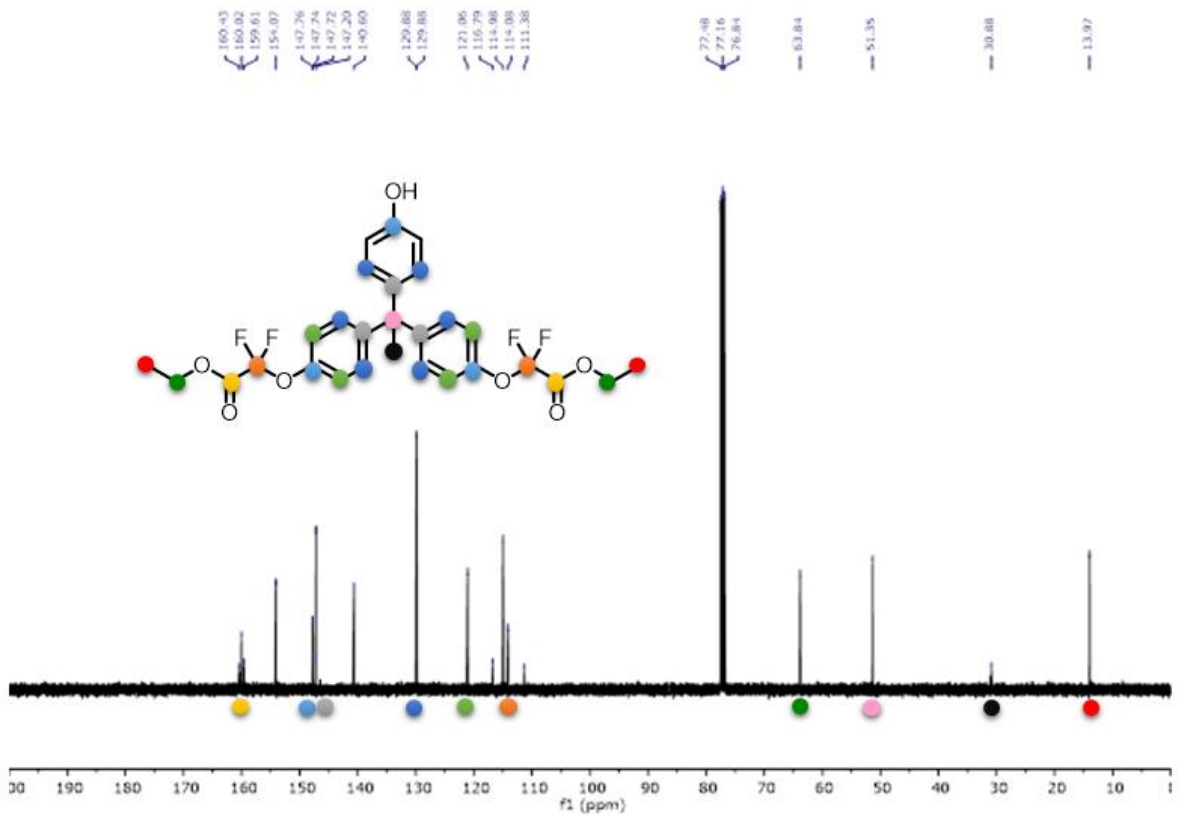

Figure S6. ^{13}C NMR spectrum of the disubstituted byproduct in $CDCl_3$

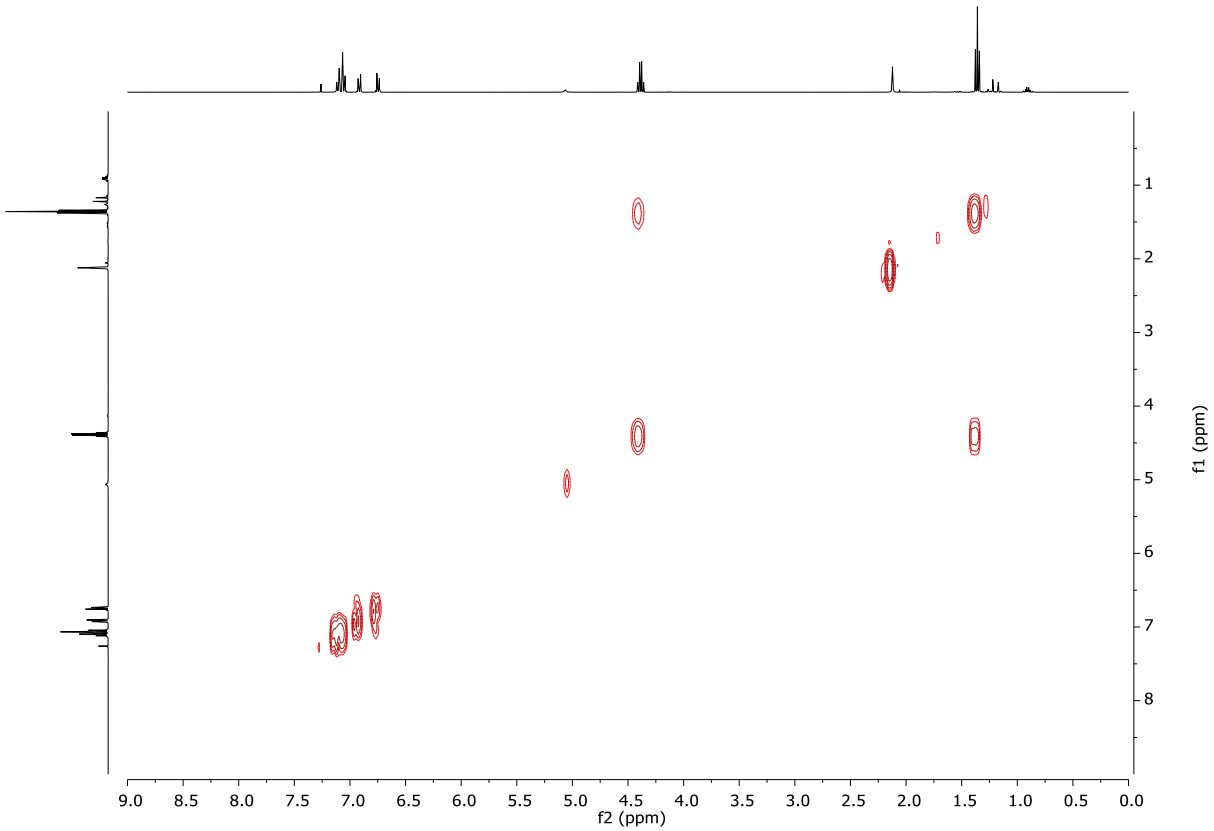

Figure S7. COSY ^{1}H NMR spectrum of the disubstituted byproduct in $CDCl_3$

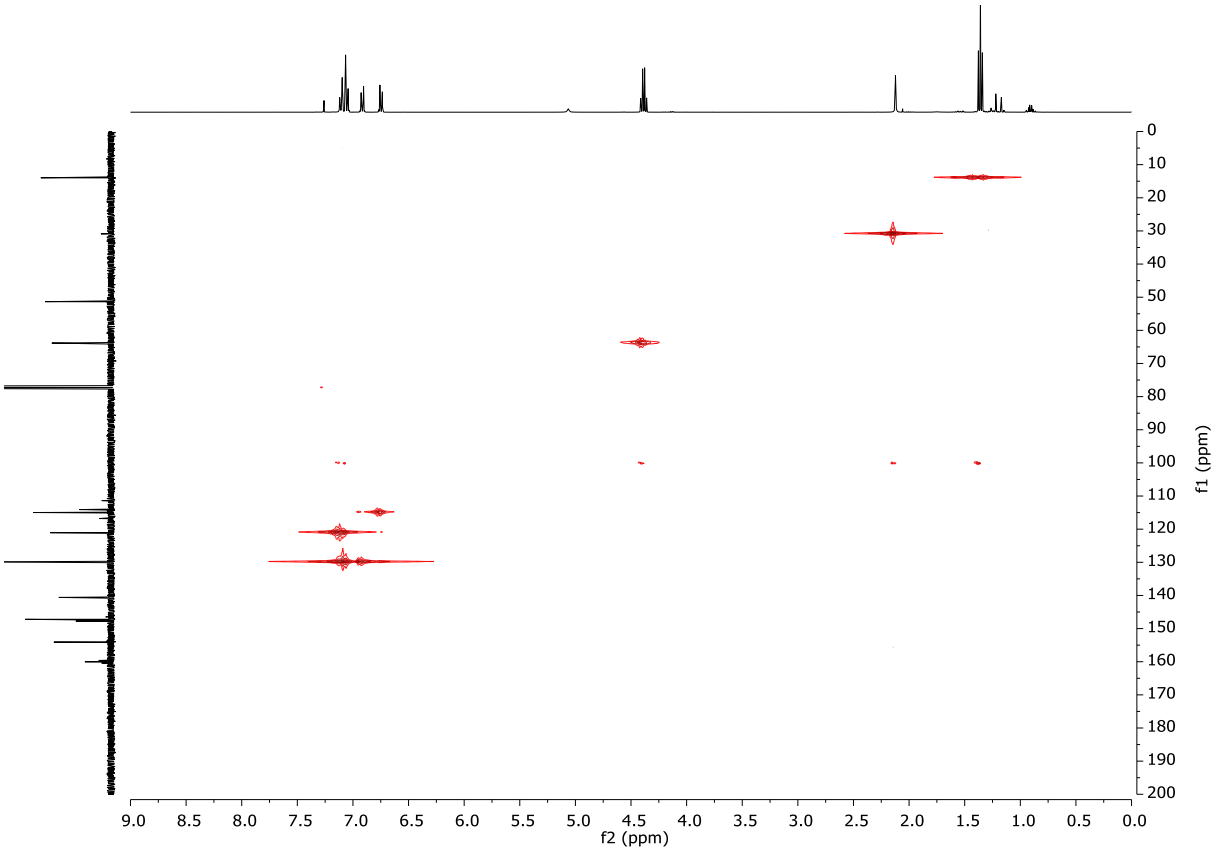

Figure S8. HSQC ^{1}H-^{13}C NMR spectrum of the disubstituted byproduct in $CDCl_3$

TPE-TAF characterizations

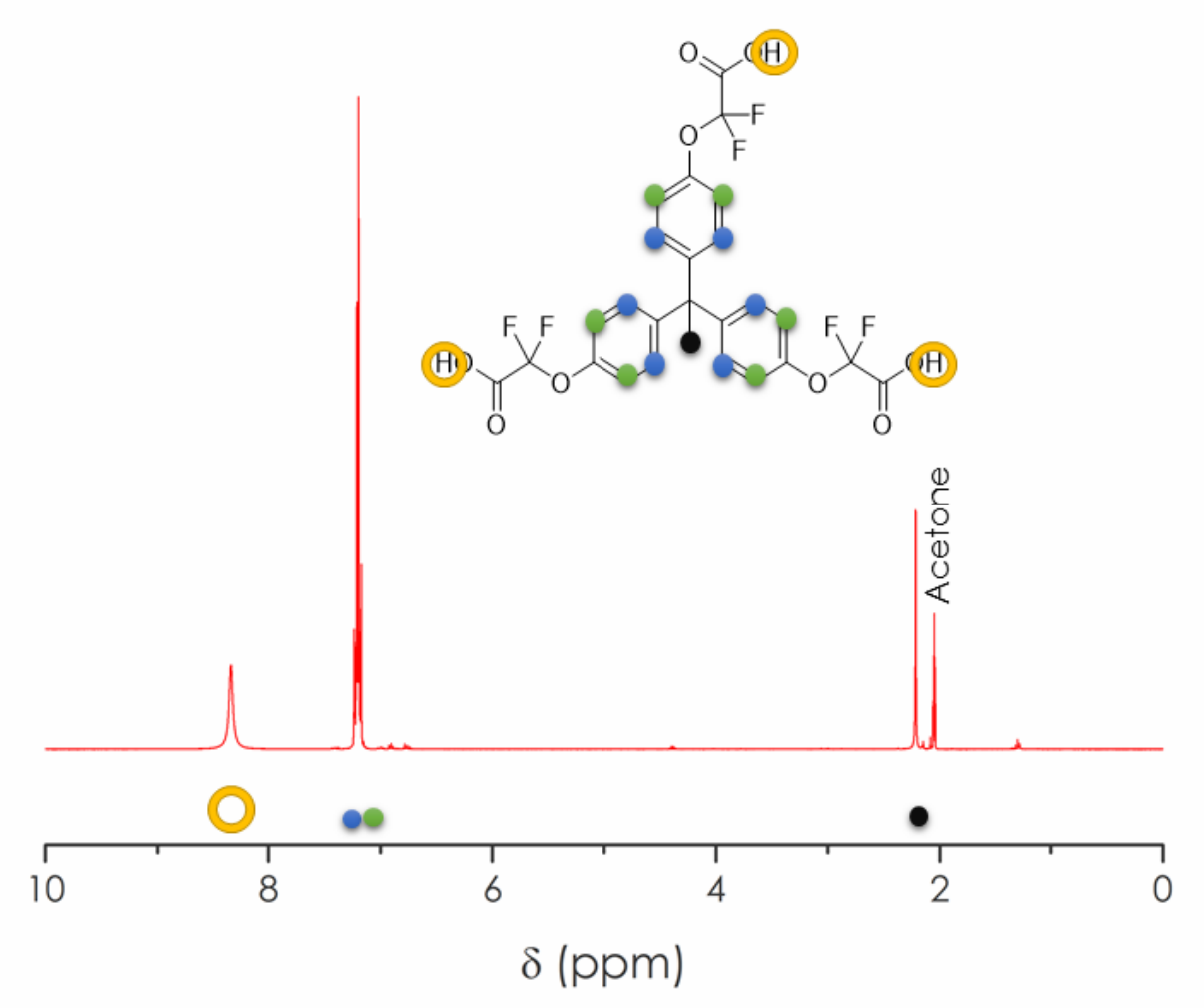

Figure S9. ^{1}H NMR spectrum of the triacid TPE-TAF in acetone-d_6.

Very small signals at 1.30 and 4.39 ppm correspond to residual ester functions (which amount to less than 2 mol% compared to the acid groups).

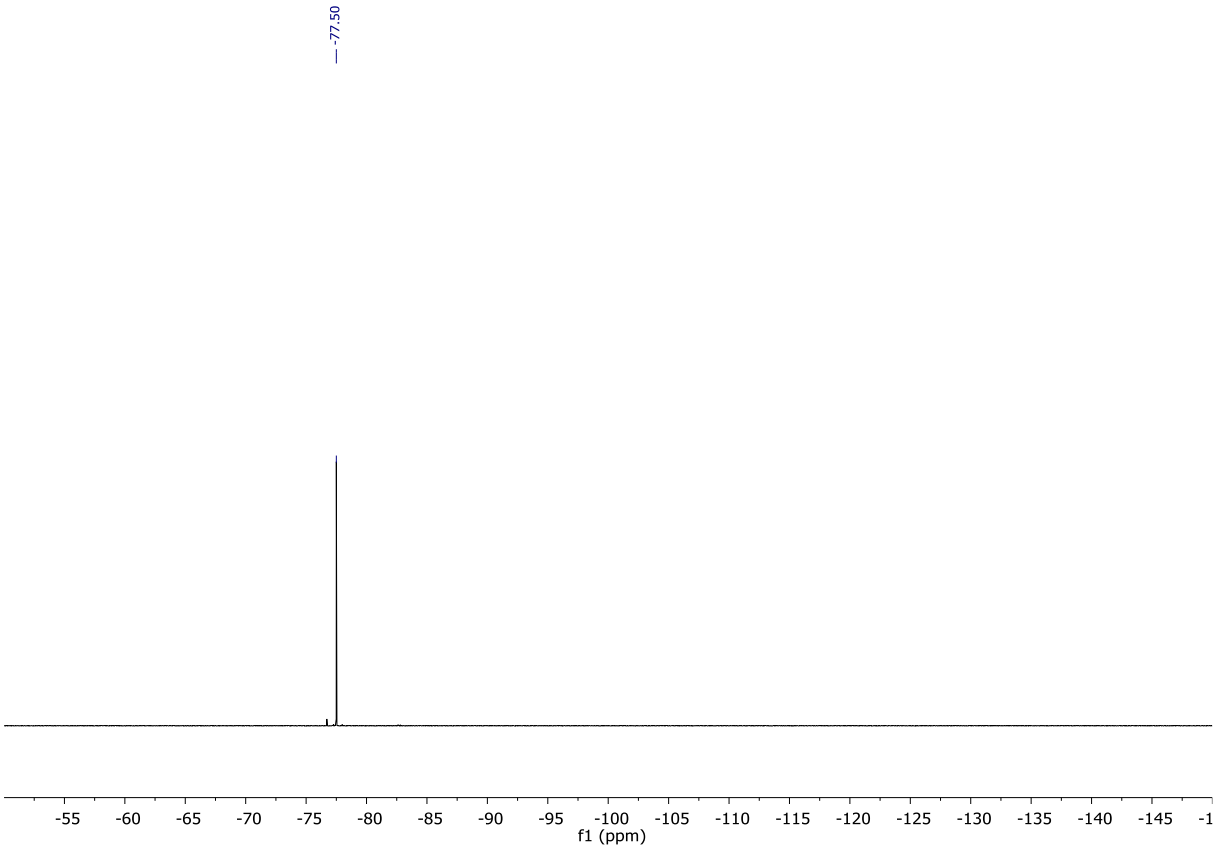

Figure S10. ^{19}F NMR spectrum of the triacid TPE-TAF in acetone-d_6

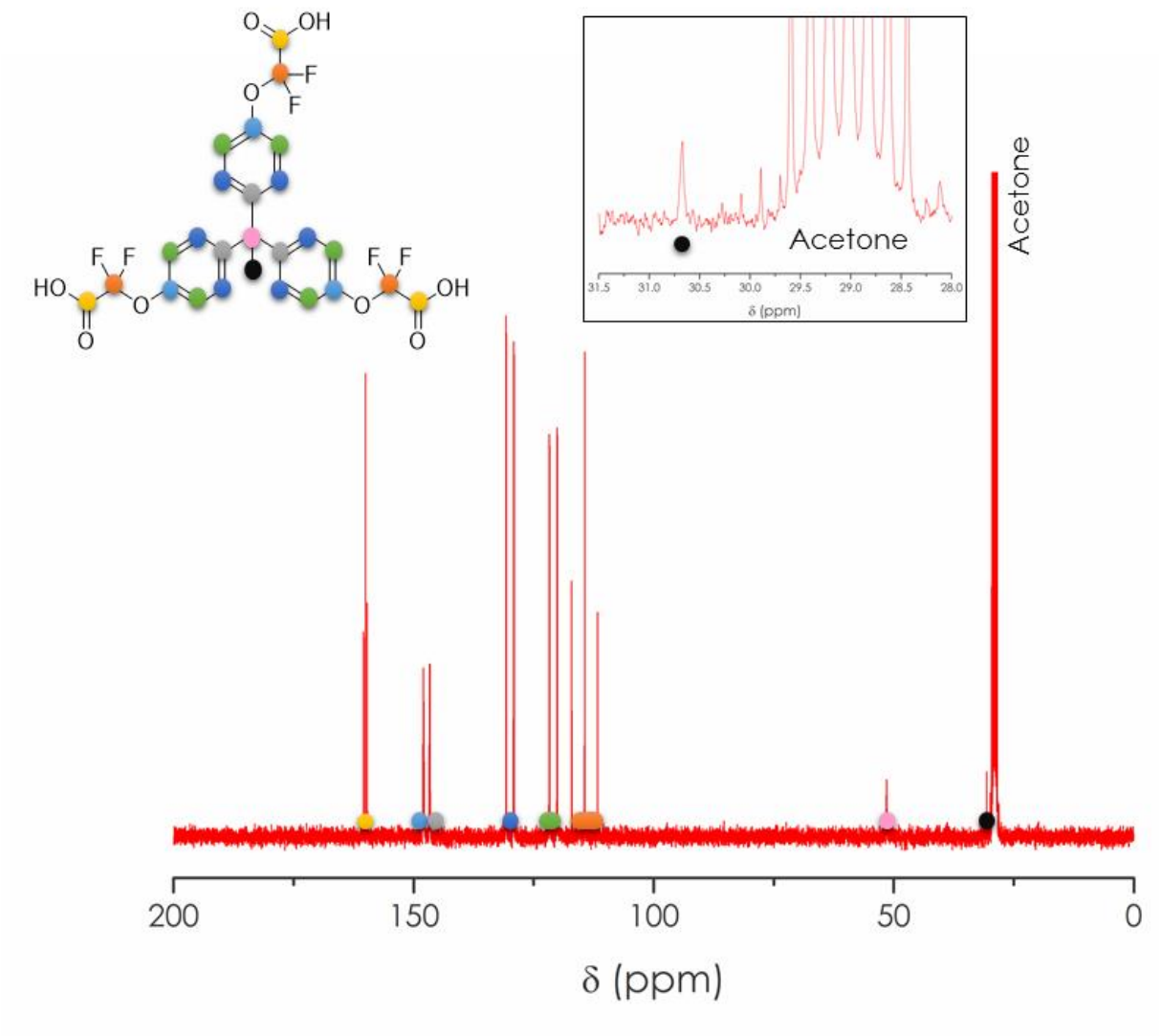

Figure S11. ^{13}C NMR spectrum of the triacid TPE-TAF in acetone-d_6

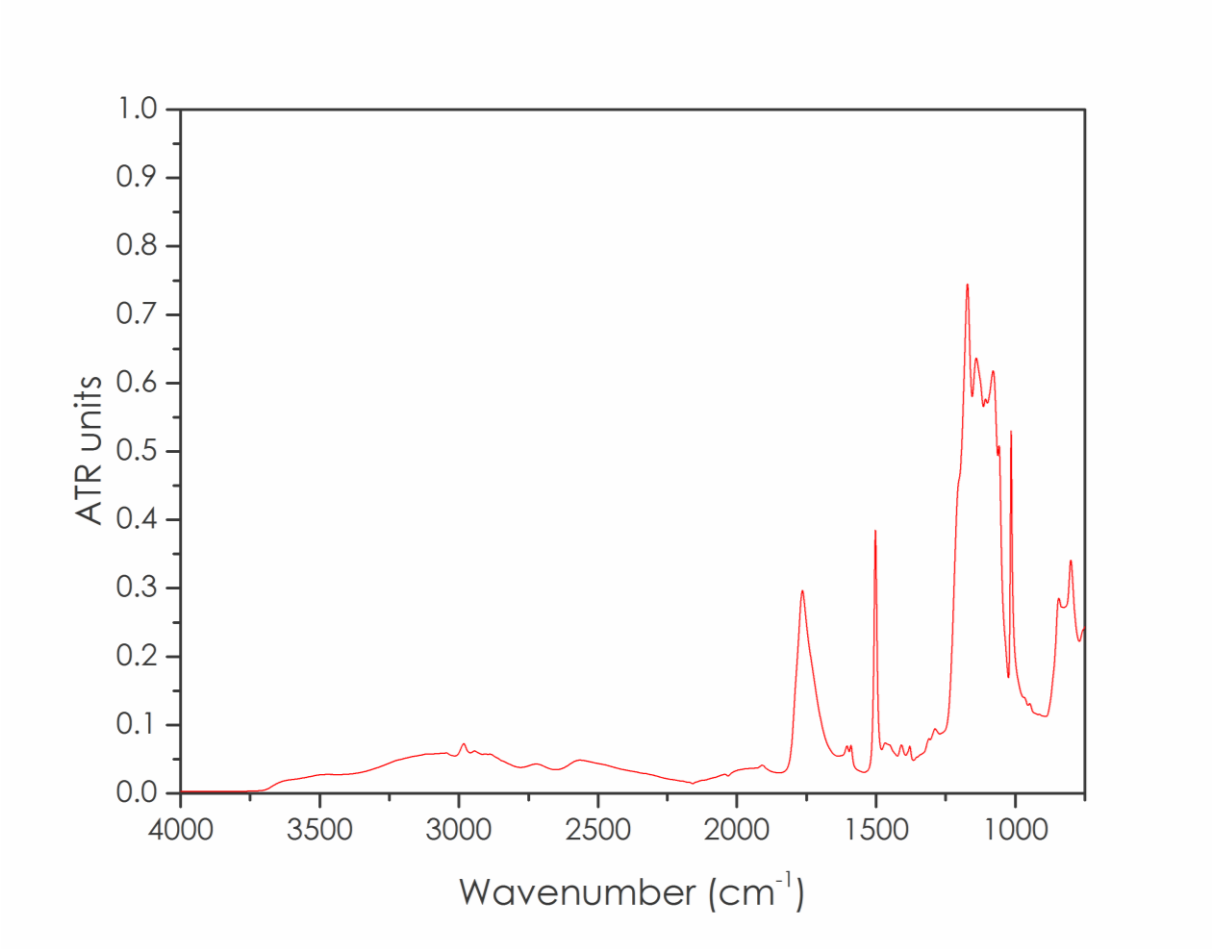

Figure S12. FTIR spectrum of the triacid TPE-TAF

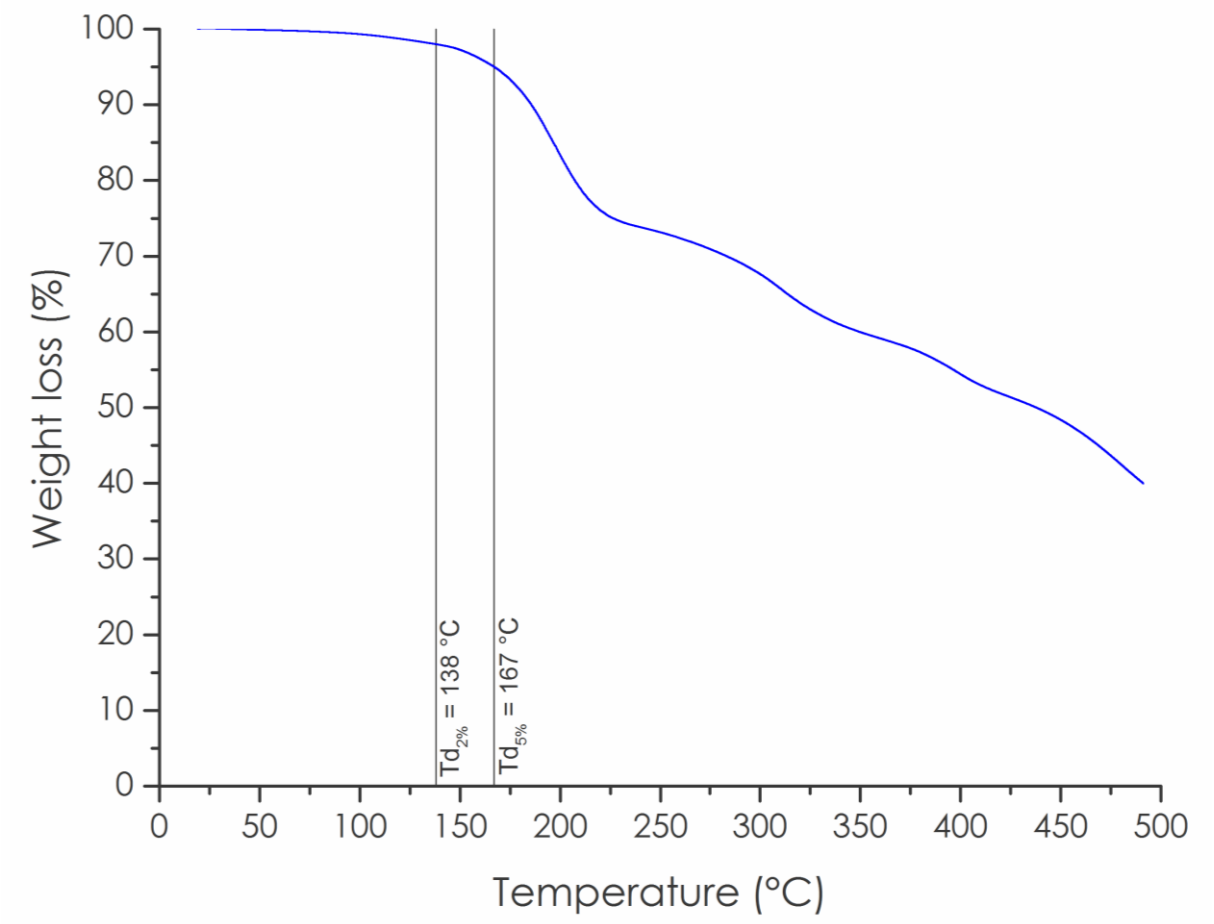

Figure S13. TGA thermogram of the triacid TPE-TAF (air, 20 °C.min^{-1})

BDGE characterizations

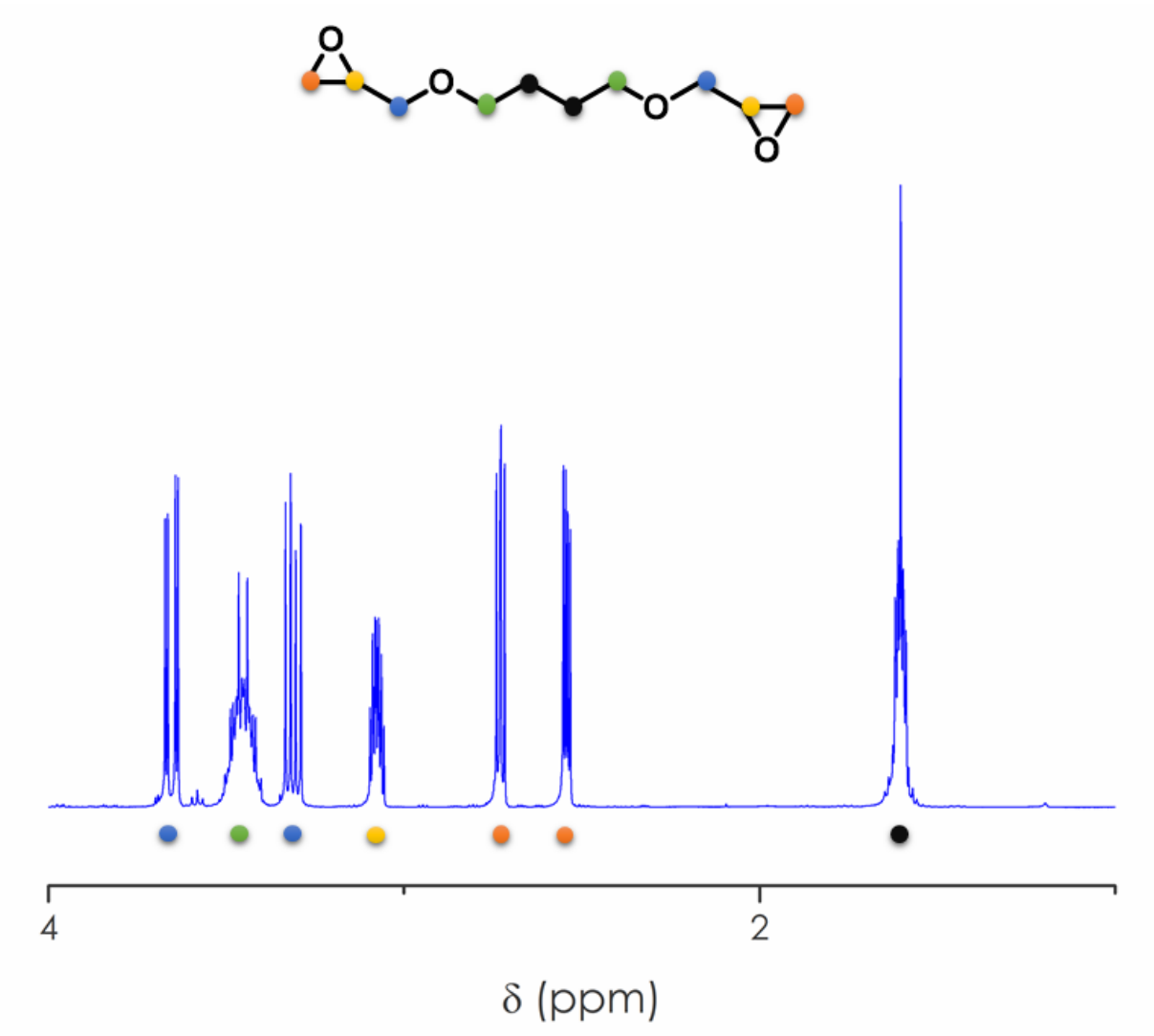

Figure S14. ^{1}H NMR spectrum of the commercial BDGE in $CDCl_3$

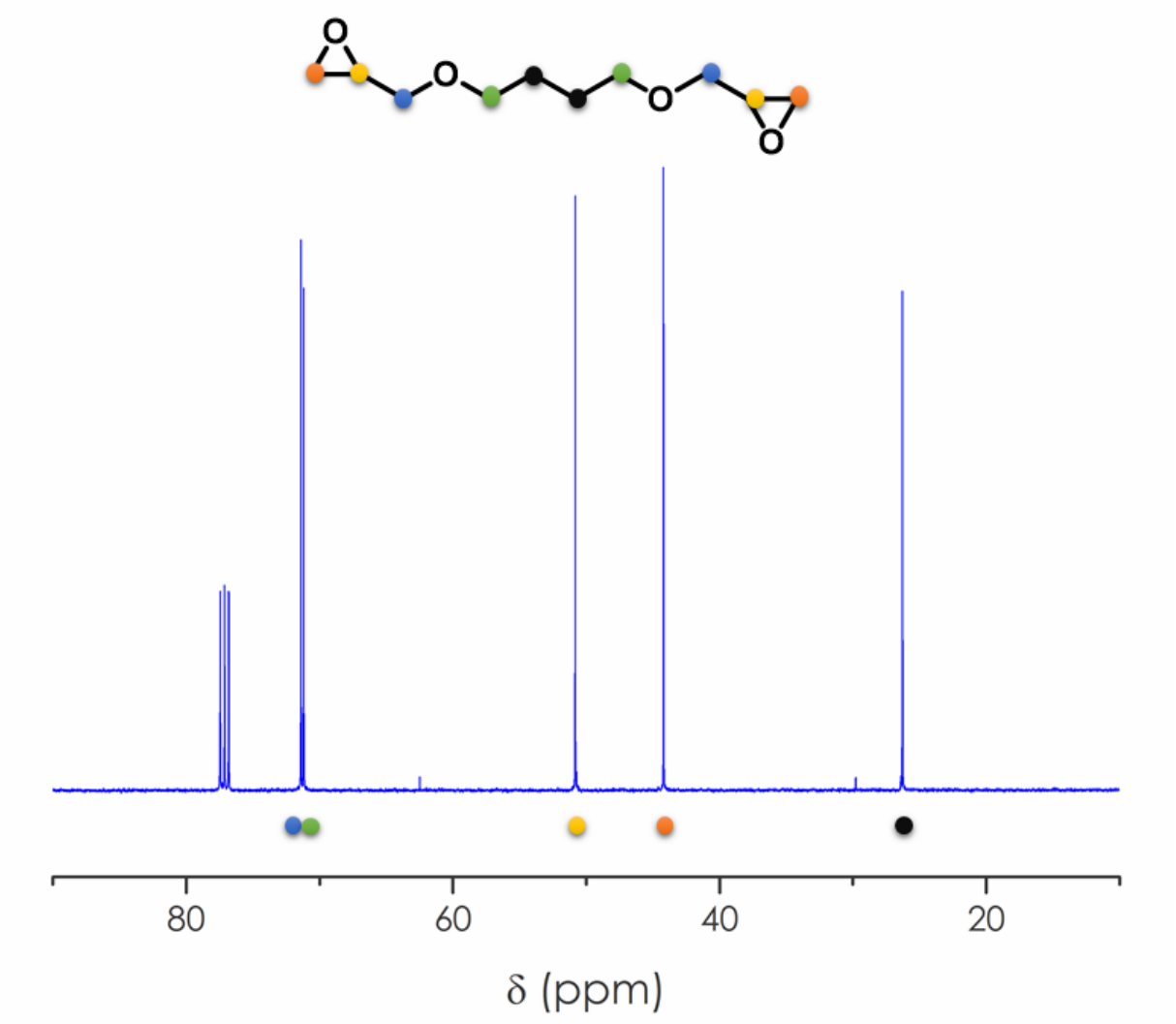

Figure S15. ^{13}C NMR spectrum of the commercial BDGE in $CDCl_3$

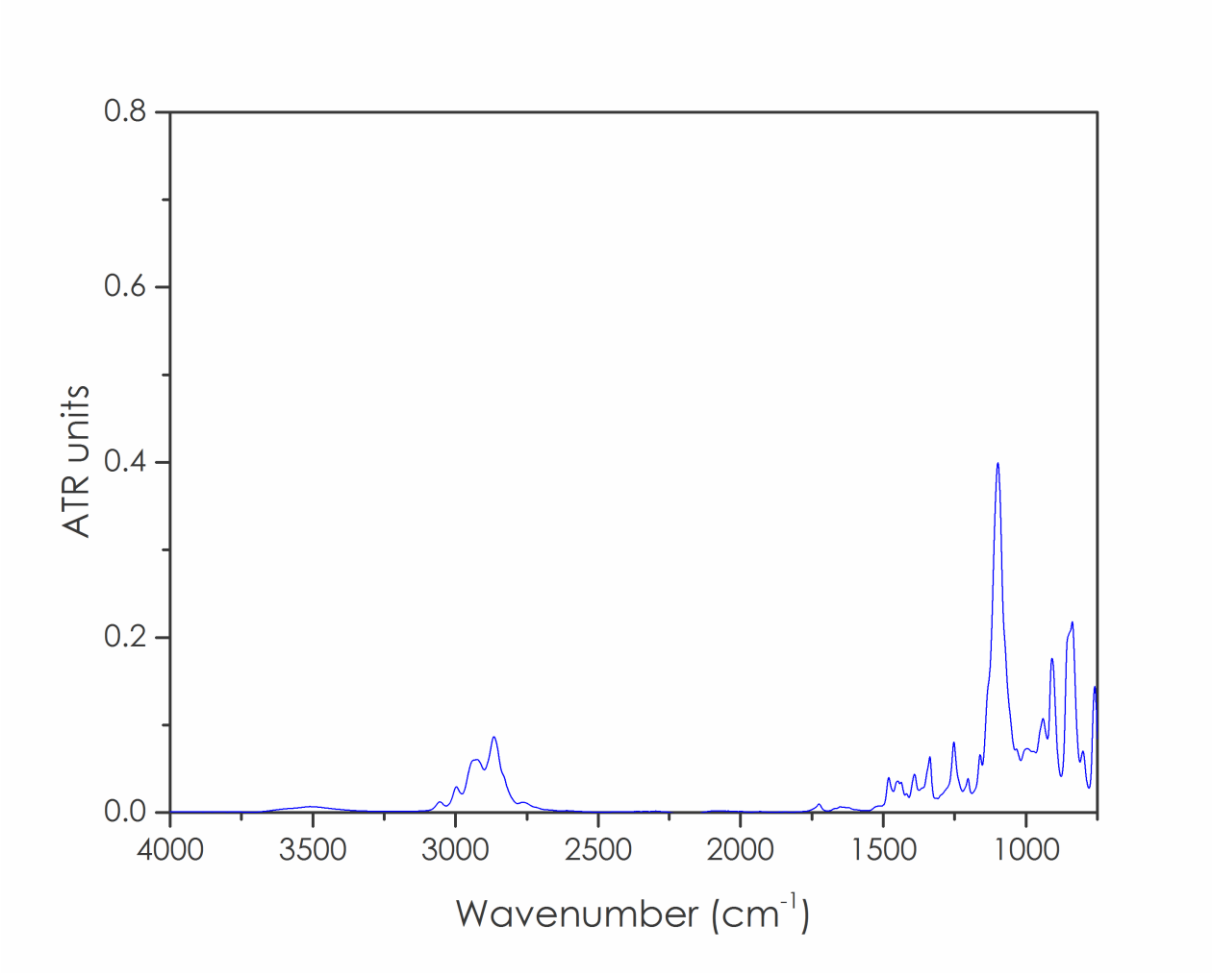

Figure S16. FTIR spectrum of the commercial BDGE

A. Experimental procedure for the determination of BDGE epoxy equivalent weight (EEW) by ^1H NMR in $CDCl_3$

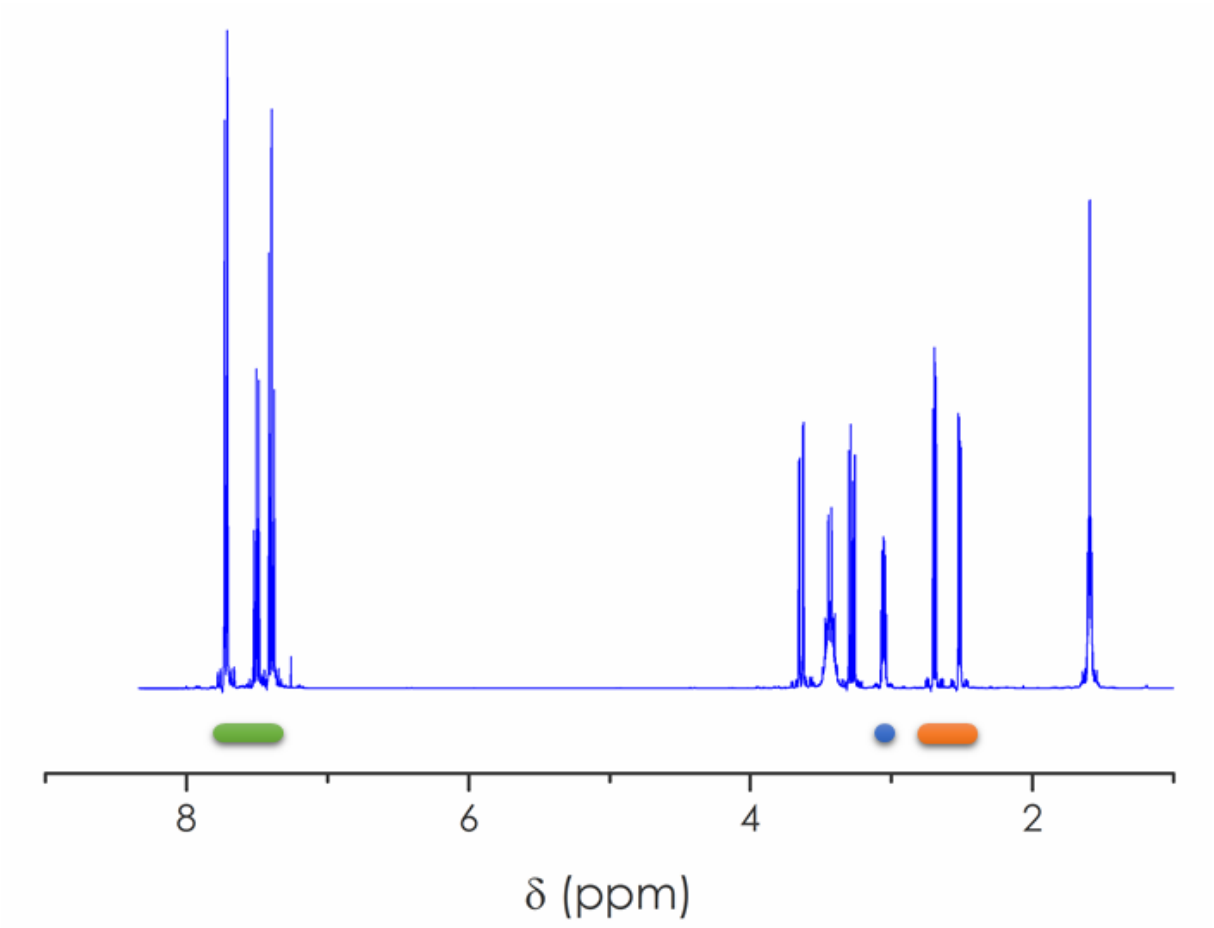

50 to 70 mg of BDGE and 50 to 80 mg of benzophenone were dissolved in deuterated chloroform. ^1H NMR spectra were integrated in the 7.87-7.28 ppm range for benzophenone protons (10 H), in the 3.19-2.97 ppm range for CH oxirane and in the 2.82-2.45 range for CH_2 oxirane. EEW was calculated as follows :

$$EEW_{CH} = \frac{m_{BDGE} \times \int_{7.28}^{7.87} benzophenone \times M_{benzophenone}}{10 \times m_{benzophenone} \times \int_{2.97}^{3.19} CH\ oxirane}$$

$$EEW_{CH_2} = \frac{2 \times m_{BDGE} \times \int_{7.28}^{7.87} benzophenone \times M_{benzophenone}}{10 \times m_{benzophenone} \times \int_{2.45}^{2.82} CH_2\ oxirane}$$

m_{BDGE} (mg)	$m_{benzophenone}$ (mg)	$\frac{\int_{2.97}^{3.19} CH\ oxirane}{\int_{7.28}^{7.87} benzophenone}$	$\frac{\int_{2.45}^{2.82} CH_2\ oxirane}{\int_{7.28}^{7.87} benzophenone}$	EEW_{CH}	EEW_{CH_2}
73.3	80.9	0.157	0.324	117	113
54.6	80.0	0.117	0.241	118	115
57.8	50.7	0.197	0.406	117	114
			Average EEW	**115 ± 4 g/eq**	

B. Experimental procedure for the determination of BDGE epoxy equivalent weight (EEW) by DSC

To confirm the EEW value obtained by NMR, a DSC study was performed. Thermosets of BDGE and succinic acid were made with different stoichiometric ratios. The T_g of the thermosets was measured by DSC, the maximum value corresponding to a acid/epoxy function ratio of 1:1, allowing to calculate the corresponding EEW, knowing the acid HEW (hydrogen equivalent weight). HEW of succinic acid is 59 g/eq.

The coarse acid powder was first crushed in a mortar to obtain a powder as thin as possible. Then it was mixed manually with the right amount of BDGE in a tube. The tube was sealed with a septum and cured overnight at 200 °C in an oven. The thermosets obtained were analysed by DSC (-100 to + 150 °C at 20 °C/min). The Tg was determined upon second heating ramp. The optimal ratio was 1:1, which confirmed the EEW determined by NMR.

$m_{succinic\ acid}$ *(mg)*	m_{BDGE} *(mg)*	*Ratio (based on NMR EEW)*	T_g *(°C)*
66.9	119	0.91	7.9
70.1	134.5	0.99	8
81.6	158.6	1.00	9.4
76.1	156	1.05	7.7
82.8	178.4	1.11	3.7
86.9	206.9	1.22	3.3

TPE-TAF / BDGE vitrimer characterizations

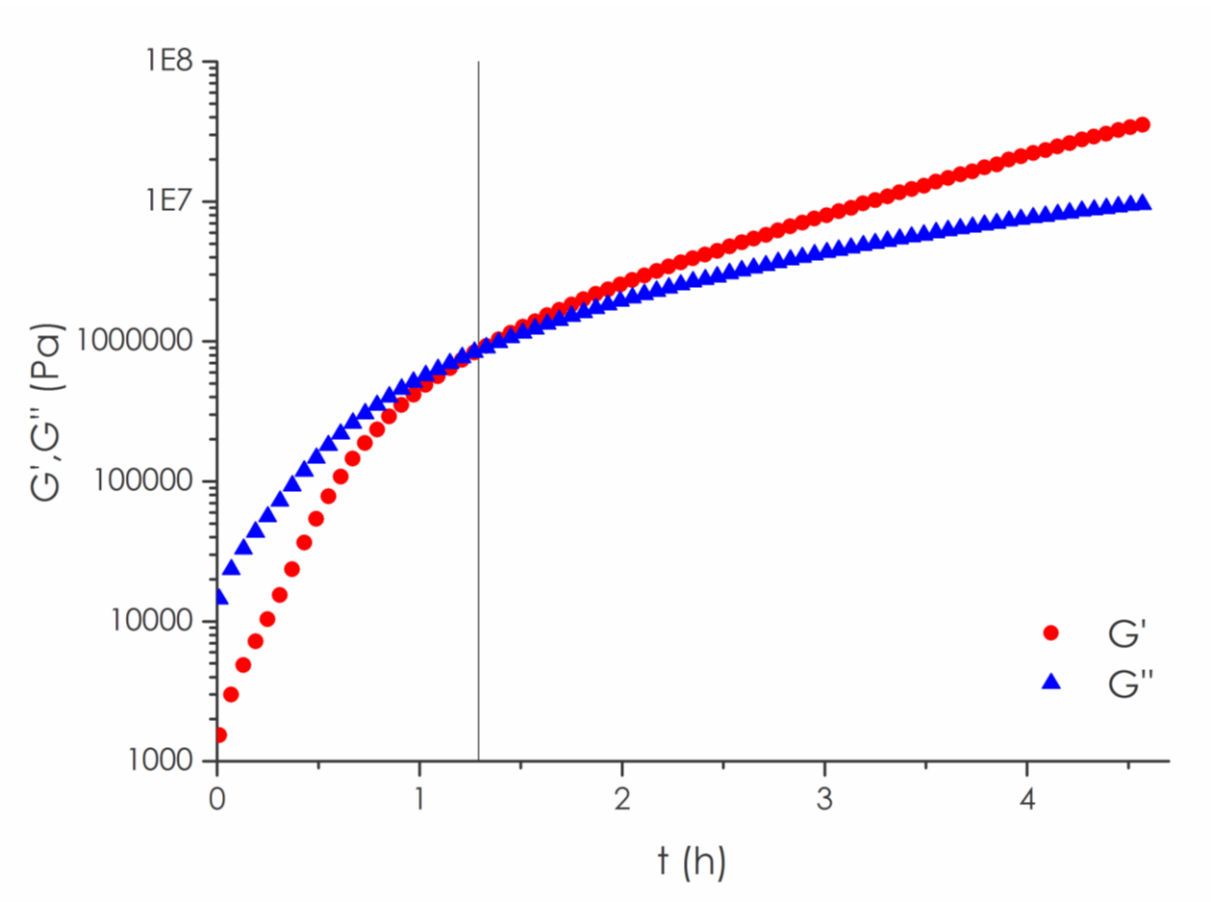

Figure S17. Determination of the gel time of the TPE-TAF/BDGE mixture at 20 °C by rheology

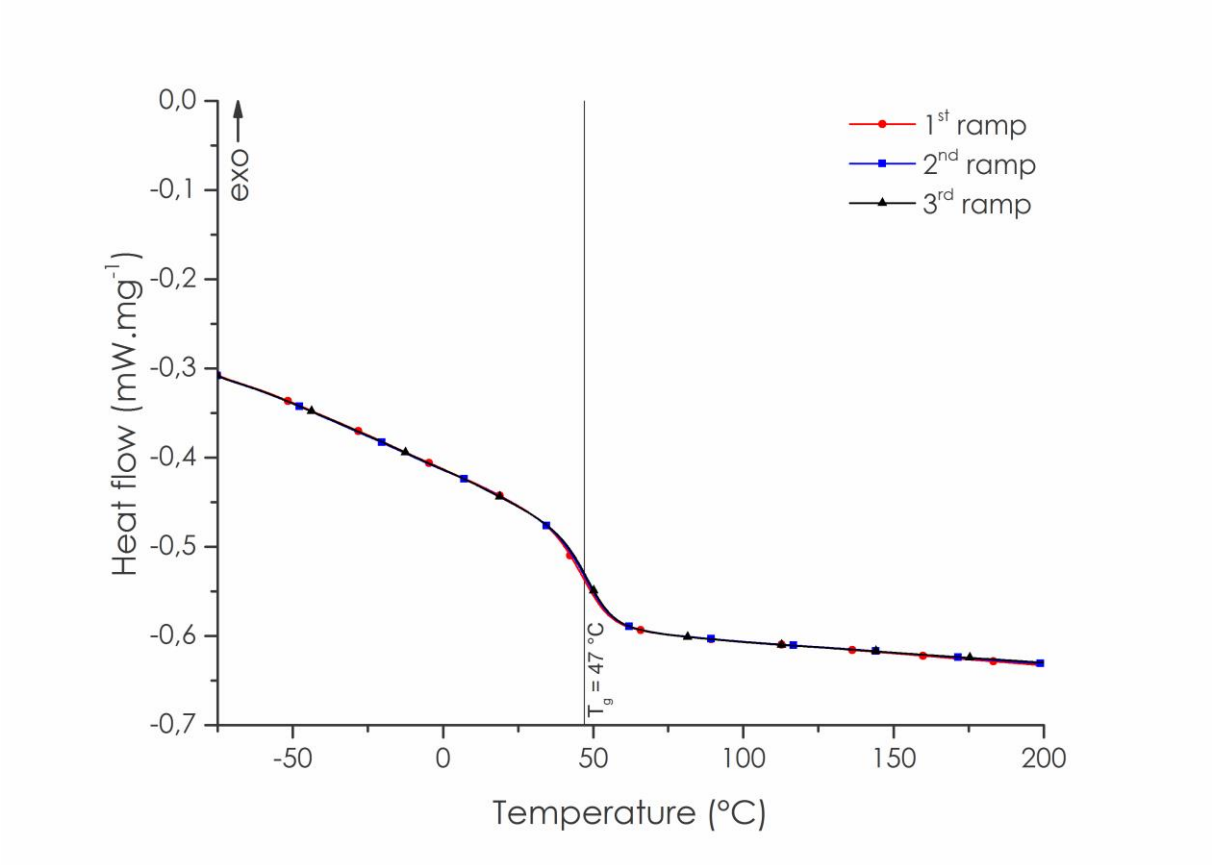

Figure S18. DSC thermogram of the TPE-TAF/BDGE material after curing 3 h at 150 °C (nitrogen, 20 °C.min-1)

Table S1. Gel content of the pristine TPE-TAF/BDGE material after curing 3 h at 150 °C in various solvents

Solvent	Acetone	THF	Toluene	Cyclohexane	DMSO	CH_2Cl_2	Acetonitrile
GC (%)	94	94	99	99	96	97	96

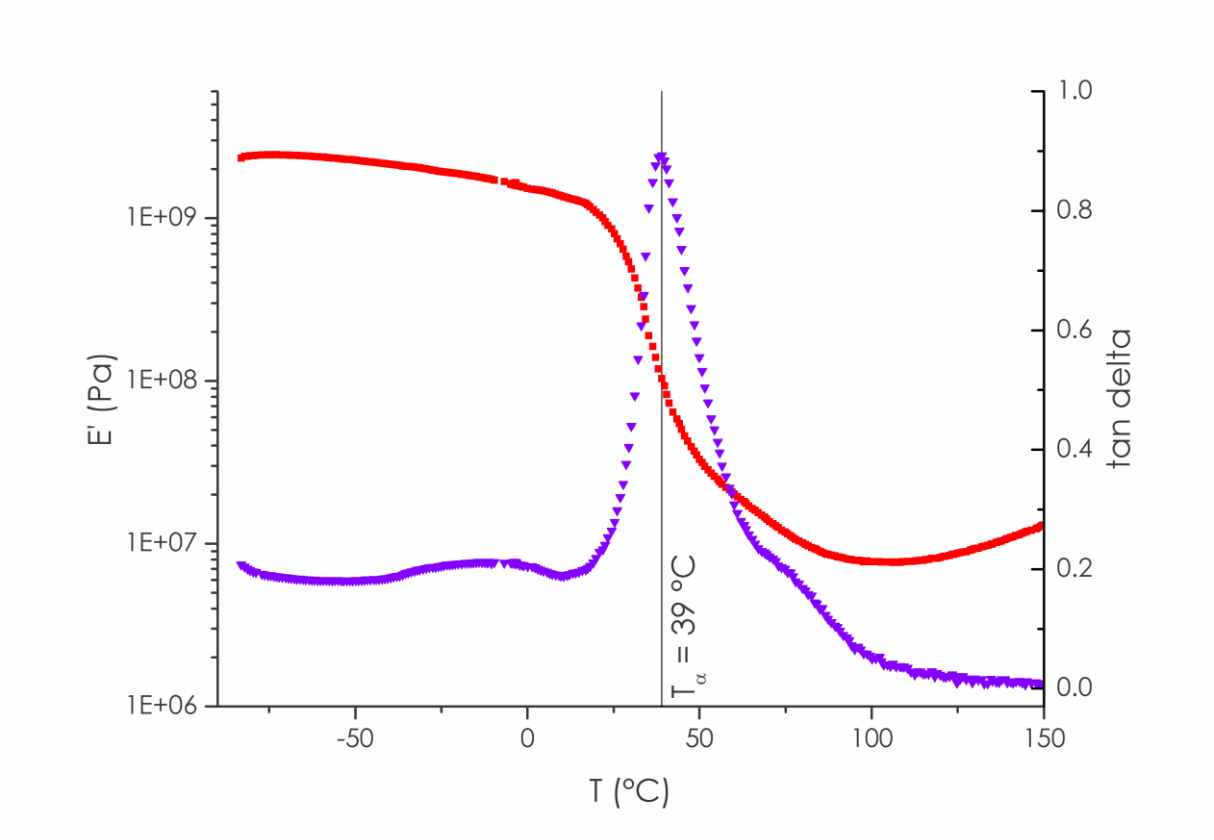

Figure S19. DMA thermogram of the pristine TPE-TAF/BDGE material after curing 3 h at 150 °C

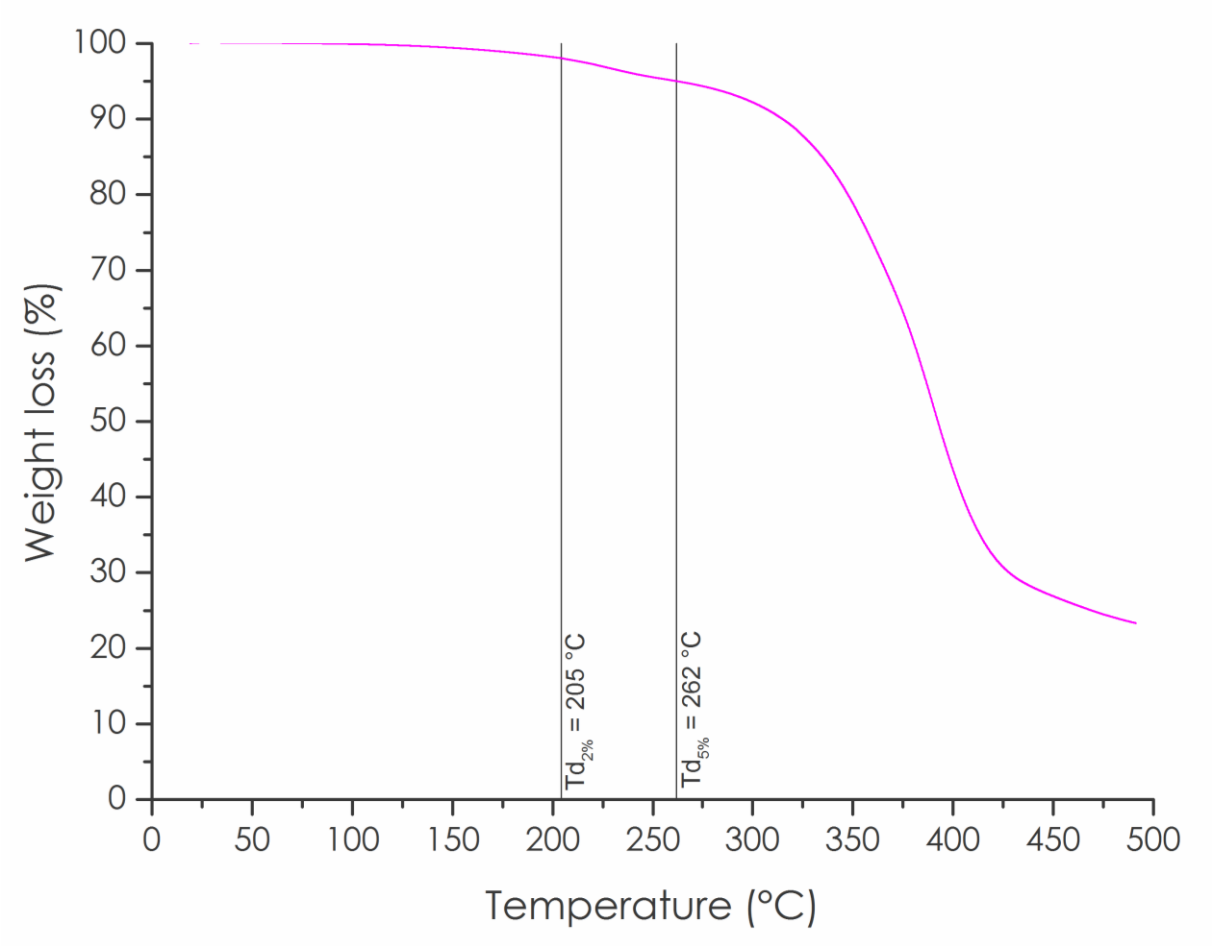

Figure S20. TGA thermogram of the pristine TPE-TAF/BDGE material after curing 3 h at 150 °C (air, 20 °C min^{-1})

Table S2. Equation and fitting parameters of the Kohlrausch-Williams-Watts stretched exponential model for the stress relaxation experiments

$\frac{G}{G_0} = e^{\left(\frac{-t}{\tau}\right)^{\beta}}$	T (°C)	170	180	190	200	210
	τ (s)	79692	43025	30376	20772	13097
	β	0.57	0.58	0.58	0.53	0.56
	R^2	0.99513	0.99975	0.99906	0.99804	0.99923

Note: for β = 1 the KWW expression is a Maxwell

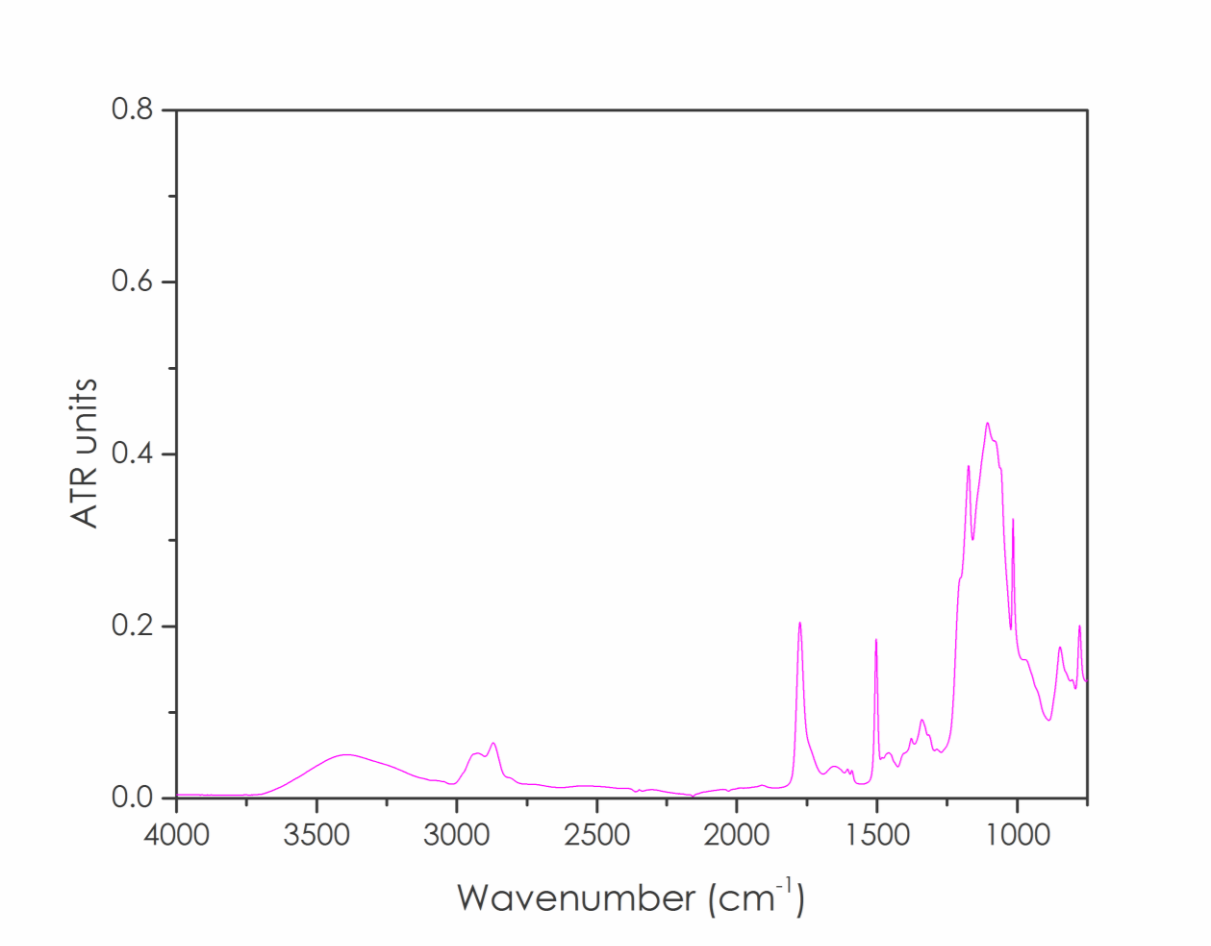

Figure S21. FTIR spectrum of the cured TPE-TAF/BDGE material

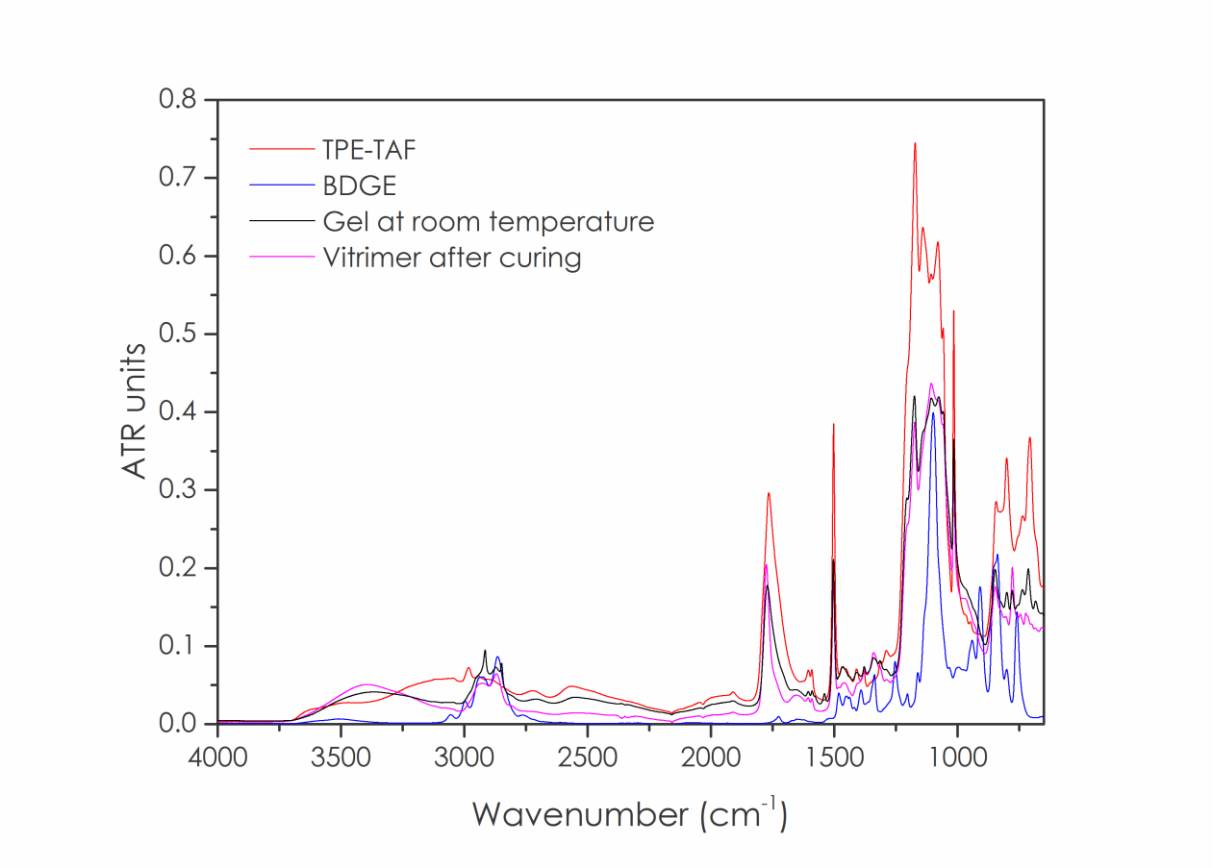

Figure S22. Stacked FTIR spectra of TPE-TAF, BDGE, material after gelation 4 days at room temperature and TPE-TAF/BDGE material after curing 3 h at 150 °C

ANNEXES B : ANNEXES AU CHAPITRE III

Supplementary Material to "Synthesis of a transesterification vitrimer activated by fluorine from an α,α-difluoro carboxylic acid and a diepoxy"

Florian Cuminet,[a] Sylvain Caillol,[a] Éric Dantras,[b] Éric Leclerc,[a] Cédric Totée,[c] Olivier Guille[d] and Vincent Ladmiral[a]

a ICGM, Univ Montpellier, CNRS, ENSCM, Montpellier, France
b CIRIMAT, Université Toulouse 3 Paul Sabatier, Physique des Polymères, 118 Route de Narbonne, 31062 Toulouse, France
c ICGM, PAC, Univ Montpellier, CNRS, ENSCM, Montpellier, France
d Institut d'Electronique et Systèmes (IES) UMR 5214, Université de Montpellier/CNRS, 34095, Montpellier, France

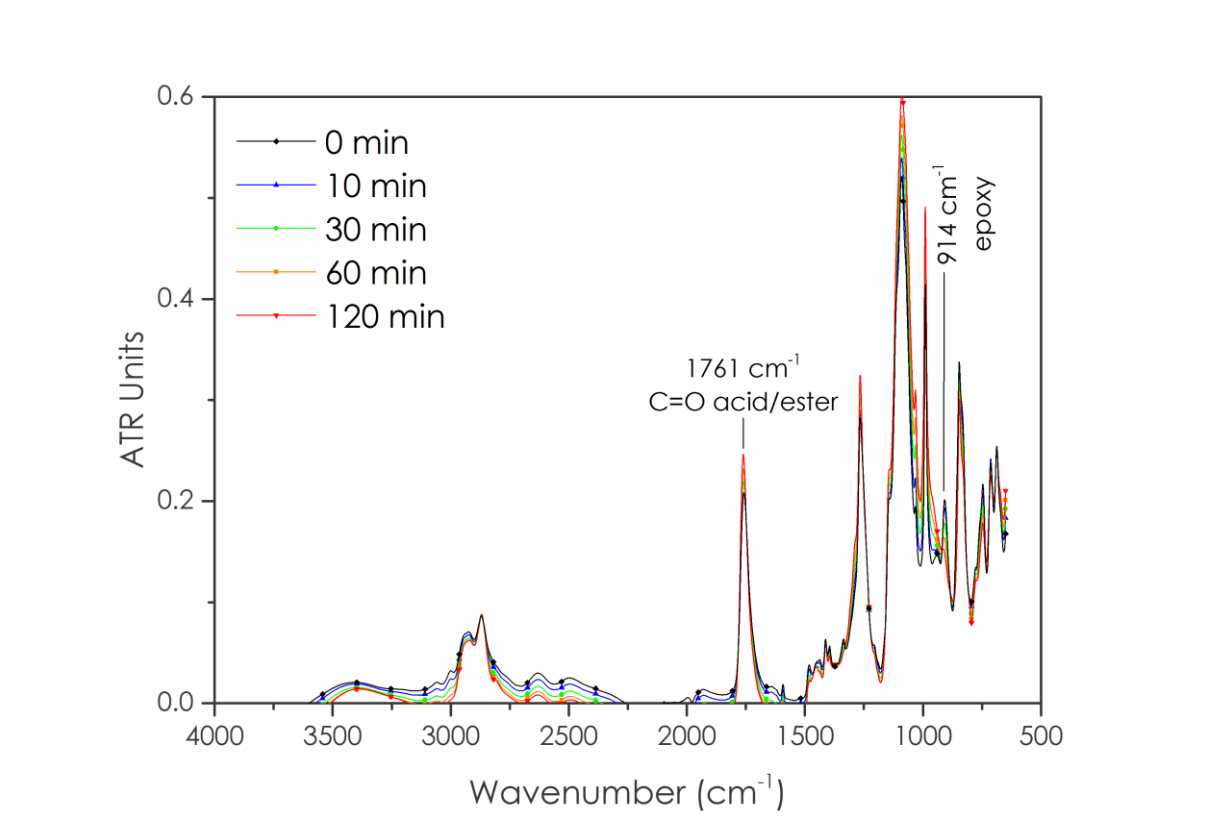

Figure S1. ATR-FTIR monitoring of the P-DAF/BDGE mixture reaction at room temperature over time

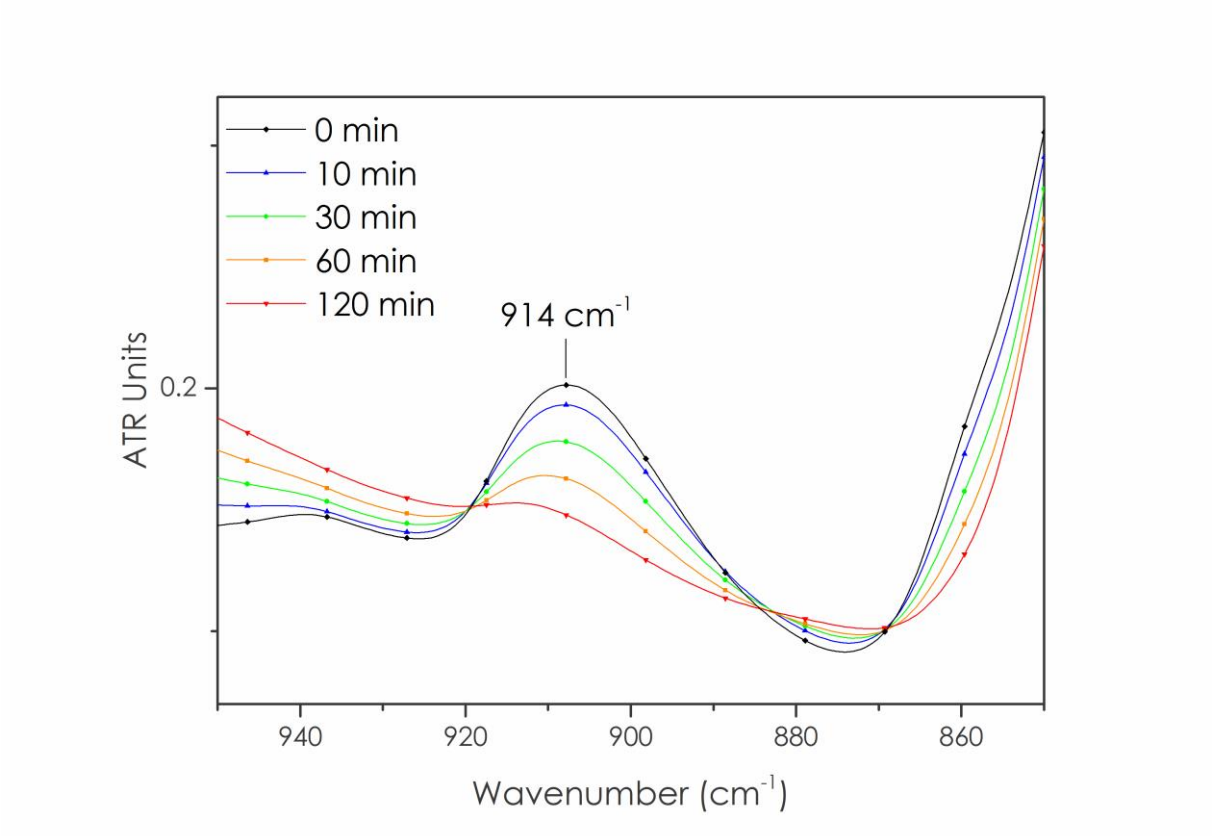

Figure S2. Evolution of the epoxy ATR-FTIR band at 914 cm^{-1} of the P-DAF/BDGE binary mixture over time at room temperature (ca. 20 °C)

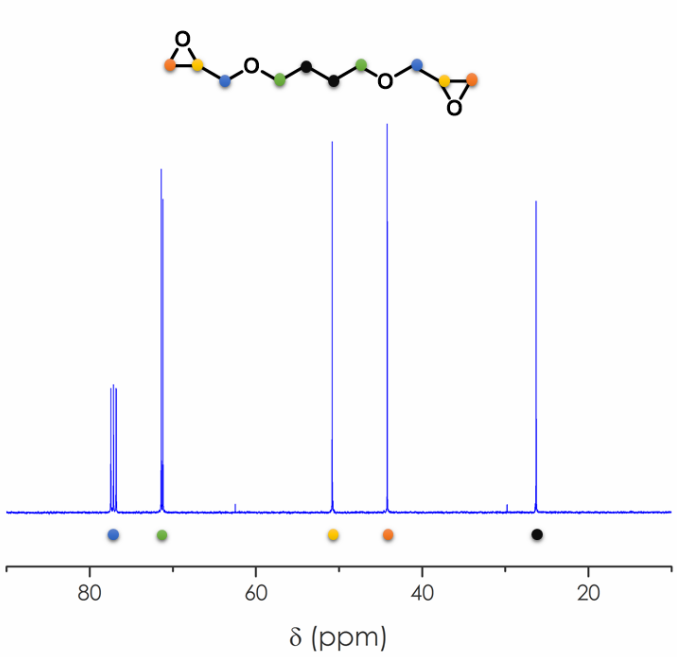

Figure S3. ^{13}C NMR spectrum of commercial butanediol diglycidyl ether (BDGE) in $CDCl_3$

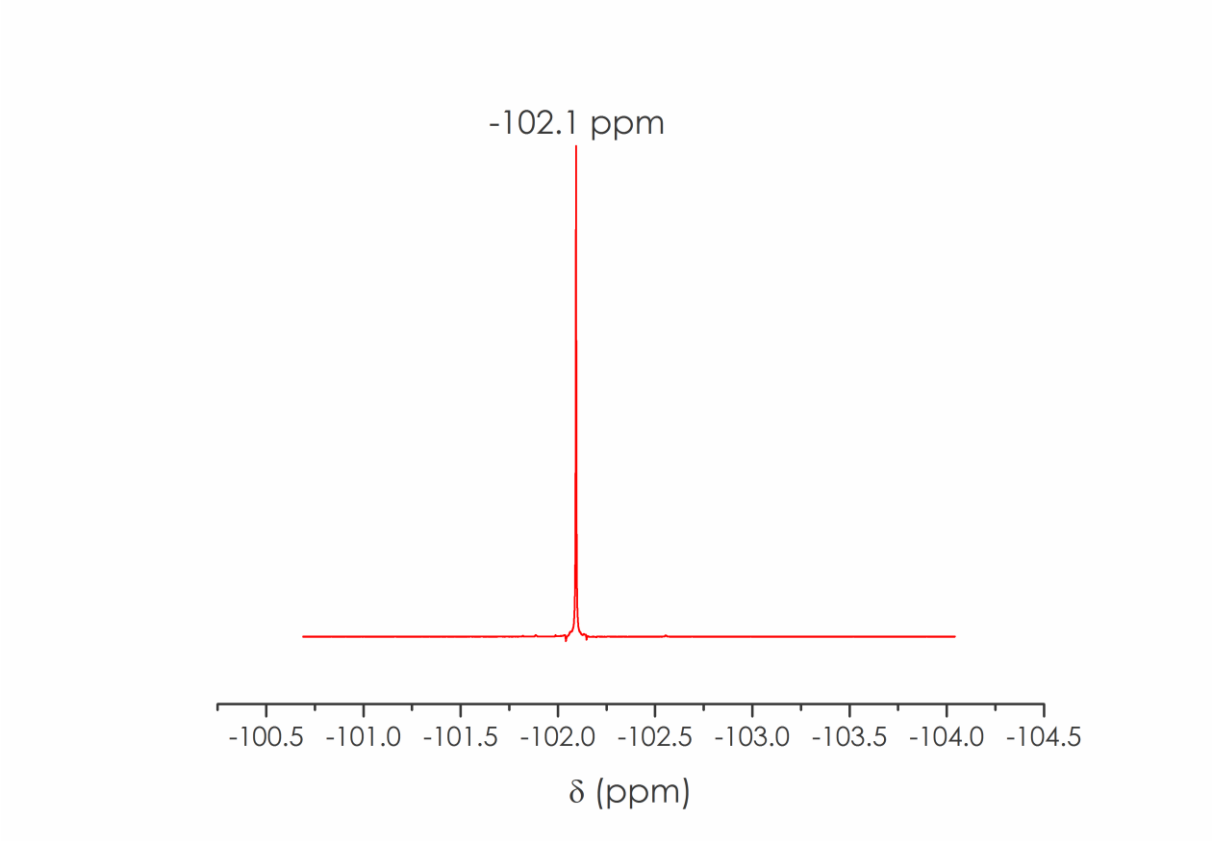

Figure S4. ^{19}F NMR spectrum of P-DE in DMSO-d_6

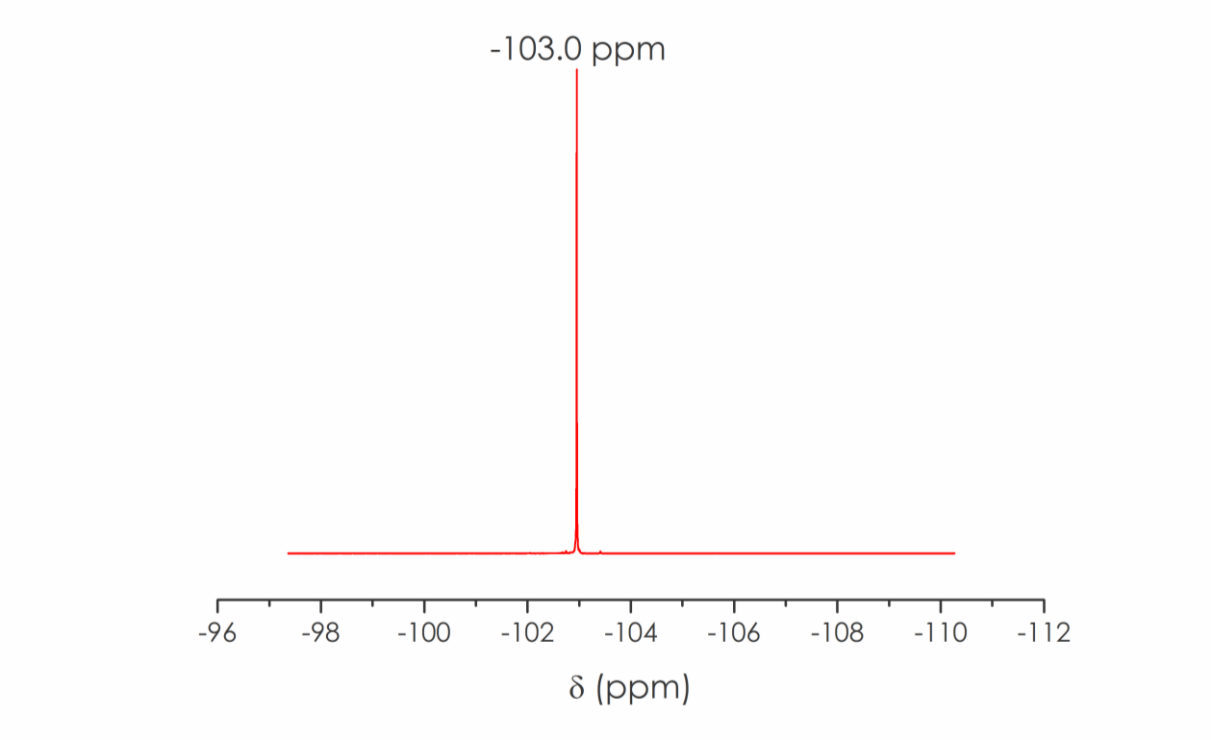

Figure S5. ^{19}F NMR spectrum of P-DAF in DMSO-d_6

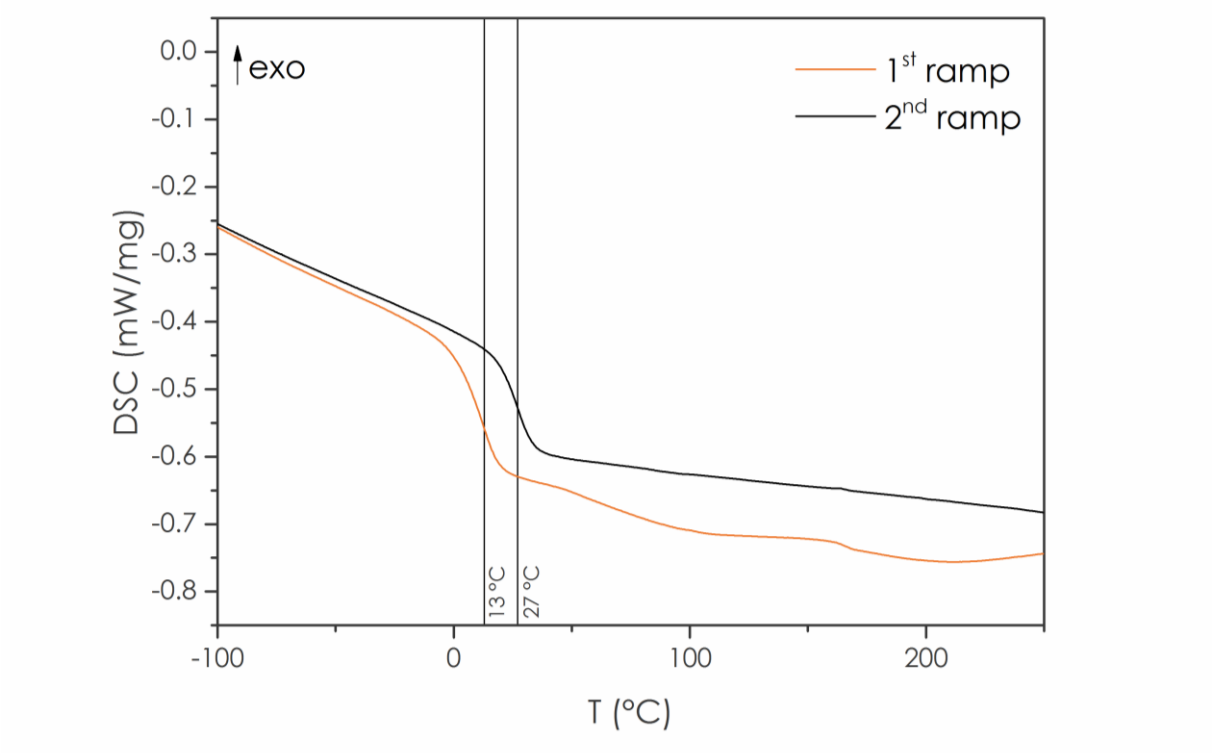

Figure S6. DSC thermograms of the BDGE/P-DAF after gelation at room temperature. Two consecutive ramps from -100 °C to +250 °C were applied

Table S1. Swelling Index and Gel Content of the BDGE/P-DAF gel after curing at room temperature in various solvents

	SI (%)	GC (%)
Acetone	99	54
Methanol	62	53
THF	162	59
Acetonitrile	35	55
DCM	168	80
Toluene	41	94
Cyclohexane	30	93

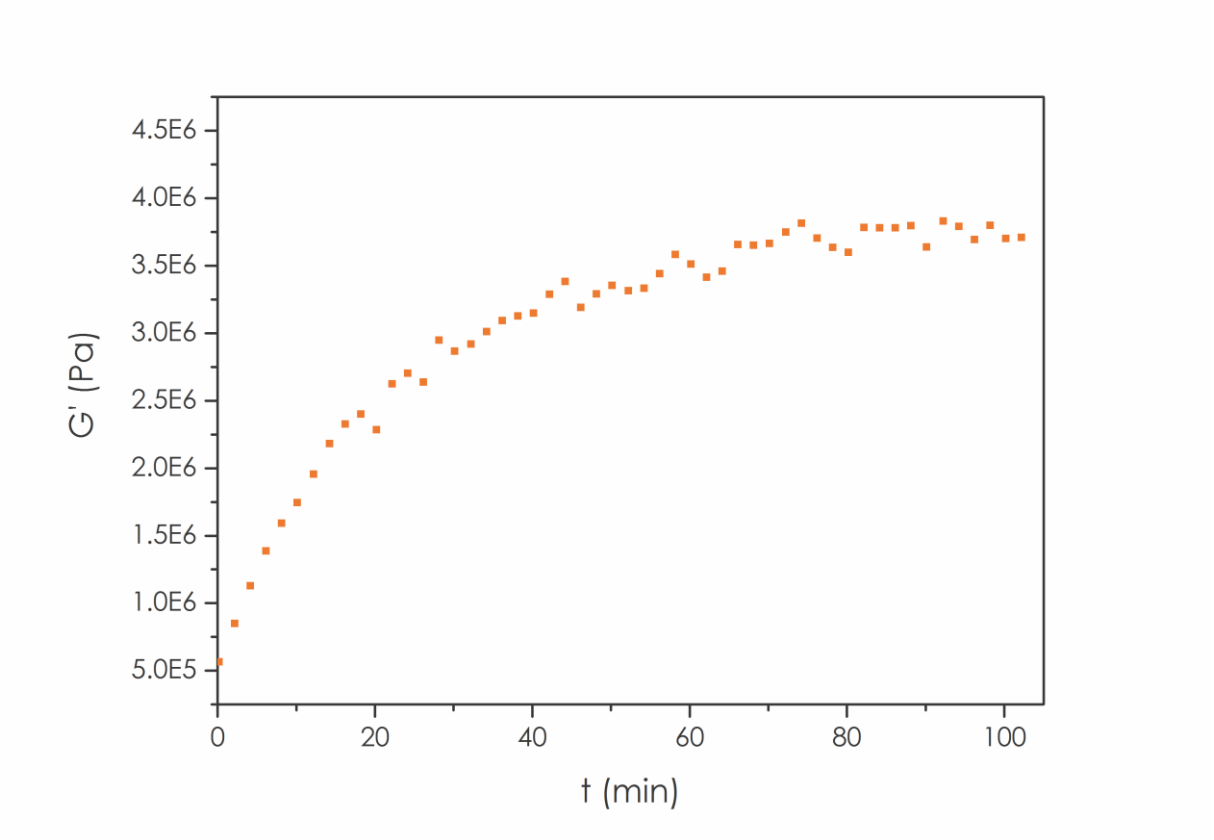

Figure S7. Monitoring of BDGE/P-DAF end of curing at 150 °C by dynamic mechanical analysis. A 0.1 % oscillation was applied every 2 minutes at an angular frequency of 1 rad/s and the storage modulus G' evolution with time was followed

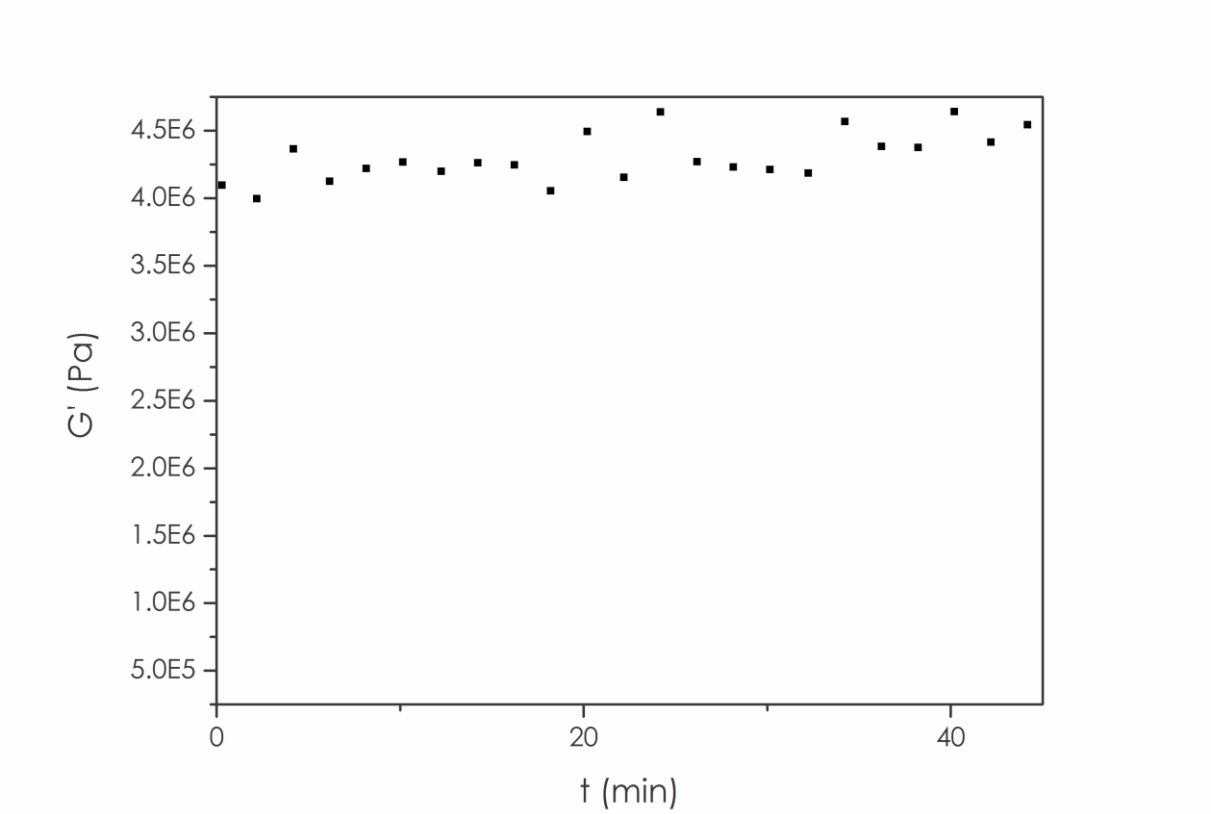

Figure S8. Check of complete curing of BDGE/P-DAF at 170 °C by dynamic mechanical analysis, after the curing step at 150 °C. A 0.1 % oscillation was applied every 2 minutes at an angular frequency of 1 rad/s and the storage modulus G' evolution with time was followed

Table S2. Swelling Index and Gel Content of the BDGE/P-DAF vitrimer after 3 h at 150 °C in various solvents

	SI (%)	GC (%)
Acetone	115 ± 9	97 ± 1
Ethanol	99 ± 21	97 ± 1
Water	159 ± 61	95 ± 4
THF	136 ± 11	96 ± 1
DMSO	237 ± 29	95.9 ± 0.4
Acetonitrile	109 ± 26	96.5 ± 0.9
DCM	148 ± 22	97.3 ± 0.2
Toluene	86 ± 68	99.0 ± 0.3
Cyclohexane	45 ± 16	99.3 ± 0.5

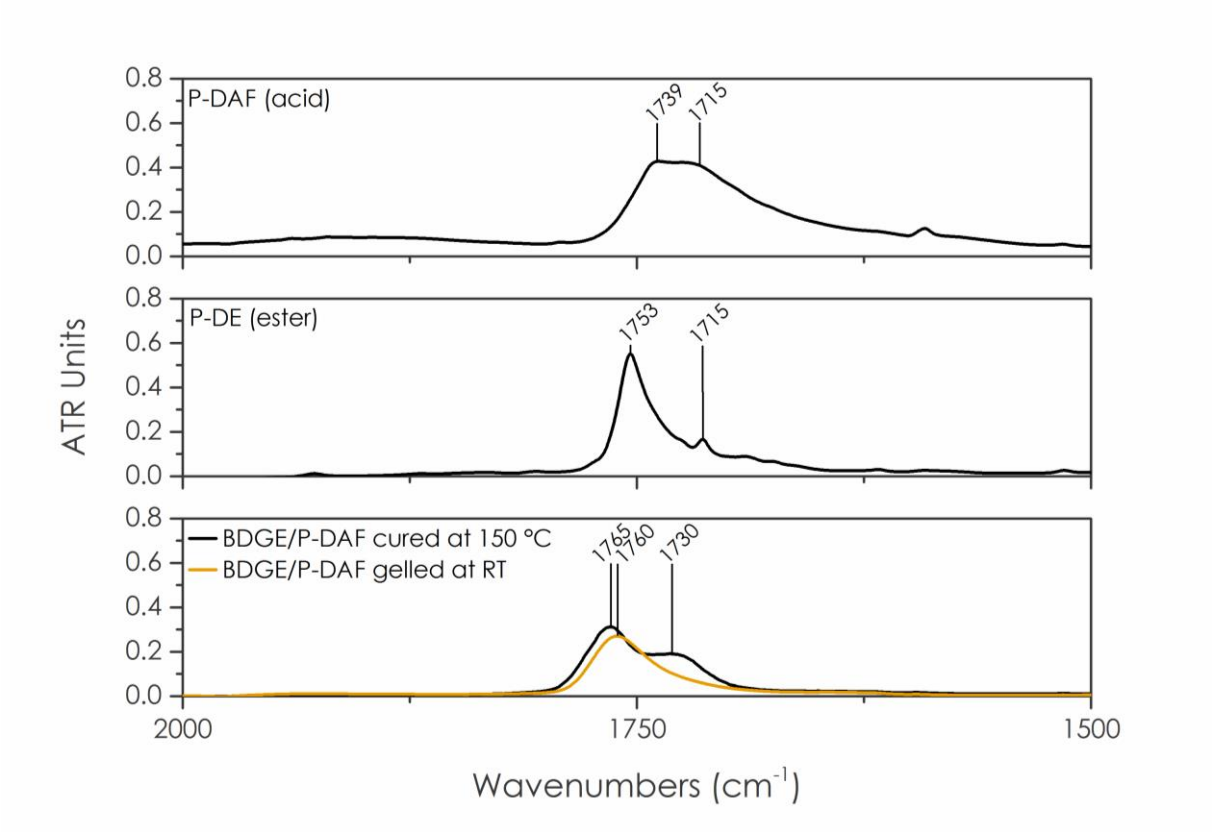

Figure S9. Comparison of the ATR-FTIR C=O bands of the P-DE (ester), the P-DAF (acid) and the BDGE/P-DAF material before and after the curing step at 150 °C

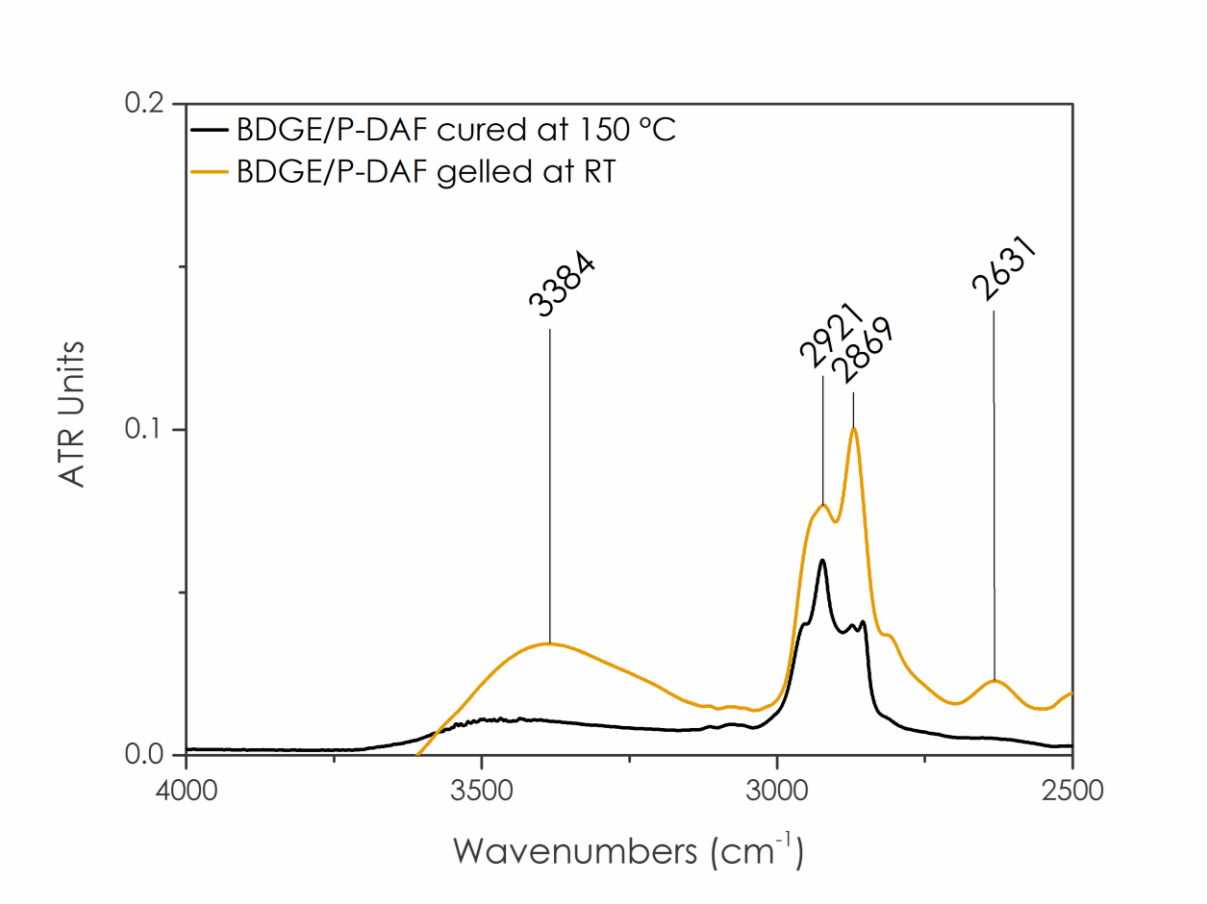

Figure S10. Zoom of the ATR-FTIR spectra on the 4000-2500 cm^{-1} area for BDGE/P-DAF before and after the curing step at 150 °C

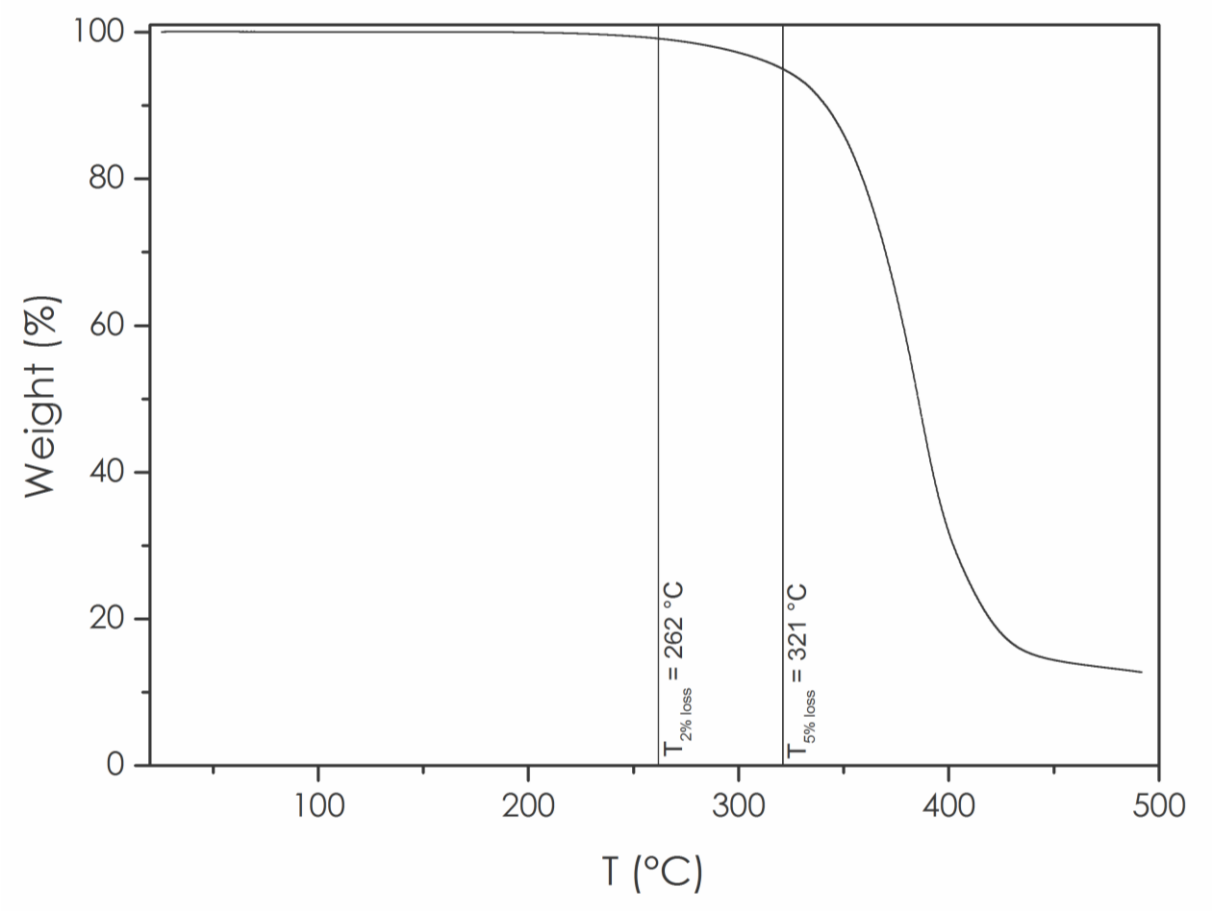

Figure S11. TGA thermogram of BDGE/P-DAF in air (20 °C/min)

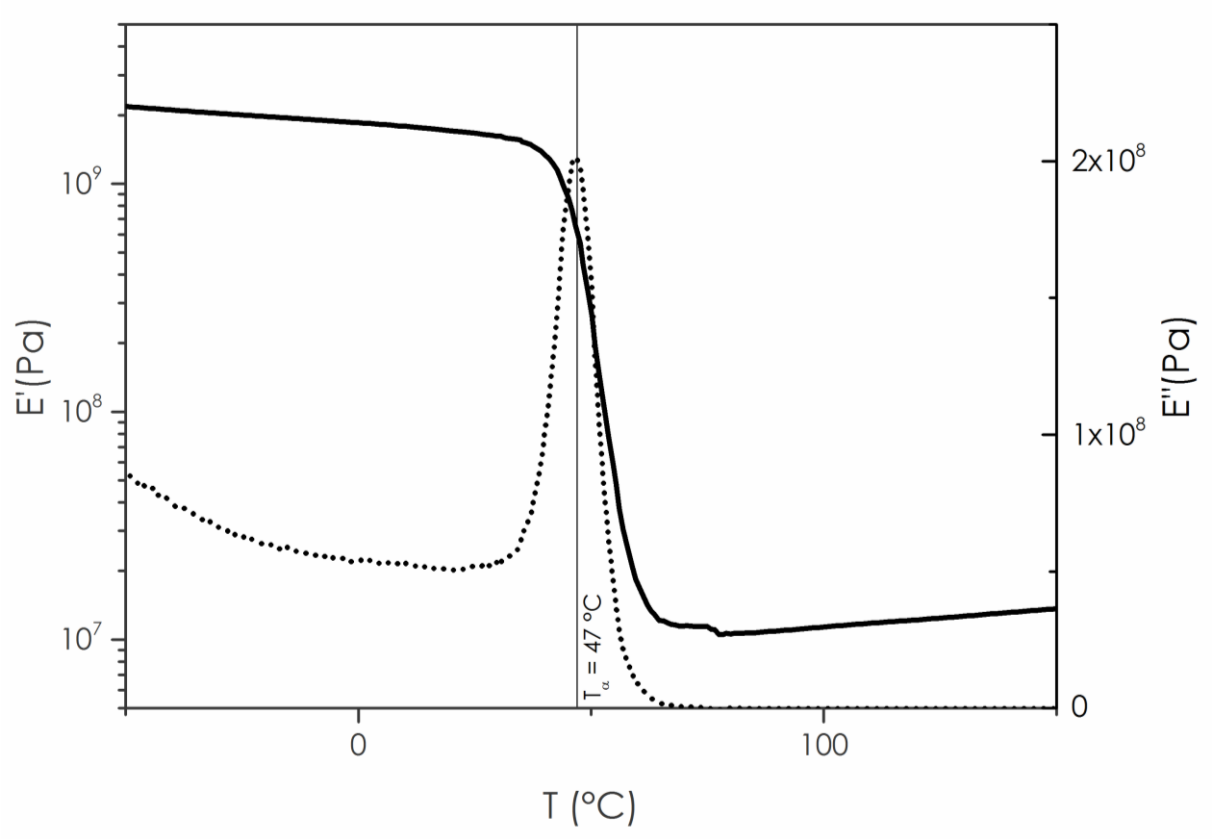

Figure S12. DMA thermograms of BDGE/P-DAF in air (3 °C/min, 1 Hz)

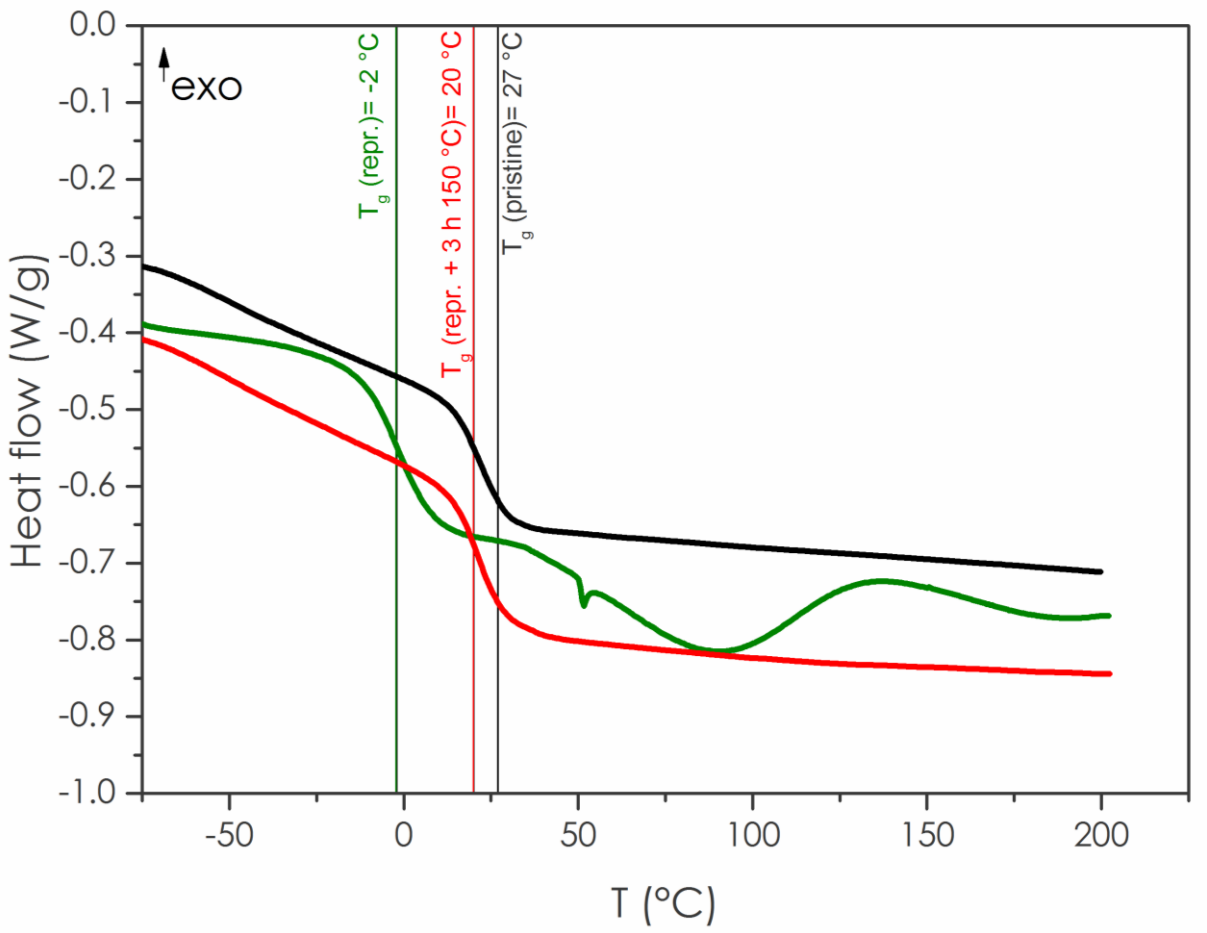

Figure S13. DSC thermograms of BDGE/P-DAF pristine (black), after reprocessing 1.5 h at 150 °C by compression molding (green), and after reprocessing by compression molding and annealing 3 h at 150 °C in an oven (red)

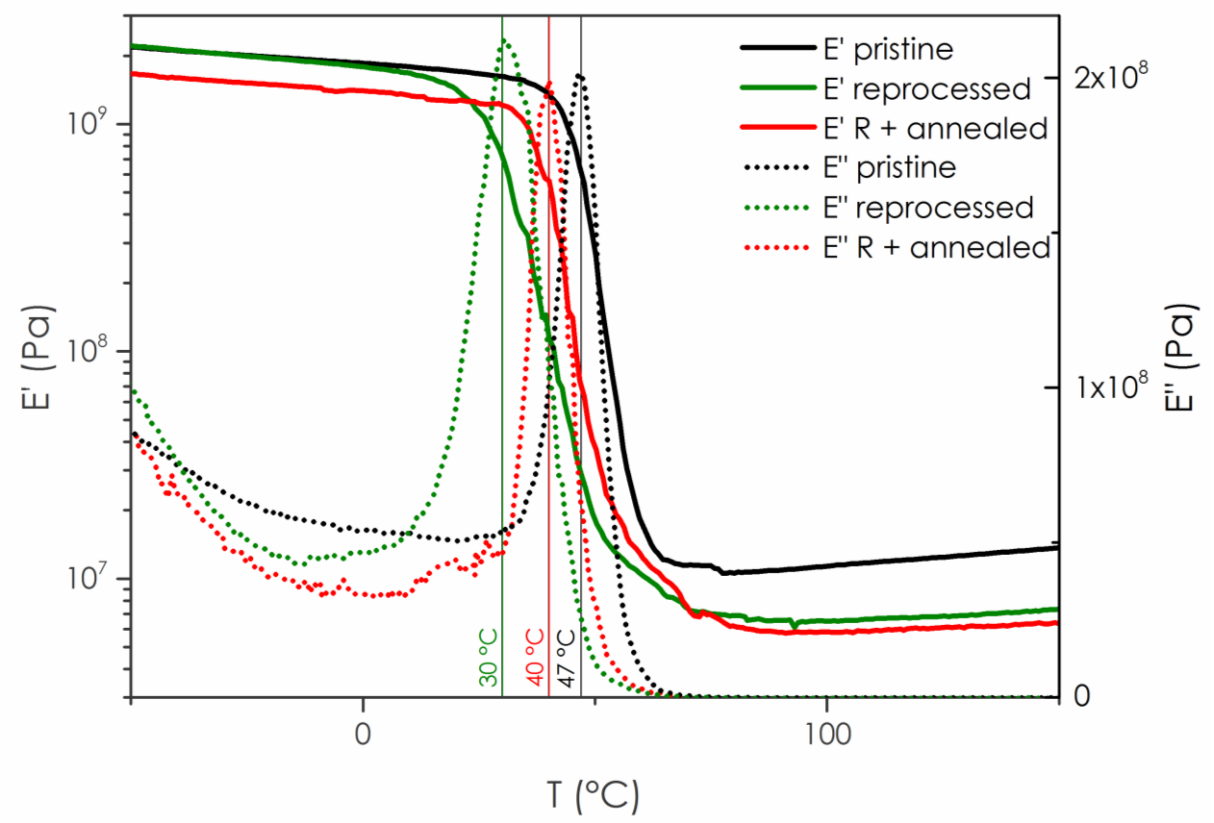

Figure S14. DMA thermograms (3°/min, 1 Hz) of BDGE/P-DAF pristine (black), after reprocessing 1.5 h at 150 °C by compression molding (green), and after reprocessing by compression molding and annealing 3 h at 150 °C in an oven (red)

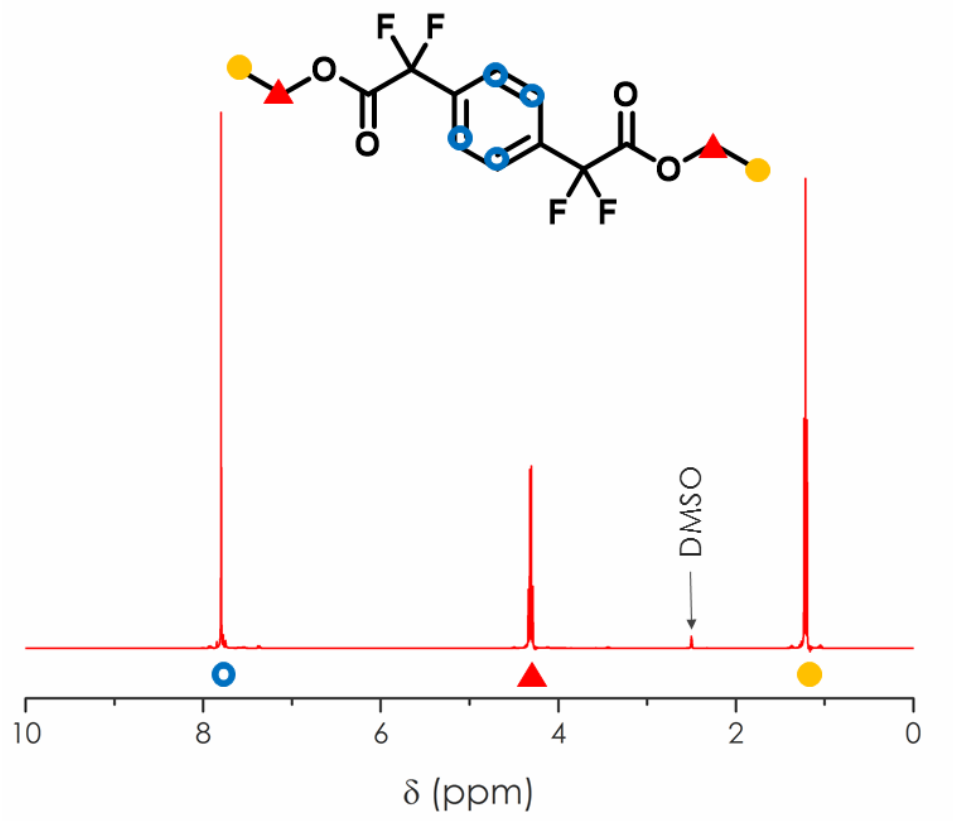

Figure S15. ^{1}H NMR spectrum of P-DE in DMSO-d_6

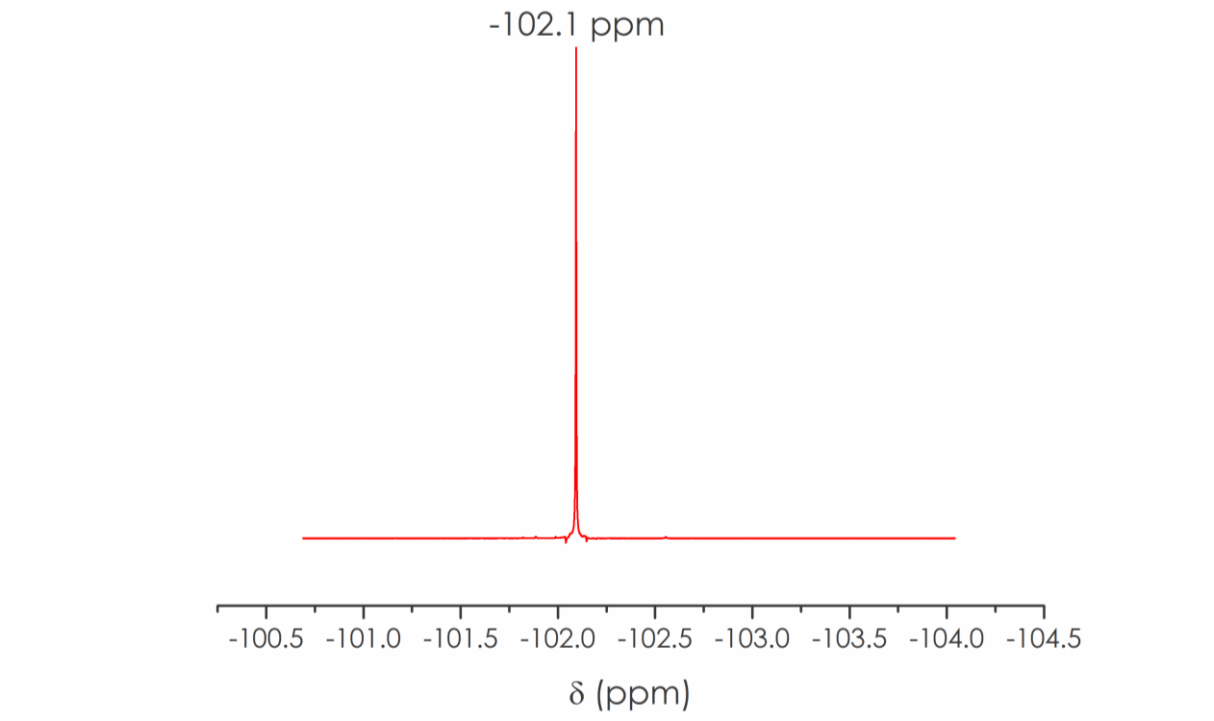

Figure S16. ^{19}F NMR spectrum of P-DE in DMSO-d_6

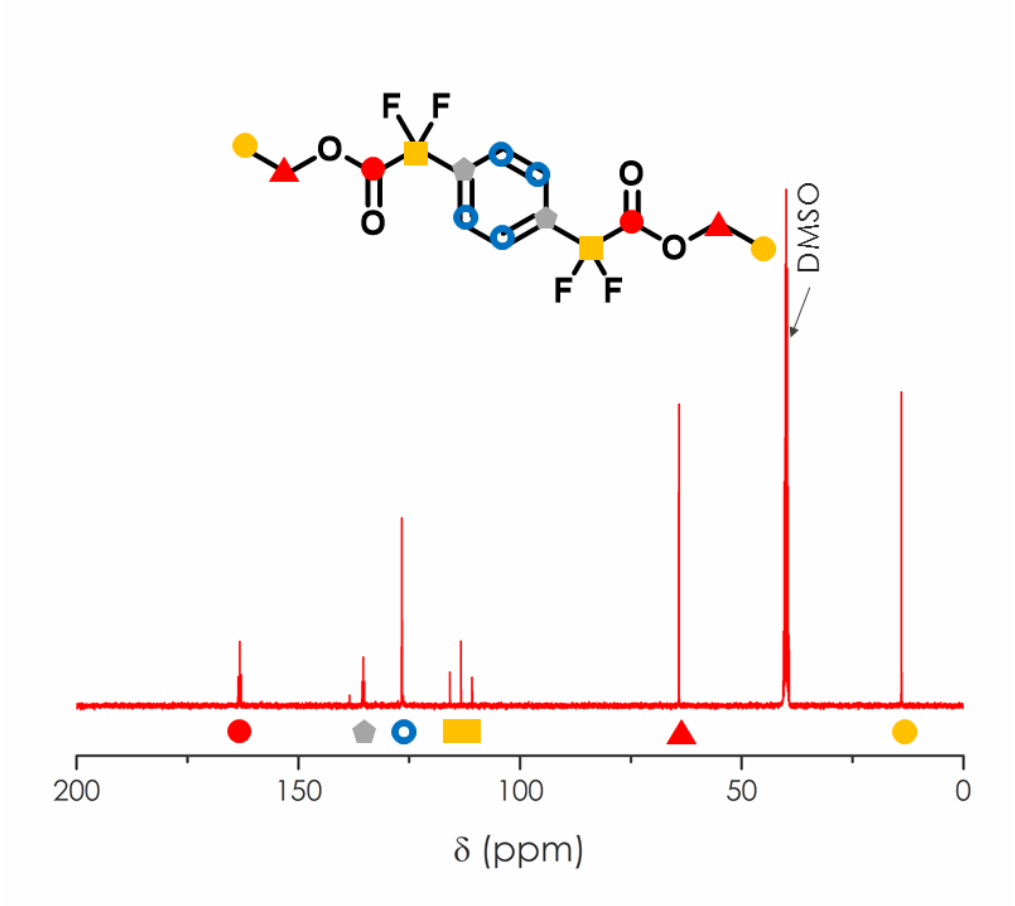

Figure S17. ^{13}C NMR spectrum of P-DE in DMSO-d_6

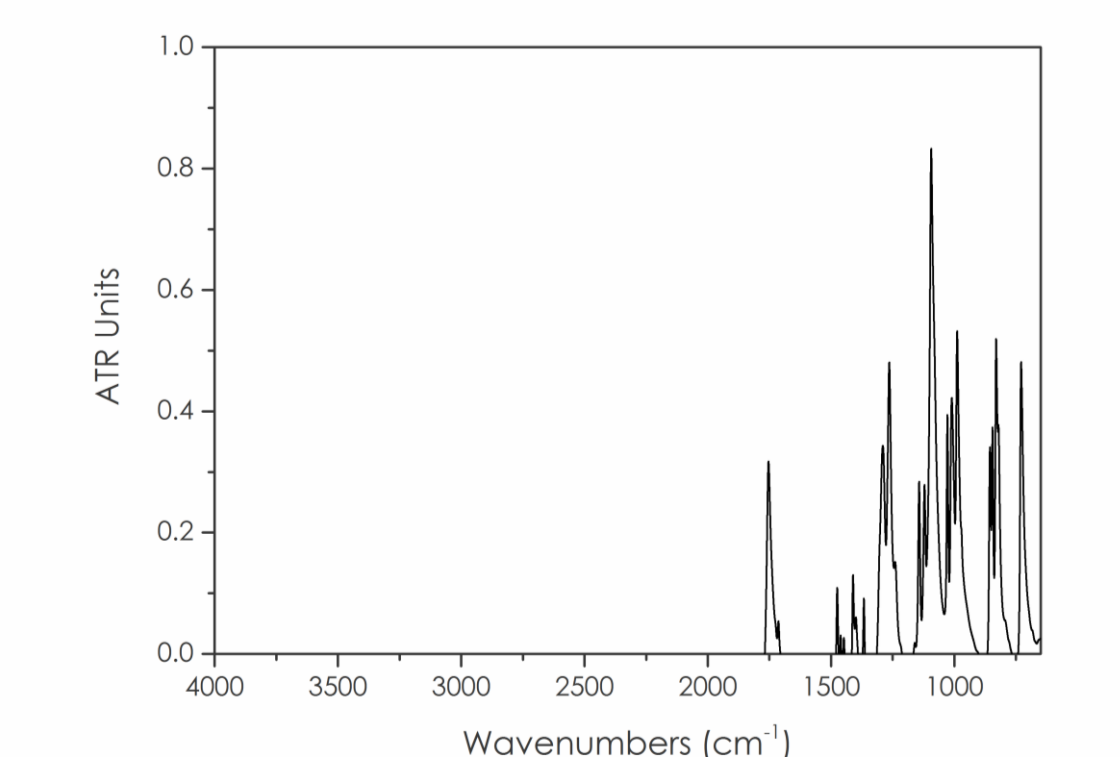

Figure S18. ATR-FTIR spectrum of P-DE

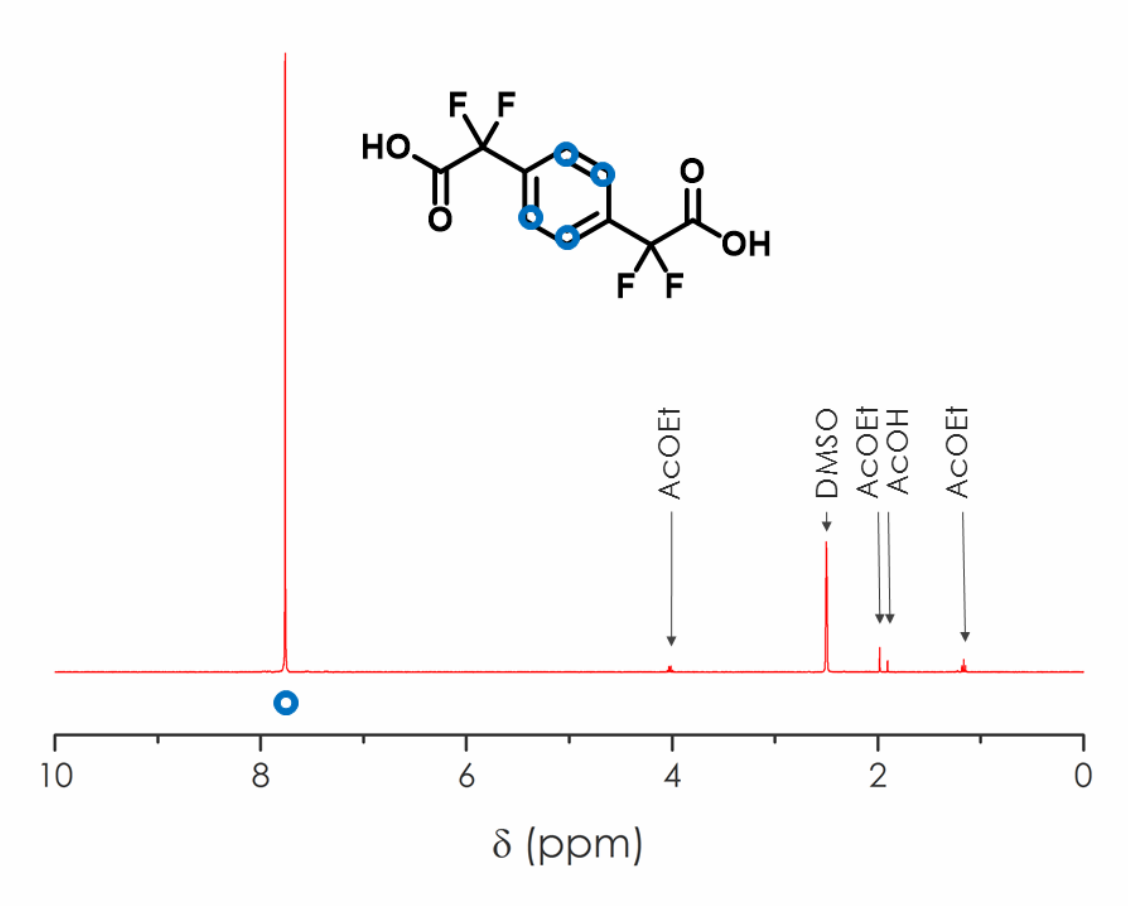

Figure S19. ^{1}H NMR spectrum of P-DAF in DMSO-d_6

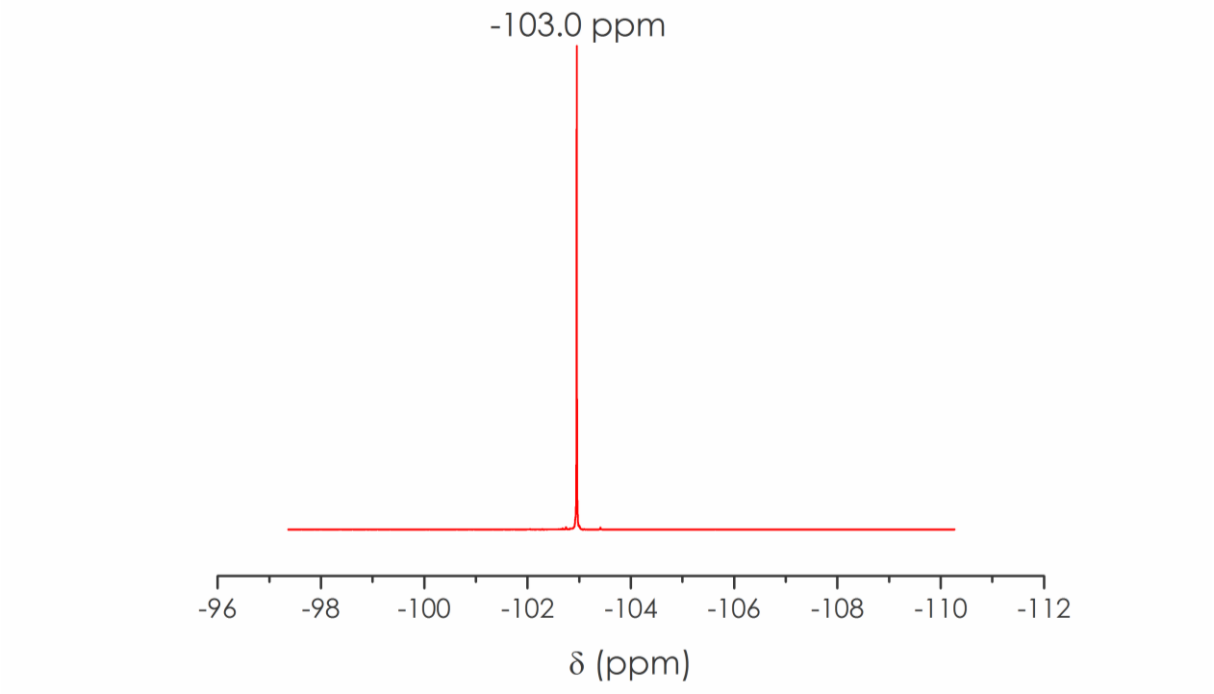

Figure S20. ^{19}F NMR spectrum of P-DAF in DMSO-d_6

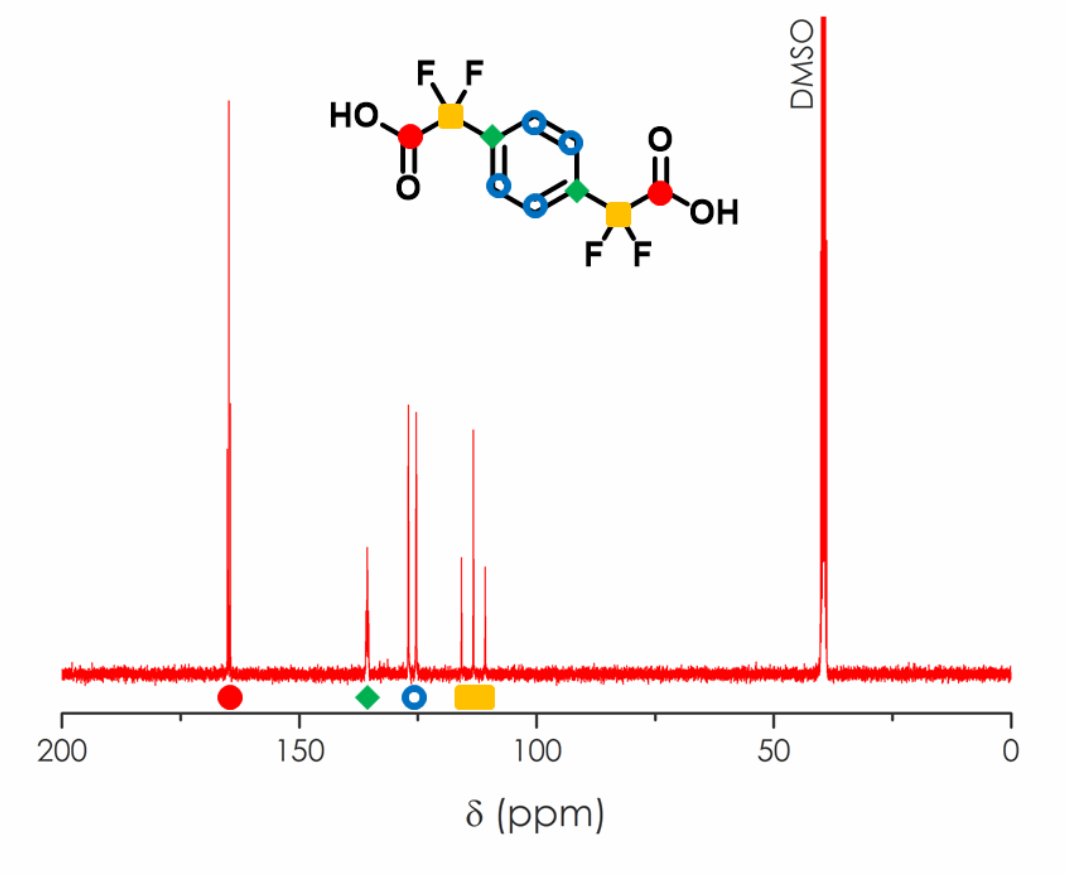

Figure S21. ^{13}C NMR spectrum of P-DAF in DMSO-d_6

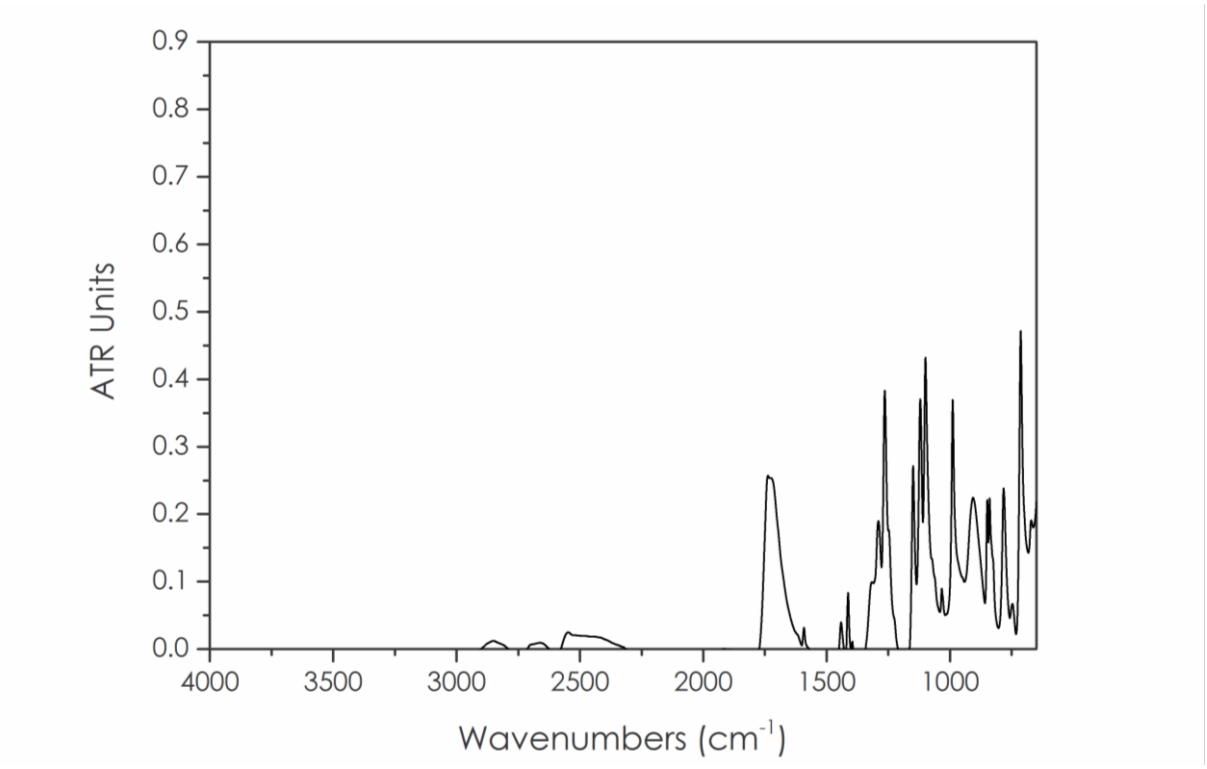

Figure S22. ATR-FTIR spectrum of P-DAF

ANNEXES C : ANNEXES AU CHAPITRE IV

Supplementary information to "From vineyards to 100 % resveratrol materials: α-CF_2 activation in biobased catalyst-free vitrimers"

Florian Cuminet,[a,b] Sébastien Lemouzy,[a] Éric Dantras,[b] Sylvain Caillol,[a] Éric Leclerc[a] and Vincent Ladmiral[a]

[a]ICGM, Univ Montpellier, CNRS, ENSCM, Montpellier, France
[b]CIRIMAT, Université Toulouse 3 Paul Sabatier, Physique des Polymères, 118 Route de Narbonne, 31062 Toulouse, France

Resveratrol α,α-difluorotriester "RvOEt" characterizations

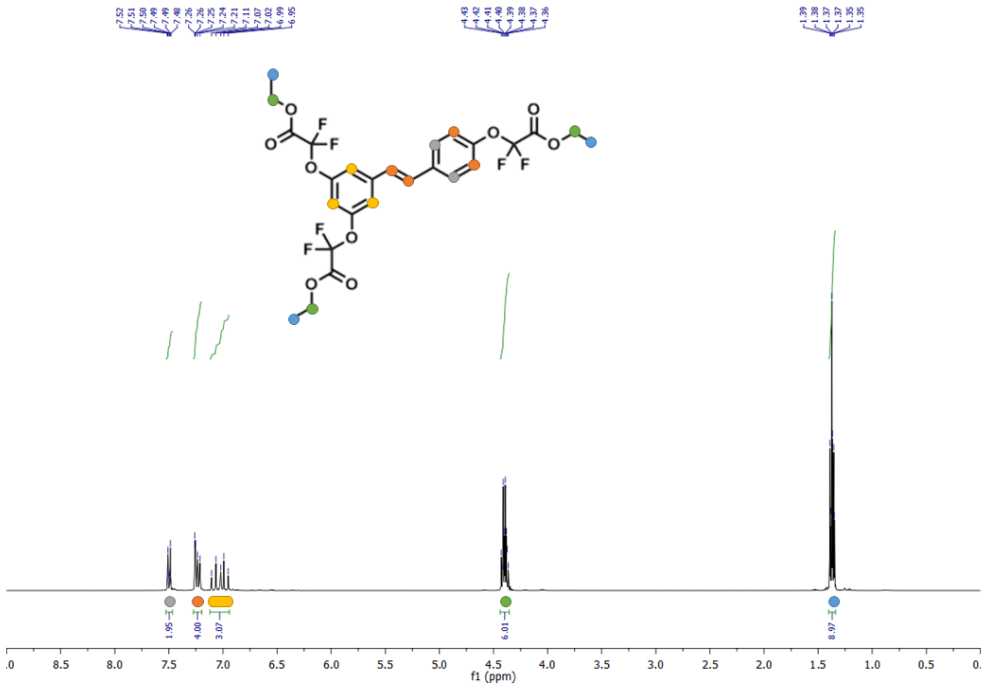

Figure S1. ^{1}H NMR spectrum of RvOEt in $CDCl_3$

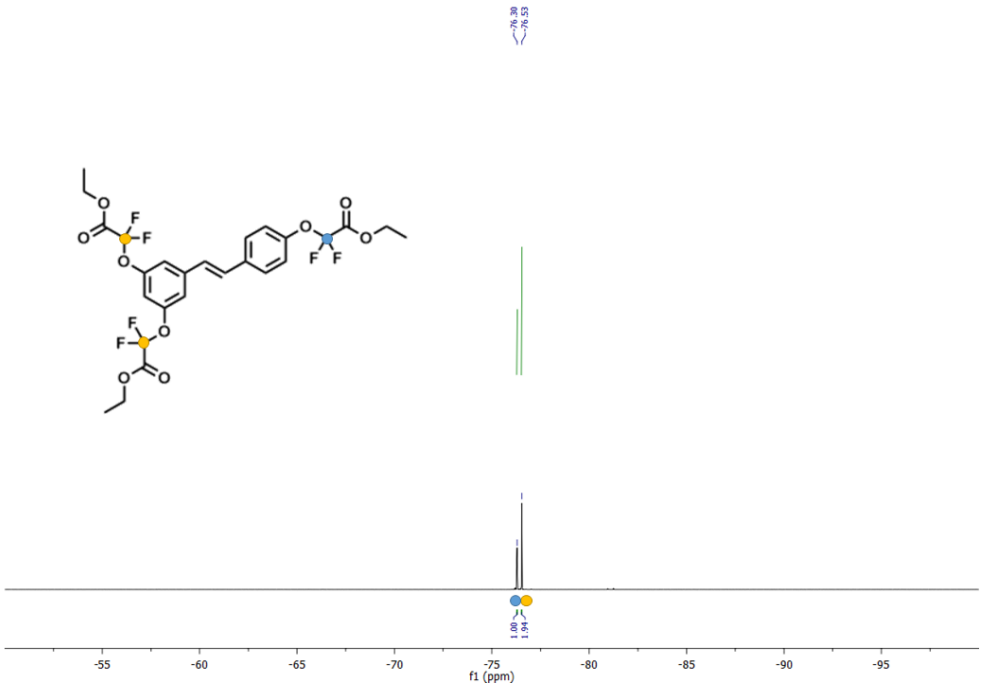

Figure S2. ^{19}F NMR spectrum of RvOEt in $CDCl_3$

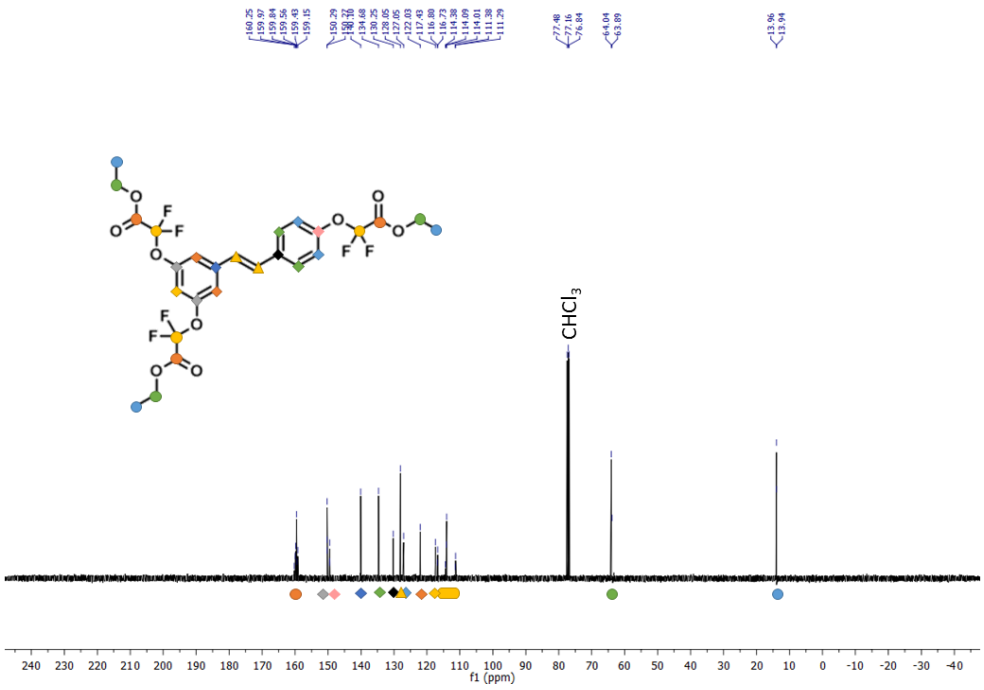

Figure S3. ^{13}C NMR spectrum of RvOEt in $CDCl_3$

Resveratrol α,α-difluorotriacid "RvOH-TAF" characterizations

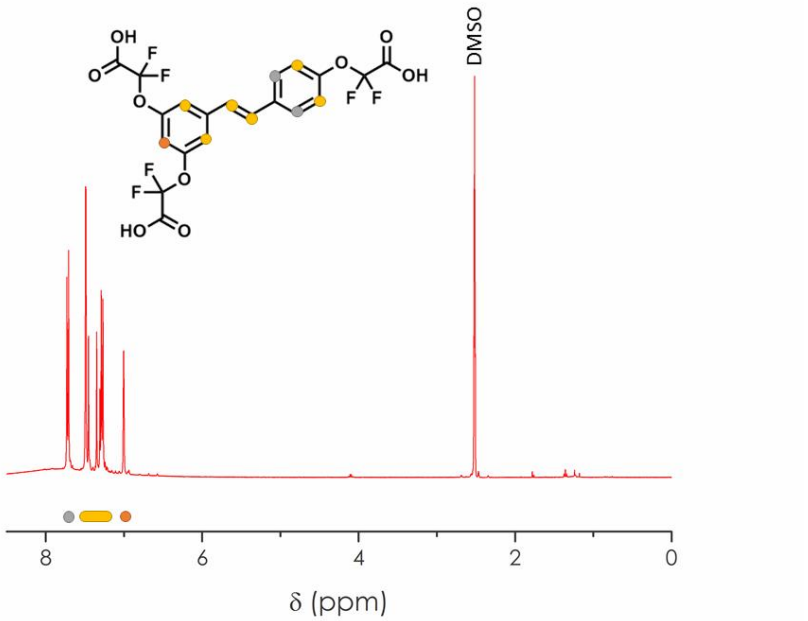

Figure S4. ^{1}H NMR spectrum of RvOH-TAF in DMSO-d_6

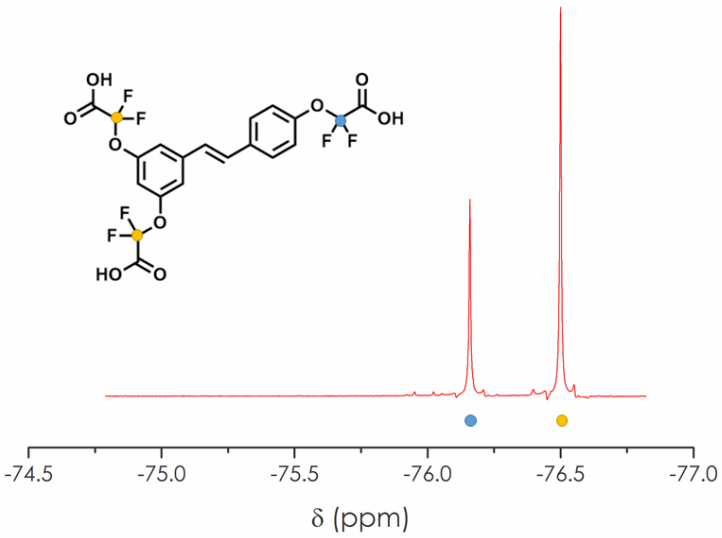

Figure S5. ^{19}F NMR spectrum of RvOH-TAF in DMSO-d_6

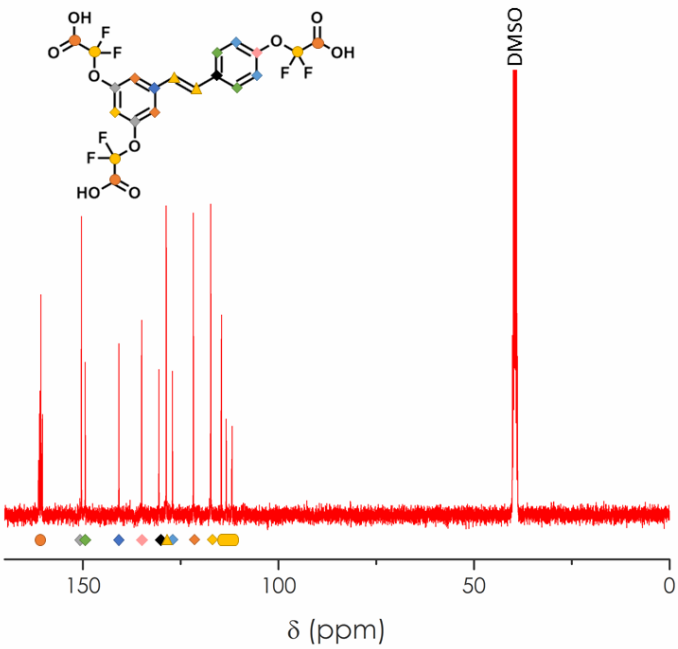

Figure S6. ^{13}C NMR spectrum of RvOH-TAF in DMSO-d_6

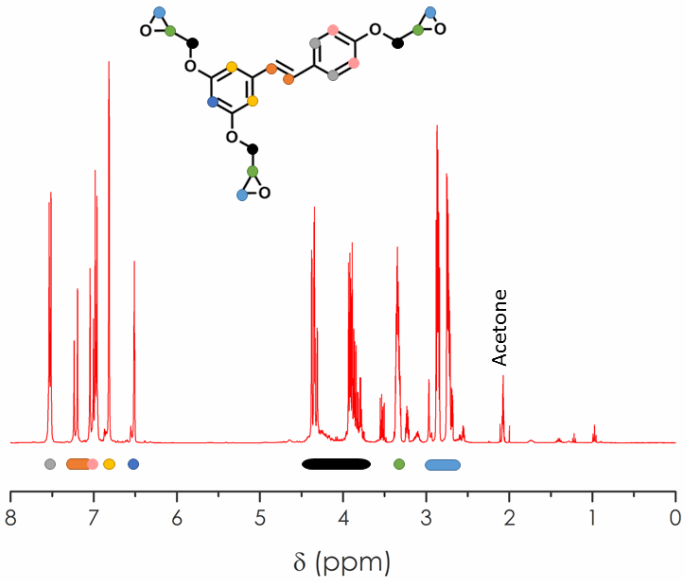

Figure S7. ^{1}H NMR spectrum of RvOGly in acetone-d_6

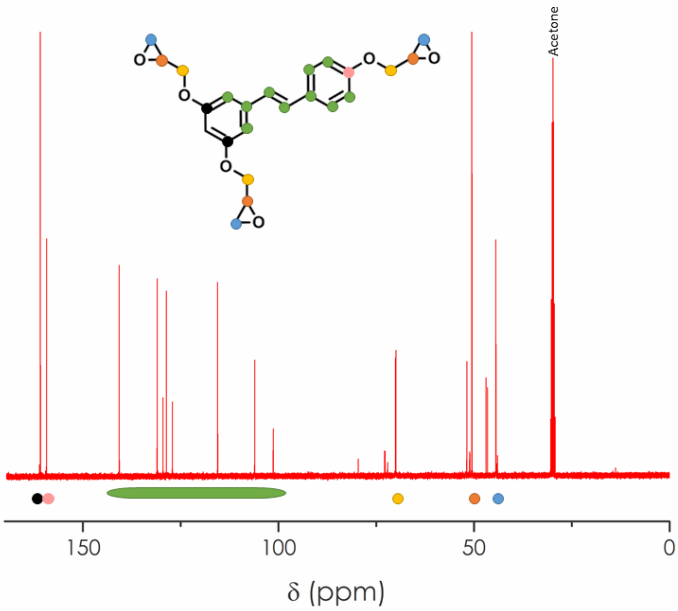

Figure S8. 13C NMR spectrum of RvOGly in acetone-d_6

A. Experimental procedure for the determination of RvOGly epoxy equivalent weight (EEW) by ^{1}H NMR

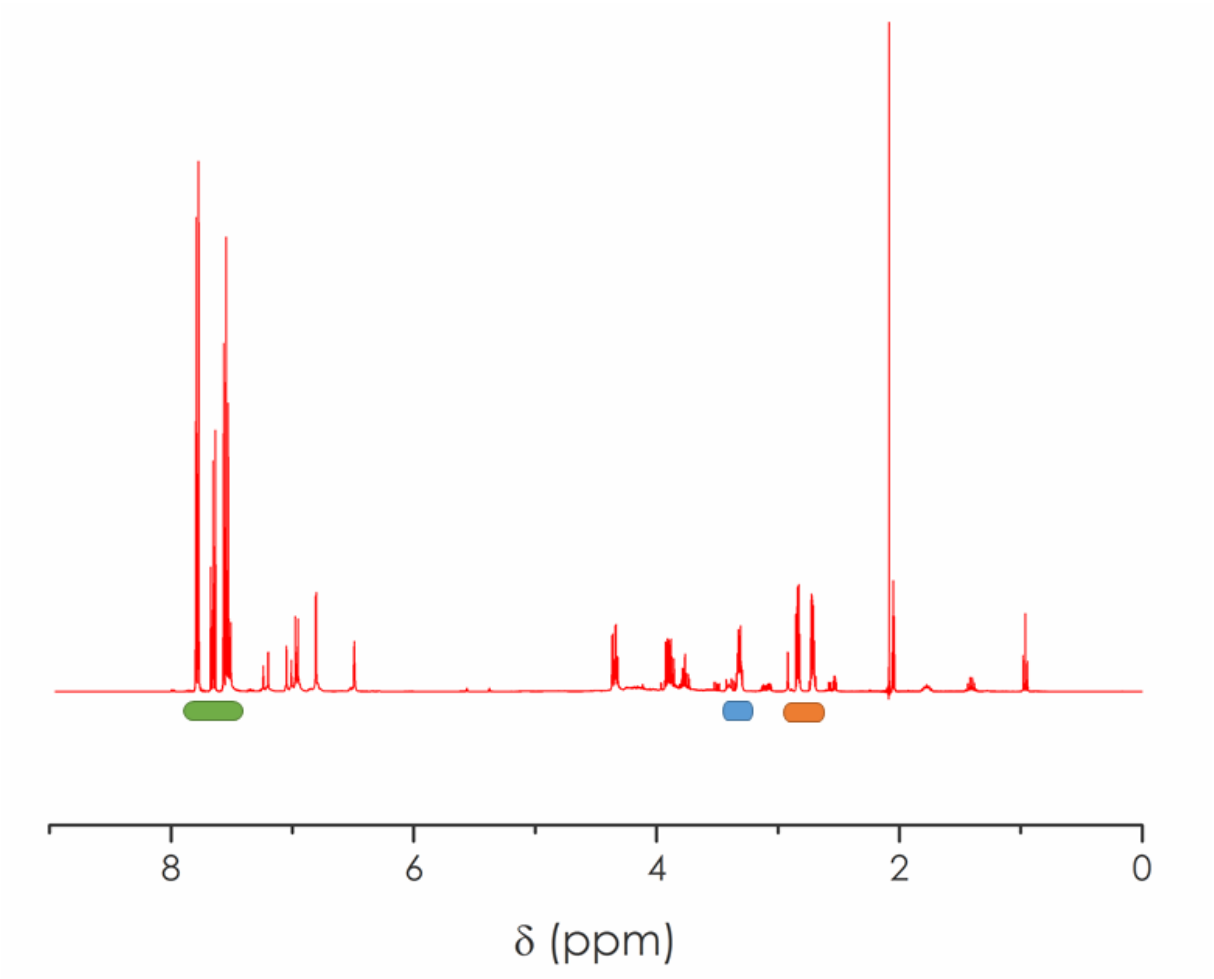

50 to 70 mg of BDGE and 50 to 130 mg of RvOGly were dissolved in deuterated acetone. ^{1}H NMR spectra were integrated in the 7.87-7.28 ppm range for benzophenone protons (10 H), in the 3.46-3.26 ppm range for CH oxirane and in the 3.0-2.65 range for CH_2 oxirane. EEW was calculated as follows :

$$EEW_{CH} = \frac{m_{BDGE} \times \int_{7.28}^{7.87} benzophenone \times M_{benzophenone}}{10 \times m_{benzophenone} \times \int_{3.26}^{3.46} CH\ oxirane}$$

$$EEW_{CH_2} = \frac{2 \times m_{BDGE} \times \int_{7.28}^{7.87} benzophenone \times M_{benzophenone}}{10 \times m_{benzophenone} \times \int_{2.65}^{3.0} CH_2\ oxirane}$$

m_{epoxy} (mg)	$m_{benzophenone}$ (mg)	$\frac{\int_{2.97}^{3.19} CH\ oxirane}{\int_{7.28}^{7.87} benzophenone}$	$\frac{\int_{2.45}^{2.82} CH_2\ oxirane}{\int_{7.28}^{7.87} benzophenone}$	EEW_{CH}	EEW_{CH_2}
55.9	39.9	0.157	0.283	163	180
94.8	44.8	0.227	0.390	170	198
125.9	54.8	0.245	0.402	171	208
			Average EEW	**182 ± 8 g/eq**	

Vitrimer characterizations (Vm-RvOH)

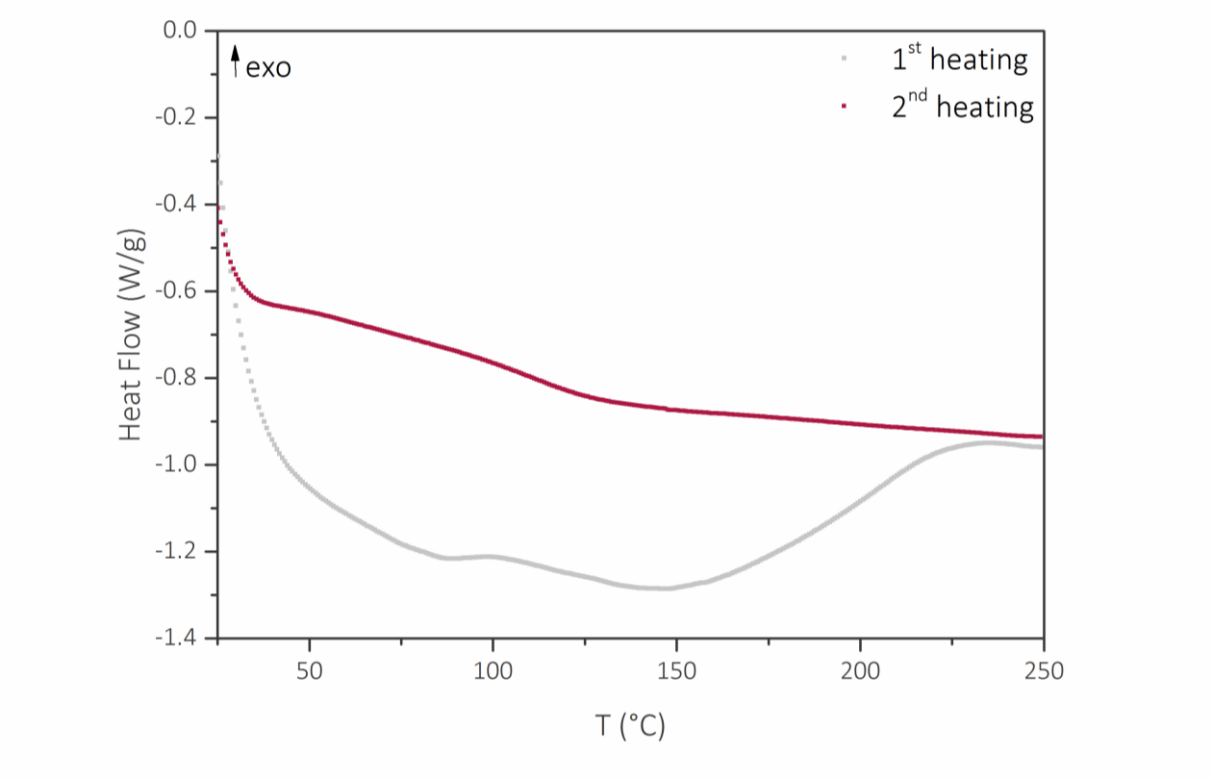

Figure S9. DSC thermogram of Vm-RvOH after curing 3 h at room temperature

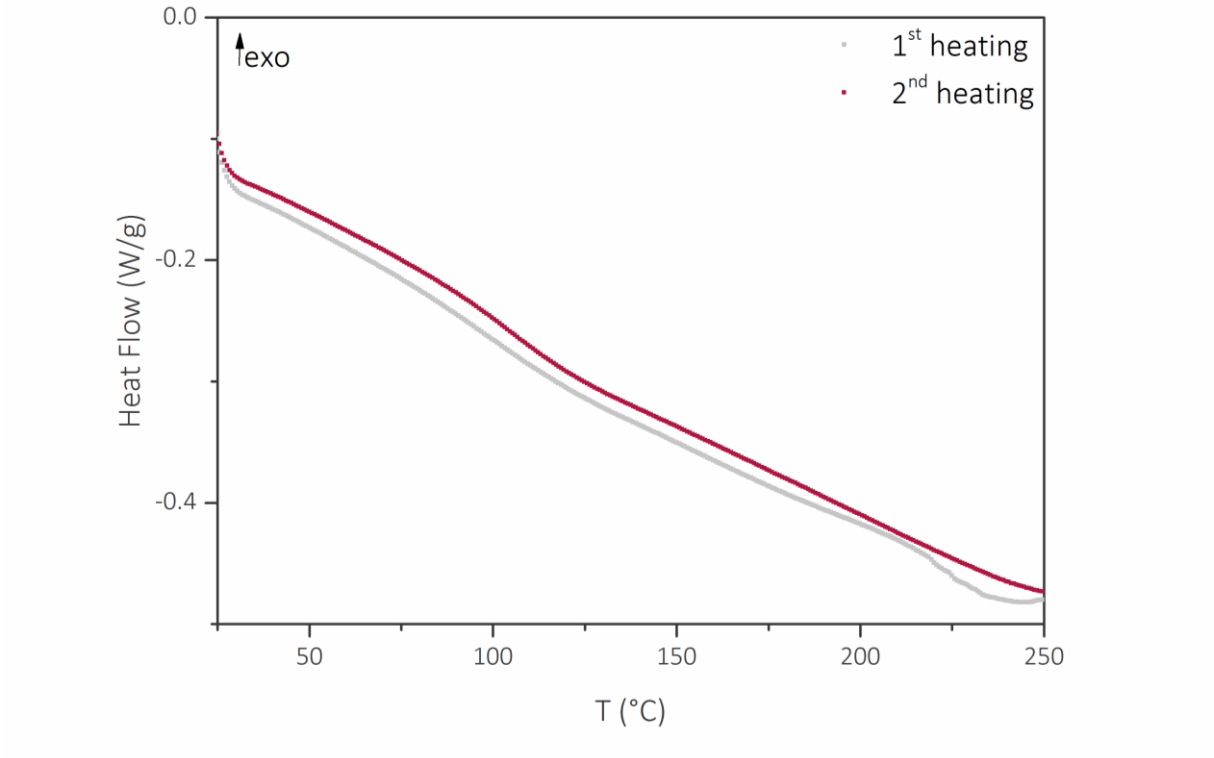

Figure S10. DSC thermogram of Vm-RvOH after curing 3 h at room temperature and 1 h at 150 °C

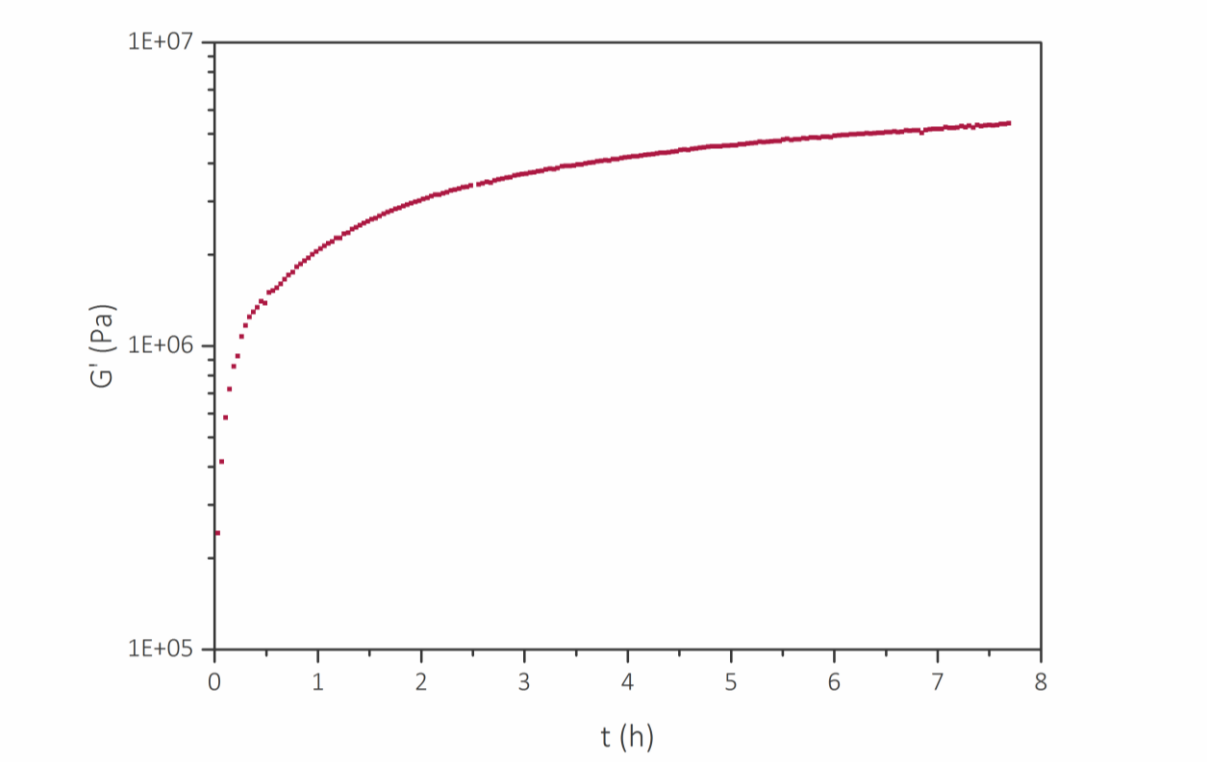

Figure S11. Curing step at 150 °C monitored by the evolution of the material storage modulus G'

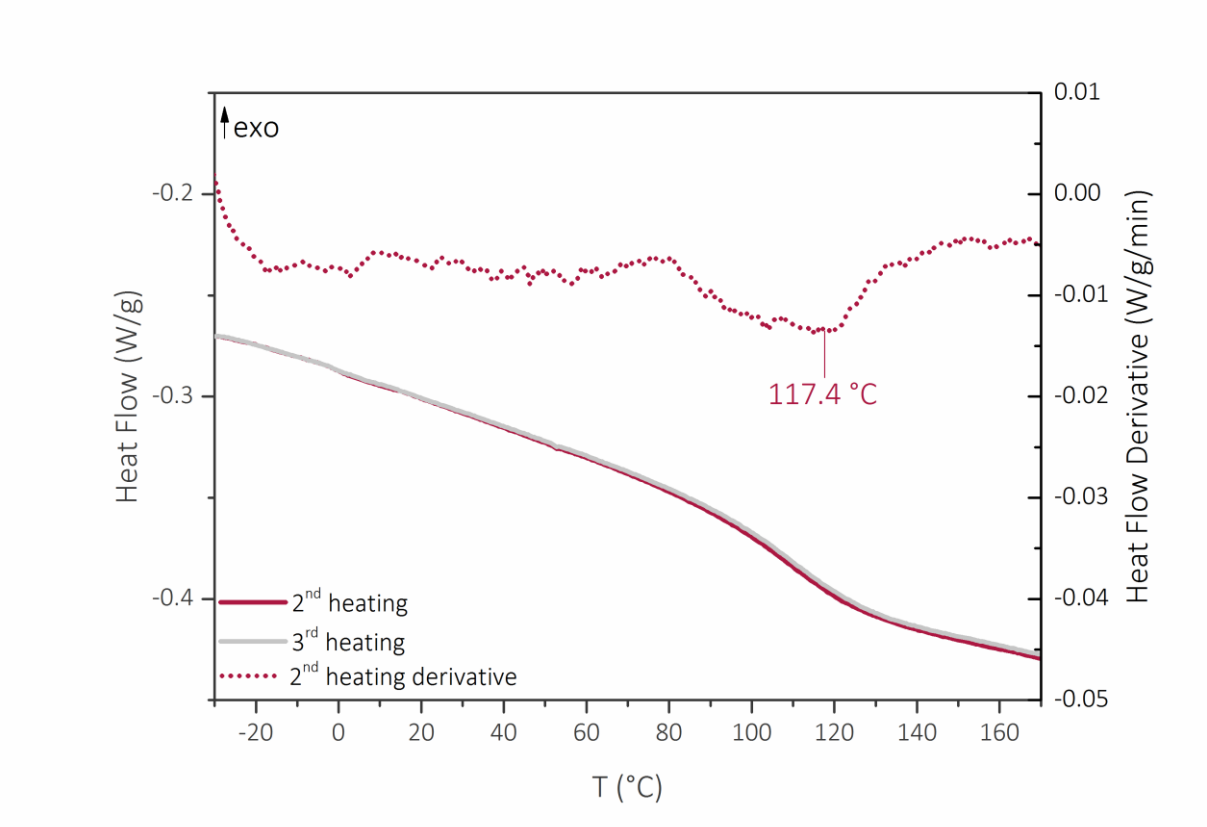

Figure S12. DSC thermogram of Vm-RvOH after complete curing 10 h at 150 °C.

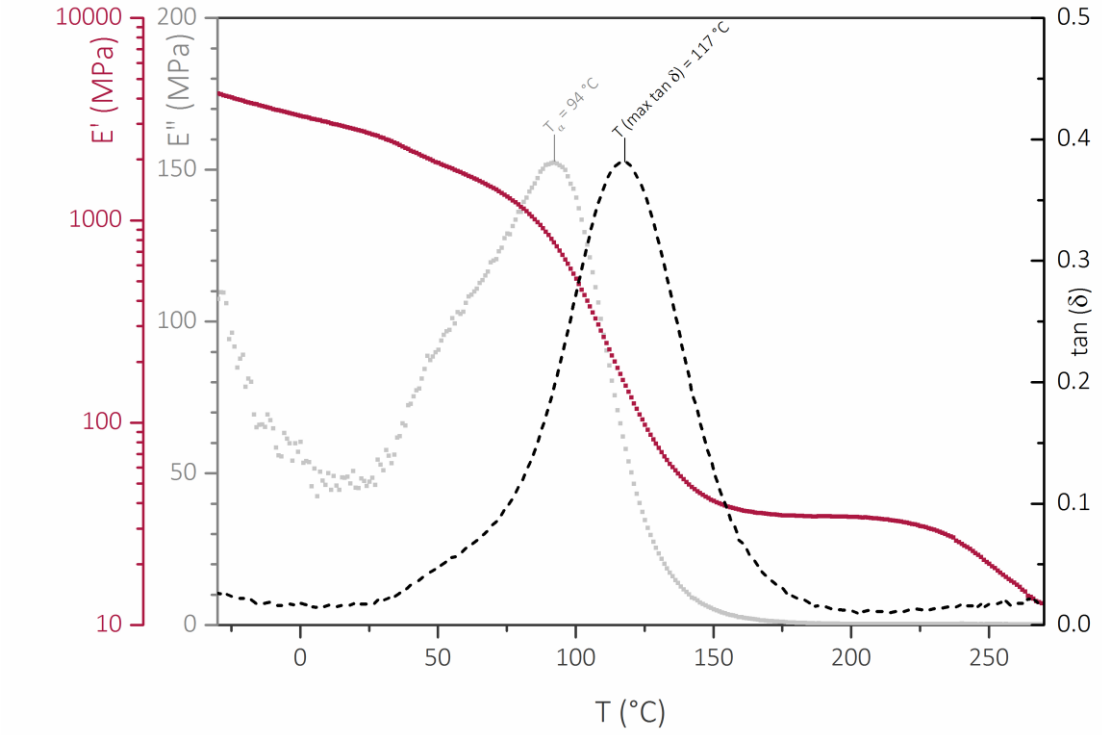

Figure S13. DMA thermogram of Vm-RvOH after complete curing 10 h at 150 °C (0.1 % strain, 1 Hz, 3 °C/min)

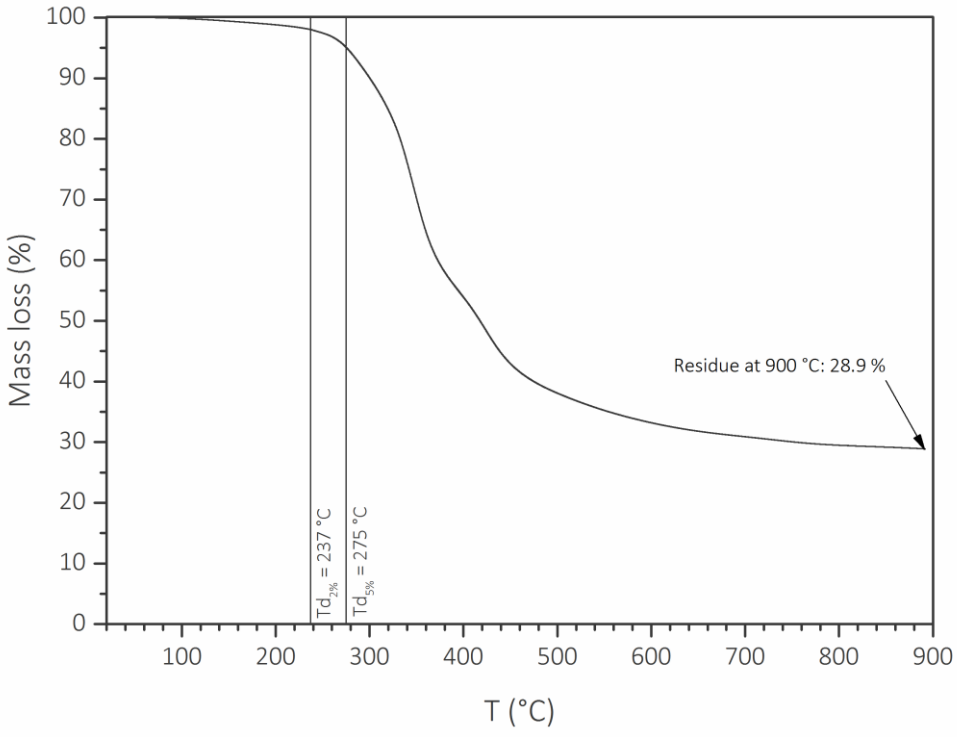

Figure S14. TGA thermogram under nitrogen of Vm-RvOH after complete curing 10 h at 150 °C

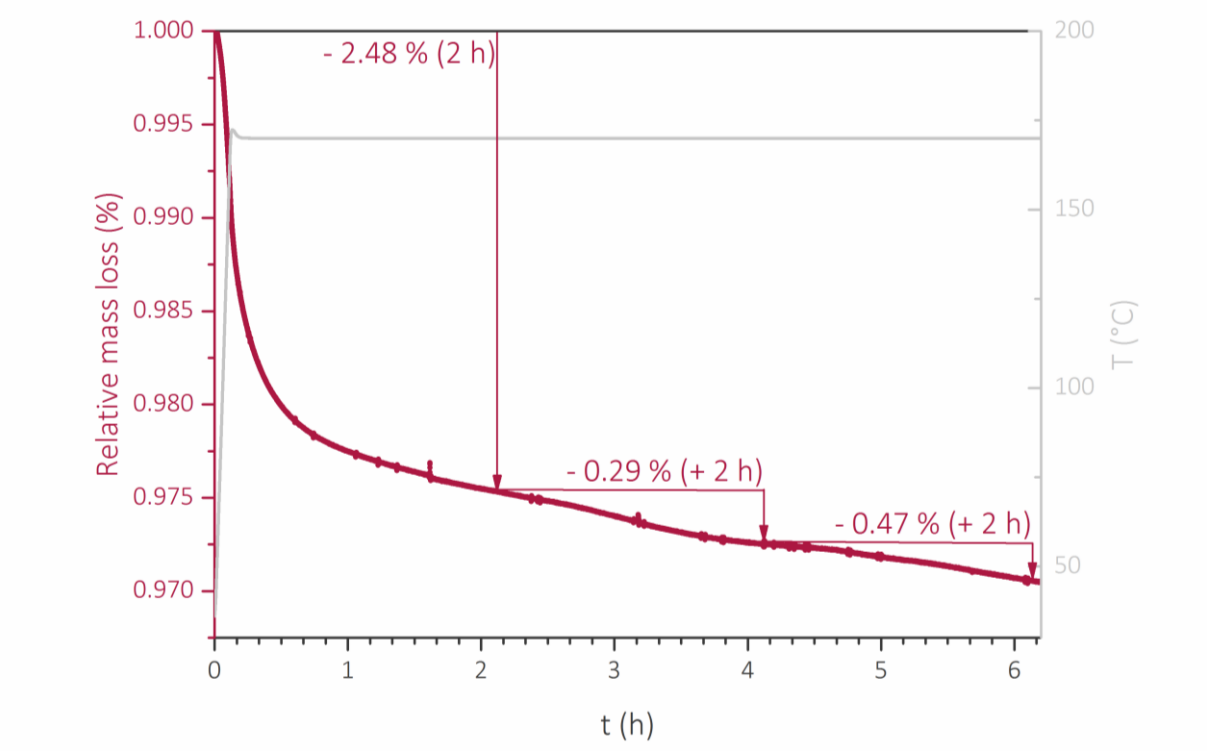

Figure S15. Isothermal TGA thermogram at 170 °C under air of Vm-RvOH after complete curing 10 h at 150 °C

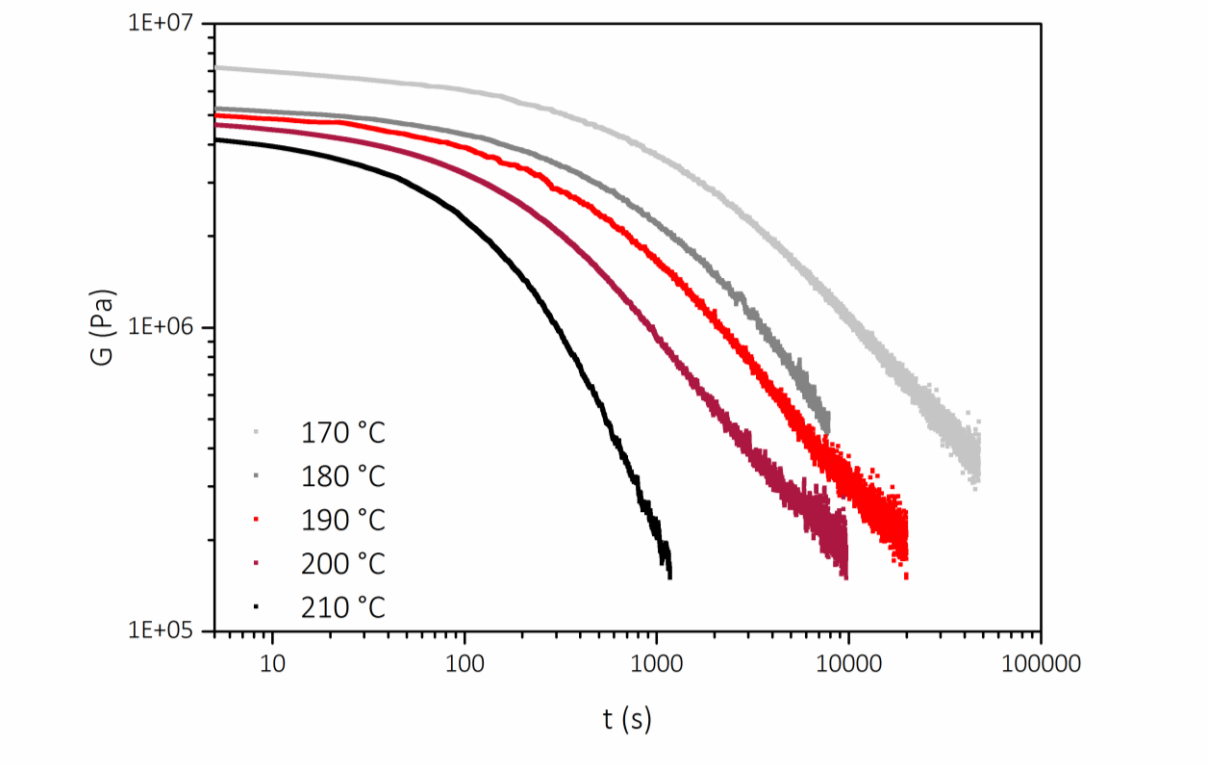

Figure S16. Stress–relaxation curves of Vm-RvOH from 170 to 210 °C with 10 °C steps (0.3 % strain)

Table S1. Equation and fitting parameters of the Kohlrausch-Williams-Watts stretched exponential for the stress relaxation experiments

$$\frac{G}{G_0} = e^{\left(\frac{-t}{\tau}\right)^{\beta}} + y_0$$

T (°C)	170	180	190	200	210
τ (s)	1827	1042	648	333	156
β	0.486	0.569	0.593	0.642	0.797
y_0	0.043	0.049	0.060	0.064	0.053
R^2	0.99962	0.99975	0.99937	0.99974	0.99979

Note: for β = 1 and y_0 = 0, the KWW expression becomes a Maxwell

Production scientifique

Articles publiés

(1) Cuminet, F.; Caillol, S.; Dantras, É.; Leclerc, É.; Ladmiral, V. Neighboring Group Participation and Internal Catalysis Effects on Exchangeable Covalent Bonds: Application to the Thriving Field of Vitrimer Chemistry. *Macromolecules* 2021, 54 (9), 3927–3961. https://doi.org/10.1021/acs.macromol.0c02706

(2) Cuminet, F.; Berne, D.; Lemouzy, S.; Dantras, E.; Joly-Duhamel, C.; Caillol, S.; Leclerc, E.; Ladmiral, V. Catalyst-Free Transesterification Vitrimers: Activation via α -Difluoroesters. Polym. Chem. 2022, 8, 5255–5446. https://doi.org/10.1039/D2PY00124A.

(3) Berne, D.; Cuminet, F.; Lemouzy, S.; Joly-Duhamel, C.; Poli, R.; Caillol, S.; Leclerc, E.; Ladmiral, V. Catalyst-Free Epoxy Vitrimers Based on Transesterification Internally Activated by an α–CF 3 Group . Macromolecules 2022, 55 (5), 1669–1679. https://doi.org/10.1021/acs.macromol.1c02538.

(4) Quienne, B.; Cuminet, F.; Pinaud, J.; Semsarilar, M.; Cot, D.; Ladmiral, V.; Caillol, S. Upcycling Biobased Polyurethane Foams into Thermosets: Toward the Closing of the Loop. ACS Sustain. Chem. Eng. 2022, 10 (21), 7041–7049. https://doi.org/10.1021/ACSSUSCHEMENG.2C00950.

(5) Lemouzy, S.; Cuminet, F.; Berne, D.; Caillol, S.; Ladmiral, V.; Poli, R.; Leclerc, E. Understanding the Reshaping of Fluorinated Polyester Vitrimers by Kinetic and DFT Studies of the Transesterification Reaction. Chem. – A Eur. J. 2022. https://doi.org/10.1002/CHEM.202201135

Articles à soumettre prochainement

(1) Cuminet, F.; Caillol, S.; Dantras, E. ; Leclerc, E. ; Totée, C. ; Guille, O. ; Ladmiral, V. Synthesis of a transesterification vitrimer activated by fluorine from an α,α-difluoro carboxylic acid and a diepoxy. To be submitted in Eur. Polym. J.

(2) Cuminet, F.; Lemouzy, S. ; Dantras, E.; Caillol, S.; Leclerc, E.; Ladmiral, V. From vineyards to 100 % resveratrol materials: α-CF2 activation in biobased catalyst-free vitrimers. To be submitted in Green Chem.

Participations à des congrès scientifiques

- Balard Chemistry Conferences – Montpellier – Juin 2021 :

Communication orale (EN) et présentation d'un poster (EN) "Catalyst-free transesterification vitrimers: the power of fluorine to activate bond exchanges"

- 48èmes Journées d'Etudes des Polymères (JEPO) – Porquerolles – 2021 :

Communication orale (FR) "Vitrimères de transestérification sans catalyseur activés par des groupements α-CF_2"

- 9èmes Journées Méditerranéennes des Jeunes Chercheur(e)s (JMJC) – Montpellier – 2021 :

Communication orale (EN) "α-CF_2 groups to activate the transesterification in catalyst-free vitrimers"

- International Symposium on Green Chemistry 2022 (ISGC 2022) – La Rochelle – 2022 :

Communication orale (EN) "Biobased Catalyst-free Vitrimers: From Vineyards to Reprocessable Networks"

- 26th Annual Green Chemistry and Engineering Conference (GC&E 2022) – Reston, VA, USA – 2022 :

Communication orale (EN) "Reprocessable biobased polyurethane foams: an asset for circular economy, from biomass to multiple recycling steps" et présentation d'un poster (EN) "From vineyards to 100 % resveratrol materials: α-CF_2 activation in biobased catalyst-free vitrimers"

- Bordeaux Polymer Conference (BPC 2022) – Bordeaux – 2022 :

Présentation d'un poster « From vineyards to 100 % resveratrol materials: α-CF_2 activation in biobased catalyst-free vitrimers"

Les vitrimères sont des matériaux polymères qui présentent une bonne résistance aux solvants, des propriétés mécaniques qui peuvent se comparer à celles des thermodurcissables, et qui peuvent être remis en œuvre par des techniques mécaniques, grâce à des liaisons échangeables au sein du réseau. En particulier, les vitrimères polyesters ont été beaucoup étudiés, du fait de la disponibilité des résines époxy dont ils sont issus. Néanmoins, un inconvénient majeur de ces vitrimères polyester réside dans l'utilisation de catalyseurs en grande quantité au sein du réseau macromoléculaire. Ces catalyseurs peuvent subir des phénomènes de lixiviation au cours de la vie du matériau, ce qui diminue sa capacité de remise en œuvre, et peut induire des risques pour l'environnement voire la santé. De plus, ces catalyseurs peuvent provoquer un vieillissement prématuré de ces matériaux au cours de leur remise en œuvre. L'objectif de cette étude a donc été de réaliser des vitrimères sans catalyseur. Pour cela, deux stratégies sont possibles. La première est d'exploiter des réactions d'échange intrinsèquement plus rapides. La deuxième stratégie est d'ajouter des groupements à proximité des sites d'échange pour activer ces échanges. Après avoir dressé un état de l'art sur les réactions d'échange disponibles et les stratégies d'activation existantes, le choix de travailler sur l'activation des liaisons ester a été fait. Des groupements CF_2 placés en α de la liaison ester ont permis d'activer la réaction de transestérification. Une preuve de concept a ainsi été obtenue sur un vitrimère formé à partir d'un α,α-difluoro acide trifonctionnel et d'un diépoxy. Un deuxième système 2+2 a été synthétisé par la suite, permettant de montrer la faisabilité d'un réseau macromoléculaire tridimensionnel à partir de deux composés difonctionnels, grâce à l'effet de la transestérification. Enfin, un troisième système a été formé à partir de monomères issus de resvératrol, un triphénol naturel extrait de la vigne. Un vitrimère sans catalyseur avec 85 % de carbone biosourcé a ainsi été synthétisé. Ces trois systèmes permettent de proposer différentes solutions afin d'améliorer la durabilité des vitrimères, depuis le choix de la matière première utilisée, jusqu'à leur remise en œuvre et leur fin de vie.

Vitrimers are a type of polymer materials featuring superior resistance to solvents, mechanical properties comparable to thermosets, and the ability to be reprocessed. Their macromolecular network embeds exchangeable bonds responsible for their ability to be reshaped upon heating. Polyester vitrimers are the most studied as they are made from very available epoxy resins. Nonetheless, a major drawback of these vitrimers is the need for large quantities of catalysts in the macromolecular network. They induce risks of leaching when the material is in use, which decreases its ability to be reprocessed and induces risks for the environment and the human health. They can also trigger a premature ageing of the material upon reprocessing. The aim of this project was to create catalyst-free vitrimers. A first strategy is to implement other exchange reactions which are faster, and do not require any catalyst. Another strategy is to accelerate the exchange reaction by activating groups in close vicinity to the exchangeable bonds. The state-of-the-art on the variety of exchangeable bonds and the activation strategies was summarized. Then, the choice to work on transesterification vitrimers was made, with the idea to activate the ester carbonyl by electroattractive inductive effects. In particular, a proof-of-concept of the activation of α-CF_2 esters towards transesterification was proven, in a catalyst-free vitrimer made of a trifunctional α,α-difluoro acid and a diepoxy. Then, a 2+2 system led to the synthesis of a second vitrimer, showing the feasibility of a crosslinked macromolecular network from difunctional monomers, thanks to the effect of the transesterification reaction. Finally, a third vitrimer was made out of resveratrol, a biobased triphenol extracted from grapes, after a 2-way functionalization. This catalyst-free vitrimer exhibited a 85 % biobased carbon content. These three systems propose different solutions toward more sustainable vitrimers, taking into account their whole life, from the sourcing of the raw materials, to their reshaping and the management of their end-of-life.